Evaluation of Fiber Reinforced Polymer Bench Scale Specimen Sizes and Prediction of Full Scale Flame Spread Testing for Building Applications

Development of a Flame Spread Screening

Tool for Fiber Reinforced Polymers

A Major Qualifying Project Report

submitted to the Faculty of

WORCESTER POLYTECHNIC INSTITUTE

in partial fulfillment of the requirements for the

Degree of Bachelor of Science

By:

_____

Christian Acosta

_____

Shawn Mahoney

_____

Nicholas Nava

_____

William Wright

May 2013

Project number: NAD FM12

_____

Professor Nicholas A. Dembsey, Advisor

Table of Contents

List of Figures

List of Tables

Authorship

Christian Acosta

- Background
- Edge Burning Analysis
- Cone Calorimeter Specimen Size Comparison

Shawn Mahoney

- Background
- Edge Burning Analysis
- Flame Length Screening Tool
- Conclusions

Nicholas Nava

- Introduction
- Background
- Edge Burning Analysis
- Cone Calorimeter Specimen Size Comparison
- International Building Code Proposed Changes
- Conclusions

William Wright

- Introduction

Authorship for Appendices is listed under the title for each Appendix.

1. Organization of Report

This MQP report consists of a 20-page conference paper which compared fire characteristics of bench scale specimen sizes and explains a flame length model created for fiber reinforced polymers. This is then followed by multiple briefs included as appendices where additional in depth information is presented. Supplemental information such as a test results database, a section of derived equations for analysis, and other data and charts can also be found in the appendices.

2. Acknowledgements

3. Abstract

Fiber Reinforced Polymers (FRPs) are quickly becoming an important building material due to their aesthetic and environmentally "green" characteristics. As with many building materials FRPs can potentially be a fire hazard in regards to flame spread. The International Building Code (IBC) limits flame spread for materials which are to be used as interior finish based on large scale ASTM E84 (Tunnel) testing. Unfortunately for manufacturers, Tunnel testing is not a particularly cost effective way for developing new materials. To make development more affordable, use of the bench scale ASTM E1354 Cone Calorimeter (Cone) test is desirable.

FRP Cone standard samples (100mm by 100mm) often exhibit non 1D behavior in terms of edge burning. Cone sample burning behavior was analyzed by comparing standard samples to enlarged samples (175mm by 175mm). Testing larger samples is thought to more clearly identify the onset of edge burning. Statistical methods helped analyze and compare the two sample sizes in terms of typical Cone data. Additional analysis involved the use of finite difference methods to compare sample temperature profiles.

A flame length model for material burning in the Tunnel test based on 1D Cone test results for material behavior was created to simulate the limited burning behavior of materials with a flame spread index 25 or less. This model can be used as a screening tool for material development. Additionally, the model can be used to establish compliance criteria for interior finish materials consistent with IBC requirements.

4. Evaluation of Fiber Reinforced Polymer Bench Scale Specimen Sizes and Prediction of Full Scale Flame Spread Testing for Building Applications

4.1 Introduction

Fiber reinforced polymers (FRP's) are quickly becoming a building material used in new construction where the owner would like the ability to use a material that is sustainable, aesthetically pleasing, and easy to mold into shapes to achieve certain architectural desires. A potential problem of placing FRP's in a building, as an interior finish, is the possibility that the material may spread flame quickly, which is not desired when placed in a building. Chapter 8 of the International Building Code (IBC) dictates requirements for interior finishes in a building.[1] The IBC classifies these materials by flame spread and smoke production as determined by testing a material in the Steiner Tunnel (tunnel) using the standard test ASTM E84[2]. The IBC classifies a Class A material as a material with a relatively slow flame spread, a Class B material has more flame spread, and a Class C material has an even higher rate of flame spread, all with a predetermined allowable amount of smoke production. The result of this test and the subsequent building classification, determines where a building material can be used (i.e. exit passageway, exit corridor, room or space).

There is significant interest from FRP material manufacturers to determine results that may be found in the tunnel test without actually running the test. The test requires a large nominal 24 foot by 2 foot material specimen, which requires significant effort from the manufacturer, and is also quite costly in comparison to other standardized tests. A screening tool that can determine the expected results, before creating the large specimen required and running a full scale test, is desired by the manufacturer for quick research and development of new specimens.

The Cone Calorimeter (Cone) tested using the ASTM E1354 test standard[3] is determined a feasible screening tool as specimens are only 100mm by 100mm and testing is rather quick, easy, and cost effective. The issue with testing using the Cone is the fact that FRP specimens tend to produce edge burning when tested in the Cone standard configuration. Edge burning occurs when the edges of the specimen ignite, which is often hard to determine due to edge flame confounding with the surface flame. Edge burning also indicates the end of burning solely on the top face, which means the ASTM E1354 test is invalid and test collection must stop. To determine when edge burning occurs, when the test becomes invalid, a larger specimen may be able to be used, allowing technicians to more easily see edge burning. In order to utilize a larger specimen, it must be determined that the standard and large specimens perform the same in the test. A technician should be notified of this edge burning phenomena and the possible remedy of testing a large specimen size as it may lead to better testing.

The use of a screening tool, which uses the results of accurate Cone testing accounting for edge burning, has the potential to save manufacturers time and money when it comes to designing new materials. In the grand scheme of things, this screening tool also has the potential to make the building environment safer for occupants. This is the result of, during development of new materials, the manufacturer trying multiple variations of an FRP material to find the safest material but also what is desired by the building owner.

4.2 Background

For this project we utilized two ASTM standards, the ASTM E1354: Standard Test Method for Heat and Visible Smoke Release Rates for Materials and Products Using an Oxygen Consumption Calorimeter[3] and ASTM E84: Standard Test Method for Surface Burning Characteristics of Building Materials[2].

4.2.1 Cone Calorimeter

The Cone calorimeter (Cone) is a bench scale testing apparatus that measures fire performance of a material specimen. The Cone was first used in the early 1980's by the National Institute of Standards and Technology (NIST) as an improved bench scale test over the current test at that time which involved measuring outflow enthalpy of enclosed systems.[4] The American Society for Testing and Materials (ASTM) created various testing standards that utilize this device. One of the standard test methods utilizing the Cone is described in ASTM E1354: Standard Test Method for Heat and Visible Smoke Release Rates for Materials and Products Using an Oxygen Consumption Calorimeter. The following Figure 1 shows schematics of the Cone apparatus.
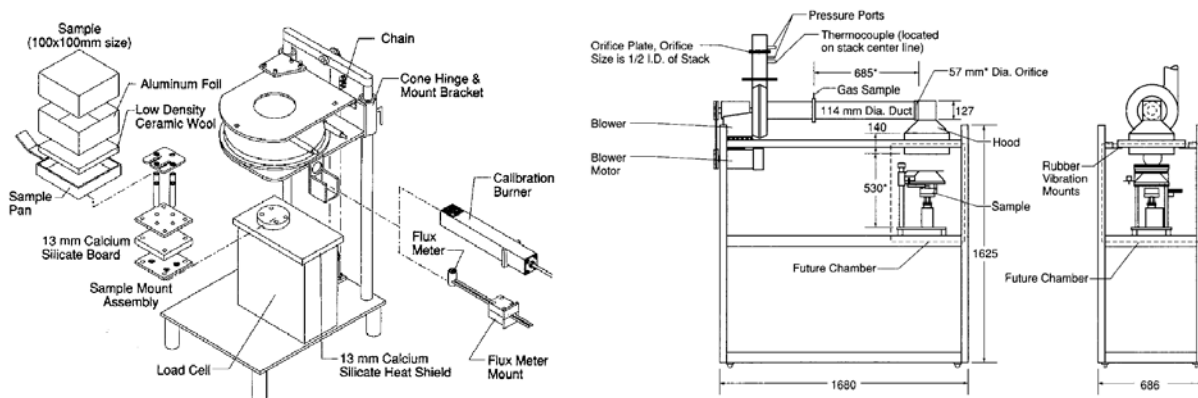
Figure 1: Cone Calorimeter Schematic Drawings (Left: Cone burner assembly. Right: entire Cone assembly.)

4.2.1.1 Cone Operation

The ASTM E1354 test involves the testing of a 100mm by 100mm (nominal 4in. by 4in.) specimen placed upon a load cell in ambient air, while exposing it to a constant heat flux. This heat flux produces a flame on the surface of the material defined as burning in one dimension. When the specimen's edges begin decomposing and support a flame, the data collection and testing stops as this is no longer one dimensional burning and is then defined as two dimensional burning and not representative of the ASTM E1354 test.

The oxygen concentration in the exhaust, exhaust rate, specimen mass-loss rate, time to ignition, and smoke obscuration are measured during testing using various data acquisition techniques. The Cone test method is based on the fact that the net heat of combustion of a test specimen is directly related to the amount of oxygen required for combustion.[3] This data acquired allows for the determination of the heat-release rate (HRR) of the specimens. The HRR is the heat energy, in kilo-watts, produced by a specimen when the surface has ignited and supports flame. The HRR can be used to predict real-scale fire behavior and is used in state-of-the-art fire models.[5] The HRR is often normalized based on the specimen surface area, often expressed as kW/m^2, which allows the fire performance to be estimated for a larger sized specimen as long as the specimen area is known. The HRR per unit area (HRRPUA) is often plotted as a function of time and can then be compared to other specimens.

4.2.1.2 Cone Specimen

The standard specimen size in the Cone is 100mm by 100mm (nominal 4in. by 4in.) specimen with varying thicknesses up to 50mm (2 in.). Products that are thinner than 6 mm (0.25 in.) shall be tested with a substrate representative of end use conditions at its back face, such that the total specimen thickness is 6 mm or more.[3] The specimen is wrapped in aluminum foil which eliminates mass transfer along all boundaries except for the burning face of the specimen and shields the edges against heating from the Cone[6]. Specimens are then placed in an edge frame that ensures the specimen does not rise up into the Cone if it begins to intumesce (expand when heated) and to ensure the specimen is in the same location for all tests. The specimen is smaller than the Cone heater which ensures that the entire specimen face is exposed to a uniform heat flux at all times throughout the test.

4.2.1.3 Edge Burning Phenomena

Edge burning is the phenomenon, as described above, when the specimen's edges decompose and support flame. This creates a two dimensional heat effect on the specimen, where the top heating from the Cone and flame and side heating from the flame contribute to the specimen heating. Edge burning must be accounted for to ensure legitimate testing. It is often hard for technicians to determine when edge burning begins because top and side flames become confounded. To account for edge burning, the ASTM E1354 test method may benefit from testing a larger specimen than its standard 100mm by 100mm (nominal 4in. by 4in.) size. This would prevent top and side lames from becoming confounded with a clear distinction of top flame and side flame. In 1986, Nussbaum and Ostma performed a study with extended 200mm by 200mm (7.9 in. by 7.9in.) specimens and standard 100mm by 100mm (nominal 4in. by 4in.) specimens, with the thought that the increased specimen size would minimize edge effects.[7] Increasing the specimen size pushes the edges out to the Cone heater's edges and in this way is assumed to minimize edge effects. Nussbaum and Ostma concluded that the general fire behavior is similar between both size specimens when using a custom made extended size Cone.[7] Further analysis regarding the specimen size's relation to edge burning should be completed to confirm this conclusion with a standard Cone.

4.2.2 ASTM E84 – Tunnel Test

The purpose of the ASTM E84 (Tunnel test) is to determine the relative burning behavior of a building material by observing the flame length over a period of 10 minutes. During the test, there is an imposed flame created by a methane or natural gas burner that impinges on a 4.5 feet long distance of the specimen, which is mounted on the ceiling of the tunnel. The resulting flame length extension past the 4.5 foot burner flame is measured along the length of the tunnel for a duration of 10 minutes. Figure 2 shows a schematic of the tunnel. The three areas shown in the figure represent the area of the specimen impinged by the burners and will prove essential in calculating the flame length in this correlation.
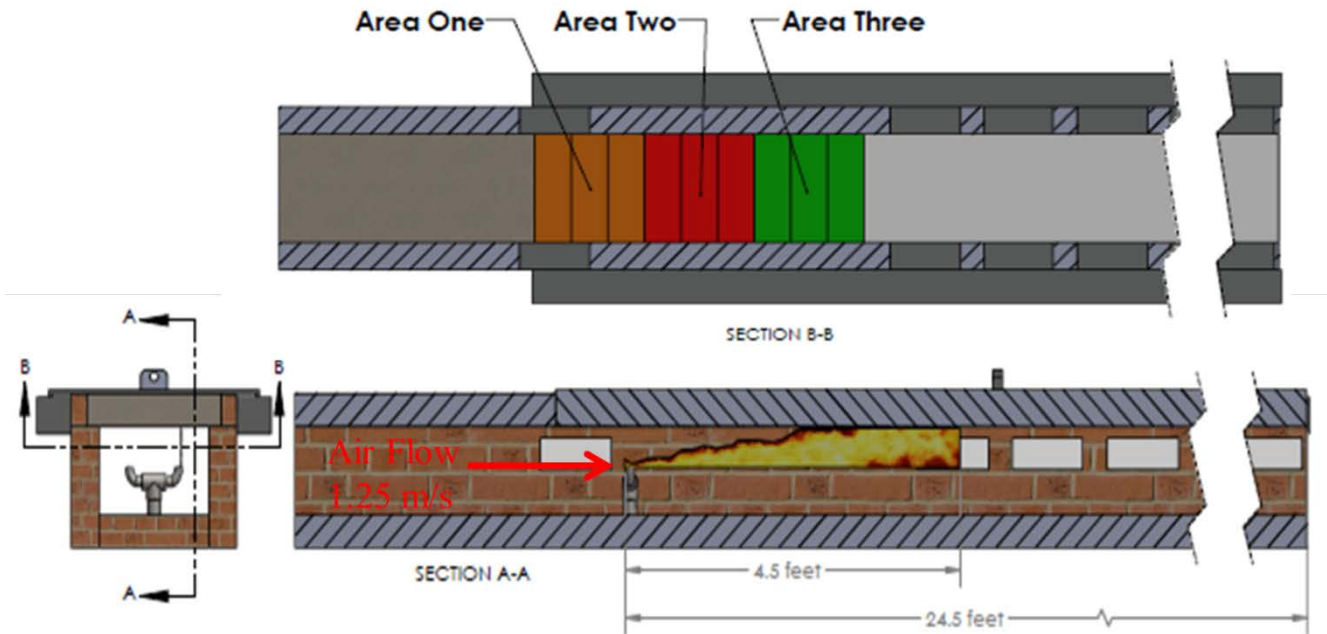
Figure 2: Schematic of Tunnel Test

From this test, a flame index and smoke index are developed for the specimen being tested. The flame spread index (FSI) is developed by calculating the area under the observed flame length extension vs. time curve. A FSI of 0-25 is classified as a Class A, 26-75 is classified as a Class B, and 76 – 200 is considered a Class C, these classifications normally include smoke production.

4.2.3   Materials Used in This Study

During this study there were seven different material specimens used. The first two specimens were Fiberglass Reinforced Polymers supplied by Kreysler and Associates. The FRP panels are made from commercially available components that include E glass reinforcement, polyester FR resin, inorganic FR additives and other fillers for FR and aesthetic purposes. The FRP panels are nominally 11mm (7/16") in thickness. The structure of the panels is an FRP laminate with a proprietary Kastone coating. The two FRP panel systems are designated as Kreysler 1 and Kreysler 2. The next three material specimens were Fiberglass Reinforced Polymers provided by Creative Pultrusions. These three FRPs were created through a pultrusion of fiber reinforced polymer and are designated by CP 286, CP 702, and CP 802. The final two material specimens were FRPs supplied by Crane Composites. These include two products from their Glasbord with Surfaseal line. One sample is their FSI- 0.075 Class A Fire-Rated 85 White Smooth FRP and the other sample is their FX-0.090 Class A Fire-Rated 85 White Pebbled Embossed FRP. These two samples are designated by FSI 0.075 and FXE 0.090.

4.2.4   International Building Code

The International Building Code (IBC), or a version of it with alterations, is a standard code adopted by all states in the United States.[8] The code establishes minimum requirements to safeguard the public health and provide: safety and general welfare through structural strength, a means of egress, stability, sanitation, adequate light and ventilation, energy conservation, and safety to life and property from fire and other hazards attributed to the built environment.[9] Most of the requirements in the code are prescriptive in nature meaning they are determined through historical data and by industry professionals and approved by the Code Development Committee.

Section 2612 of the 2012 IBC addresses the use of FRPs, and allows their use as an interior finish or an exterior wall granted it meets the requirements set forth in the code. The interior finish requirements are separated by space and are: interior passageways, exit access corridors, and rooms, where each allows a specific material classification (A, B, or C). The requirements for interior finishes can be found in Appendix 5.1. Exterior FRP finish is allowed to be used as long as certain requirements are met, including but not limited to, the fact that the material FSI of 25 or less.

4.3 Edge Burning Analysis

To determine when edge burning is likely to occur in a sample a semi-infinite one-dimensional analysis was performed to confirm our hypothesis for why and when edge burning occurs. It is hypothesized that edge burning is a result of decomposition below the surface of a sample. The interior of the sample decomposes and the glass resin on the surface prevents decomposition vapors from venting out of the top of the specimen and instead forces the vapors to travel out the side. The vapors then ignite when they reach their auto ignition temperature, resulting in edge burning. The following analysis describes methods used to confirm this hypothesis.

4.3.1   Semi-Infinite Analysis: One-Dimensional Case

Upon further analysis of the burning behaviors of samples in the Cone; the samples burned have been assumed to be lumped capacitors in a one-dimensional semi-infinite model. This assumption was made to help distinguish temperature change throughout the tested material. If the material reaches the decomposition temperature range of 200-300° C[10] beneath the surface, this will verify that the preliminary stage of edge burning is occurring.

This semi-infinite model is unlike the typical cases which contain one type of burning component. This semi-infinite model accounted for radiation from the cone heater to the surface of the specimen along with convective and radiative cooling. In reality there would also be radiative and convective cooling along the sides of the specimen, but since this model only accounts for one dimensional heating they have been ignored. The equation used was found in *Conduction of Heat in Solids* by Carslaw and Jaeger.[11] The exact formula found in the text was derived using an advanced mathematical approach; however to make the equation more understandable, it was derived once more using common variables. The final derivation can be seen below.

$$\Delta T = \frac{q''}{h_{tot}} erfc\left(\frac{x}{2\sqrt{\alpha t}}\right) - \frac{q''}{h_{tot}} \exp\left(\frac{h_{tot}}{k}x + \frac{h_{tot}^2}{k^2}\alpha t\right) erfc\left(\frac{x}{2\sqrt{\alpha t}} + \frac{h_{tot}\sqrt{\alpha t}}{k}\right) \qquad \mathbf{1}$$

q'' - Incident Heat Flux $\left(\frac{W}{m^2}\right)$ **x** – Depth through the specimen (m)

h_{tot} – Total Heat Transfer Coef. $\left(\frac{W}{m^2 K}\right)$ **t** – Time throughout (sec)

α – Thermal diffusivity $\left(10^{-7}\frac{m^2}{s}\right)$ **k** – Thermal Conductivity of the specimen $\left(.5\frac{W}{m*K}\right)$

ΔT – Change in Temperature (K)

This equation would allow users to solve for the one-dimensional temperature change at any depth in the material at any moment in time for any radiative heat flux to the surface of the specimen. For further analysis on how the results are obtained of the equation view Appendix 5.4.

4.3.2 Results

Using the minimal heat flux for ignition found in Cone testing, the ignition temperatures for the three IHF tested were derived, the equation can be found in Appendix 5.4. The theoretical ignition temperature has been found to be 524 degrees Celsius. The results below display that the temperature beneath the surface of the sample does in fact reach the resins decomposition temperature (200-300° C). Decomposition through the material and surface ignition occurred at different time periods for each of the three incident heat fluxes. In Figure 3 below, the temperature profiles of the specimen at given times can be seen when the specimen is heated at an IHF of 50 kW/m². It can be seen that both surface ignition and decomposition at depth in the specimen occurred around the same time. However for the case of 25 kW/m² the IHF was not significantly hot enough to ignite the specimen. The constant heat flux merely heated the entire specimen over an extensive amount of time causing the first few layers to slowly converge to the same temperature. The graphs for IHF 25 kW/m² and 75 kW/m² can be viewed in Appendix 5.4.

Semi-Infinite Analysis at 50kW/m²
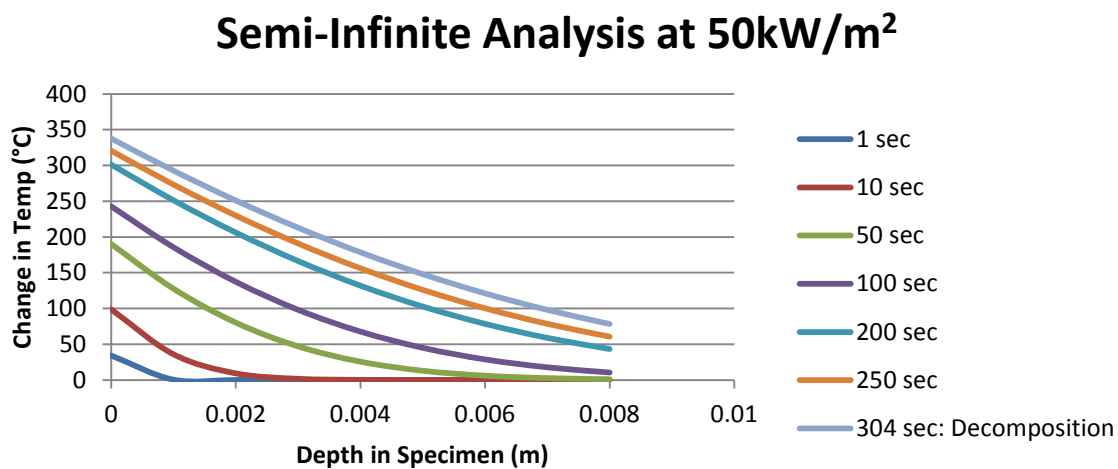
Figure 3: Semi-Infinite Analysis at 50kW/m²

These calculated times to interior decomposition were then compared to observations of the specimen burning in the Cone Calorimeter. It was found that the calculated time to interior decomposition occurred at times analogous to the observed time of edge burn in the Cone. This information supports our hypothesis that edge burn occurs when there is a decomposition of the interior of the specimen.

4.4 Cone Calorimeter Specimen Size Comparison

The difference between standard [100mm by 100mm (nominal 4in. by 4in.)] and extended [175mm by 175mm (nominal 7in. by 7in.) specimens was first approached theoretically and then the conclusions made through theoretical work were confirmed via actual ASTM E1354 testing. These specimen sizes were provided by manufactures for testing, so these sizes were analyzed to ensure continuity in results. The theoretical comparison of specimen size was completed by comparing temperature profiles found using finite difference methods. If temperature profiles were similar (in profile and temperature) throughout both specimens, actual specimen testing was to be performed. The comparison of specimen size via testing was completed statistically by comparing several specific fire characteristics.

4.4.1 Temperature Profile Comparison

The temperature profiles were determined for both standard and extended size samples. The temperature profiles of the specimen configurations was determined using two dimensional steady state finite difference methods with boundary conditions consistent with those of the actual ASTM E1354 test.

The standard 8mm (0.3 in.) thick sample was examined with 46mm (1.8 in.) fiber board backing and 2mm (0.08 in.) thick edge frame along the side and 2 mm (0.08 in.) in from the edges on the top surface it as it would be during testing. The analysis was performed with an induced incident heat flux (IHF) on the top face and a radiative fraction (heat flux multiplied by a view factor) along the sides. Natural convective cooling on the top was determined using Janssens' equation for determining the convective heat transfer coefficient[12] and natural convective cooling on the side and back faces was determined using a standard convective heat transfer coefficient. The extended 8mm (0.3 in.) thick sample was examined with 46mm (1.8 in.) fiber board backing and no edge frame, as is the testing configuration for this sample size. The analysis was performed with an induced heat flux on the top face under the Cone, where the edges outside of the Cone's area were exposed to a radiative fraction (heat flux multiplied by a view factor) and sides received no heat flux. The convective cooling was the same as for the standard samples. The thermal conductivity for the FRP specimen, fiber board, and steel edge frame were determined based on literature review and practical experience and remained consistent throughout the calculations, see Appendix 5.5 for more details.

See Figure 4 for results of finite difference calculations using the equations in Appendix 5.5, which shows the temperature contours for standard and extended size specimens at the three IHF's tested.
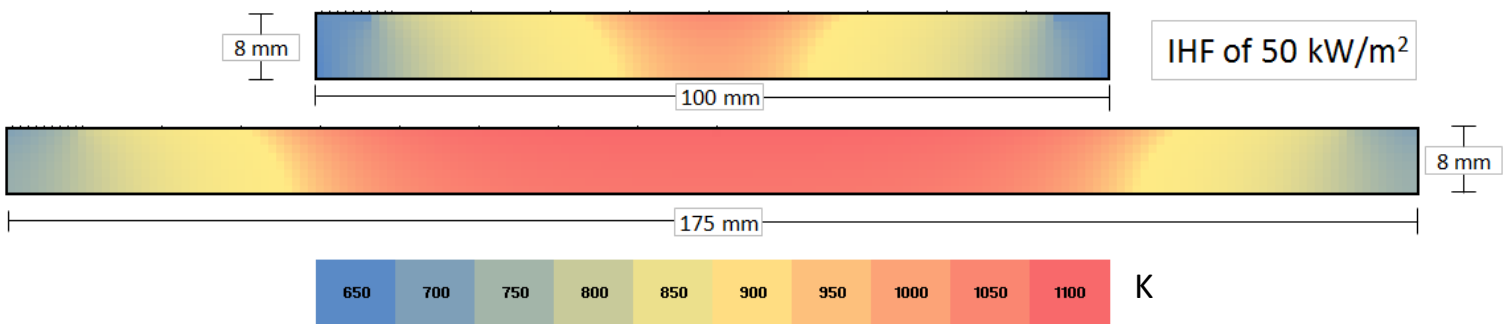
Figure 4: Steady state temperature profiles for both sample sizes at IHF ok 50kW/m^2.

4.4.2 Temperature Profile Comparison Results

Figure 4 shows similar temperature profiles when comparing standard and extended specimens of the same IHF. The figure shows slightly higher temperatures for the extended specimen which is explained below where profiles are compared. A plot of the temperatures over a normalized distance of -1 (left edge) to 1 (right edge) was created to compare the specimen sizes for each IHF it was exposed to. The plot for an IHF of 50 kW/m^2 is shown in Figure 5. This figure shows that that the temperature at the surface, 3 mm down, and at the back face, tracks similarly for both size specimens. The profiles are similar which indicates similarity between the specimens yet the profiles of the larger samples indicate higher temperatures. The difference in temperatures is indicative of the larger sample receiving more heat because of its size. Since fire performance in the Cone is normalized by surface area burned, the fact that the extended sample receives higher temperatures will be accounted for when normalized by size. This explanation helps to confirm theoretically that these specimen

sizes are similar. To determine if they are quantitatively similar, not significantly different, testing of both specimen sizes in the Cone was performed.
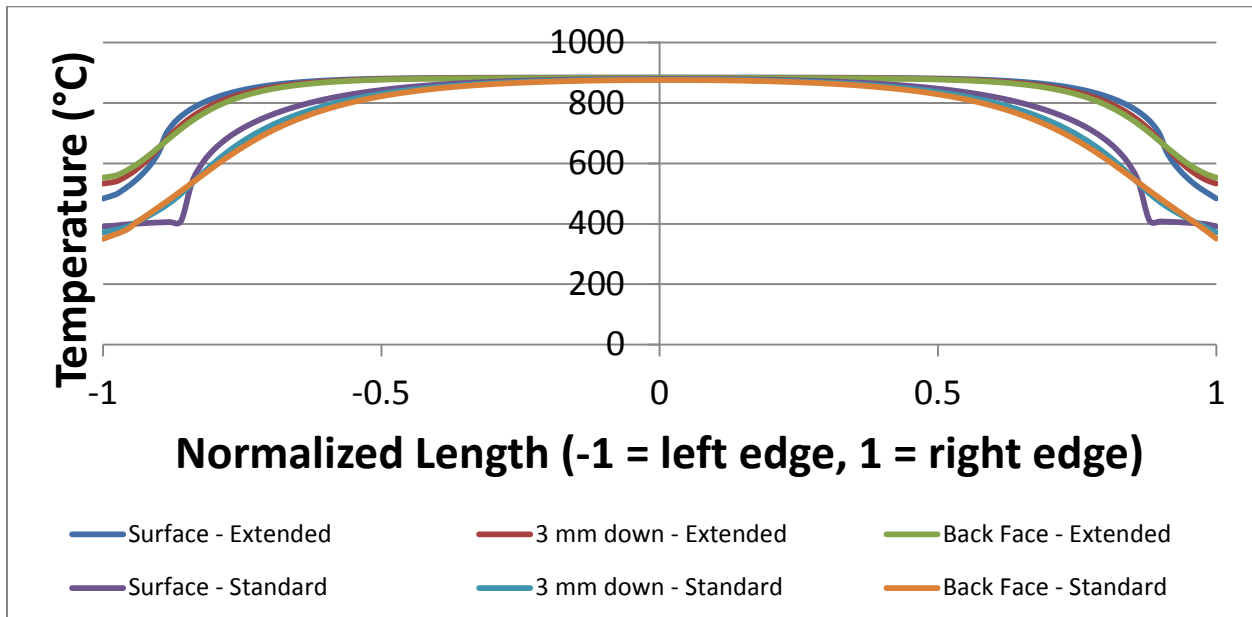
Figure 5: Temperature Profiles at 50 kW/m^2 IHF (Standard and Extended Size)

4.4.3 Cone Testing Procedure

The hope of the team was to confirm the similarity in sample size though actual ASTM E1354 testing. The team received five different specimens from Kreysler and Associates and Creative Pultrusions in the standard and extended specimen sizes. These specimens were tested in the standard Cone calorimeter apparatus in the WPI Fire Lab. Three specimen configurations were tested and the procedure for each configuration can be found in Chapter 4.4.3.1, 4.4.3.2, and 4.4.3.3.

4.4.3.1 100mm by 100mm Testing - Standard Configuration

The standard size specimens were tested in the Cone using standard operating procedures specified in the ASTM E1354 test standard. The individual samples were wrapped in aluminum foil and housed in an edge frame. Table 1 shows the specimens tested and the incident heat flux (IHF) each were exposed to. In general, two samples of each specimen were tested at three IHF's.

Table 1: Cone Specimens Tested

Specimen	Incident Heat Flux Tested		
Kreysler 1 - A	25 kW/m^2	50 kW/m^2	75 kW/m^2
Kreysler 1 - B	25 kW/m^2	50 kW/m^2	75 kW/m^2
Kreysler 2 - A	25 kW/m^2	50 kW/m^2	75 kW/m^2
Kreysler 2 - B	25 kW/m^2	50 kW/m^2	75 kW/m^2
CP 286 - A	25 kW/m^2	50 kW/m^2	75 kW/m^2
CP 286 - B	25 kW/m^2	50 kW/m^2	75 kW/m^2
CP 702 - A	25 kW/m^2	50 kW/m^2	75 kW/m^2
CP 702 - B	25 kW/m^2	50 kW/m^2	75 kW/m^2
CP 802 - A	25 kW/m^2	50 kW/m^2	75 kW/m^2
CP 802 - B	25 kW/m^2	50 kW/m^2	75 kW/m^2

During testing, the time when the specimen began edge burning was noted. The results of testing, such as HRRPUA, time to ignition, and time when edge burning began, can be seen in Appendix 5.9.

4.4.3.2 100mm by 100mm Testing - No Edge Frame

This configuration consists of a standard size specimen wrapped in aluminum foil placed on the standard burning pedestal with no edge frame covering the sample. The steel frame was omitted from this testing configuration to prevent what is assumed to be additional heating that the edge frame would cause, while also allowing the tester to verify visually when edge burning is occurring. The same specimens were tested as in Table 1 but only at an IHF of 50kW/m^2. HRRPUA curves can be found in Appendix 5.9 for this testing. Further analysis was not performed for these samples based on the fact that the results obtained from testing at an incident heat flux of 50kW/m^2 did not better provide an indication of edge burning over the standard testing configuration utilizing the edge frame.

4.4.3.3 175mm by 175mm Testing

The extended specimens were tested using the standard Cone calorimeter with a few adjustments. The Cone's outer protective box was sealed with aluminum foil to ensure produced smoke did not escape to the environment outside of the collection hood. A picture of the Cone with its adjustments can be seen in below.

Figure 6: Cone Calorimeter Adjustments for 175mm by 175mm Specimen

The specimen was placed on an extended frame with no edge frame surrounding the specimen. The specimen was exposed to a constant heat flux and allowed to burn until it was deemed "unsafe" for testing, due to its large flame impinging on the Cone's sensitive equipment, upon which time the specimens was extinguished. The specimen was never extinguished before edge burning began so extinguishment did not have an effect on data analyzed. The specimens that were tested were the same ones tested for the standard configuration specimen testing see Table 1. Again, the time when the specimen began edge burning was noted during testing.

After the specimen was extinguished and allowed to cool, the burn diameter was measured. Figure 7 shows an extended specimen post-burn, where the red lines indicate how the burn diameter was measured. The burn diameter was used to solve for the entire burn area, which allowed for the HRRPUA to be determined.
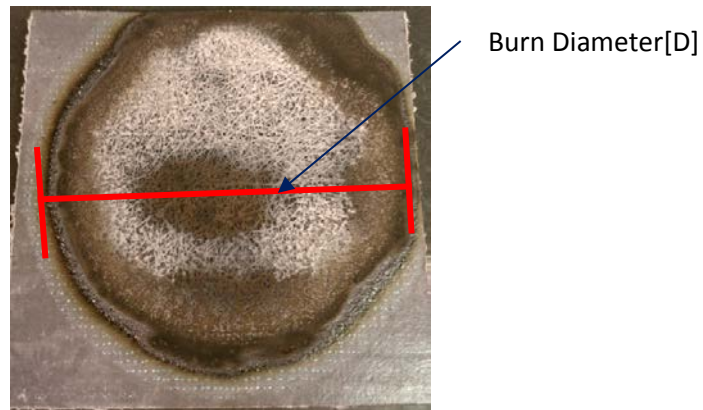
Burn Diameter[D]

Figure 7: Burn Diameter Diagram of extended sample.

The results of testing, such as HRR per unit area, time to ignition, and time when edge burning begins, can be seen in Appendix 5.8.

4.4.4 ASTM E1354 Test Specimen Comparison

From Cone testing of specimens, the time to ignition was analyzed along with a few subsets of the HRRPUA truncated based on the determination of when edge burning occurred. Truncation was performed due to the fact that at this moment when edge burning occurs, the Cone is no longer burning in one dimension and testing is no longer valid. Along with time to ignition, the average HRRPUA of the truncated data for several time intervals (Ignition to 30s, Ignition to 60s, Ignition to 90s, Ignition to 120s), was compared between samples of the same specimen (material, size configuration, and IHF). Additionally, standard and extended specimens of the same material and IHF were compared. The specimens were compared to ensure the difference in these values addressed between the same specimens was insignificant as defines in the following sections.

4.4.4.1 Statistical Comparison

The time to ignition and average HRRPUA over several time intervals (Ignition to 30s, Ignition to 60s, Ignition to 90s, Ignition to 120s) were compared for the two samples of each specimen tested at the same IHF. The percent difference between the two samples tested was calculated which gives a difference in testing a specimen i.e. the time to ignition for a 100mm by 100mm Kreysler 1 at 25kW/m^2 yielded a percent difference of 18% between Sample 1 and 2. This procedure was completed for all standard and extended size specimens at each IHF tested. Equations and sample calculations can be found for this in Appendix 5.6. The values for percent difference here indicate a difference between samples for a specimen size, shown for both standard specimens and again for extended specimens.

The percent difference between the specimen sizes was also calculated using an average of the value of time to ignition or average HRRPUA for the same time interval to calculate a percent difference between the sizes themselves. Equations and sample calculations can be found for this in Appendix 5.6. For example, the percent difference between a 100mm by 100mm and 175mm by 175 mm specimen tested at 25kW/m^2 for the average time to ignition value was 35%. The values for percent difference here indicate a percent difference between specimen sizes in the Cone.

To compare the difference within a sample size and the difference between the specimen sizes, the root square sum (RSS) of the difference within a standard sample and extended sample was calculated. Equations and sample calculations can be found for this in Appendix 5.6. This RSS value created a population of differences

expected between Cone samples during testing, where the average difference was found along with a standard deviation. The difference between specimen sizes was compared to this average value plus or minus a standard deviation. If the percent difference between specimen sizes did not exceeded the average RSS value plus a standard deviation, the difference between specimen sizes was considered to be an insignificant difference for that specific value being analyzed. The lower range was determined unimportant because it simply indicated more insignificance as this just indicated a decrease in difference.

4.4.4.2 Heat Release Rate per Unit Area (HRRPUA) Difference Plot Comparison

The difference between the HRRPUA of the standard and extended samples was graphed along with both specimen size ignition times at the incident heat fluxes of 25 kW/m^2, 50 kW/m^2 and 75 kW/m^2 for the Kreysler specimens and 50 kW/m^2 and 75 kW/m^2 for the Creative Pultrusion specimens. The finals graphs can be viewed in Appendix 5.5. Next the uncertainties were calculated for the time to ignition and HRRPUA. This included the use of both inter-(r) and intra-(R) laboratory uncertainties that were found in the ASTM E1354. Inter-Laboratory uncertainty refers to the uncertainty allowable between two tests completed within the same lab and Intra-Laboratory uncertainty refers to the allowable uncertainty between two identical tests completed at different laboratories.5.3 The average 'r' and 'R' values obtained for the entire test for time to ignition were calculated using the corresponding equations found in Appendix 5.7. The results demonstrate the repeatability factor when obtaining time to ignition for both the standard size and extended size samples. The repeatability diminishes as the incident heat flux increases, which in turn proves that the results would be difficult to duplicate. The average repeatability factors were also calculated for the HRRPUA. The calculated values were roughly the same for every incident heat flux and provide a range that is very large compared to the lowest and highest points on the graph. In this case, the tests are repeatable, and will help prove statistically that there is not a significant difference in testing the two sample sizes.

4.4.5   Result of Comparing Tested Specimens

At the conclusion of the statistical and temperature profile comparison, it has been determined that specimen sizes are not significantly different and can be tested in place of one another. Through in-depth statistical analysis it quickly became clear that the variation between Cone samples and between specimens sizes was quite similar, indicating no significant difference between sample sizes. Appendix 5.6 shows calculations for results in Table 2. This table displays highlights cells red when the specific value is significantly different between specimen sizes. As shown in Table 2, very few specimens tested at one of the IHF's showed significant differences defined as at as a difference between specimen sizes results that exceeded one standard deviation of the average RSS value (the difference within a sample size). This confirms the fact that statistically, there is no difference between the two specimen sizes.

Table 2: Significant Difference Chart between Specimen Sizes for Multiple Variables

	Difference between Samples Size (Average Time to Ignition)	Difference between Samples Size (Average HRRPUA Ignition - 30s)	Difference between Samples Size (Average HRRPUA Ignition - 60s)	Difference between Samples Size (Average HRRPUA Ignition - 90s)	Difference between Samples Size (Average HRRPUA Ignition - 120s)
Kreysler 1 - 25 kW/m^2	34%	29%	26%	18%	21%
Kreysler 2 - 25 kW/m^2	55%	46%	48%	33%	15%
Kreysler 1 - 50 kW/m^2	23%	21%	3%	5%	9%
Kresyler 2 - 50 kW/m^2	7%	3%	0%	4%	5%
Kreysler 1 - 75 kW/m^2	29%	7%	32%	52%	61%
Kreysler 2 - 75 kW/m^2	18%	3%	20%	40%	62%
CP 286 - 25 kW/m^2	31%	25%	18%	15%	31%
CP 702 - 25 kW/m^2	34%	16%	34%	46%	54%
CP 802 - 25 kW/m^2	12%	42%	33%	29%	25%
CP 286 - 50 kW/m^2	17%	6%	10%	42%	65%
CP 702 - 50 kW/m^2	11%	5%	12%	16%	17%
CP 802 - 50 kW/m^2	23%	2%	13%	20%	24%
CP 286 - 75 kW/m^2	13%	7%	2%	1%	26%
CP 702 - 75 kW/m^2	10%	19%	10%	7%	17%
CP 802 - 75 kW/m^2	61%	8%	15%	19%	8%
Average RSS	21%	16%	20%	27%	36%
Standard Deviation RSS	14%	12%	17%	31%	40%

4.5 Flame Length Screening Tool

For this correlation it was necessary to determine the type of flame spread that is occurring in the tunnel test. For this model the idea of static concurrent flame lengths was used. This means that the pyrolysis zone (burn area) does not change as the specimen burns and the flame is extending in the direction in which the air is moving. These assumptions are valid for this correlation because limited pyrolysis movement is a characteristic of specimens with a flame spread rating of less than 25 which is the classification of materials in which this correlation will be created for and there is an imposed air flow in the tunnel test as specified in ASTM E84 of 1.25 m/s in the direction in which the flame propagates[2]. After determining these two assumptions it was then possible to create a governing equation to predict a flame length of the specimen in the tunnel test given Heat Release Rate data that was collected in the ASTM E1354 cone calorimeter test.

4.5.1 Governing Equation

To create a correlation between data collected in the ASTM E1354 cone calorimeter test and the ASTM E84 tunnel test it was necessary to determine a governing equation that could be adjusted utilizing specimens in which the flame lengths in the tunnel test were known. For some pre-existing correlations to adapt we referred to such scientists as Newman[13], Consalvi[14], Drysdale[15], Quintiere[16], Hasemi[17], and King-Mon-Tu[18]. To create a governing equation the assumption that the heat release rate of the specimen and burners in the tunnel test could be distilled into a point source line fire was used. This equation also needed to account for a point source that would move as the specimen began burning in the tunnel test. This has led to the creating of the governing equation that can be seen below.

$$L_{f=}(\beta + \gamma) * \dot{Q}'^n$$

2

Beta is a constant that was found to create a flame length of 4.5 feet when just the burners are on. Gama is a constant that was found to add in when the specimen begins to burn utilizing an ignition delay time that is found in the cone calorimeter. Q' is found as the heat release per unit width of the specimen and the burners. And the

value of n will be adjusted utilizing known flame lengths in the tunnel test. For further information on the governing equation refer to Appendix 5.10.

4.5.2   ASTM E1354 Cone Calorimeter Test Procedure

To create an optimal correlation model it was necessary to represent the conditions of the tunnel test while collecting data in the ASTM E1354 cone calorimeter. The insult heat flux on the specimen burn area in the tunnel test has been found by William Parker to change as the distance from the burner increases and as the time into the test increases[19]. Figure 8 shows the simplified imposed heat flux over time and distance of the three respective areas of the Tunnel as shown in Figure 2. This was then simplified into three time dependent IHF curves corresponding to their respective areas in the tunnel. See Figure 9 below.
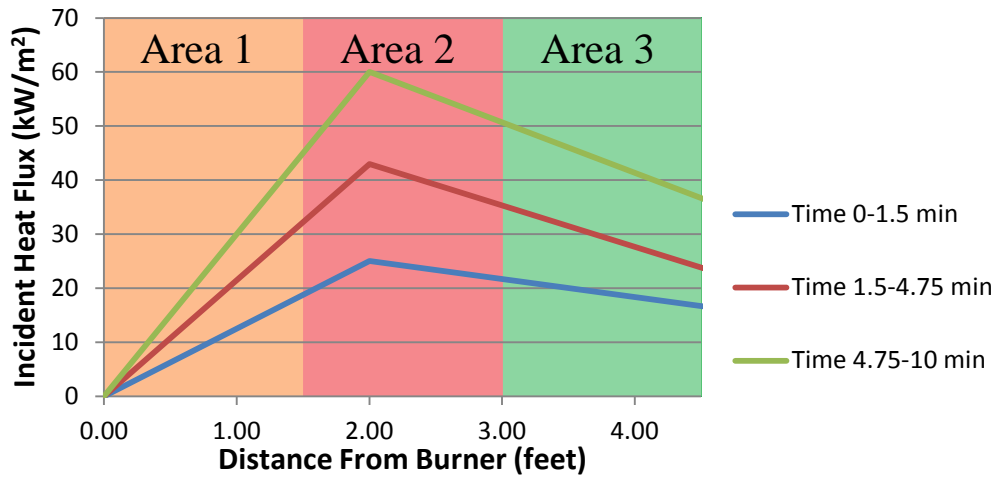
Figure 8: Incident Heat Flux over the First 4.5 Feet for 3 Time Segments
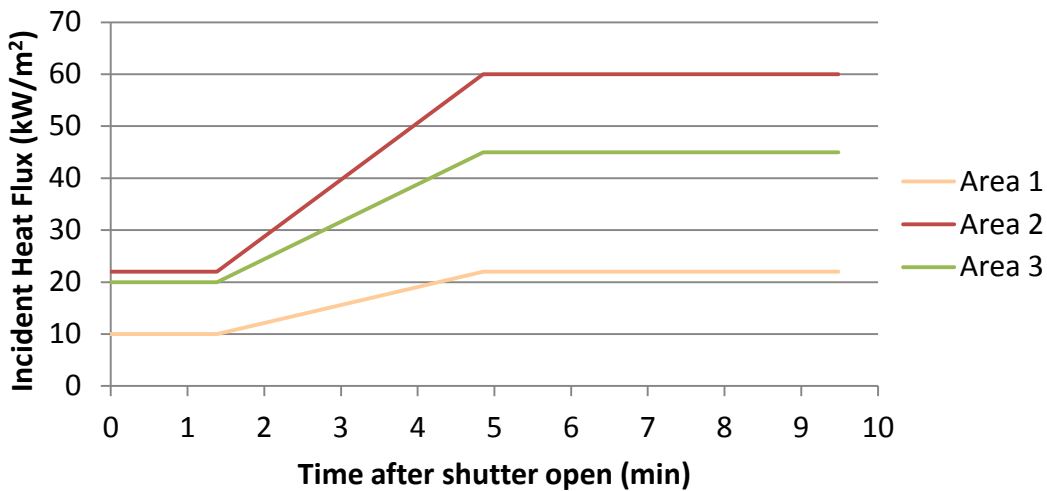
Figure 9: Incident Heat Flux over Time for the 3 Burn Areas

These three simplified imposed incident heat flux curves in the Tunnel were then used in the Cone to test each specimen. To collect the data in the ASTM E1354 cone calorimeter it is necessary to run two samples of each specimen at each of the three incident heat flux time dependent curves that are shown in Figure 9,

resulting in a total of six data sets. For more information pertaining to testing the specimen in the Cone refer to Appendix 5.10 under the ASTM 1354 Test Procedure section.

4.5.3   Creating Composite Heat Release Rate

In order to use the data collected from the cone calorimeter, a composite heat release rate per unit width per time curve that will be used in the correlation was created. To do this first the heat release rate per unit areas of the two samples run at each of the three incident heat flux curves must be averaged. This must be completed for each second of all three of the incident heat flux curves for a total of three average heat release rates per unit area curves for each specimen that was run in the test. This creates three different heat release rate per unit area curves, one for each of the three areas in the 4.5 foot (1.4 meter) distance. After this was completed the heat release rate per unit area must be converted into a heat release rate. This was done by multiplying each heat release rate curve that was created by the area of one third of the first 4.5 foot (1.4 meter) section of the curve. This is because each heat release rate per unit area curve is only applied to the section of the burn area that is affected by that incident heat flux. After converting each curve for each area to a heat release rate they must be added together in order to create a total heat release rate for the first 4.5 feet (1.4 meters) of the tunnel. This heat release rate must be converted to a heat release rate per unit width. In the case of the Tunnel, the width is 17 inches. This was converted to meters and divided the total heat release rate in order to arrive at a heat release rate per unit width.

These calculations are to be completed at each second for the first 600 seconds after shutter open in order to create a total composite heat release rate per unit width over time. Below in Figure 10 the calculation of the total composite heat release rate can be seen. Area 1, 2, and 3 correspond to the heat release rate data collected from the Cone when running each of the three time dependent incident heat flux curves shown in Figure 9. The total composite heat release rate shows the results when completing the calculations completed above.
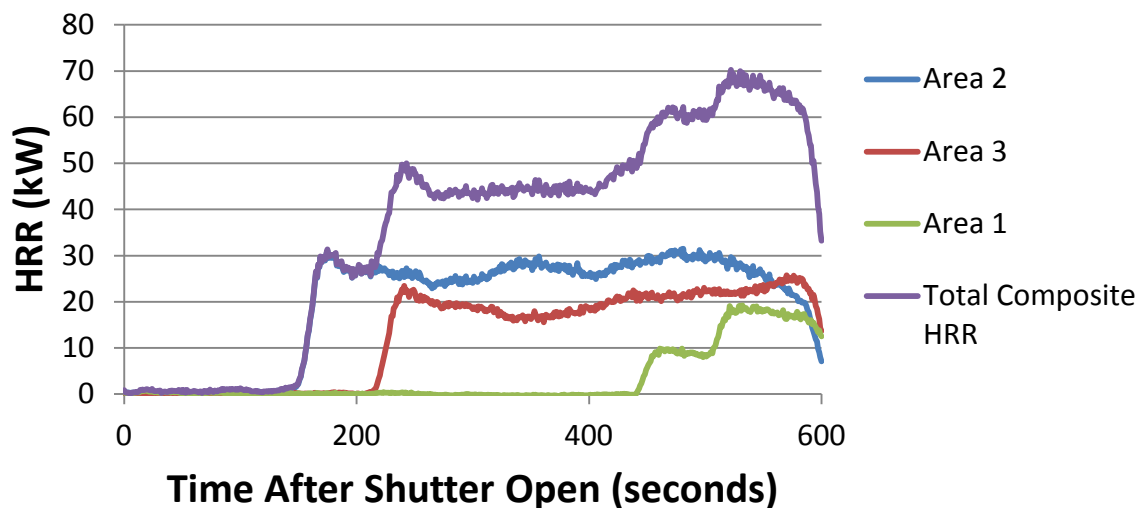
Figure 10: Composite Heat Release Rate for CP 286

This heat release rate per unit width over time curve will then be used in the correlation to determine the flame length in the tunnel test. For sample calculations refer to Appendix 5.10 under the Composite Heat Release Rate Calculations section.

4.5.4 Ignition Delay

In order for this correlation to best represent the conditions in the tunnel test, an ignition delay was utilized to determine when to start calculating the flame extension of the specimen. Through statistical analysis it was found that the best representation of a time to ignition in the tunnel test was found as the time to ignition of the specimen when testing in the cone calorimeter at an incident heat flux of 40 kW/m^2. This time identifies when to begin calculating a flame extension in the tunnel test. For simplicity a flame extension of zero feet will be inserted for all times less than the time to ignition found when testing the specimen at 40 kW/m^2. For more information pertaining to the ignition delay refer to Appendix 5.10 under the Ignition Delay section.

4.5.5 Final Correlation

Utilizing tunnel test results and cone calorimeter data for Kreysler 1, CP 286, FSI 0.75, and FXE 0.090 a final correlation between the ASTM E84 tunnel test and ASTM E1354 cone calorimeter test was found. Kreysler 1 had a proprietary Kastone coating and the other three did not have any coating. In order to account for the different burning characteristics of these two types of fiberglass reinforced polymers, two different correlations were created. These correlations can be seen below as Equation 3 and Equation 4. For each equation the calculated composite heat release rate per time is used as Q for each second to calculate a flame length at each of the 600 seconds of the test.

Proprietary Kastone Coating Correlation:
$$L_{f=} \left((0.2211) * (Q' + \dot{}204)^{0.6709} \right) - 4.5 \tag{3}$$

Non-Coated FRP Correlation:
$$L_{f=} \left((0.1647) * (Q' + \dot{}204)^{0.6709} \right) - 4.5 \tag{4}$$

Apply a flame extension of zero feet for all time before ignition as predicted from testing the specimen in an ASTM E1354 Cone Calorimeter at an incident heat flux of 40 kW/m²

$$L_f \text{ is Flame Extension in Tunnel Test } (ft)$$

$$\dot{Q}' \text{ is the composite heat release rate per unit width of the specimen } \left(\frac{kW}{m} \right)$$

These correlations were used to calculate the flame length vs. time in the Tunnel test of each of the four specimens. This information was then used to calculate the Flame Spread Index by calculating the area under the curve and multiplying it by a constant of .515 as specified in ASTM E84. This calculated FSI was then compared to the known values found in the Tunnel Test. Due to the fact that there was only one specimen with a Proprietary Kastone Coating and available Tunnel Test data, the percent error was zero. The percent error of the correlation for the three specimens without a coating can be seen below in Table 3. For more information pertaining to calculating the Flame Spread Index, refer to Appendix 5.10 under the Comparison section.

Table 3: Percent Error for Non-Coated Composite HRR Correlation

	FSI Calculated from Correlation	Known FSI from Tunnel Test	Percent Error between Known and Calculated	
CP 286	13.7	16.0	14.4	
FSI .075	16.0	13.7	17.1	
FXE .090	14.4	14.4	0.3	
			10.6	Average Percent Error

This correlation proves to be extremely accurate when calculating the FSI of the specimen in the tunnel test with an average error of 10.6 percent. The calculated flame extension and known flame extension of CP 286 used to calculate the FSI above can be seen below in Figure 11.
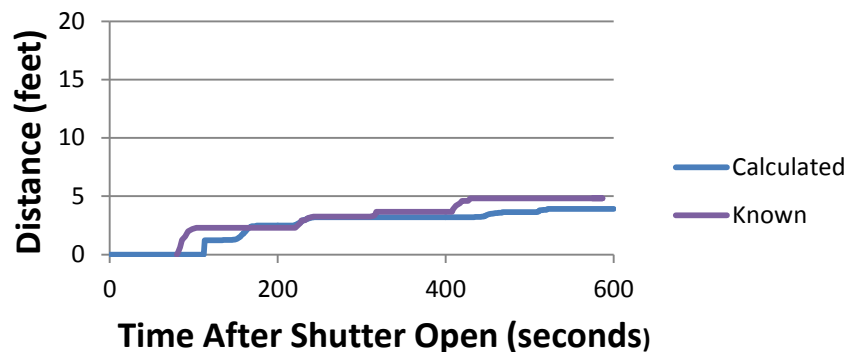
Figure 11: Calculated Flame Length Extension vs. Known of CP 286

For more information on the composite heat release rate correlation refer to Appendix 5.10 under the Final Adjustments to Model section.

4.5.6 Single Incident Heat Flux Correlation

For most manufacturers who want to get an idea of how their material will perform in the tunnel test, performing seven different tests may prove to be more than necessary. To reduce the amount of testing needed in the cone calorimeter a second set of equations was created to predict the flame extension in the Tunnel of a specimen only utilizing heat release rate per unit area per time data that is collected in the cone calorimeter at an incident heat flux of 40 kW/m^2. The heat release per unit area is then put into the correlation and a flame length is calculated utilizing the equation for each second of the 600 second test. These equations can be seen below.

Proprietary Kastone Coating Correlation:
$$L_{f=} \left((0.2322) * (\frac{(Q * .6\dot{0}) + 88}{.43})^{0.6494} \right) - 4.5 \qquad \text{5}$$

Non-Coated FRP Correlation:
$$L_{f=} \left((0.1574) * (\frac{(Q * .6\dot{0}) + 88}{.43})^{0.6494} \right) - 4.5 \qquad \text{6}$$

Apply a flame extension of zero feet for all time before ignition as predicted from testing the specimen in an ASTM E1354 Cone Calorimeter at an incident heat flux of 40 kW/m2

$$L_f \text{ is Flame Extension in Tunnel Test } (ft)$$

$$\dot{Q} \text{ is the heat release per unit area retrieved from testing the specimen in the Cone at an IHF } (\frac{kW}{m^2})$$

This method proves to be much easier than calculating the composite heat release of the specimen, but in return there is a loss of accuracy in the model. The calculated percent error of the calculated FSI versus the Know FSI in the Tunnel can be seen below in Table 4.

Table 4: Percent Error for Non-Coated Single IHF Correlation

	FSI Calculated from Correlation	Known FSI from Tunnel Test	Percent Error between Known and Calculated
CP 286	11.8	16.0	26.5
FSI .075	18.5	13.7	35.4
FXE .090	16.2	14.4	12.7

	Average Percent Error
24.9	

This correlation is not as accurate as the composite heat release rate model, but it still gives a calculated flame spread index that is close enough to give the manufacturer an idea of how well their material will perform. The calculated flame extension in the Tunnel and known flame extension in the Tunnel of CP 286 can be seen below in Figure 12.
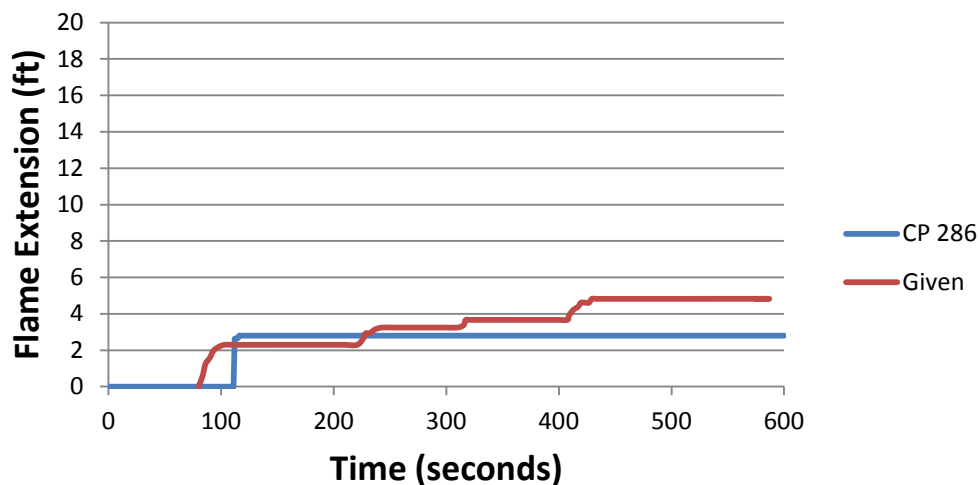
Figure 12: Calculated Flame Length Extension vs. Known of CP 286

For more information on the single incident heat flux model refer to Appendix 5.10.

4.5.7   Ability to Pass ASTM E84 Quick Screen

Now that there is a correlation to relate the heat release rate of a specimen when tested in the ASTM E1354 Cone Calorimeter and a constant incident heat $40 \frac{kW}{m^2}$ a way to quick screen a material based upon both the peak heat release rate and the ignition temperature can be created. This quick screen will show the maximum peak heat release rate for each time to ignition in order to receive a flame spread index of 25 or below. In order to do this the assumption is made that as soon as the specimen ignites it reaches its peak heat release rate. Our correlation was created utilizing specimens with time to ignitions of 100 seconds, because of this our quick screen can only sensibly correlate peak heat release rates for time to ignitions up to 300 seconds. This information was then used to create proposed requirements for The International Building Code. For more information refer to section 4.6.

4.6 International Building Code Proposed Changes

The current 2012 edition of the International Building Code (IBC) indicates the following requirements regarding interior wall and ceiling finish materials.

Interior wall and ceiling finish materials shall be classified in accordance with ASTM E 84 (Tunnel test) or UL 723. Such interior finish materials shall be grouped in the following classes in accordance with their flame spread and smoke-developed indexes.

Class A:=Flame spread index 0-25; smoke-developed index 0-450.
Class B:=Flame spread index 26-75; smoke-developed index 0-450.
Class C:=Flame spread index 76-200; smoke-developed index 0-450.[1]

Table 803.9 of the IBC then states where these specific materials are permitted based on classification.

The team proposes changes to this section's code language where results of a cone calorimeter ASTM E1354 test will govern the material classification, which will again govern its use. The new proposed language is applicable to only the materials classified as "Class A" materials. The new code language is as follows:

Kastone coated FRPs with a time to ignition and a HRR per unit area corresponding to a value that falls below the curve in Figure 13, shall be considered a Class A material.
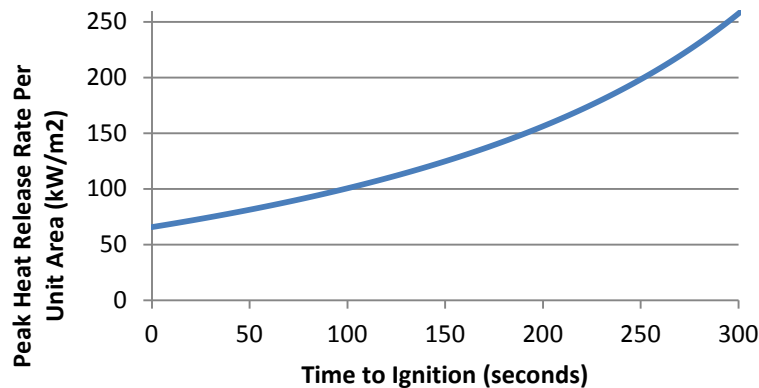
Figure 13: Peak HRR per unit area versus Time to Ignition to Receive FSI of 25 for Proprietary Kastone Coated FRPs

Additionally,

Non-coated FRPs with a time to ignition and a HRR per unit area corresponding to a value that falls below the curve in Figure 14, shall be considered a Class A material.
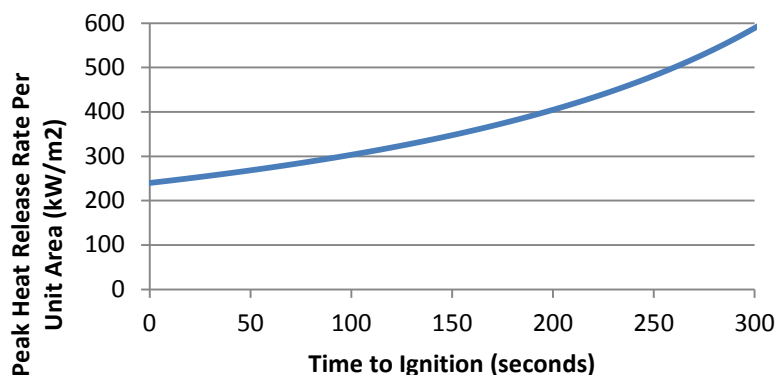
Figure 14: Peak HRR per unit area versus Time to Ignition to Receive FSI of 25 for Non-coated FRPs

The curves in Figure 13 and Figure 14 were determined by using the flame length model created in this study. In the future the same procedure can be used to determine the time to ignition and HRR per unit area requirements for a Class B and Class C material. The usefulness of this new code requirement is the ability to test a material relatively quickly and inexpensively than the ASTM E84 tunnel test.

4.7 Conclusions

The cone calorimeter suffers from the fundamental notion of edge burning when testing samples, specifically FRP samples, which skews test results. The ASTM E1354 test is only valid when the specimen is burning on the top face only. Through analysis of theoretical data and experimental data, analyzed statistically, it was determined that the specimen size does not significantly affect results. This means that a technician can now test an extended sample if edge burning will be an issue during testing when proper cone calorimeter adjustments are made. The extended samples allow for better notification of edge burning which will lead to more accurate testing.

Two sets of equations to predict the flame extension down an ASTM E84 Tunnel Test have been created. One set of equations requires testing the specimen at three different incident heat flux steps. The resulting heat release rate per unit area must then be converted to a heat release rate by multiplying by the area of each section. These three heat release rate curves must be added. After that is completed the heat release rate must be converted to a heat release rate per unit width by dividing the rate by the width of the tunnel. Finally in order to calculate the distance the flame traveled down the tunnel, insert the heat release rate into the respective equation depending if the FRP has a Proprietary Kastone Coating or not and apply a flame extension of zero feet for all time before ignition as predicted from testing the specimen in an ASTM E1354 Cone Calorimeter at an incident heat flux of $40 \frac{kW}{m^2}$.

The next set of equations that were created utilize heat release rate data collected from running a sample at a single incident heat flux in the ASTM E1354 Cone Calorimeter. As before apply a flame extension of zero feet for all time before ignition as predicted from testing the specimen in an ASTM E1354 Cone Calorimeter at an incident heat flux of $40 \frac{kW}{m^2}$. Both of these sets of equations create a flame length versus time graph. The flame spread index of the material can then be calculated by determining the area under the curve and multiplying it by a constant of .515.

From this information a quick screen to determine the feasibility of receiving a FSI of 25 or less was created based upon the peak heat release rate and time to ignition of a specimen when tested in the cone calorimeter at an incident heat flux of 40 kW/m^2. These three methods will prove to be a great asset for Fiberglass Reinforced Polymer manufacturers because now they can prescreen their materials before sending them to be tested in the ASTM-E84 Tunnel Test.

4.8 References

[1] "Wall and Ceiling Finishes."*2012 International Building Code*. Country Club Hills, IL: ICC, Inc., 2011. 803.

[2] ASTM Standard E84,2012, "Standard Test Method for Surface Burning Characteristics of Building Materials," ASTM International, West Conshohocken, PA, 2012 DOI : 10.1520/E0084-12A, www.astm.org.

[3] ASTM Standard E1354, 2003, "Standard Test Method for Heat and Visible Smoke Release Rates for Materials and Products Using an Oxygen Consumption Calorimeter," ASTM International, West Conshohocken, PA, 2011, DOI: 10.1520/E1354-11B, www.astm.org.

[4] "Fire Testing Technology - Cone Calorimeter." *Fire Testing Technology*. Fire Testing Technology Ltd., n.d. Web. 19 Apr. 2013. <http://www.fire-testing.com/cone-calorimeter-dual>

[5] Babrauskas, Dr. Vytenis. "Ten Years of Heat Release Research with the Cone Calorimeter ." Fire Science and Technology Inc. N.p., n.d. Web. 1 Apr. 2013. <http://www.doctorfire.com/cone.html>.

[6] Babrauskas, Vytenis , William Twilley, and William Parker. "Effects of Specimen Edge Conditions on Heat Release Rate." *Fire and Materials* Mar. - Apr. 1993: 51-63.

[7] Nussbaum, Ralph, and Birgit Ostman. "Larger specimens for determining rate of heat release in the cone calorimeter." *Fire and Materials* Sep. 1986: 151-160.

[8]"International Codes-Adoption by State." *ICC Safe*. ICC, Inc., n.d. Web. 1 Apr. 2013. <www.iccsafe.org/gr/Documents/stateadoptions.pdf>.

[9] "Scope." *2012 International Building Code*. Country Club Hills, IL: ICC, Inc., 2011. 101.2.

[10] Ricciardi, Maria, Vincenza Antonucci, Michelle Giordano, and Mauro Zarrelli. "Thermal Decomposition and Fire Behavior of Glass Fiber-reinforced Polyester Resin Composites Containing Phosphate-based Fire-retardant Additives." *Journal of Fire Sciences* 2012.30 (2012): 318-30.

[11] Carslaw, H. S., and J. C. Jaeger. *Conduction of heat in solids*. 2d ed. Oxford: Clarendon Press, 1959.

[12] Janssens, Marc. "Improved Method for Analyzing Ignition Data from the Cone Calorimeter in the Vertical Orientation." *International Association for Fire Safety Science.*

[13] Jeffrey S Newman, Christopher J Wieczorek, Chemical flame heights, Fire Safety Journal, Volume 39, Issue 5, July 2004, Pages 375-382, ISSN 0379-7112, 10.1016/j.firesaf.2004.02.003.

[14] J.L. Consalvi, Y. Pizzo, B. Porterie, J.L. Torero, On the flame height definition for upward flame spread, Fire Safety Journal, Volume 42, Issue 5, July 2007, Pages 384-392, ISSN 0379-7112, 10.1016/j.firesaf.2006.12.008.

[15] Chung Tsai, K.-. and Drysdale, D. (2002), Flame height correlation and upward flame spread modeling. Fire Mater., 26: 279–287. doi: 10.1002/fam.809

[16] Grove, Brian, and James Quintiere. "Calculating Entrainment and Flame Height in Fire Plumes of Axisymmetric and Infinite Line Geometries. Linear and axisymmetric fires." Journal of Fire Protection Engineering 12 (2002): 117-137. Print

[17] Hasemi, Y., 1986. Thermal Modeling Of Upward Wall Flame Spread. Fire Safety Science 1: 87-96. doi:10.3801/IAFSS.FSS.1-87

[18] Tu, King-Mon (08/01/1991). "Wall flame heights with external radiation". *Fire technology (0015-2684)*, 27 (3), p. 195

[19] Parker, William. "An Investigation of the Fire Environment in the ASTM E 84 Tunnel Test." National Bureau of Standards technical note 945 (1977): 28. Print.

5. Appendices

5.1 Appendix - International Building Code

Primary Author: William Wright

Secondary Author: Nicholas Nava

Past experiences have shown that two key factors in flame-propagation are a building's interior finish and its decorative materials. In order to limit the development and spread of fire, the International Building Code (IBC) requires the materials used as interior finishes and decorations to meet specific flame-spread index criteria. Performance of these materials is evaluated based on test standards.

Flame-spread index (FSI) is a comparative measure, derived from data acquired in the ASTM E84 Tunnel test. The FSI is essentially a measurement of the area under the curve of the graph of spread of fire across tested material's surface versus time. The units of FSI are dimensionless, and given by Equation 7:

$$FSI = 0.515 \times A_T \hspace{4cm} 7$$

where,

A_T = Calculated Area (Integral of Distance vs. Time)[1]

An example of a flame spread curve is shown in Figure 15 where A = A1 + A2 indicating that the flame front is not allowed to recede when determining FSI.
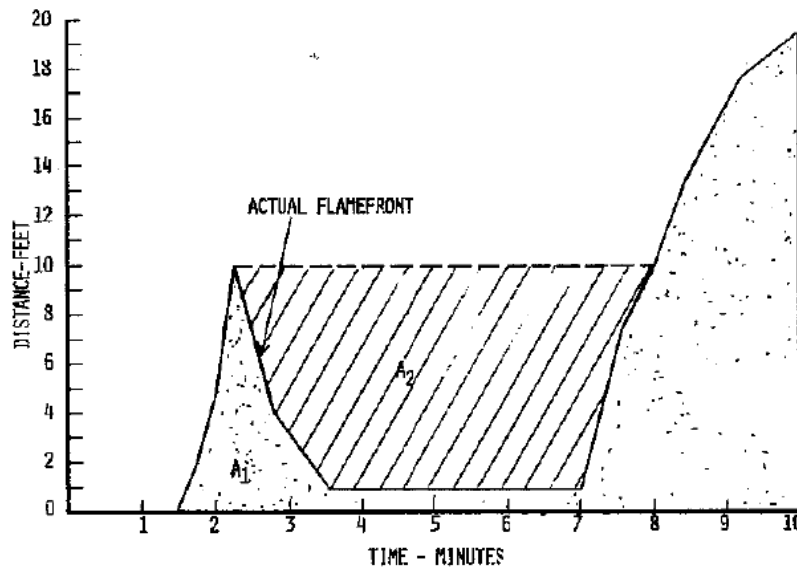
Figure 15: Flame Front Distance vs. Time Example

Interior wall and ceiling finish materials are divided into three classes based on their FSI and smoke developed index. The material classification is as follows:

Class A: Flame-spread index 0-25; smoke-developed index 0-450

Class B: Flame-spread index 26-75; smoke-developed index 0-450

Class C: Flame-spread index 76-200; smoke-developed index 0-450.[2]

In order to be used in certain location, Table 803.9 of the IBC shall be examined. It gives the minimum classification that shall be required is based on occupancy classification, sprinklered/non sprinklered, and location in the building. See Figure 16 for material classification requirements.

TABLE 803.9
INTERIOR WALL AND CEILING FINISH REQUIREMENTS BY OCCUPANCY[a]

GROUP	SPRINKLERED[l]			NONSPRINKLERED		
	Exit enclosures and exit passageways[a, b]	Corridors	Rooms and enclosed spaces[c]	Exit enclosures and exit passageways[a, b]	Corridors	Rooms and enclosed spaces[c]
A-1 & A-2	B	B	C	A	Ad	Be
A-3[f], A-4, A-5	B	B	C	A	Ad	C
B, E, M, R-1	B	C	C	A	B	C
R-4	B	C	C	A	B	B
F	C	C	C	B	C	C
H	B	B	Cg	A	A	B
I-1	B	C	C	A	B	B
I-2	B	B	Bh,i	A	A	B
I-3	A	Aj	C	A	A	B
I-4	B	B	Bh,i	A	A	B
R-2	C	C	C	B	B	C
R-3	C	C	C	C	C	C
S	C	C	C	B	B	C
U	No restrictions			No restrictions		

For SI: 1 inch = 25.4 mm, 1 square foot = 0.0929m².

a. Class C interior finish materials shall be permitted for wainscotting or paneling of not more than 1,000 square feet of applied surface area in the grade lobby where applied directly to a noncombustible base or over furring strips applied to a noncombustible base and fireblocked as required by Section 803.11.1.

b. In exit enclosures of buildings less than three stories above grade plane of other than Group I-3, Class B interior finish for nonsprinklered buildings and Class C interior finish for sprinklered buildings shall be permitted.

c. Requirements for rooms and enclosed spaces shall be based upon spaces enclosed by partitions. Where a fire-resistance rating is required for structural elements, the enclosing partitions shall extend from the floor to the ceiling. Partitions that do not comply with this shall be considered enclosing spaces and the rooms or spaces on both sides shall be considered one. In determining the applicable requirements for rooms and enclosed spaces, the specific occupancy thereof shall be the governing factor regardless of the group classification of the building or structure.

d. Lobby areas in Group A-1, A-2 and A-3 occupancies shall not be less than Class B materials.

e. Class C interior finish materials shall be permitted in places of assembly with an occupant load of 300 persons or less.

f. For places of religious worship, wood used for ornamental purposes, trusses, paneling or chancel furnishing shall be permitted.

g. Class B material is required where the building exceeds two stories.

h. Class C interior finish materials shall be permitted in administrative spaces.

i. Class C interior finish materials shall be permitted in rooms with a capacity of four persons or less.

j. Class B materials shall be permitted as wainscotting extending not more than 48 inches above the finished floor in corridors.

k. Finish materials as provided for in other sections of this code.

l. Applies when the exit enclosures, exit passageways, corridors or rooms and enclosed spaces are protected by an automatic sprinkler system installed in accordance with Section 903.3.1.1 or 903.3.1.2.

Figure 16: IBC Table 803.9 giving interior wall and ceiling finish requirements.

References

[1] ASTM Standard E84,2012, "Standard Test Method for Surface Burning Characteristics of Building Materials," ASTM International, West Conshohocken, PA, 2012 DOI : 10.1520/E0084-12A, www.astm.org.

[1] "Wall and Ceiling Finishes."*2012 International Building Code*. Country Club Hills, IL: ICC, Inc., 2011. 803.

5.2 Appendix – ASTM E84 Tunnel Test

Primary Author: Christian Acosta
Secondary Author: William Wright

5.2.1 ASTM –E84

This section describes ASTM-E84: *Standard Test Method for Surface Burning Characteristics of Building Materials.* This is a standard used in the manufacturing industry for comparative surface burning behaviors that applies for exposed surfaces such as walls and ceilings. The purpose of this test is to determine the relative burning behavior of a material by observation of the flame spread and data acquisition of smoke production for a sample. Results of this test provide classification of building materials relative to red oak and fiber cement boards.

5.2.2 Dimensions of Test Chamber

Width: 17 3⁄4 (+ or -) 1⁄4 in. (451 (+ or -) 6.3 mm) measured between the top ledges along the side walls, and 17 5⁄8 (+ or -) 3⁄8 in. (448 (+ or -) 10mm) at all other points.

Depth: 12 (+ or -) 1⁄2 in. (305 (+ or -) 13 mm) measured from the bottom of the test chamber to the top of the ledges on which the specimen is supported. This measurement includes the 1⁄8 in. (3.2 mm) thickness of the 1 1⁄2 in. (38 mm) wide woven fiberglass gasket tape.

Length: 25 ft. (+ or -) 3 in. (7.62 m (+ or -) 76 mm).
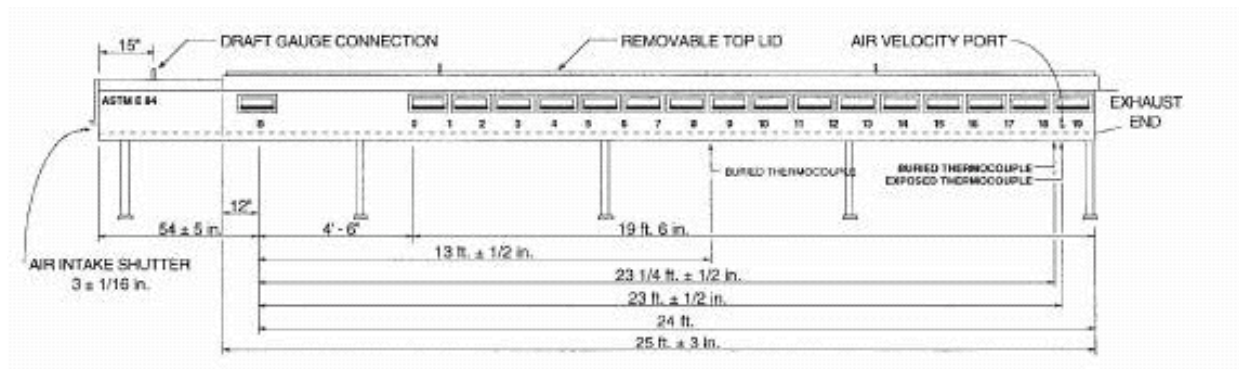
5.2.3 Testing Conditions

Testing calls for a specimen which must be 24ft long by 20 in wide. During testing, there is controlled air flow and a fire exposed to the specimen in order to create a flame along the entire length of it. The velocity of air within the tunnel is approximately 1.22 m/s. This fire end shall be provided with two gas burners delivering flames upward against the surface of the test sample. The fire rest chamber should be supplied with natural or methane gas fuel.

5.2.4   Testing Procedures

1. Place the test specimen on the test chamber ledges that have been covered completely with gasketing tape.
2. While the specimen is mounted in the chamber, have the furnace draft operating for 120s prior to the use of the test flame.
3. Ignite the gas burner; observe and record the distance and time of maximum flame front travel. -Continue the test for 10 minutes and only conclude the test prior of the time when the specimen is completely consumed in the fire area.
4. Record the photoelectric prior to testing and every 2s during the test.
5. Record the gas pressure, the pressure differential across the orifice plate, and the volume of gas used in each test.
   Plot the flame spread distance, temperature, and change in photoelectric cell readings for the duration of the test for use in determining the flame-spread and smoke-developed indexes as outlined in Section 9. Flame front advancement shall be recorded at the time of occurrence or at least every 30 s if no advancement is noted. Flame spread distance shall be determined as the observed distance minus 4½ ft. (1.37 m).

5.2.5   Specimen Classifications

After testing is completed in the tunnel, the recorded distance of flame spread versus the 10 minute duration is plotted. In order to determine the classification of the specimen tested, the area under the curve is then calculated. If the total area under the curve is less than or equal to 97.5, the area is multiplied by .515 to obtain the flame spread index (FSI). FSI = 0.515 *AT. If the total area is greater than 97.5 the FSI is calculated as 4900/(195-AT).

5.2.6   References

ASTM Standard E84,2012, "Standard Test Method for Surface Burning Characteristics of Building Materials," ASTM International, West Conshohocken, PA, 2012 DOI : 10.1520/E0084-12A, www.astm.org.

5.3 Appendix – ASTM E1354 Cone Calorimeter

Primary Authors: Shawn Mahoney, Nicholas Nava

5.3.1 Cone Calorimeter

The cone calorimeter is a fire testing device that uses the principle of oxygen consumption during combustion to collect data that is then used to find properties of materials. These properties are then used for calculations and fire models to help predict fire behavior [4]. The cone calorimeter is considered the best tool for finding heat release rate and also effective heat of combustion, mass loss rate, ignitability, and production of smoke, soot, and toxic gases as a function of time [1 + 3]. Before operation, the following information should be consulted; ASTM E 1354, the calorimeters user manual, as well as the manufacturers instruction manual [1].
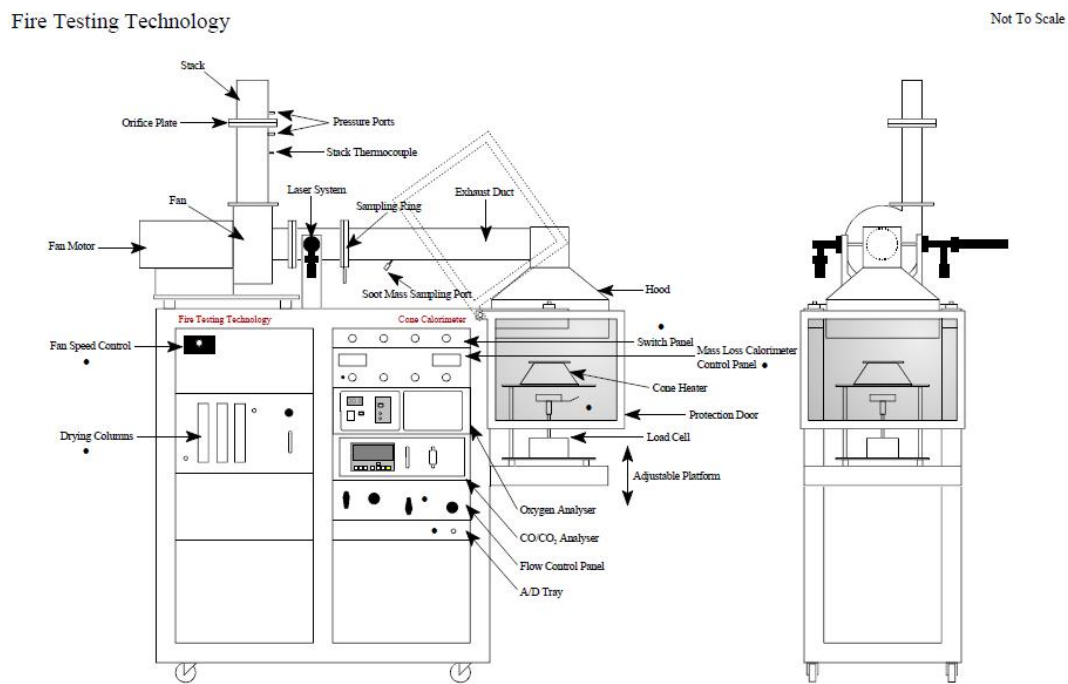
Figure 1: Schematic Diagram Of The FTT Standard Cone Calorimeter

Figure 17: Cone Schematic

As seen above in Figure 17, the cone calorimeter consists of conical radiant electric heater which is composed of over 3 meters of resistance wire wrapped in a conical shape and packed in magnesium oxide refractory [4]. This heater has a heating flux range of 0 to 100 kilowatts per square meter. Located one inch below the lower rim of the heater is a specimen holder designed to hold a specimen of 100 mm by 100 mm and up to 50 mm in thickness. The Specimen must be conditioned to moisture equilibrium at an ambient temperature of 23 ± 3°C and a relative humidity of 50 ± 5 %. The edges of the specimen are covered in aluminum foil so only the surface of the specimen is exposed to the heater. This specimen is traditionally oriented horizontally, but for exploratory studies it may be oriented vertically [1]. The specimen is located on top of a load cell in order to measure mass loss during burning. This load cell is able to read up to 500g with a measuring resolution of 0.005g. Half of an inch above the specimen there

is an electric spark igniter used as a source of ignition. And finally, gases are collected in a hood above the burner; these gases are then flowed through a flue using a fan located in the flue. The gases first flow through two filters in the flue to collect particles. They then travel through a cold trap and drying agent to remove water from the gases before they enter a gas sampling ring. The exhaust gases also flow through an orifice plate in order to create a pressure difference that is measured in order to calculate the flow of exhaust gases.
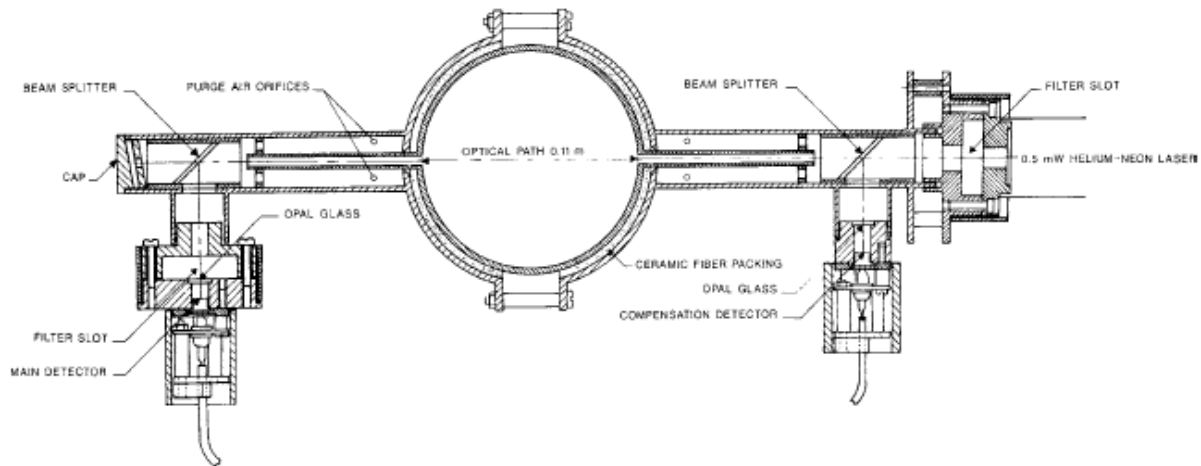
FIG. 10 Smoke Obscuration Measuring System

Figure 18: Smoke Measuring System

Inside the flue there is also a laser photometric beam that is used to measure the amount of smoke that is being produced by the burning specimen, as seen in Figure 18. The gas sampled from the exhaust is then run through an oxygen analyzer, but with some more complex cone calorimeters the gases are also analyzed for carbon monoxide and carbon dioxide [4].

5.3.2 Procedure [5]

Preparation

Check CO_2 trap and final moisture trap and drain excess water.

Turn on cone heater and exhaust blower.

Complete the following procedures for calibration:

- Heater flux calibration
- Oxygen analyzer calibration
- Heat release rate calibration
- Load cell calibration
- Smoke meter calibration

Test Execution:

Position the specimen into the appropriate holder in the appropriate location. The specimen holder shall be centered with respect to the cone heater.

Start data collection (at intervals of 5 s or less).

Record times when flashing or transitory flaming occur.

Sustained flaming occurs when flame exists over most of the test specimen surface for at least 4 s. When sustained flaming occurs, record the time when flaming was initially observed and turn off the spark.

If the specimen does not ignite in 30 minutes, remove and discard.

Test three samples and the 180-s mean heat release rate ratings shall be compared. If any of these readings differ by more than 10% from the average, additional samples shall be tested.

5.3.3   Data Acquired [5]
- Cone Irradiance
- Oxygen Analyzer reading (Oxygen Consumption)
- Exhaust Flow Rate
- Pressure Differential through orifice
- Temperature at orifice meter
- Specimen initial mass
- Specimen final mass
- Time to Ignition
- Time to Flameout
- Total Heat Released
- Peak Heat Release Rate
- Beam Intensity (with and without smoke)

5.3.4   Calculations [5]
The ASTM 1354 standard lists equations to solve for the following:

Calibration Constant

$$C = \frac{5.0}{1.10\,(12.54 \times 10^3)}\sqrt{\frac{T_e}{\Delta P}}\,\frac{1.105 - 1.5\,X_{O_2}}{X_{O_2}^{\,0} - X_{O_2}}$$

C = calibration constant for oxygen consumption analysis, $m_{1/2} - kg_{1/2} - K_{1/2}$.
T_e = absolute temperature of gas at the orifice meter, K.
ΔP = orifice meter pressure differential, Pa.
X_{O_2} = oxygen analyzer reading, before delay time correction (–).
X_{O_20} = oxygen analyzer reading, mole fraction O_2(–).

Heat Release Rate

$$X_{O_2}(t) = X_{O_2}{}^1(t + t_d)$$

X_{O_2} = oxygen analyzer reading, before delay time correction (–).
$X_{O_2 1}$ = oxygen analyzer reading, mole fraction O_2(–).
t = time, s.
t_d = oxygen analyzer delay time, s.

$$\dot{Q}(t) = \left(\frac{\Delta h_c}{r_o}\right)(1.10)\, C\, \sqrt{\frac{\Delta P}{T_e}}\, \frac{(X_{O_2}{}^0 - X_{O_2}(t))}{1.105 - 1.5\, X_{O_2}(t)}$$

$\dot{q}$ = heat release rate, kW.
$\Delta h_c/r$ for the test specimen equal to 13.1 x 10_3 kJ/kg unless a more exact value is known for the test material
C = calibration constant for oxygen consumption analysis, $m_{1/2} - kg_{1/2} - K_{1/2}$.
T_e = absolute temperature of gas at the orifice meter, K.
ΔP = orifice meter pressure differential, Pa.
X_{O_2} = oxygen analyzer reading, before delay time correction (–).
$X_{O_2 0}$ = oxygen analyzer reading, mole fraction O_2(–).

$$\dot{q}''(t) = \frac{\dot{q}(t)}{A_s}$$

$\dot{q}$ = heat release rate, kW.
A_s = nominal specimen exposed surface area, 0.01 m^2.

Mass Loss Rate

13.3.2.1 For the first scan ($i = 0$):

$$-\left[\frac{dm}{dt}\right]_{i=0} = \frac{25 m_0 - 48 m_1 + 36 m_2 - 16 m_3 + 3 m_4}{12\Delta t} \tag{7}$$

13.3.2.2 For the second scan ($i = 1$):

$$-\left[\frac{dm}{dt}\right]_{i=1} = \frac{3 m_0 + 10 m_1 - 18 m_2 + 6 m_3 - m_4}{12\Delta t} \tag{8}$$

13.3.2.3 For any scan for which $1 < i < n - 1$ (where n = total number of scans):

$$-\left[\frac{dm}{dt}\right]_i = \frac{-m_{i-2} + 8 m_{i-1} - 8 m_{i+1} + m_{i+2}}{12\Delta t} \tag{9}$$

13.3.2.4 For the last scan but one ($i = n - 1$):

$$-\left[\frac{dm}{dt}\right]_{i=n-1} \tag{10}$$

$$= \frac{-3 m_n - 10 m_{n-1} + 18 m_{n-2} - 6 m_{n-3} + m_{n-4}}{12\Delta t}$$

13.3.2.5 For the last scan ($i = n$):

$$-\left[\frac{dm}{dt}\right]_{i=n} \tag{11}$$

$$= \frac{-25 m_n + 48 m_{n-1} - 36 m_{n-2} + 16 m_{n-3} - 3 m_{n-4}}{12\Delta t}$$

Effective Heat of Combustion

$$\Delta h_{c,eff} = \frac{\Sigma_i \, \dot{q}_i(t) \, \Delta t}{m_i - m_f}$$

$\dot{q}$ = heat release rate, kW.
m_f = final specimen mass, kg.
m_i = initial specimen mass, kg.
t = time, s.

Smoke Obscuration

$$k = \left(\frac{1}{L}\right) \ln \frac{I_o}{I}$$

L = extinction beam path length, m.
I = actual beam intensity.
I_o = beam intensity with no smoke.
k = smoke extinction coefficient, m^{-1}.

$$\sigma_{f(Avg)} = \frac{\Sigma_i \, \dot{V}_i \, k_i \, \Delta t_i}{m_i - m_f}$$

σ_f = specific extinction area, for smoke, m^2/kg.
$\dot{V}$ = volume exhaust flow rate, measured at the location of the laser photometer, m^3/s.
k = smoke extinction coefficient, m^{-1}.
m_f = final specimen mass, kg.
m_i = initial specimen mass, kg.
t = time, s.

5.3.5 References

1) Babrauskas, V. (1995). The Cone Calorimeter. Heat release in fires (pp. 62-65). London: E & FN Spon.

2) Twilley, W. H., & Babrauskas, V. (2001). User's Guide for the Cone Calorimeter. Fire Testing Technology Limited, 1, 85.

3) ASTM E1354: Cone Calorimeter. (2012). Fire Testing and Evaluation Center. Retrieved August 29, 2012, from http://www.firetec.umd.edu/testing/standard/astm_e1354

4) Lindholm, J., Brink, A., & Hupa, M. (n.d.). CONE CALORIMETER â€" A TOOL FOR MEASURING HEAT RELEASE RATE. Flame Days. Retrieved August 29, 2012, from www.ffrc.fi/FlameDays_2009/4B/LindholmPaper.pdf

5) E1354-11b Standard Test Method for Heat and Visible Smoke Release Rates for Materials and Products Using an Oxygen Consumption Calorimeter

5.4 Appendix - Edge Burning Analysis

Primary Authors: Christian Acosta

Many of the parameters found in equation 1 were constant for the specimen, however h_{tot} needed to be solved for to be used in the equation. To begin that process, the underlying heat transfer equation had to be manipulated to solve for T_{ig}.

$$q'' = \varepsilon\sigma\left(T_{ig}^4 - T_\infty^4\right) + h_c\left(T_{ig} - T_\infty\right)$$

The constant h_c was found by using a quadratic expression developed by Janssens which incorporated the heat flux of any given test in the cone calorimeter. In this case we used the incident heat fluxes of 25 kW/m^2, 50 kW/m^2 and 75 kW/m^2.

$$h_c = 1.4 * 10^{-4}(q'') + 2.4 * 10^{-6}\,(q'')^2$$

Once the h_c variable was incorporated to the overall heat transfer equation for this case and T_{ig} was solved for the corresponding heat fluxes necessary, the T_{ig} values were then used to solve for h_{rad} in the linearized radiation equation shown below.

$$h_{rad} = \frac{\varepsilon\sigma\left(T_{ig}^4 - T_\infty^4\right)}{T_{ig} - T_\infty}$$

The convective and radiative heat transfer coefficient were then added together to solve for the total heat transfer coefficient for the overall case in the cone calorimeter.

$$h_{tot} = h_c + h_{rad}$$

The corresponding h_{tot} values were then utilized with the analogous heat flux within the equation to develop a temperature profile along a distributed depth over a matter of time.

5.4.1 Graphed Temperature Changes: IHF of 25kW/m² , 50kW/m² & 75kW/m²
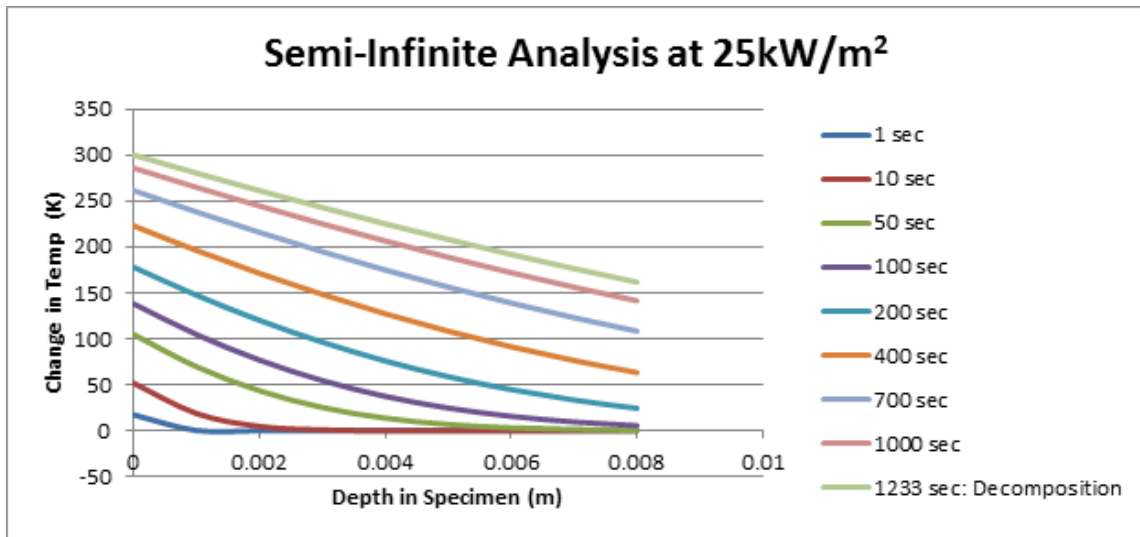
Figure 19: Temperature at Depth IHF 25 kW/m²
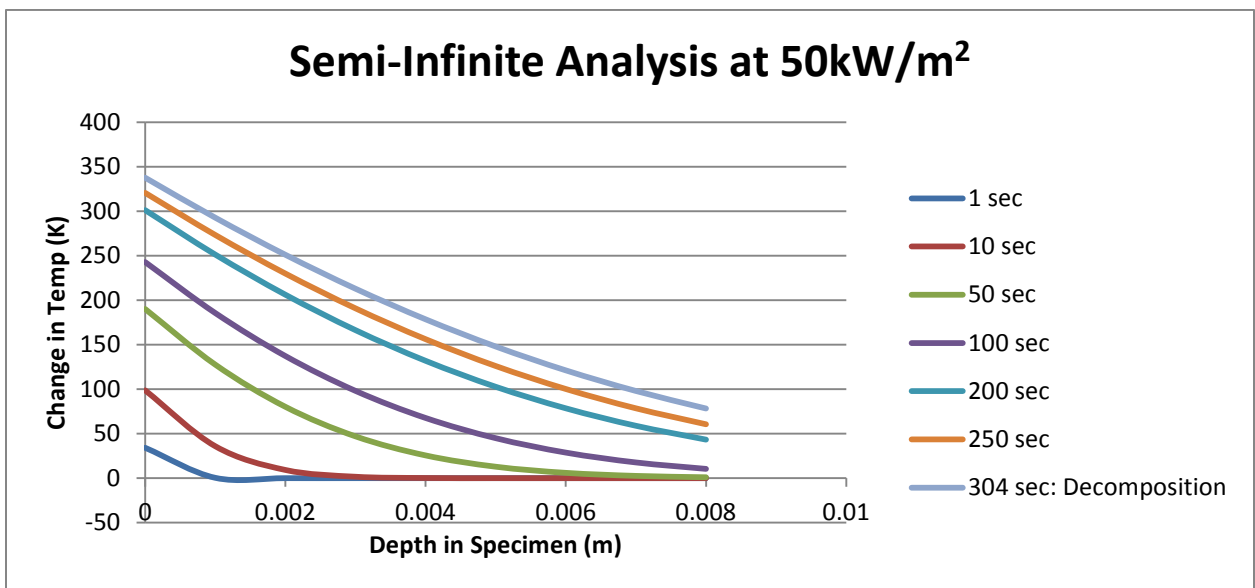
Figure 20: Temperature at Depth IHF 50 kW/m²
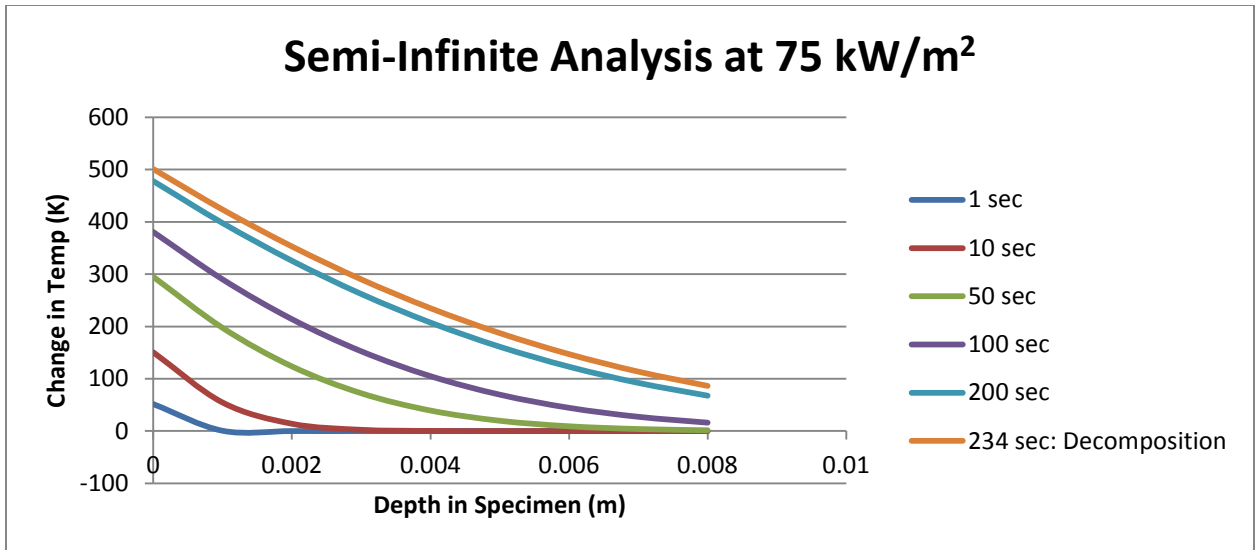
Figure 21: Temperature at Depth IHF 75 kW/m^2

5.5 Appendix – Theoretical Temperature Profiles

Primary Author: Nicholas Nava

Temperature profiles were determined theoretically using finite difference methods. The Fundamentals of Heat and Mass Transfer, Incropera provided a fundamental understanding of finite difference methods, where equations for different nodes were derived.

Finite difference methods requires a nodal network be created, which involves subdividing the samples into smaller regions. For this calculation the regions were decided to be 1mm by 1mm. Each node will be represented by an equation which is determined to be essentially the average of the temperatures around it for interior nodes. Exterior node or boundary nodes are determined by temperatures around the node with the addition of boundary conditions such as a radiative incident heat flux or convective cooling.

The standard 8mm (0.3 in.) thick sample was examined with 46mm (1.8 in.) fiber board backing and 2mm (0.08 in.) thick edge frame along the side and 2 mm (0.08 in.) in from the edges on the top surface it as it would be during testing. The analysis was performed with an induced incident heat flux (IHF) on the top face and a radiative fraction (heat flux multiplied by a view factor) along the sides. Natural convective cooling on the top was determined using Janssens' equation for determining the convective heat transfer coefficient [1] and natural convective cooling on the side and back faces was determined using a standard convective heat transfer coefficient. The extended 8mm (0.3 in.) thick sample was examined with 46mm (1.8 in.) fiber board backing and no edge frame, as is the testing configuration for this sample size. The analysis was performed with an induced heat flux on the top face under the Cone, where the edges outside of the Cone's area were exposed to a radiative fraction (heat flux multiplied by a view factor) and sides received no heat flux. The convective cooling was the same as for the standard samples. The thermal conductivity for the FRP specimen, fiber board, and steel edge frame were determined based on literature review and practical experience and remained consistent throughout the calculations.

To determine the equation for the nodes, they were derived using methods in the energy balance method as outline in Incropera. [1] The following was copied from Incropera page 215 and 216.
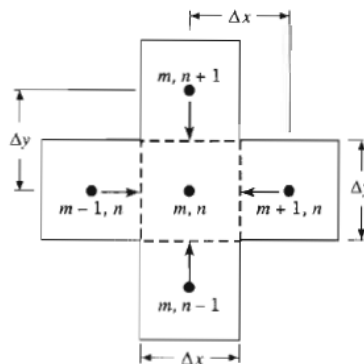
$$\dot{E}_{in} + \dot{E}_{g} = 0$$

$$\sum_{i=1}^{4} q_{(i) \to (m,n)} + \dot{q}(\Delta x \cdot \Delta y \cdot 1) = 0$$

$$q_{(m-1,n) \to (m,n)} = k(\Delta y \cdot 1)\frac{T_{m-1,n} - T_{m,n}}{\Delta x}$$

$$q_{(m+1,n) \to (m,n)} = k(\Delta y \cdot 1)\frac{T_{m+1,n} - T_{m,n}}{\Delta x}$$

$$q_{(m,n+1) \to (m,n)} = k(\Delta x \cdot 1)\frac{T_{m,n+1} - T_{m,n}}{\Delta y}$$

$$q_{(m,n-1) \to (m,n)} = k(\Delta x \cdot 1)\frac{T_{m,n-1} - T_{m,n}}{\Delta y}$$

$$T_{m,n+1} + T_{m,n-1} + T_{m+1,n} + T_{m-1,n} + \frac{\dot{q}(\Delta x)^2}{k} - 4T_{m,n} = 0$$

$$T_{m,n+1} + T_{m,n-1} + T_{m+1,n} + T_{m-1,n} - 4T_{m,n} = 0$$

These equations taken from Incropera are for an interior node where q the internal energy is taken to be zero. Solving for T_{mn} will give the temperature at that node. The other nodes were determined based on a derivation of this method.

5.5.1   Boundary Conditions

The boundary conditions for this analysis are as follows:

The thermal conductivity was determined based on known values in literature and estimates for FRP samples since it was not exactly known. It is important to note exact values are not needed when comparing temperature profiles as long as the same boundary condition was used for both standard and extended samples.

k_e (k of edge frame) = 41 W/mK [2]

k_s (k of FRP sample) = .5 W/mK (Estimated based on value expected from MQP Group B)

k_f (k of fiber board) = .05 W/mK [3]

h (convective heat transfer coefficient in free convection) = 5 W/m^{2}K [4]

Δ_x (size of node) = 0.001 m

T_{amb} = 299 K (Average of ambient temperature in lab during testing)

q (Incident Heat Flux {IHF}) = 25000 W/m^2, 50000 W/m^2, 75000 W/m^2 (Depending on test condition)

e (emissivity) = 1 (assumed for simplicity)

sigma (Stefan Boltzmann constant) = 5.67E-08 W/m^{2}K^4

Finally, the convective heat transfer coefficient varied based on location of node on sample. If the node was not exposed to a heat flux (back face of both specimens sizes, edge of extended specimen size), the convective heat transfer coefficient is just h, the heat transfer coefficient in free convection. Nodes where the sample is exposed to a heat flux, the convective heat transfer coefficient is determined based on a total convective heat transfer coefficient of the convective heat transfer coefficient as a function of the heat flux (hs) and the convective heat transfer coefficient due to radiation from the surface (hr).

h_tot = hs + hr

hs = $\dfrac{1.4 \cdot 10^{-4} \dot{q}_e'' + 2.4 \cdot 10^{-6} (\dot{q}_e'')^2}{}$ [5]

hs = 5 W/m^{2}K, 13 W/m^{2}K, 24 W/m^{2}K, respectively, for IHF of 25000 W/m^2, 50000 W/m^2, 75000 W/m^2

hr = σ (T$_s^4$ - T$_{amb}^4$) / (T$_s$ - T$_{amb}$) = (Derived for the equation for basic radiation)

where, T_s = T_{ig} to keep calculation simple. T_{ig} is the ignition temperature of the FRP material based on a minimum heat flux to ignition of 25000 W/m^2 and determined to be 797 K.

This will give a hr = 45.1 W/m^{2}K.

It is important to note this value of hr would be higher, indicating more cooling, if T_s was used vice T_{ig} but again to keep calculation simple T_{ig} was used. The reason using the T_s will be more computationally demanding is due to the fact that hundreds of additional iterations will need to be performed to

determine hr which will determine T_s which will be affected by h_r in addition to the surrounding temperatures so using a standard T_{ig} will eliminate these additional iterations.

5.5.2 Shape Factors

In order to complete the finite difference model for the 100 mm and 175mm specimens, it was necessary to determine the imposed heat flux on the side of the edge frame from the cone heater and the edges of the 175 mm sample that were not directly under the cone heater. To determine this the IHF is to be multiplied by a shape of view factor. The hand written calculations for the derivation of these shape factors can be seen below.
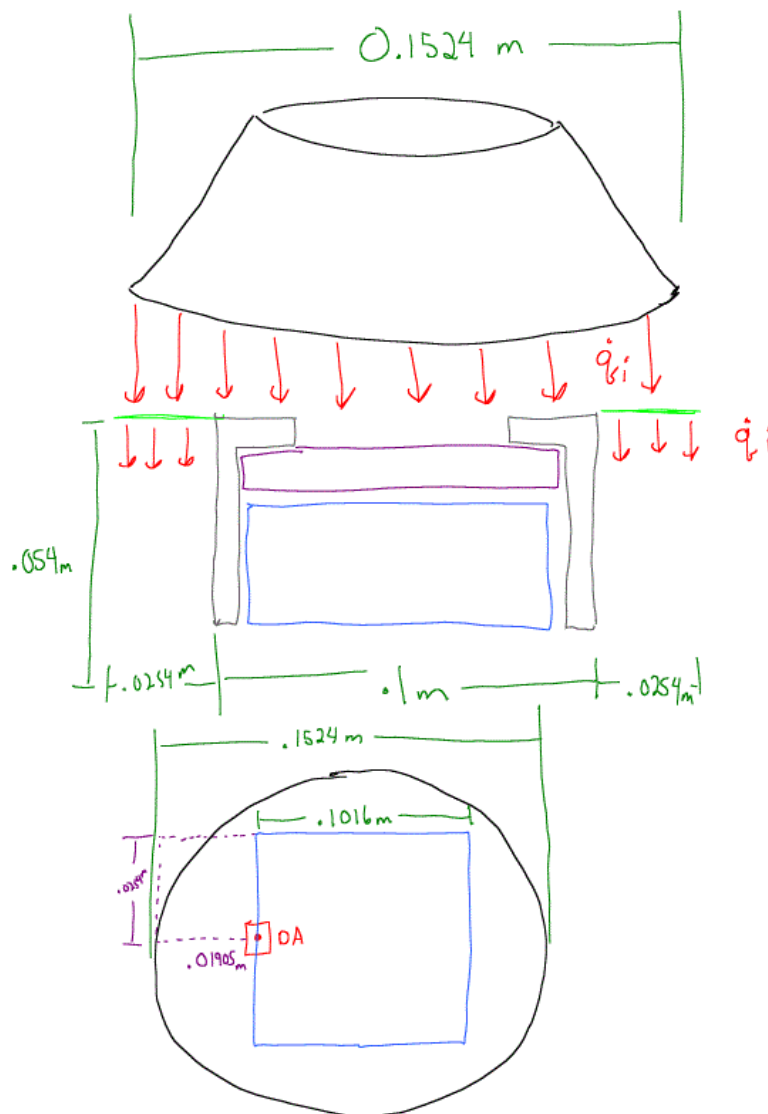
To find factor for entire side it will utalize two times the shape factor

Shape factor Calculation

From SFPE T1-4.1 Pg 1-78   [6]

$x = a/b$

$y = c/b$
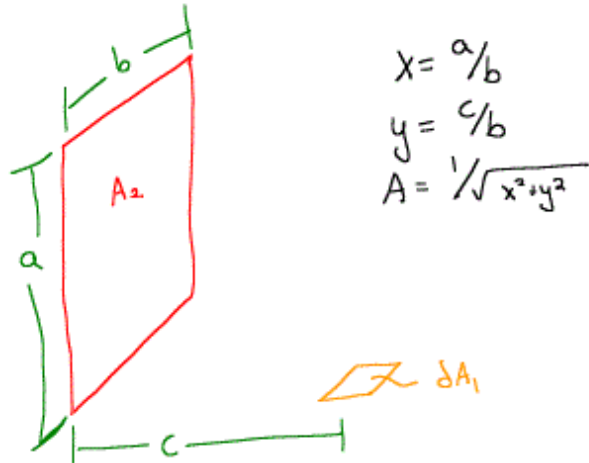
$A = 1/\sqrt{x^2 + y^2}$

$a = 0.0254\,m$

$b = 0.01905\,m$

$0 \leq C \leq 0.054\,m$

$$F_{1-2} = \frac{1}{2\pi}\left(Tan^{-1}\left(1/y\right) - AY\left(Tan^{-1}(A)\right)\right)$$

$$X = \frac{0.0254}{0.01905} = 1.33 \qquad Y = \frac{C}{0.01905} \qquad A = 1/\sqrt{1.778 + \left(c/0.01905\right)^2}$$

$$F_{1-2}(c) = \frac{1}{2\pi}\left(Tan^{-1}\left(\frac{0.01905}{c}\right)\right) - \frac{c}{0.01905\sqrt{1.778 + \left(c/0.01905\right)^2}}\left(Tan^{-1}\left(1/\sqrt{1.778 + \left(c/0.0195\right)^2}\right)\right)$$

Derivation of incident flux on flame

$$F_{C-F}\, A_{cone}\, \varepsilon_{cone}\, \sigma\, T^4_{cone} = \dot{Q}_{cone-fr}$$

$$\dot{q}''_{fr} = \frac{\dot{Q}_{cone-fr}}{A_{fr}}$$

$$\dot{q}''_{fr} = \frac{F_{c-fr}\, A_{cone}}{A_{fr}}\, \varepsilon_{cone}\, \sigma\, T^4_{cone}$$

$$\dot{q}''_{bfr} = \left(F_{Fr\cdot c}\right)\left(\varepsilon_{cone}\,\sigma\,T_{cone}^4\right)$$

$$\dot{q}''_{bfr} = 2\left(F_{1-2}(c)\right)\left(\dot{q}''_{b\,incident}\right)$$

where

$$F_{1-2}(c) = \frac{1}{2\pi}\left(Tan^{-1}\left(\frac{0.01905}{c}\right)\right) - \frac{c}{0.01905\sqrt{1.778 + \left(\frac{c}{0.01905}\right)^2}}\left(Tan^{-1}\left(\frac{1}{\sqrt{1.778 + \left(\frac{c}{0.01905}\right)^2}}\right)\right)$$

Shape factor Calculations Cone to Specimen.
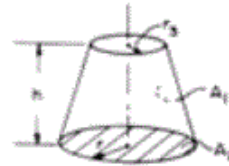
Definitions:

$H = h/r_3; R = r/r_3;$
$X = (1 + R^2 + H^2)$

Governing Equation:

$r_3 = .1016 \, m$
$h = .0762 \, m$
$r = .1524 \, m$

$$F_{1-2} = \frac{2R^2 - X + (X^2 - 4R^2)^{1/2}}{2(X - 2R)^{1/2} \cdot (1 + R)} \qquad [7]$$

$$H = \frac{h}{r_3} = \frac{0.0762}{.1016} = .75$$

$$R = \frac{r}{r_3} = \frac{.1524}{.1016} = 1.5$$

$$X = (1 + R^2 + H^2) = 3.8125$$

$$F_{c-s} = \frac{2R^2 - X + (x^2 - 4R^2)^{1/2}}{2(x - 2R)^{1/2} \cdot (1 + R)} = \frac{4.5 - 3.8125 + (5.1875)^{1/2}}{1.803 \cdot 2.5} = \frac{3.040}{4.5075}$$

$$F_{c-s} = 0.674$$
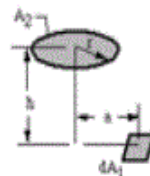
$x = .1524$
$h = .0254$
$.0762 \le a \le .0889$

Definitions: $H=h/a; R=r/a; Z=1+R^2+H^2$

Governing equation:

$$F_{d1-2} = \frac{1}{2}\left[1 - \frac{Z - 2R^2}{(Z^2 - 4R^2)^{1/2}} \right] \qquad [8]$$

$$H = \frac{.0254}{a} \qquad R = \frac{.1524}{a} \qquad Z = 1 + R^2 + H^2$$

$$F_{cs}(a) = \frac{1}{2}\left[1 - \frac{\left(1 + \left(\frac{.1524}{a}\right)^2 + \left(\frac{.0254}{a}\right)^2\right) - 2\left(\frac{.1524}{a}\right)^2}{\left(\left(1 + \left(\frac{.1524}{a}\right)^2 + \left(\frac{.0254}{a}\right)^2\right)^2 - 4\left(\frac{.1524}{a}\right)^2\right)^{(1/2)}}\right]$$

where a is the distance from the center of the cone

Cone Rad Cont.

$$F_{1-2} \, A_1 \, \epsilon \, \sigma \, T^4_{cone} = \dot{Q}_{cone}$$

Frustum of a Right Circular Cone

r = radius of upper base
R = radius of lower base
s = slant height
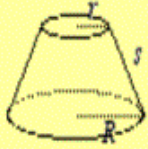
Volume $= \frac{1}{3}\pi h\left(r^2 + rR + R^2\right)$

Lateral Surface Area $= \pi(r + R)s$
$= \pi(r + R)\sqrt{(R-r)^2 + h^2}$

Total Surface Area $= \pi(r + R)s + \pi r^2 + \pi R^2$
$= \pi(r + R)\sqrt{(R-r)^2 + h^2} + \pi r^2 + \pi R^2$

[9]

$r = .1016 \text{ m}$

$R = .1524 \text{ m}$

$$A_1 = \pi(.1016 + .1524)\sqrt{(.1524 - .1016)^2 + .0762}$$

$A_1 = 0.224 \text{ m}^2$

$\epsilon = 1$

$\sigma = 5.67037 \times 10^{-8} \, W/m^2 K^4$

assume cone temp of 500 K

$$0.674 \cdot 0.224 \text{m}^2 \cdot 1 \cdot 5.67 \times 10^{-8} \, W/m^2 K^4 \cdot 500^4 K = 535.0212 \text{ watts}$$

$$\text{flux at cone opening} = \frac{535.0212 \text{ watts}}{\pi(.0762)^2 \text{ m}^2} = 29{,}329.94 \, W/m^2$$

flux at distance a from the center

$$\dot{q}''_{outer} = F_{c-s}\left(29{,}329.94 \, W/m^2\right)$$

where (Next Page)

$$F_{cs}(a) = \frac{1}{2}\left[1 - \frac{\left(1 + \left(\frac{.1524}{a}\right)^2 + \left(\frac{.0254}{a}\right)^2\right) - 2\left(\frac{.1524}{a}\right)^2}{\left(\left(1 + \left(\frac{.1524}{a}\right)^2 + \left(\frac{.0254}{a}\right)^2\right)^2 - 4\left(\frac{.1524}{a}\right)^2\right)^{(1/2)}}\right]$$

The resulting shape factors used in calculation are shown in Table 5 and Table 6.

Table 5: Extended Sample Shape Factor

Distance Across	1 mm	2 mm	3 mm	4 mm	5 mm	6 mm	7 mm	8 mm	9 mm	167 mm	168 mm	169 mm	170 mm	171 mm	172 mm	173 mm	174 mm	175 mm
View Factor	0.264816	0.280188	0.296186	0.312775	0.329911	0.34754	0.365598	0.384015	0.402713	0.402713	0.384015	0.365598	0.34754	0.329911	0.312775	0.296186	0.280188	0.264816

Table 6: Shape Factor along edge of Standard Sample

Depth Down Edge'	View Factor
1 mm	0.475493812
2 mm	0.45089045
3 mm	0.426595225
4 mm	0.402750716
5 mm	0.379486618
6 mm	0.35691682
7 mm	0.335137452
8 mm	0.314225895
9 mm	0.294240704
10 mm	0.275222301
11 mm	0.257194256
12 mm	0.240165009
13 mm	0.22412982
14 mm	0.209072833
15 mm	0.194969124
16 mm	0.181786632
17 mm	0.169487932
18 mm	0.15803181
19 mm	0.147374622
20 mm	0.137471429
21 mm	0.128276948
22 mm	0.119746294
23 mm	0.111835574
24 mm	0.104502324
25 mm	0.09770583
26 mm	0.091407347
27 mm	0.085570227
28 mm	0.080159994
29 mm	0.075144349
30 mm	0.070493154
31 mm	0.066178367
32 mm	0.062173972
33 mm	0.058455881
34 mm	0.055001833
35 mm	0.051791289
36 mm	0.04880532
37 mm	0.046026498
38 mm	0.043438793
39 mm	0.041027465
40 mm	0.038778969
41 mm	0.036680864
42 mm	0.034721719
43 mm	0.032891037
44 mm	0.031179177
45 mm	0.029577282
46 mm	0.028077213
47 mm	0.026671494
48 mm	0.025353248
49 mm	0.024116153
50 mm	0.022954393
51 mm	0.021862613
52 mm	0.020835884
53 mm	0.019869663
54 mm	0.018959762

Table 6: Shape Factor along edge of Standard Sample

5.5.3   Equations Used in Calculation

5.5.3.1 Standard Specimen Equations

Additional Nomenclature:

T_{mn} = Temperature at node in K

T_{m+1} = Temperature to the right of the node

T_{m-1} = Temperature to the left of the node

T_{n+1} = Temperature above node

T_{n-1} = Temperature below node

F = View factor

The following is a list of equations used to solve for the temperature profiles for the standard sample configuration. See Figure 22 for where each equation applies where gray indicates edge frame, tan indicates fiber board, and green indicates the FRP specimen. Note these equations apply to the left half of the configuration, see Figure. For the right side of the equation, the equations directly mirror the left side equations where the center of the sample is the mirror pivot point.

Break to 50 mm, Eq 22, 7, 12, 11, 7, 6 continue

Mirror about line for other side of specimen

	1 mm	2 mm	1 mm	2 mm	3 mm	4 mm	5 mm	6 mm	7 mm	8 mm	50 mm
1 mm	1				20					19	
2 mm		7			17					21	
1 mm			16			18					22
2 mm		14	15				7				
3 mm											
4 mm											
5 mm											
6 mm											
7 mm											
8 mm			13				12				
9 mm			10				11				
10–53 mm	2	9	8				7				
54 mm	3	4	5				6				

Figure 22: Standard Specimen Configuration Equation Numbering

Equation 1

$$T_{mn} = \frac{(T_{m+1} + T_{n-1}) + \left(\frac{2 * (hs + hr) * \Delta x * T_{amb}}{K_e}\right) + \left(\frac{2 * q * \Delta x}{K_e}\right)}{2 + \frac{2 * (hs + hr) * \Delta x}{K_e}}$$

Equation 2

$$T_{mn} = \frac{(2 * K_e * T_{m+1} + K_e * T_{n+1} + K_e * T_{n-1}) + ((h + hr) * \Delta x * 2 * T_{amb}) + 2 * F * q * \Delta x}{4 * K_e + (h + hr) * 2 * \Delta x}$$

Equation 3

$$T_{mn} = \frac{(K_e * T_{n+1} + K_e * T_{m+1}) + ((h + hr) * \Delta x * 2 * T_{amb}) + 2 * F * q * \Delta x}{2 * K_e + (h + hr) * 2 * \Delta x}$$

Equation 4

$$T_{mn} = \frac{\left((2 * T_{n+1} * K_e) + (T_{m+1} * K_f) + (T_{m-1} * K_e)\right) + \left(\frac{h * \Delta x}{2}\right) * T_{amb}}{3 * K_e + K_f + \frac{h * \Delta x}{2}}$$

Equation 5

$$T_{mn} = \frac{\left((2 * T_{n+1} * K_f) + (T_{m+1} * K_f) + (T_{m-1} * K_e)\right) + \left(\frac{h * \Delta x}{2}\right) * T_{amb}}{3 * K_f + K_e + \frac{h * \Delta x}{2}}$$

Equation 6

$$T_{mn} = \frac{\left((2 * T_{n+1}) + T_{m+1} + T_{m-1}\right) + \left(\frac{2 * h * \Delta x}{K_f}\right) * T_{amb}}{2 * \left(\left(\frac{h * \Delta x}{K_f}\right) + 2\right)}$$

Equation 7

$$T_{mn} = \frac{T_{n+1} + T_{m+1} + T_{n-1} + T_{m-1}}{4}$$

Equation 8

$$T_{mn} = \frac{T_{n+1} * K_f + T_{m-1} * K_e + T_{n-1} * K_f + T_{m+1} * K_f}{K_e + 3 * K_f}$$

Equation 9

$$T_{mn} = \frac{T_{n+1} * K_e + T_{m-1} * K_e + T_{n-1} * K_e + T_{m+1} * K_f}{K_f + 3 * K_e}$$

Equation 10

$$T_{mn} = \frac{T_{n+1} * K_s + T_{m-1} * K_e + T_{n-1} * K_f + T_{m+1} * K_f}{K_e + K_s + 2 * K_f}$$

Equation 11

$$T_{mn} = \frac{T_{n+1} * K_s + T_{m-1} * K_f + T_{n-1} * K_f + T_{m+1} * K_f}{K_s + 3 * K_f}$$

Equation 12

$$T_{mn} = \frac{T_{n+1} * K_s + T_{m-1} * K_s + T_{n-1} * K_f + T_{m+1} * K_s}{K_f + 3 * K_s}$$

Equation 13

$$T_{mn} = \frac{T_{n+1} * K_s + T_{m-1} * K_e + T_{n-1} * K_f + T_{m+1} * K_s}{K_e + K_f + 2 * K_s}$$

Equation 14

$$T_{mn} = \frac{T_{n+1} * K_e + T_{m-1} * K_e + T_{n-1} * K_e + T_{m+1} * K_s}{K_s + 3 * K_e}$$

Equation 15

$$T_{mn} = \frac{T_{n+1} * K_s + T_{m-1} * K_e + T_{n-1} * K_s + T_{m+1} * K_s}{K_e + 3 * K_s}$$

Equation 16

$$T_{mn} = \frac{T_{n+1} * K_e + T_{m-1} * K_e + T_{n-1} * K_s + T_{m+1} * K_s}{2 * K_e + 2 * K_s}$$

Equation 17

$$T_{mn} = \frac{T_{m+1} * K_e + T_{m-1} * K_e + T_{n-1} * K_s + T_{m+1} * K_e}{K_s + 3 * K_e}$$

Equation 18

$$T_{mn} = \frac{T_{n+1} * K_e + T_{m-1} * K_s + T_{n-1} * K_s + T_{m+1} * K_s}{K_e + 3 * K_s}$$

Equation 19

$$T_{mn} = \frac{(T_{n-1} + T_{m-1}) + \left(\frac{2*(hs+hr)*\Delta x*T_{amb}}{K_e}\right) + \left(\frac{2*q*\Delta x}{K_e}\right)}{2 + \frac{2*(hs+hr)*\Delta x}{K_e}}$$

Equation 20

$$T_{mn} = \frac{(2*T_{n-1} + T_{m-1} + T_{m+1}) + \left(\frac{2*(hs+hr)*\Delta x*T_{amb}}{K_e}\right) + \left(\frac{2*q*\Delta x}{K_e}\right)}{4 + \frac{2*(hs+hr)*\Delta x}{K_e}}$$

Equation 21

$$T_{mn} = \frac{(2*K_e*T_{m+1} + K_e*T_{n+1} + K_e*T_{n-1}) + \left((h+hr)*\Delta x*1.5*T_{amb}\right) + 1.5*q*\Delta x}{4*K_e + (h+hr)*1.5*\Delta x}$$

Equation 22

$$T_{mn} = \frac{(2*T_{n-1} + T_{m+1} + T_{m-1}) + \left(\frac{2*(hs+hr)*\Delta x*T_{amb}}{K_s}\right) + \left(\frac{2*q*\Delta x}{K_s}\right)}{4 + \frac{2*(hs+hr)*\Delta x}{K_s}}$$

5.5.3.2 Extended Specimen Equations

Additional Nomenclature:

T_{mn} = Temperature at node in K

T_{m+1} = Temperature to the right of the node

T_{m-1} = Temperature to the left of the node

T_{n+1} = Temperature above node

T_{n-1} = Temperature below node

F = View factor (See Shape Factors Section)

qf = q_{outer}= heat flux in kW used in view factor equation - different from q which is the IHF (See Shape Factors Section)

The following is a list of equations used to solve for the temperature profiles for the extended sample configuration. See Figure 23 for where each equation applies where tan indicates fiber board and green indicates the FRP specimen. Note these equations apply to the left half of the configuration, see Figure. For the right side of the equation, the equations directly mirror the left side equations where the center of the sample is the mirror pivot point.

Figure 23: Extended Specimen Configuration Equation Numbering

Equation 1

$$T_{mn} = \frac{(K_s * T_{m+1} + K_s * T_{n-1}) + ((hs + hr) * \Delta x * 2 * T_{amb}) + 2 * qf * F * \Delta x}{2 * K_s + (hs + hr) * 2 * \Delta x}$$

Equation 2

$$T_{mn} = \frac{(2 * T_{n-1} + T_{m+1} + T_{m-1}) + \left(\frac{2 * (hs + hr) * \Delta x * T_{amb}}{K_s}\right) + \left(\frac{2 * qf * F * \Delta x}{K_s}\right)}{4 + \frac{2 * (hs + hr) * \Delta x}{K_s}}$$

Equation 3

$$T_{mn} = \frac{(2 * T_{n-1} + T_{m+1} + T_{m-1}) + \left(\frac{2 * (hs + hr) * \Delta x * T_{amb}}{K_s}\right) + \left(\frac{2 * q * \Delta x}{K_s}\right)}{4 + \frac{2 * (hs + hr) * \Delta x}{K_s}}$$

Equation 4

$$T_{mn} = \frac{(2 * K_s * T_{m+1} + K_s * T_{n+1} + K_s * T_{n-1}) + (h * \Delta x * 2 * T_{amb})}{4 * K_s + (h * 2 * \Delta x)}$$

Equation 5

$$T_{mn} = \frac{(2 * K_s * T_{m+1} + K_s * T_{n+1} + K_f * T_{n-1}) + (h * \Delta x * 2 * T_{amb})}{3 * K_s + K_f + (h * 2 * \Delta x)}$$

Equation 6

$$T_{mn} = \frac{(2 * K_f * T_{m+1} + K_s * T_{n+1} + K_f * T_{n-1}) + (h * \Delta x * 2 * T_{amb})}{3 * K_f + K_s + (h * 2 * \Delta x)}$$

Equation 7

$$T_{mn} = \frac{(2 * K_f * T_{m+1} + K_f * T_{n+1} + K_f * T_{n-1}) + (h * \Delta x * 2 * T_{amb})}{4 * K_f + (h * 2 * \Delta x)}$$

Equation 8

$$T_{mn} = \frac{(K_f * T_{m+1} + K_f * T_{n+1}) + (h * \Delta x * 2 * T_{amb})}{2 * K_f + (h * 2 * \Delta x)}$$

Equation 9

$$T_{mn} = \frac{\left((2 * T_{n+1}) + T_{m-1} + T_{m+1}\right) + \left(\frac{2 * h * \Delta x}{K_f}\right) * T_{amb}}{2 * \left(\left(\frac{h * \Delta x}{K_f}\right) + 2\right)}$$

Equation 10

$$T_{mn} = \frac{T_{n+1} + T_{m+1} + T_{n-1} + T_{m-1}}{4}$$

Equation 11

$$T_{mn} = \frac{T_{n+1} * K_s + T_{m-1} * K_f + T_{n-1} * K_f + T_{m+1} * K_f}{K_s + 3 * K_f}$$

Equation 12

$$T_{mn} = \frac{T_{n+1} * K_s + T_{m-1} * K_s + T_{n-1} * K_f + T_{m+1} * K_s}{K_f + 3 * K_s}$$

5.5.4 Results

Figure 24 shows the resulting temperature profiles for the 3 IHF's experienced in the cone using boundary conditions and equations described above. Calculations were performed using Microsoft Excel's ability to perform iterative calculations.
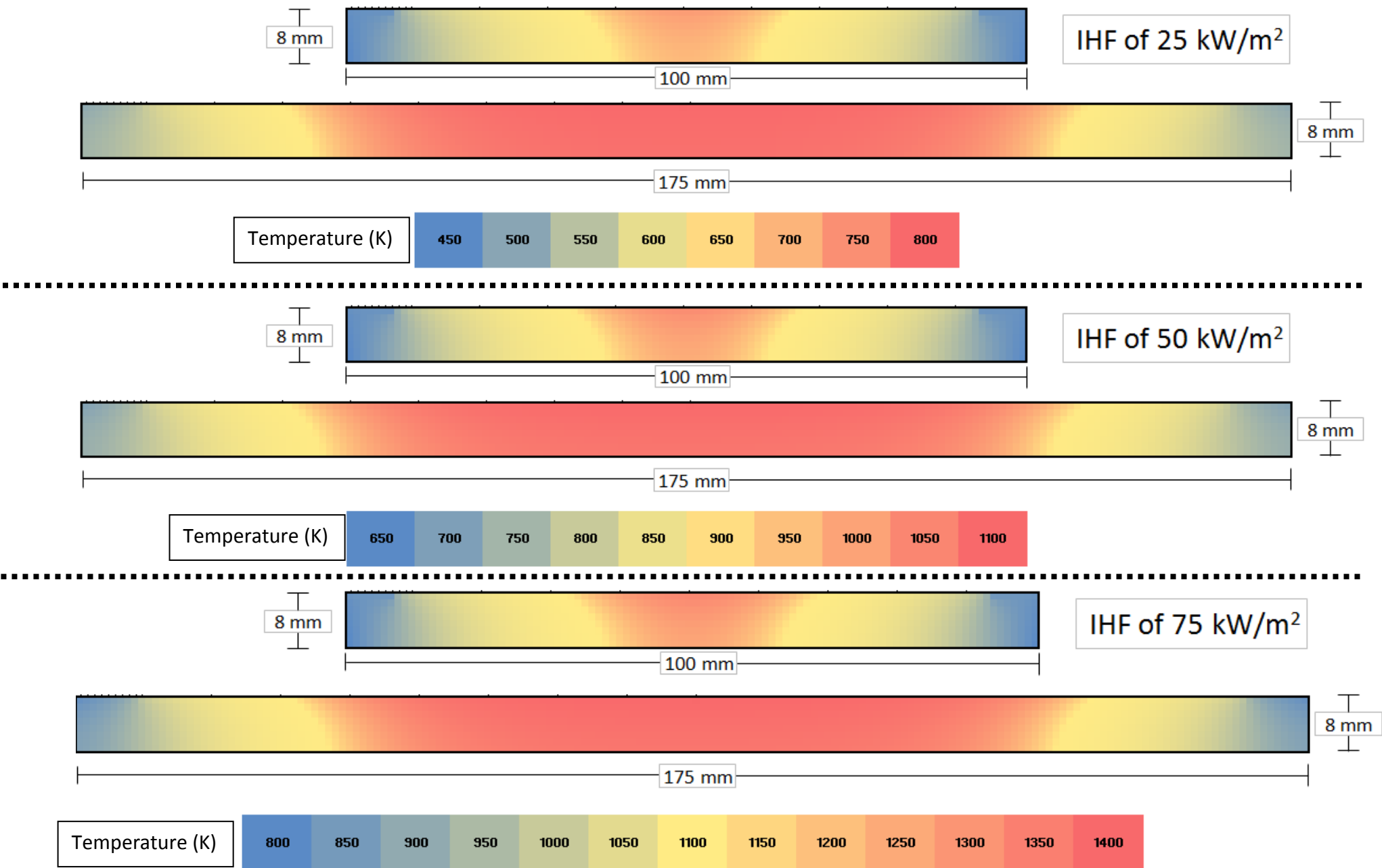
Figure 24: Steady state temperature profiles for both sample sizes at various IHF's.

Plots of these temperature profiles were also created to compare these values quantitatively. The charts are displayed in degrees Celsius for the reader to better relate to the values. These values are the same as in Figure 24, but in Celsius found simply by subtracting 273 degrees form values. See Figure 25 - Figure 27 for these plots.
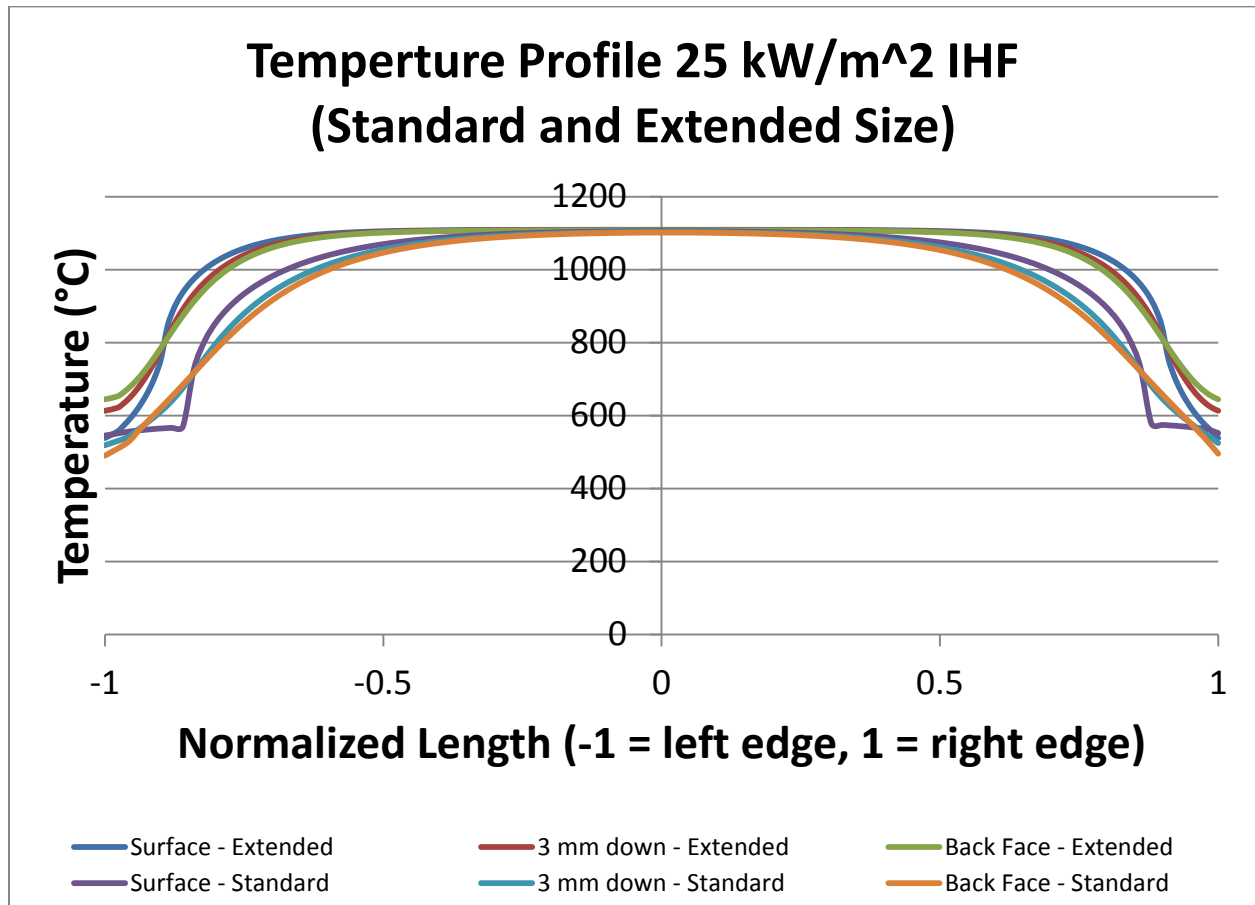
Figure 25: Temperature Profile Graph at IHF of 25 kW/m^2
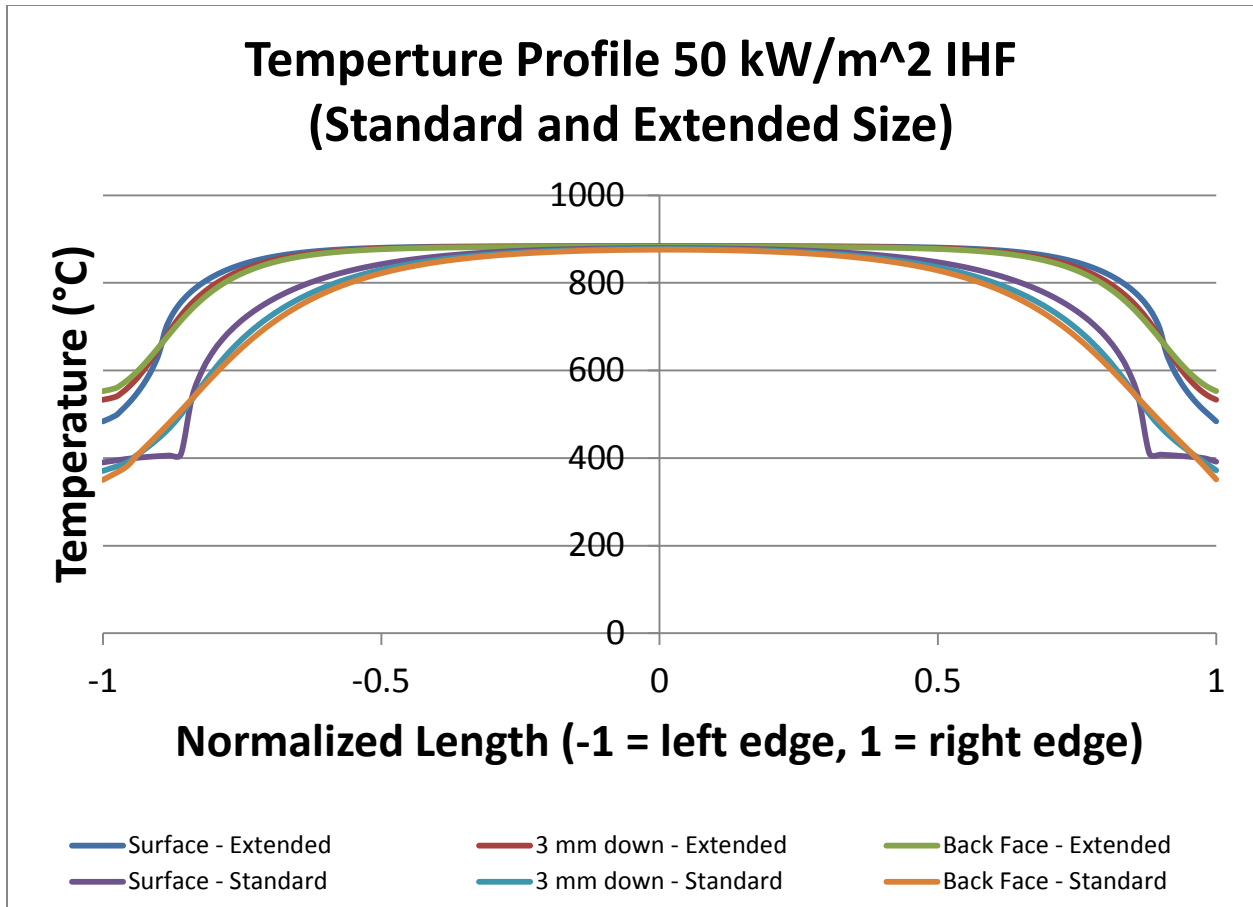
Figure 26: Temperature Profile Graph at IHF of 50 kW/m^2
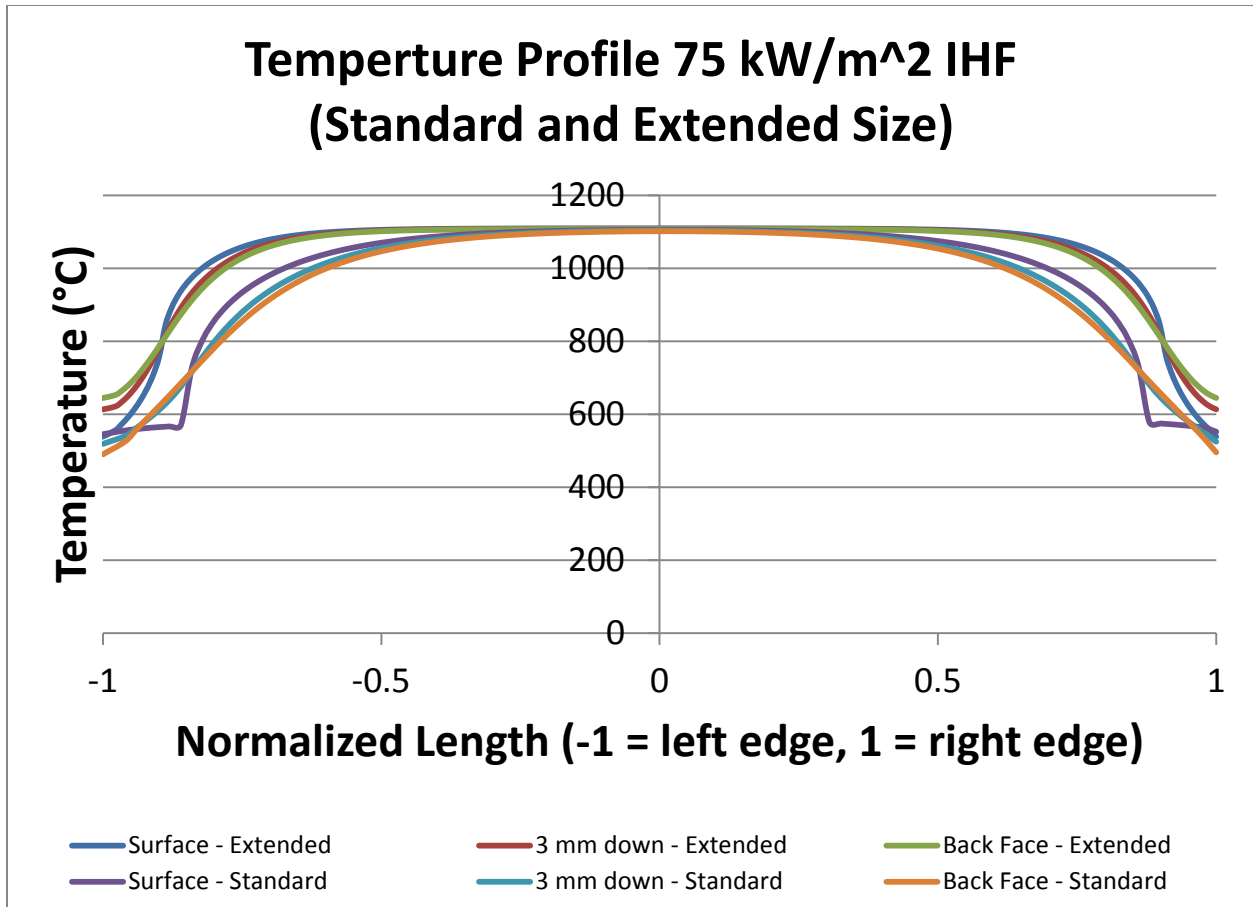
Figure 27: Temperature Profile Graph at IHF of 50 kW/m²

5.5.5   Conclusion

Figure 25 - Figure 27 show that that the temperature at the surface, 3 mm down, and at the back face, track similarly for both size specimens at various IHF's. The profiles are similar which indicates similarity between the specimens yet the profiles of the larger samples indicate higher temperatures. The difference in temperatures is indicative of the larger sample receiving more heat because of its size. Since fire performance in the Cone is normalized by surface area burned, the fact that the extended sample receives higher temperatures will be accounted for when normalized by size. This explanation helps to confirm theoretically that these specimen sizes are similar. To determine if they are quantitatively similar, not significantly different, testing of both specimen sizes in the Cone was performed.

5.5.6 References

[1] Incropera, Frank P. *Fundamentals of Heat and Mass Transfer.* Hoboken, NJ: John Wiley, 2011. Print.

[2] "Ceramic Fiber Board in Houston Texas, 2300°F, Refractory Ceramic Fiber Board,0.5", 1.0" 2.0" *Ceramic Fiber Board, Ceramic Fiber Blanket, Ceramic Fiber Paper, IFB,Ceramic Fiber products." Ceramic fiber blanket, ceramic fiber board*. N.p., n.d. Web. 5 Apr. 2013. <http://www.ktrefractories.com/CeramicFiberProducts/CeramicFiberBoard.htm>.

[3] "Mechanical Charts - Thermal Conductivity of Materials at 20 degree Celsius." *Free Online Calculators for Engineers - Electrical, Mechanical, Electronics, Chemical,Construction, Optical, Medical, Physics, etc.* N.p., n.d. Web. 5 Apr. 2013. <http://www.calculatoredge.com/charts/mthconm.htm>. [4] Whitelaw, Jim H. "Convective Heat Transfer". http://www.thermopedia.com/content/660/

[5] Janssens, Marc L. "Improved Method for Analyzing Ignition Data from the Cone Calorimeter in the Vertical Orientation".

[6] DiNenno, P. J. (2008). SFPE handbook of fire protection engineering (4th ed.). Quincy, Mass.: National Fire Protection Association pg 1-78

[7] College of Engineering - University of Kentucky College of Engineering. "Interior of frustum of right circular cone to base." Radiation Configuration Factors C-111.html. http://www.engr.uky.edu/rtl/Catalog/sectionc/C-111.html (accessed April 23, 2013).

[8] College of Engineering - University of Kentucky College of Engineering. "Planar element dA1 to a circular disk A2 in a parallel plane. Element is offset from normal to disk center by distance a." Radiation Configuration Factors B-14.html. http://www.engr.uky.edu/rtl/Catalog/sectionb/B-14.html (accessed April 23, 2013).

[9] "Frustum of a Cone." Ditutor. http://www.ditutor.com/solid_gometry/frustum_cone.html (accessed April 23, 2013).

5.6 Appendix - Cone Calorimeter Statistical Analysis

5.6.1   Terminology/Nomenclature

Specimen - The size and material tested. See all specimens tested.

- 100mm by 100mm Kreysler 1
- 100mm by 100mm Kreysler 2
- 100mm by 100mm Creative Pultrusion 286
- 100mm by 100mm Creative Pultrusion 702
- 100mm by 100mm Creative Pultrusion 802
- 175mm by 175mm Kreysler 1
- 175mm by 175mm Kreysler 2
- 175mm by 175mm Creative Pultrusion 286
- 175mm by 175mm Creative Pultrusion 702
- 175mm by 175mm Creative Pultrusion 802

Sample - An individual test run in the cone. See all samples tested for selected specimens. (Similar samples for all other specimens)

- 100mm by 100mm Kreysler 1, Sample 1
- 100mm by 100mm Kreysler 1, Sample 2
- 175mm by 175mm Kreysler 1, Sample 1
- 175mm by 175mm Kreysler 1, Sample 2

AVG(...) = average of the values in parentheses

|...| = absolute value of values surrounded by bars

Standard Size = 100mm by 100mm (4"x4")

Extended Size = 175mm by 175mm (7"x7")

5.6.2   Procedure/Agenda

Compare the HRRPUA curves for time to ignition and HRRPUA averages for time intervals. Two samples were tested for each standard sized specimen that was tested and then two extended sized sample of the same specimen were tested. Testing was performed at 25 kW/m^2, 50 kW/m^2, and 75 kW/m^2 incident heat fluxes for two specimens provided by Kreysler and Associates (Kreysler 1 and Kreysler 2) and by Creative Pultrusions (CP 286, CP 702, and CP 802).

5.6.3   Analysis

The parameters analyzed for both samples sizes for all specimens tested are time to ignition and HRRPUA averages for time intervals: Ignition to 30 seconds, Ignition to 60 seconds, Ignition to 90 seconds, and Ignition to 120 seconds. It is important to note that averages and standard deviations were not used solely for statistical analysis because there were only two samples of each specimen tested. It is recommended that at least one additional sample of each specimen be tested to give a distribution of

data for more meaningful statistical analysis. Since this testing was not possible in the timeline of this project the analysis will continue with the data the team did gather.

Two samples of each specimen and size were tested and often did not result in the same value for the parameters analyzed, therefore, the percent difference for each specimen was determined. The percent difference was found using Equation 13:

$$\% \; difference \; standard \; size \; specimen = \frac{|x_1 - x_2|}{AVG(x_1, x_2)} \qquad \textbf{13}$$

where,

x_1 = parameter value of sample 1, standard size specimen

x_2 = parameter value of sample 2, standard size specimen

The same procedure was completed for extended samples, using Equation 14:

$$\% \; difference \; extended \; size \; specimen = \frac{|y_1 - y_2|}{AVG(y_1, y_2)} \qquad \textbf{14}$$

where,

y_1 = parameter value of sample 1, extended specimen

y_2 = parameter value of sample 2, extended specimen

The next step in analyzing the effect specimen size is to compute the percent difference between the standard sized specimens and extended sized specimens shown in Equation 15 - Equation 17.

$$\% \; difference \; between \; standard \; and \; extended = \frac{|x_a - y_a|}{AVG(x_a, y_a)} \qquad \textbf{15}$$

where,

$$x_a = AVG(x_1, x_2) \qquad \textbf{16}$$

where,

x_1 = parameter value of sample 1, standard size specimen

x_2 = parameter value of sample 2, standard size specimen

$$y_a = AVG(y_1, y_2) \qquad \textbf{17}$$

where,

y_1 = parameter value of sample 1, extended size specimen

y_2 = parameter value of sample 2, extended size specimen

This percent difference between the standard sized specimens and extended sized specimens found using Equation 15 is then compared to the difference in the standard sample size values found using Equation 13 and in the extended sample values found using Equation 14.

To determine if there is a significant difference between standard and extended sized samples, the percent difference between the standard sized specimens and extended sized specimens found using Equation 15 will be compared to the percent difference between samples of the same size, deemed an error that will be seen in the cone and is not a function of the different sample size. Since the percent difference in the standard sample values found using Equation 13 and in the extended sample values found using Equation 14 are often different, the root sum of the squares (RSS) will be found for each specimen and then will be compared to the percent difference between standard sized specimens and extended sized specimens. The RSS was performed for each specimen and is intended to give a combination of both standard samples and extended samples percent differences to get a total uncertainty or in this case percent difference. The RSS for each specimen can be found using Equation 18.

$$RSS = SQRT[(\% \ difference \ standard)^2 + (\% \ difference \ extended)^2] \qquad \textbf{18}$$

This RSS value created a population of differences expected between Cone samples during testing, where the average difference was found along with a standard deviation. The difference between specimen sizes was compared to this average value plus or minus a standard deviation. If the percent difference between specimen sizes did not exceeded the average RSS value plus a standard deviation, the difference between specimen size was considered to be an insignificant difference for that specific value being analyzed. The lower range was determined unimportant because it simply indicated more insignificance as this just indicated a decrease in difference.

This analysis helped the team determine if extended sized specimens are not significantly different from standard sized specimens. An extended specimen is determined to be significantly different if the percent difference in a specimen size at a specific IHF, size, and material exceeds the average RSS value plus a standard deviation, deemed as statistically different. This then allowed the team to assess the value of testing extended sized specimens versus the standard sized specimens to get a better understanding on when one dimensional burning stops.

See Appendix 5.6.7 for sample calculations of all the equations used above.

5.6.4   Time to Ignition

The time to ignition is defined using terminology from ASTM E1354 shown here,

> "Sustained flaming occurs once a flame exists over most of the test specimen surface for at least 4 s. The time to be reported as the time to sustained flaming is the time when the flaming was initially observed, not the time when the 4 s period elapsed."[1]

The time to ignition of the samples is first compared for standard sized specimens, i.e. sample 1 of standard specimen 1 is compared to sample 2 of standard specimen 1 and then for extended sized specimens. Table 7 gives the time to ignition percent difference values for standard sized specimens and for extended sized specimens.

	% Difference 100mm	% Difference 175mm
Kreysler 1 25 kW/m^2	18%	45%
Kreysler 2 25 kW/m^2	3%	17%
Kreysler 1 50 kW/m^2	5%	5%
Kreysler 2 50 kW/m^2	1%	10%
Kreysler 1 75 kW/m^2	24%	2%
Kreysler 2 75 kW/m^2	3%	4%
CP 286 25 kW/m^2	8%	17%
CP 702 25 kW/m^2	1%	35%
CP 802 25 kW/m^2	16%	2%
CP 286 50 kW/m^2	2%	6%
CP 702 50 kW/m^2	0%	14%
CP 802 50 kW/m^2	14%	18%
CP 286 75 kW/m^2	8%	11%
CP 702 75 kW/m^2	3%	19%
CP 802 75 kW/m^2	0%	53%

Table 7: Time to Ignition Percent Difference

Table 7 shows that standard sized specimens show better repeatability for time to ignition then all of the extended sized specimens. After comparing the times to ignition in between same sized samples, the percent difference between the standard sized specimens and extended sized specimens was found using Equation 15- Equation 17. Table 8 shows these values for each specimen at specific heat fluxes.

	% Difference Comparing 100mm and 175mm
Kreysler 1 25 kW/m^2	35%
Kreysler 2 25 kW/m^2	55%
Kreysler 1 50 kW/m^2	23%
Kreysler 2 50 kW/m^2	7%
Kreysler 1 75 kW/m^2	29%
Kreysler 2 75 kW/m^2	18%
CP 286 25 kW/m^2	32%
CP 702 25 kW/m^2	34%
CP 802 25 kW/m^2	13%
CP 286 50 kW/m^2	17%
CP 702 50 kW/m^2	12%
CP 802 50 kW/m^2	23%
CP 286 75 kW/m^2	14%
CP 702 75 kW/m^2	11%
CP 802 75 kW/m^2	62%

Table 8: Percent Difference Table between Average between Samples

Table 8 shows a rather large percent difference between the average time to ignition of standard sized samples of a specimen and the average time to ignition of extended sized samples of a specimen, which may allude to the fact that testing extended sized samples in lieu of standard sized samples may not be adequate. Although, it is possible that the large percent difference in samples of extended sized specimens may have carried through to give the large percent difference seen in Table 8.

As described in the Analysis section, the RSS was found for each specimen because it is intended to give a combination of both standard sized samples and extended sized samples percent differences to get a total uncertainty or in this case percent difference. Table 9 gives calculated RSS values and percent difference values between standard sized samples and extended sized samples given in Table 8 and indicates whether the extended samples are significantly different than the standard sample sizes based on criteria explained in Analysis section.

Time to Ignition			
	RSS for 100mm and 175mm	% Difference Comparing 100mm and 175mm	Is difference significant?
Kreysler 1 25 kW/m^2	48%	34%	Not Significant
Kreysler 2 25 kW/m^2	17%	55%	Significant
Kreysler 1 50 kW/m^2	7%	23%	Not Significant
Kreysler 2 50 kW/m^2	10%	7%	Not Significant
Kreysler 1 75 kW/m^2	24%	29%	Not Significant
Kreysler 2 75 kW/m^2	5%	18%	Not Significant
CP 286 25 kW/m^2	19%	31%	Not Significant
CP 702 25 kW/m^2	35%	34%	Not Significant
CP 802 25 kW/m^2	16%	12%	Not Significant
CP 286 50 kW/m^2	6%	17%	Not Significant
CP 702 50 kW/m^2	14%	11%	Not Significant
CP 802 50 kW/m^2	22%	23%	Not Significant
CP 286 75 kW/m^2	14%	13%	Not Significant
CP 702 75 kW/m^2	20%	10%	Not Significant
CP 802 75 kW/m^2	53%	61%	Significant
Average RSS	21%	Avg + 1 Stand Dev.	35%
Stand. Dev RSS	14%		

Table 9: Time to Ignition Significance Chart

Table 9 shows a majority of the % differences comparing standard and extended samples are not significantly different than the average plus 1 standard deviation of the RSS value indicating that standard and extended sized samples are not significantly different for time to ignition.

5.6.5 Average HRRPUA from Time to Ignition - 30 s, - 60 s, - 90, - 120 s

The HRRPUA data was obtained by taking HRR data in the cone and dividing by the burn area of the specimen, see Equation 19

$$HRRPUA = \frac{HRR}{A_S}$$

19

where,

HRR = Heat Release Rate (1 second data acquisition interval)

A_S : Burn Area of Sample

For standard sized specimens the A_S was a constant .009 m^2.

For extended sized specimens the A_S varied from test to test and was determined after the test by examining the burn area of the sample. Figure 28 shows a sample post testing which shows the burn area diameter by red lines. This value varies per sample tested but ranged from roughly .02 m^2 to .025 m^2.
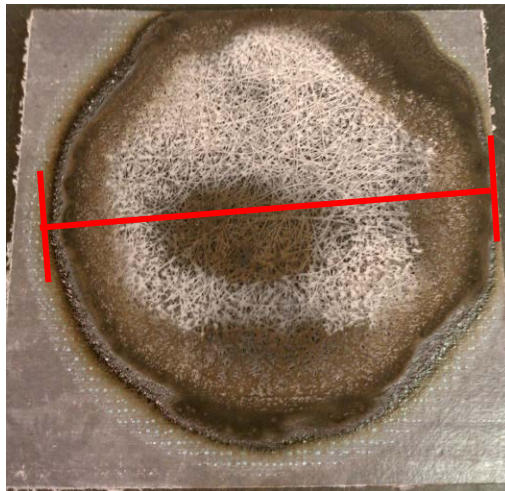
Figure 28: Burn area determination for extended samples.

The following equation was then used to find the Average HRRPUA.

$$Average\ HRRPUA = \frac{SUM\big(HRRPUA(Ignition), \dots, HRRPUA(t)\big)}{n}$$

20

where,

t = time duration of average (30 s, 60 s, 90 s, 120s)

n = number of data points

5.6.5.1 Average HRRPUA from Time to Ignition to 30 seconds

The same procedure is followed for the average HRRPUA comparisons as the procedure comparing time to ignition. Table 10 and Table 11 show percent differences between standard sized samples and percent difference between extended sized samples for Time to Ignition - 30 s average HRRPUA.

Percent Difference between 100mm 0-30 s Average HRRPUA		
IHF	**25kW/m^2**	**50kW/m^2**	**75kW/m^2**
Krey 1	50%	15%	6%
Krey 2	26%	1%	9%
IHF	**25kW/m^2**	**50kW/m^2**	**75kW/m^2**
CP 286	13%	0%	8%
CP 702	17%	1%	10%
CP 802	1%	5%	3%

Table 10: Percent difference between 100mm samples HRRPUA (Ignition - 30s)

Percent Difference between 175mm 0-30 s Average HRRPUA		
IHF	**25kW/m^2**	**50kW/m^2**	**75kW/m^2**
Krey 1	12%	8%	19%
Krey 2	4%	5%	8%
IHF	**25kW/m^2**	**50kW/m^2**	**75kW/m^2**
CP 286	12%	6%	7%
CP 702	7%	9%	9%
CP 802	20%	6%	4%

Table 11: Percent difference between 175mm samples HRRPUA (Ignition - 30s)

After comparing the average HRRPUA from time to ignition to 30s in between same sized samples, the percent difference between the standard sized specimens and extended sized specimens was found using Equation 15- Equation 17. Table 12 shows these values for each specimen at specific heat fluxes.

Percent Difference between 100mm and 175mm 0-30 s Average HRRPUA		
IHF	**25kW/m^2**	**50kW/m^2**	**75kW/m^2**
Krey 1	29%	21%	7%
Krey 2	46%	3%	3%
IHF	**25kW/m^2**	**50kW/m^2**	**75kW/m^2**
CP 286	25%	6%	7%
CP 702	16%	5%	19%
CP 802	42%	2%	8%

Table 12: Percent difference of average HRRPUA (Ignition - 30s) between 100mm and 175mm samples

Table 12 shows varying percent differences between the average HRRPUA of standard sized samples of a specimen and the average HRRPUA of extended sized samples of a specimen, which may allude to the fact that testing extended sized samples in lieu of standard sized samples may not be adequate.

As described in the Analysis section, the RSS was found for each specimen because it is intended to give a combination of both standard sized samples and extended sized samples percent differences to get a total uncertainty or in this case percent difference. Table 13 gives calculated RSS values and percent difference values between standard sized samples and extended sized samples given in Table 12 and indicates whether, the extended samples are significantly different than the standard sample sizes based on criteria explained in Analysis section.

Ignition - 30 s Average HRRPUA				
Sample	IHF	RSS for 100mm and 175mm	% Difference Comparing 100mm and 175mm	If difference significant?
Kreysler 1	25 kW/m^2	52%	29%	Significant
Kreysler 2	25 kW/m^2	26%	46%	Significant
Sample				
CP 286	25 kW/m^2	17%	25%	Not Significant
CP 702	25 kW/m^2	18%	16%	Not Significant
CP 802	25 kW/m^2	20%	42%	Significant

Ignition - 30 s Average HRRPUA				
Sample	IHF	RSS for 100mm and 175mm	% Difference Comparing 100mm and 175mm	If difference significant?
Kreysler 1	50 kW/m^2	17%	21%	Not Significant
Kreysler 2	50 kW/m^2	5%	3%	Not Significant
Sample				
CP 286	50 kW/m^2	6%	6%	Not Significant
CP 702	50 kW/m^2	9%	5%	Not Significant
CP 802	50 kW/m^2	8%	2%	Not Significant

Ignition - 30 s Average HRRPUA				
Sample	IHF	RSS for 100mm and 175mm	% Difference Comparing 100mm and 175mm	If difference significant?
Kreysler 1	75 kW/m^2	20%	7%	Not Significant
Kreysler 2	75 kW/m^2	12%	3%	Not Significant
Sample				
CP 286	75 kW/m^2	11%	7%	Not Significant
CP 702	75 kW/m^2	14%	19%	Not Significant
CP 802	75 kW/m^2	5%	8%	Not Significant

Average RSS		16%	Avg + 1 Stand Dev.	28%
Stand Dev. RSS		12%		

Table 13: HRRPUA (Ignition - 30s) Significance Chart

Table 13 shows a majority of the % differences comparing standard and extended samples are not significantly different than the average plus 1 standard deviation of the RSS value indicating that standard and extended sized samples are not significantly different for HRRPUA (Ignition to 30s).

5.6.5.2 Average HRRPUA from Time to Ignition to 60 seconds

The same procedure is followed for this section as with the proceeding section rendering similar conclusions. The same procedure is followed for average HRRPUA comparisons as the procedure comparing time to ignition. Table 14 and Table 15 show percent differences between standard sized samples and percent difference between extended sized samples for Time to Ignition - 60 s Average HRRPUA.

Percent Difference between 100mm 0-60 s Average HRRPUA			
IHF	25kW/m^2	50kW/m^2	75kW/m^2
Krey 1	51%	15%	50%
Krey 2	28%	9%	23%
IHF	25kW/m^2	50kW/m^2	75kW/m^2
CP 286	10%	0%	6%
CP 702	16%	2%	8%
CP 802	5%	6%	3%

Table 14: Percent difference between 100mm samples HRRPUA (Ignition - 60s)

Percent Difference between 175mm 0-60 s Average HRRPUA			
IHF	25kW/m^2	50kW/m^2	75kW/m^2
Krey 1	7%	0%	6%
Krey 2	4%	5%	10%
IHF	25kW/m^2	50kW/m^2	75kW/m^2
CP 286	7%	6%	5%
CP 702	48%	6%	6%
CP 802	15%	7%	3%

Table 15: Percent difference between 175mm samples HRRPUA (Ignition - 60s)

After comparing the average HRRPUA from time to ignition to 60s in between same sized samples, the percent difference between the standard sized specimens and extended sized specimens was found using Equation 15- Equation 17. Table 16 shows these values for each specimen at specific heat fluxes.

Percent Difference between 100mm and 175mm 0-60 s Average HRRPUA			
IHF	**25kW/m^2**	**50kW/m^2**	**75kW/m^2**
Krey 1	26%	3%	32%
Krey 2	48%	0%	20%
IHF	**25kW/m^2**	**50kW/m^2**	**75kW/m^2**
CP 286	18%	10%	2%
CP 702	34%	12%	10%
CP 802	33%	13%	15%

Table 16: Percent difference of average HRRPUA (Ignition - 60s) between 100mm and 175mm samples

Table 16 shows varying percent differences between the average HRRPUA of standard sized samples of a specimen and the average HRRPUA of extended sized samples of a specimen, which may allude to the fact that testing extended sized samples in lieu of standard sized samples may not be adequate.

As described in the Analysis section, the RSS was found for each specimen because it is intended to give a combination of both standard sized samples and extended sized samples percent differences to get a total uncertainty or in this case percent difference. Table 17 gives calculated RSS values and percent difference values between standard sized samples and extended sized samples given in Table 16 and indicates whether, the extended samples are significantly different than the standard sample sizes based on criteria explained in Analysis section.

Ignition - 60 s Average HRRPUA				
Sample	IHF	RSS for 100mm and 175mm	% Difference Comparing 100mm and 175mm	If difference significant?
Kreysler 1	25 kW/m^2	51%	26%	Not Significant
Kreysler 2	25 kW/m^2	28%	48%	Significant
Sample				
CP 286	25 kW/m^2	12%	18%	Not Significant
CP 702	25 kW/m^2	51%	34%	Not Significant
CP 802	25 kW/m^2	16%	33%	Not Significant

Ignition - 60 s Average HRRPUA				
Sample	IHF	RSS for 100mm and 175mm	% Difference Comparing 100mm and 175mm	If difference significant?
Kreysler 1	50 kW/m^2	15%	3%	Not Significant
Kreysler 2	50 kW/m^2	11%	0%	Not Significant
Sample				
CP 286	50 kW/m^2	6%	10%	Not Significant
CP 702	50 kW/m^2	6%	12%	Not Significant
CP 802	50 kW/m^2	10%	13%	Not Significant

Ignition - 60 s Average HRRPUA				
Sample	IHF	RSS for 100mm and 175mm	% Difference Comparing 100mm and 175mm	If difference significant?
Kreysler 1	75 kW/m^2	50%	32%	Not Significant
Kreysler 2	75 kW/m^2	25%	20%	Not Significant
Sample				
CP 286	75 kW/m^2	8%	2%	Not Significant
CP 702	75 kW/m^2	10%	10%	Not Significant
CP 802	75 kW/m^2	4%	15%	Not Significant
Average RSS		20%	Avg + 1 Stand Dev.	37%
Stand Dev. RSS		17%		

Table 17: HRRPUA (Ignition - 60s) Significance Chart

Table 17 shows that a majority of the % differences comparing standard and extended samples are not significantly different than the average plus 1 standard deviation of the RSS value indicating that standard and extended sized samples are not significantly different for HRRPUA (Ignition to 60s).

5.6.5.3 Average HRRPUA from Time to Ignition to 90 seconds

The same procedure is followed for this section as with the proceeding section rendering similar conclusions. The same procedure is followed for average HRRPUA comparisons as the procedure

comparing time to ignition. Table 18and Table 19 show percent differences between standard sized samples and percent difference between extended sized samples for Time to Ignition - 90 s Average HRRPUA.

Percent Difference between 100mm 0-90 s Average HRRPUA		
IHF	**25kW/m^2**	**50kW/m^2**	**75kW/m^2**
Krey 1	73%	14%	84%
Krey 2	11%	11%	54%
IHF	**25kW/m^2**	**50kW/m^2**	**75kW/m^2**
CP 286	10%	6%	3%
CP 702	17%	0%	7%
CP 802	6%	6%	3%

Table 18: Percent difference between 100mm samples HRRPUA (Ignition - 90s)

Percent Difference between 175mm 0-90 s Average HRRPUA		
IHF	**25kW/m^2**	**50kW/m^2**	**75kW/m^2**
Krey 1	47%	1%	1%
Krey 2	3%	3%	9%
IHF	**25kW/m^2**	**50kW/m^2**	**75kW/m^2**
CP 286	5%	9%	2%
CP 702	77%	3%	11%
CP 802	12%	8%	3%

Table 19: Percent difference between 175mm samples HRRPUA (Ignition - 90s)

After comparing the average HRRPUA from time to ignition to 90s in between same sized samples, the percent difference between the standard sized specimens and extended sized specimens was found using Equation 15- Equation 17. Table 20 shows these values for each specimen at specific heat fluxes.

Percent Difference between 100mm and 175mm 0-90 s Average HRRPUA		
IHF	**25kW/m^2**	**50kW/m^2**	**75kW/m^2**
Krey 1	18%	5%	52%
Krey 2	33%	4%	40%
IHF	**25kW/m^2**	**50kW/m^2**	**75kW/m^2**
CP 286	15%	42%	1%
CP 702	46%	16%	7%
CP 802	29%	20%	19%

Table 20: Percent difference of average HRRPUA (Ignition - 90s) between 100mm and 175mm samples

Table 20 shows varying percent differences between the average HRRPUA of standard sized samples of a specimen and the average HRRPUA of extended sized samples of a specimen, which may allude to the fact that testing extended sized samples in lieu of standard sized samples may not be adequate.

As described in the Analysis section, the RSS was found for each specimen because it is intended to give a combination of both standard sized samples and extended sized samples percent differences to get a total uncertainty or in this case percent difference. Table 21 gives calculated RSS values and percent difference values between standard sized samples and extended sized samples given in Table 20 and indicates whether, the extended samples are significantly different than the standard sample sizes based on criteria explained in Analysis section.

Ignition - 90 s Average HRRPUA				
Sample	IHF	RSS for 100mm and 175mm	% Difference Comparing 100mm and 175mm	If difference significant?
Kreysler 1	25 kW/m^2	87%	18%	Not Significant
Kreysler 2	25 kW/m^2	11%	33%	Not Significant
Sample				
CP 286	25 kW/m^2	11%	15%	Not Significant
CP 702	25 kW/m^2	79%	46%	Not Significant
CP 802	25 kW/m^2	14%	29%	Not Significant

Ignition - 90 s Average HRRPUA				
Sample	IHF	RSS for 100mm and 175mm	% Difference Comparing 100mm and 175mm	If difference significant?
Kreysler 1	50 kW/m^2	14%	5%	Not Significant
Kreysler 2	50 kW/m^2	12%	4%	Not Significant
Sample				
CP 286	50 kW/m^2	10%	42%	Not Significant
CP 702	50 kW/m^2	3%	16%	Not Significant
CP 802	50 kW/m^2	10%	20%	Not Significant

Ignition - 90 s Average HRRPUA				
Sample	IHF	RSS for 100mm and 175mm	% Difference Comparing 100mm and 175mm	If difference significant?
Kreysler 1	75 kW/m^2	84%	52%	Not Significant
Kreysler 2	75 kW/m^2	55%	40%	Not Significant
Sample				
CP 286	75 kW/m^2	3%	1%	Not Significant
CP 702	75 kW/m^2	13%	7%	Not Significant
CP 802	75 kW/m^2	4%	19%	Not Significant

Average RSS		27%	Avg + 1 Stand Dev.	59%
Stand Dev. RSS		31%		

Table 21: HRRPUA (Ignition - 90s) Significance Chart

Table 21 shows that all % differences comparing standard and extended samples are not significantly different than the average plus 1 standard deviation of the RSS value indicating that standard and extended sized samples are not significantly different for HRRPUA (Ignition to 90s).

5.6.5.4 Average HRRPUA from Time to Ignition to 120 seconds

The same procedure is followed for this section as with the proceeding section rendering similar conclusions. The same procedure is followed for HRRPUA comparisons as the procedure comparing time to ignition. Table 22 and Table 23 show percent differences between standard sized samples and percent difference between extended sized samples for Time to Ignition - 120 s HRRPUA.

Percent Difference between 100mm 0-120 s Average HRRPUA		
IHF	**25kW/m^2**	**50kW/m^2**	**75kW/m^2**
Krey 1	94%	15%	105%
Krey 2	15%	13%	57%
IHF	**25kW/m^2**	**50kW/m^2**	**75kW/m^2**
CP 286	11%	6%	1%
CP 702	17%	1%	9%
CP 802	6%	4%	2%

Table 22: Percent difference between 100mm samples HRRPUA (Ignition - 120s)

Percent Difference between 175mm 0-120 s Average HRRPUA		
IHF	**25kW/m^2**	**50kW/m^2**	**75kW/m^2**
Krey 1	77%	1%	2%
Krey 2	8%	4%	8%
IHF	**25kW/m^2**	**50kW/m^2**	**75kW/m^2**
CP 286	6%	0%	2%
CP 702	95%	0%	41%
CP 802	9%	9%	29%

Table 23: Percent difference between 175mm samples HRRPUA (Ignition - 120s)

After comparing the average HRRPUA from time to ignition to 120s in between same sized samples, the percent difference between the standard sized specimens and extended sized specimens was found using Equation 15- Equation 17. Table 24 shows these values for each specimen at specific heat fluxes.

Percent Difference between 100mm and 175mm 0-120 s Average HRRPUA			
IHF	**25kW/m^2**	**50kW/m^2**	**75kW/m^2**
Krey 1	21%	9%	61%
Krey 2	15%	5%	62%
IHF	**25kW/m^2**	**50kW/m^2**	**75kW/m^2**
CP 286	31%	65%	26%
CP 702	54%	17%	17%
CP 802	25%	24%	8%

Table 24: Percent difference of average HRRPUA (Ignition - 120s) between 100mm and 175mm samples

Table 24 shows varying percent differences between the average HRRPUA of standard sized samples of a specimen and the average HRRPUA of extended sized samples of a specimen, which may allude to the fact that testing extended sized samples in lieu of standard sized samples may not be adequate.

As described in the Analysis section, the RSS was found for each specimen because it is intended to give a combination of both standard sized samples and extended sized samples percent differences to get a total uncertainty or in this case percent difference. Table 25 gives calculated RSS values and percent difference values between standard sized samples and extended sized samples given in Table 24 and indicates whether, the extended samples are significantly different than the standard sample sizes based on criteria explained in Analysis section.

Ignition - 120 s Average HRRPUA				
Sample	IHF	RSS for 100mm and 175mm	% Difference Comparing 100mm and 175mm	If difference significant?
Kreysler 1	25 kW/m^2	121%	21%	Not Significant
Kreysler 2	25 kW/m^2	17%	15%	Not Significant
Sample				
CP 286	25 kW/m^2	12%	31%	Not Significant
CP 702	25 kW/m^2	96%	54%	Not Significant
CP 802	25 kW/m^2	11%	25%	Not Significant

Ignition - 120 s Average HRRPUA				
Sample	IHF	RSS for 100mm and 175mm	% Difference Comparing 100mm and 175mm	If difference significant?
Kreysler 1	50 kW/m^2	15%	9%	Not Significant
Kreysler 2	50 kW/m^2	13%	5%	Not Significant
Sample				
CP 286	50 kW/m^2	6%	65%	Not Significant
CP 702	50 kW/m^2	1%	17%	Not Significant
CP 802	50 kW/m^2	10%	24%	Not Significant

Ignition - 120 s Average HRRPUA				
Sample	IHF	RSS for 100mm and 175mm	% Difference Comparing 100mm and 175mm	If difference significant?
Kreysler 1	75 kW/m^2	105%	61%	Not Significant
Kreysler 2	75 kW/m^2	58%	62%	Not Significant
Sample				
CP 286	75 kW/m^2	3%	26%	Not Significant
CP 702	75 kW/m^2	42%	17%	Not Significant
CP 802	75 kW/m^2	29%	8%	Not Significant

Average RSS		36%	Avg + 1 Stand Dev.	76%
Stand Dev. RSS		40%		

Table 25: HRRPUA (Ignition - 120s) Significance Chart

Table 25 shows that all % differences comparing standard and extended samples are not significantly different than the average plus 1 standard deviation of the RSS value indicating that standard and extended sized samples are not significantly different for HRRPUA (Ignition to 120s).

5.6.6 Conclusion

In conclusion, if standard sized specimens and extended sized specimens of the same material exposed to the same incident heat flux are compared directly for values of time to ignition and average HRRPUA it appears they are not significantly different. This can be seen in Table 26 where red highlighted cells indicate significant differences. Where these is a significant difference it really means the difference between standard and extended samples is more than the average difference between individual samples of both sizes plus a standard deviation. Since this is only the case for a few configurations and a certain set of fire characteristics it is determined the two specimen sizes are not significantly different and can be tested in lieu of one another, where an extended sample would be preferred where edge burning may occur.

	Difference between Samples Size (Average Time to Ignition)	Difference between Samples Size (Average HRRPUA Ignition - 30s)	Difference between Samples Size (Average HRRPUA Ignition - 60s)	Difference between Samples Size (Average HRRPUA Ignition - 90s)	Difference between Samples Size (Average HRRPUA Ignition - 120s)
Kreysler 1 - 25 kW/m^2	34%	29%	26%	18%	21%
Kreysler 2 - 25 kW/m^2	55%	46%	48%	33%	15%
Kresyler 1 - 50 kW/m^2	23%	21%	3%	5%	9%
Kresyler 2 - 50 kW/m^2	7%	3%	0%	4%	5%
Kresyler 1 - 75 kW/m^2	29%	7%	32%	52%	61%
Kresyler 2 - 75 kW/m^2	18%	3%	20%	40%	62%
CP 286 - 25 kW/m^2	31%	25%	18%	15%	31%
CP 702 - 25 kW/m^2	34%	16%	34%	46%	54%
CP 802 - 25 kW/m^2	12%	42%	33%	29%	25%
CP 286 - 50 kW/m^2	17%	6%	10%	42%	65%
CP 702 - 50 kW/m^2	11%	5%	12%	16%	17%
CP 802 - 50 kW/m^2	23%	2%	13%	20%	24%
CP 286 - 75 kW/m^2	13%	7%	2%	1%	26%
CP 702 - 75 kW/m^2	10%	19%	10%	7%	17%
CP 802 - 75 kW/m^2	61%	8%	15%	19%	8%
Average RSS	21%	16%	20%	27%	36%
Standard Deviation RSS	14%	12%	17%	31%	40%

Table 26: Significance Difference Chart

---

[1] ASTM Standard E1354, 2003, "Standard Test Method for Heat and Visible Smoke Release Rates for Materials and Products Using an Oxygen Consumption Calorimeter," ASTM International, West Conshohocken, PA, 2011, DOI: 10.1520/E1354-11B, www.astm.org.

5.6.7 Appendix - Sample Calcs

The following shows sample calculations for Kreysler 1 specimens at exposed to a IHF of 50kW/m^2 for time to ignition.

$x_1 := 128s$ $\qquad\qquad\qquad\qquad$ $y_1 := 101s$

$x_2 := 134s$ $\qquad\qquad\qquad\qquad$ $y_2 := 106s$

$Eq_1 := \dfrac{\left|x_1 - x_2\right|}{\text{hmean}\left(x_1, x_2\right)}$ $\qquad\qquad$ $Eq_2 := \dfrac{\left|y_1 - y_2\right|}{\text{hmean}\left(y_1, y_2\right)}$

$Eq_1 = 0.046$ $\qquad\qquad\qquad$ $Eq_2 = 0.048$

$x_a := \text{hmean}\left(x_1, x_2\right)$ $\qquad\qquad$ $y_a := \text{hmean}\left(y_1, y_2\right)$

$x_a = 130.931s$ $\qquad\qquad\qquad$ $y_a = 103.44s$

$Eq_3 := \dfrac{\left|x_a - y_a\right|}{\text{hmean}\left(x_a, y_a\right)}$

$Eq_3 = 0.238$

$Eq_5 := \sqrt{\left(Eq_1\right)^2 + \left(Eq_2\right)^2} = 0.067$

Compare the % difference between standard and extended specimens to the average of the population of RSS (Eq.5) values for all time to ignition data plus the standard deviation of this data to determine if difference is significance. It turns out the average RSS + standard deviation is .35, so the Kreysler 1 specimen sizes are not significantly different tested at IHF of 50 kW/m^2 for the time to ignition parameter.

5.7 Appendix: Cone Calorimeter Inter- and Intra- Differences

Primary Author: Christian Acosta

For the case of time of ignition the two equations used were

$$r = 4.1 + .125t_{ig}$$

$$R = 7.4 + .220t_{ig}$$

And for the case of HRPUA, the equations used were for a heat release rate of a max of 180 since there was not an equation which applied to the measured max of 120

$$r = 23.3 + .037q_{prime}$$

$$R = 25.5 + .151q_{Prime}$$

The difference in both variables is that 'r' represents the repeatability found within one laboratory during multiple tests. However the variable 'R' represents the repeatability found when a different laboratory runs the same test.

The numbers calculated for the time to ignition provide us with the 95% probability that the results of the second test for inter-® laboratory will fall within the range and for the results of that laboratory for intra-® laboratory testing will fall within that range given.

The following table shows the average 'r' and 'R' values obtained for the entire test we ran for time of ignition.

Table 27: Time to Ignition Uncertainty Values at Various IHF's

Samples at IHF	4x4 TOI(sec)	175mm by 175mm TOI(sec)	r-Avg for TOI(s)	R-Avg for TOI(s)
Kreysler 1-25kW/m^2	0	303	23.6983	27.1256
Kreysler 2-25 kW/m^2	0	291	24.0211	28.4428
Kreysler 1-50 kW/m^2	118	97	17.5375	31.05
Kreysler 2-50 kW/m^2	105	99	25.6287	35.0035
Kreysler 1-75 kW/m^2	37	44	9.1625	16.31
Kreysler 2-75 kW/m^2	49	64	11.1625	19.83
CP 286-50 kW/m^2	47	37	9.35	16.64
CP 702-50 kW/m^2	67	59	11.975	21.26
CP 802-50 kW/m^2	30	24	7.475	13.34
CP 286-75 kW/m^2	8	15	5.5375	9.93
CP 702-75 kW/m^2	19	21	6.6	11.8
CP-802-75 kW/m^2	4	1	4.4125	7.95

The difference values between the HRRPUA for both standard and extended samples were graphed along with both specimen size ignition times at the incident heat fluxes of 25 kW/m2, 50 kW/m2 and 75 kW/m2 for both Kreysler specimen and 50 kW/m2 and 75 kW/m2 for the Creative Pultrusion specimens.

This type of comparison is useful in the sense of understanding how the HRRPUA varies for each test and how much both sample sizes deviate from each other throughout testing. The steady line found at the beginning of the graphs is the difference in HRRPUA pre-ignition, which is why this line is found at the zeroed area. The peak found after this point is due to the ignition of one of the specimen sizes. The size of the peak will highly depend on how fast the first specimen size ignites in comparison to the other. The noise found after the large peak translate to being the difference in HRRPUA during sustained burning. Looking at the graphs, not only does it show us that the time of ignition is usually earlier for the 7"x7" specimens than the 4"x4", but it also burns at a level of 20-30kw/m^2 greater than the 4"x4" specimen.

This was the case found at the majority of the incident heat fluxes, however for a few case it was different. At the incident heat flux of 25kw, for both Kreysler 1 and Kreysler 2, the HRRPUA for 7"x7" were the only values recorded because the 4"x4" had not ignited until after the 7"x7" burnt out. However, for the case of the 7"x7" testing, a lot of the times, the test were ended sooner than specimen burnt out due to the fact that the test had gotten out of control. This may have in fact disrupted the data and caused for a flame out time that was sooner than normal. Also, there were 3 cases where the 4"x4" specimens ignited sooner than the 7"x7" specimen which caused a concave peak in the negative region. Though, after ignition, the steady noise rose back into the positive 20-30kw/m^2 range.

Note: For simplicity graphs are labeled in English units i.e. 4x4, which is 100mm by 100mm, and 7x7, which is 175mm by 175mm.
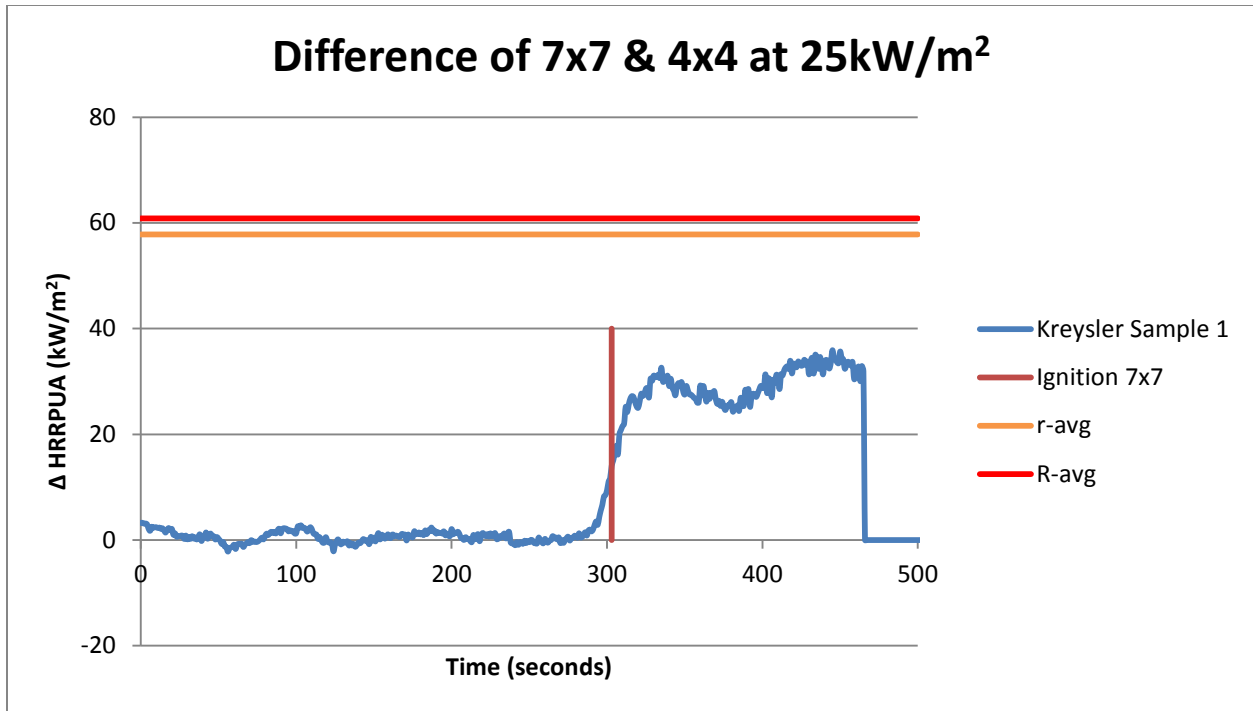
Figure 29: Kreysler 1 HRRPUA Difference Graph at IHF of 25 kW/m^2
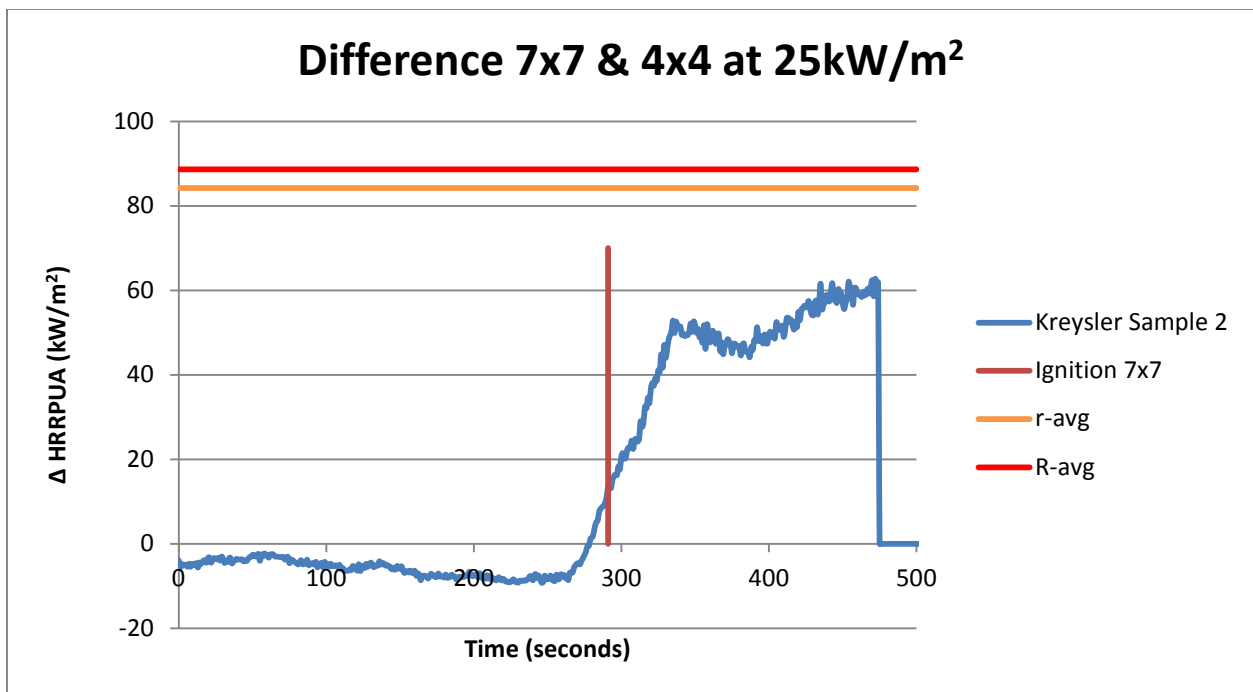
Figure 30: Kreysler 2 HRRPUA Difference Graph at IHF of 25 kW/m^2
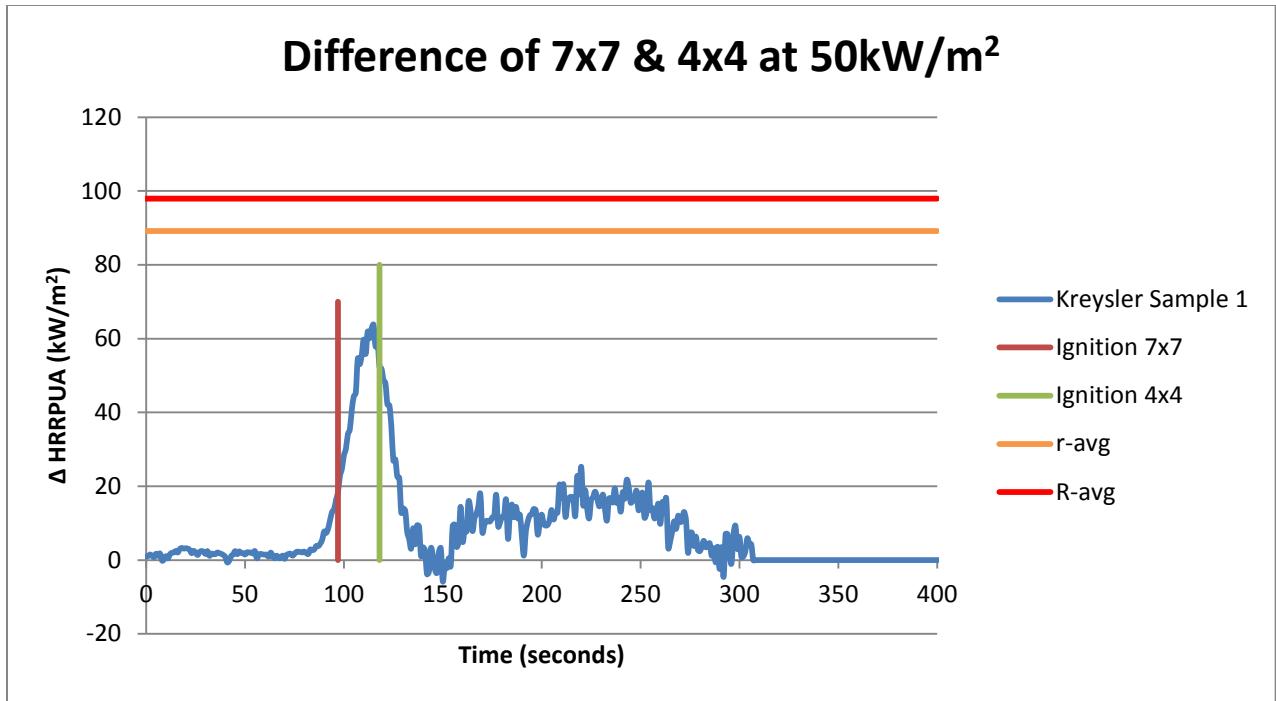
Figure 31: Kreysler 1 HRRPUA Difference Graph at IHF of 50 kW/m^2
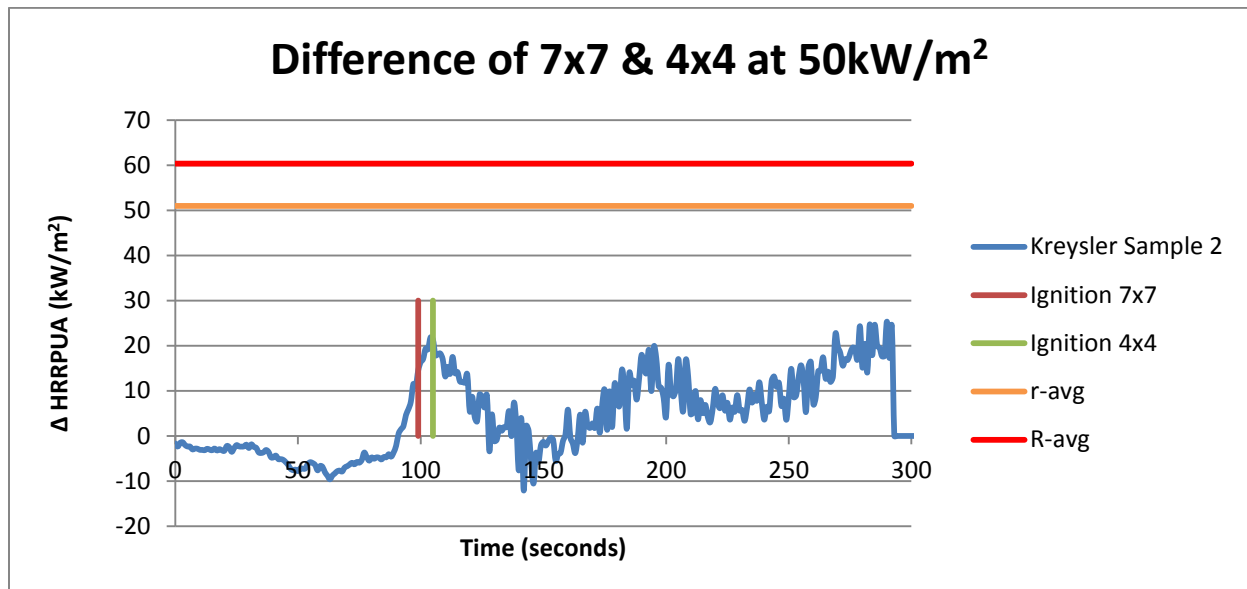
Figure 32: Kreysler 2 HRRPUA Difference Graph at IHF of 50 kW/m^2
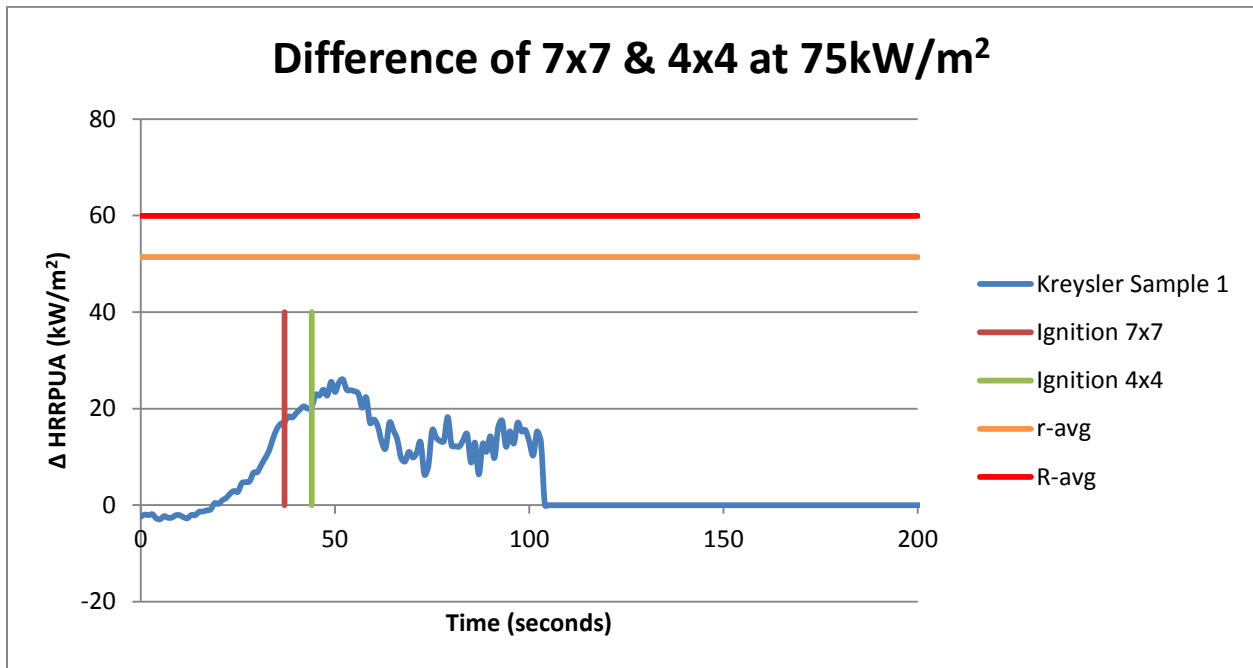
Figure 33: Kreysler 1 HRRPUA Difference Graph at IHF of 75 kW/m^2
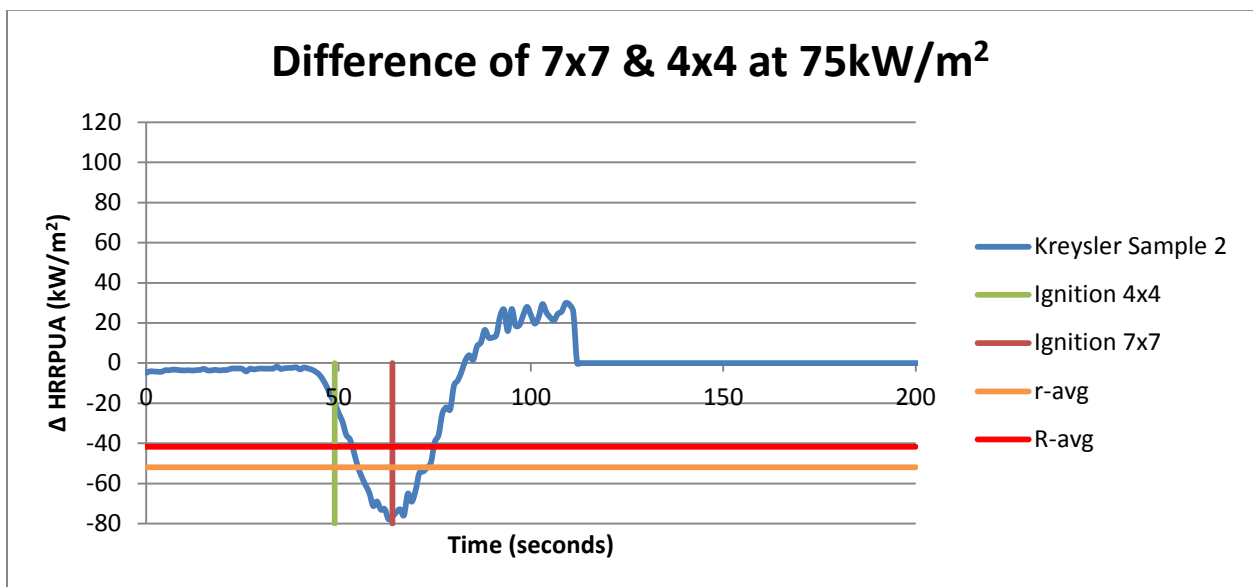
Figure 34: Kreysler 2 HRRPUA Difference Graph at IHF of 75 kW/m^2
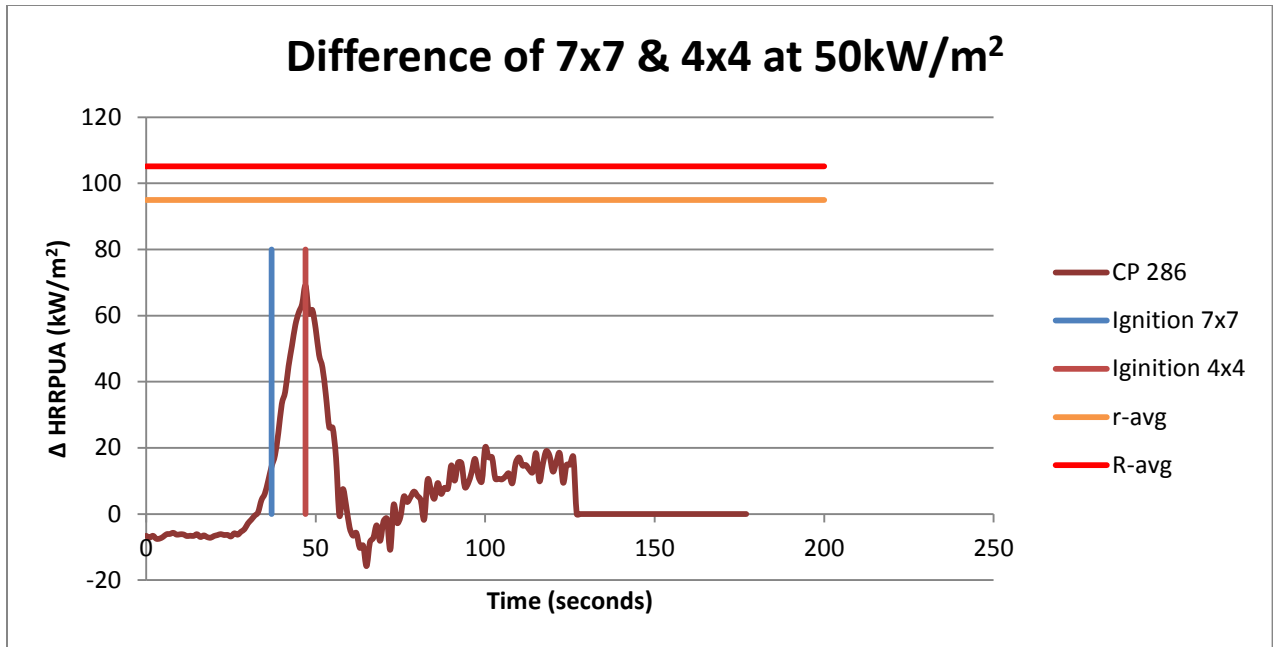
Figure 35: CP 286 HRRPUA Difference Graph at IHF of 50 kW/m²
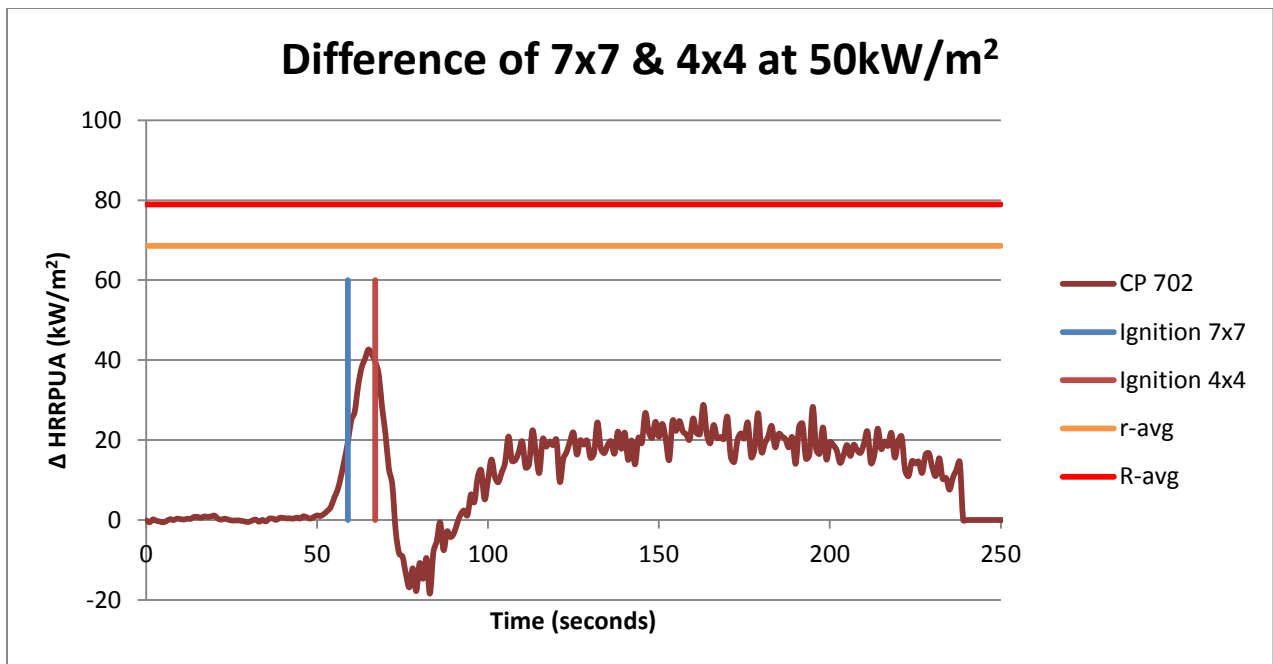
Figure 36 CP 702 HRRPUA Difference Graph at IHF of 50 kW/m²
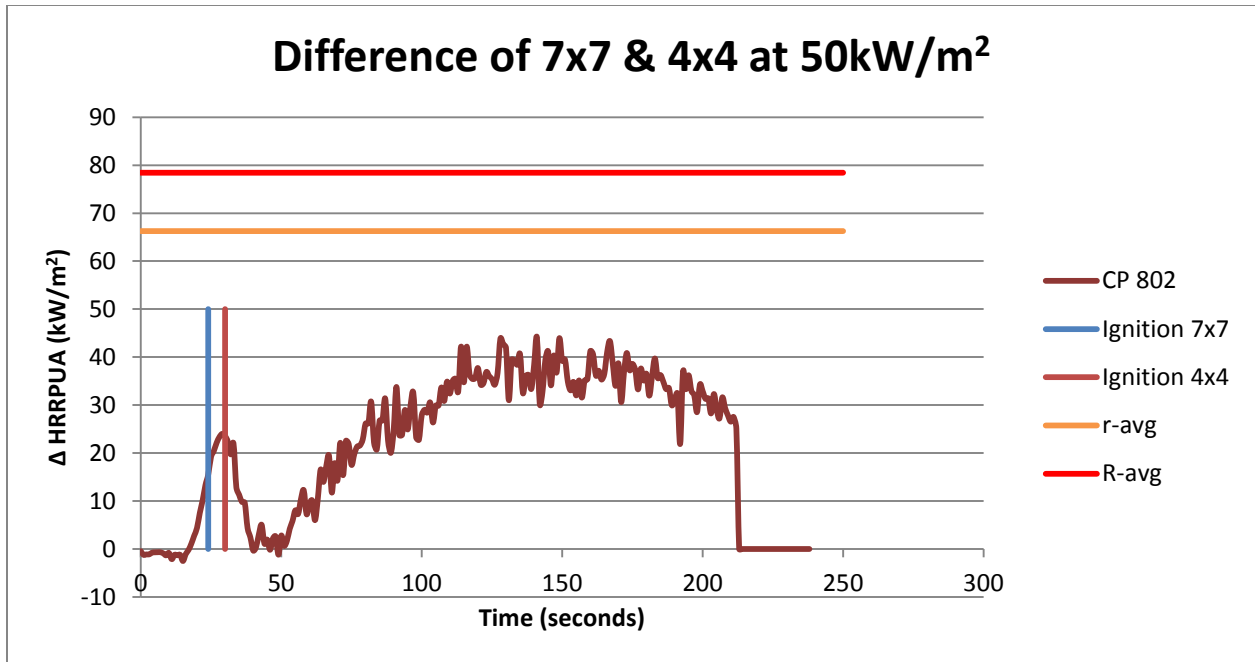
Figure 37: CP 802 HRRPUA Difference Graph at IHF of 50 kW/m²
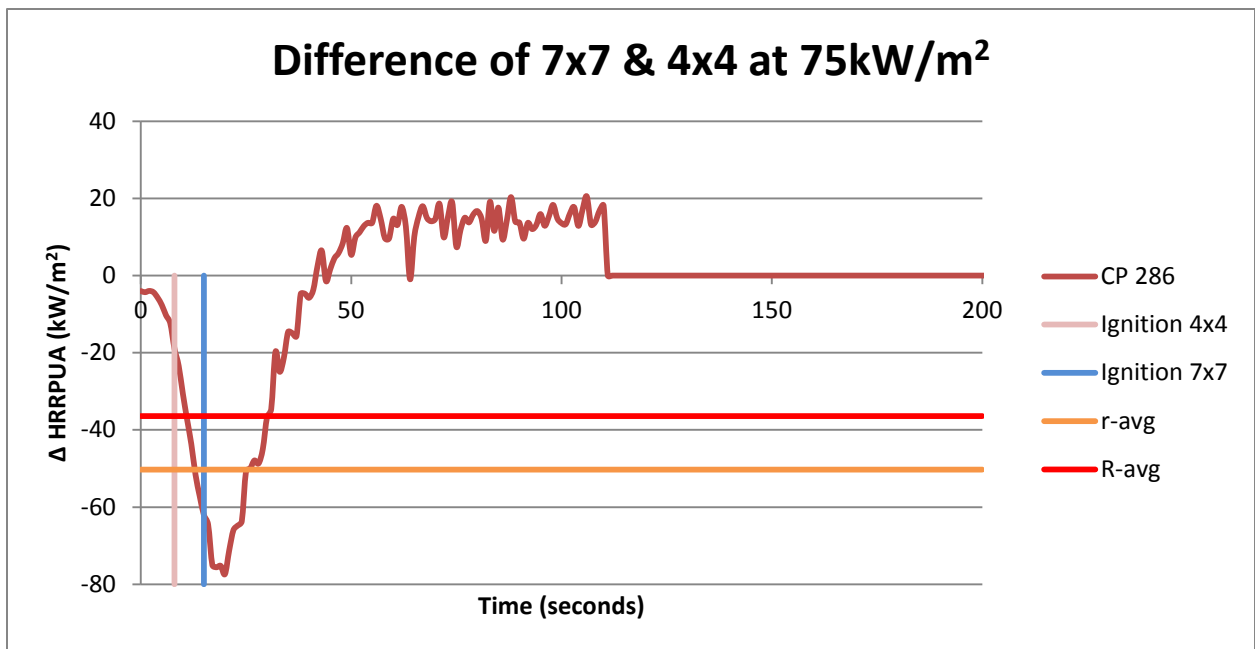
Figure 38 CP 286 HRRPUA Difference Graph at IHF of 75 kW/m²
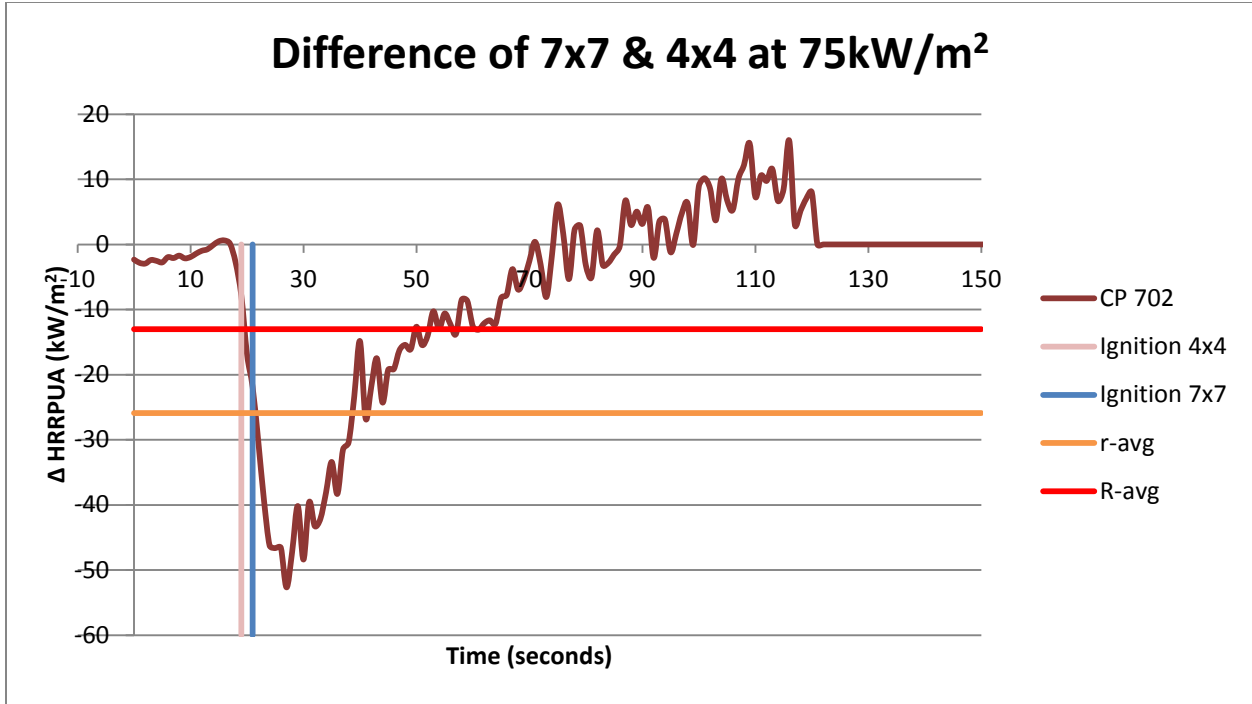
Figure 39: CP 702 HRRPUA Difference Graph at IHF of 75 kW/m²
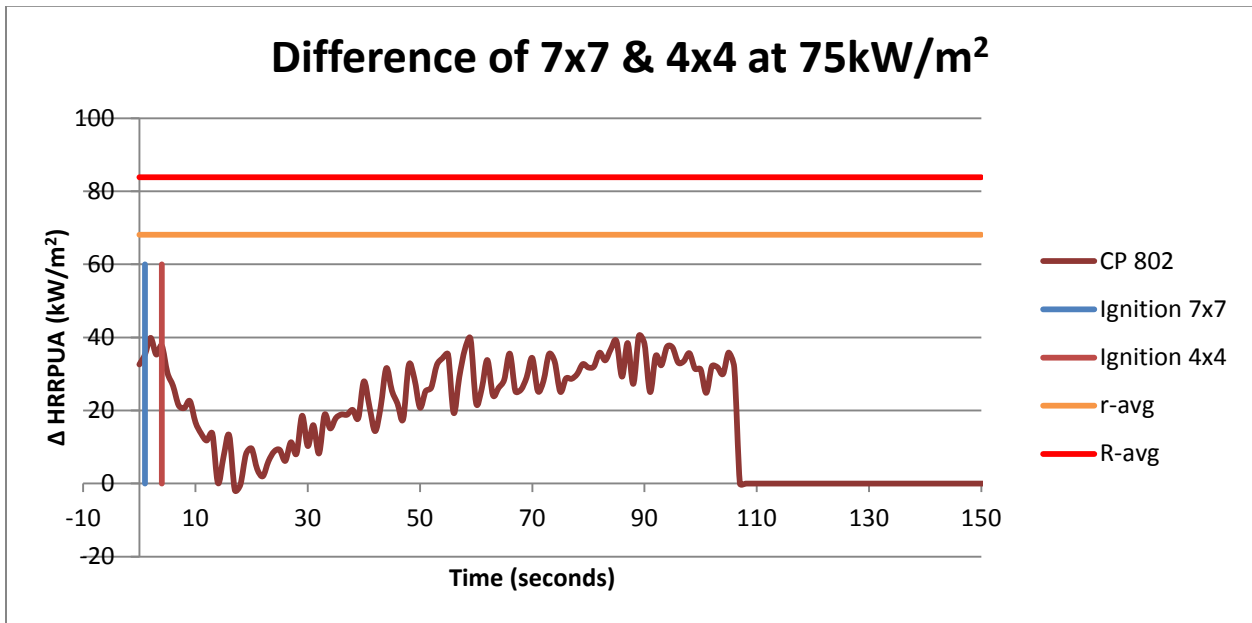
Figure 40: CP 802 HRRPUA Difference Graph at IHF of 75 kW/m²

5.8 Appendix - B Parameter

Primary Author: Nicholas Nava

The flammability parameter (B-parameter) as defined and described in Mowrer and Williamson was used to assess whether or not a material will propagate.[1] The equation used for the B-parameter was:

$$B = .01*(HRRPUA)-1-(Tig/Tb)$$

The tables below show the charts for the Kreysler and Creative Pultrusion samples which were used to solve for the B Parameter.

Table 28: B Parameter Table for Kreysler Samples

	B	.01 * HRRPUA - 1 - (Tig/Tb)			
	Tig	Time to ignition - shutter open time			
	Tb	Burn time - time to ignition			
Heat Flux (kW/m^2)	Sample	Average HRRPUA (kW/m^2)	Tig (s)	Tb (s)	B-Parameters
25	Kreysler System 1, Sample 1	33.2884	619	136	-5.2186
25	Kreysler System 1, Sample 2	50.2023	515	118	-4.8624
25	Kreysler System 2, Sample 1	63.9033	542	230	-2.7175
25	Kreysler System 2, Sample 2	81.4302	525	301	-1.9299
30	Kreysler System 1, Sample 1	48.7721	251	119	-2.6215
30	Kreysler System 1, Sample 2	64.0654	298	77	-4.2295
30	Kreysler System 2, Sample 1	77.8241	278	153	-2.0388
30	Kreysler System 2, Sample 2	68.1013	273	205	-1.6507
40	Kreysler System 1, Sample 1	57.8741	201	111	-2.2321
40	Kreysler System 1, Sample 2	70.0721	175	141	-1.5404
40	Kreysler System 2, Sample 1	84.1502	194	111	-1.9062
40	Kreysler System 2, Sample 2	88.7924	195	110	-1.8848
50	Kreysler System 1, Sample 1	74.1754	128	273	-0.7271
50	Kreysler System 1, Sample 2	80.2299	134	320	-0.6165
50	Kreysler System 2, Sample 1	89.3685	118	339	-0.4544
50	Kreysler System 2, Sample 2	75.1500	117	336	-0.5967
75	Kreysler System 1, Sample 1	69.9252	55	146	-0.6775
75	Kreysler System 1, Sample 2	74.2788	70	130	-0.7957
75	Kreysler System 2, Sample 1	93.2415	62	89	-0.7642
75	Kreysler System 2, Sample 2	90.1302	64	87	-0.8343

Table 29: B Parameter Table for CP Samples

	B	.01 * HRRPUA - 1 - (Tig/Tb)			
	Tig	Time to ignition - shutter open time			
	Tb	Burn time - time to ignition			
Heat Flux (kW/m^2)	Sample	Average HRRPUA (kW/m^2)	Tig (s)	Tb (s)	B-Parameters
15	Creative Pultrusion 286, Sample 1	66.6354592	646	124	-5.54332
15	Creative Pultrusion 286, Sample 2	0	933	-937	0
15	Creative Pultrusion 802, Sample 1	59.45696559	536	185	-3.30273
15	Creative Pultrusion 802, Sample 2	66.55816947	741	189	-4.25505
20	Creative Pultrusion 286, Sample 1	96.91956667	407	89	-4.60384
20	Creative Pultrusion 286, Sample 2	78.01693578	398	108	-3.90502
20	Creative Pultrusion 702, Sample 1	0	611	-615	0
20	Creative Pultrusion 702, Sample 2	0	603	-607	0
20	Creative Pultrusion 802, Sample 1	84.28420041	335	241	-1.54720
20	Creative Pultrusion 802, Sample 2	75.97688777	299	277	-1.31965
25	Creative Pultrusion 702, Sample 1	86.25988431	389	152	-2.69661
25	Creative Pultrusion 702, Sample 2	72.83838511	386	140	-3.02876
30	Creative Pultrusion 286, Sample 1	82.3008	176	164	-1.25016
30	Creative Pultrusion 286, Sample 2	87.5749	162	164	-1.11206
30	Creative Pultrusion 702, Sample 1	79.3482	255	121	-2.31396
30	Creative Pultrusion 702, Sample 2	89.9181	224	134	-1.77246
30	Creative Pultrusion 802, Sample 1	88.1609	148	107	-1.50157
30	Creative Pultrusion 802, Sample 2	84.7373	174	90	-2.08596
40	Creative Pultrusion 286, Sample 1	84.2954	115	136	-1.00263
40	Creative Pultrusion 286, Sample 2	78.7760	111	124	-1.10740
40	Creative Pultrusion 702, Sample 1	87.5061	133	133	-1.12494
40	Creative Pultrusion 702, Sample 2	89.3807	142	132	-1.18195
40	Creative Pultrusion 802, Sample 1	103.2999	112	89	-1.22543
40	Creative Pultrusion 802, Sample 2	103.5492	109	99	-1.06552
50	Creative Pultrusion 286, Sample 1	93.3300	63	102	-0.68435
50	Creative Pultrusion 286, Sample 2	93.8431	62	86	-0.78250
50	Creative Pultrusion 702, Sample 1	88.3320	82	97	-0.96204
50	Creative Pultrusion 702, Sample 2	89.2315	82	81	-1.12003
50	Creative Pultrusion 802, Sample 1	88.3736	46	93	-0.61089
50	Creative Pultrusion 802, Sample 2	85.4011	40	38	-1.19862
75	Creative Pultrusion 286, Sample 1	111.5730	23	65	-0.2381
75	Creative Pultrusion 286, Sample 2	110.5507	25	44	-0.4627
75	Creative Pultrusion 702, Sample 1	107.3199	35	89	-0.3201
75	Creative Pultrusion 702, Sample 2	118.3305	34	54	-0.4463
75	Creative Pultrusion 802, Sample 1	110.2291	18	77	-0.1315
75	Creative Pultrusion 802, Sample 2	106.9687	18	67	-0.1990

The following plots show the B Parameter for Kreysler samples and Creative Pultrusion samples as a function of indicant heat flux.
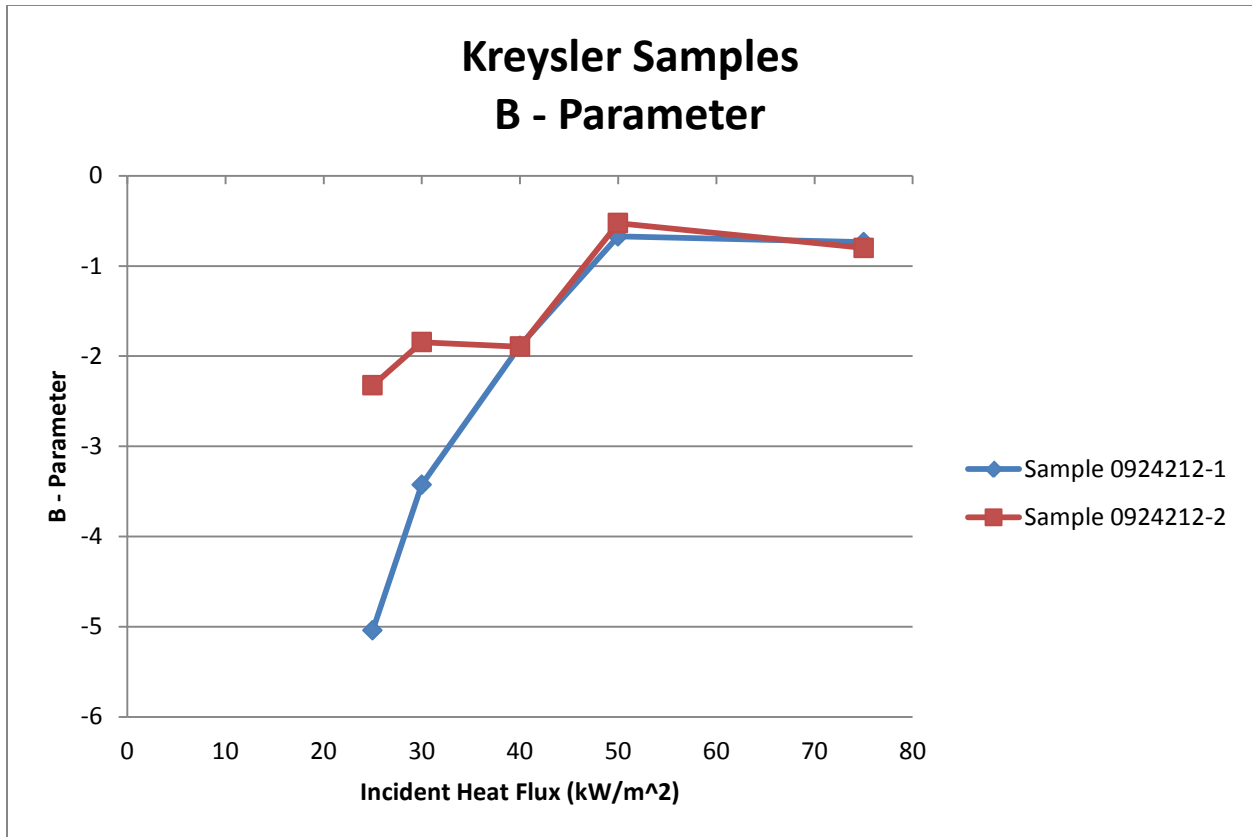
Figure 41: Kreysler B Parameter Graph
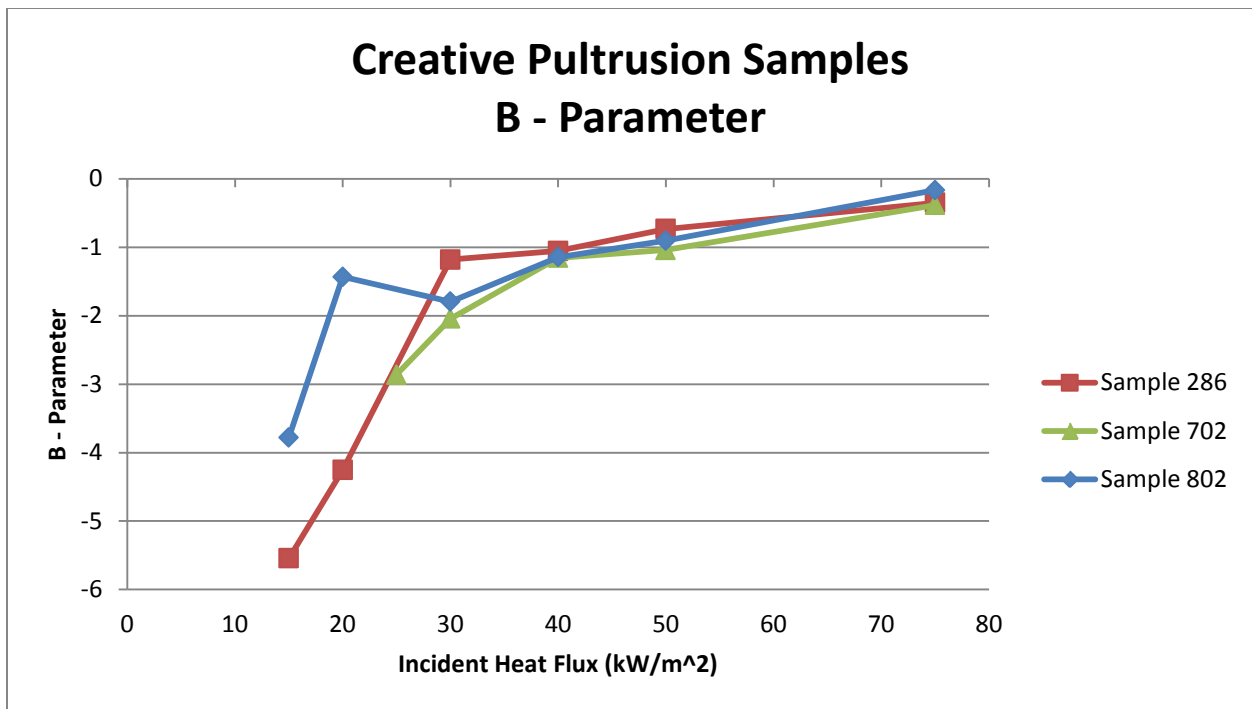
Figure 42: CP Samples B Parameter Graph
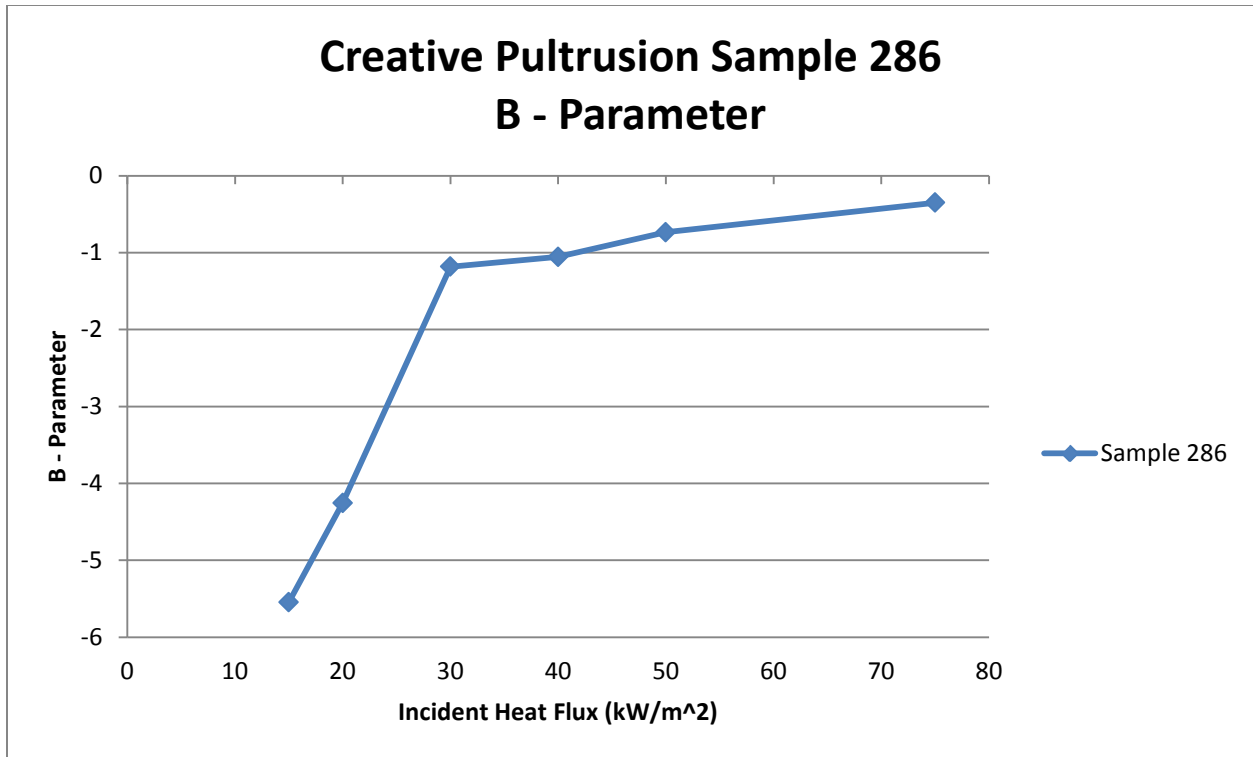
Figure 43: CP 286 Sample B Parameter Graph
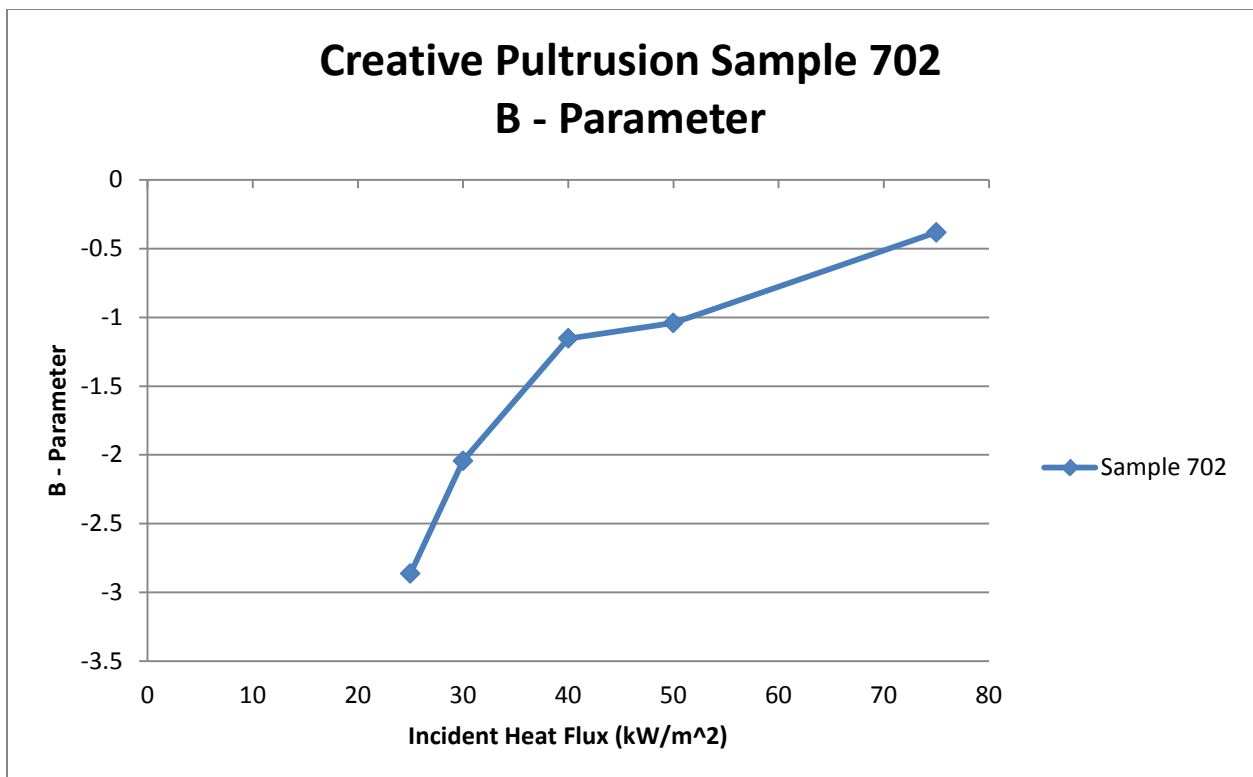
Figure 44: CP 702 Samples B Parameter Graph
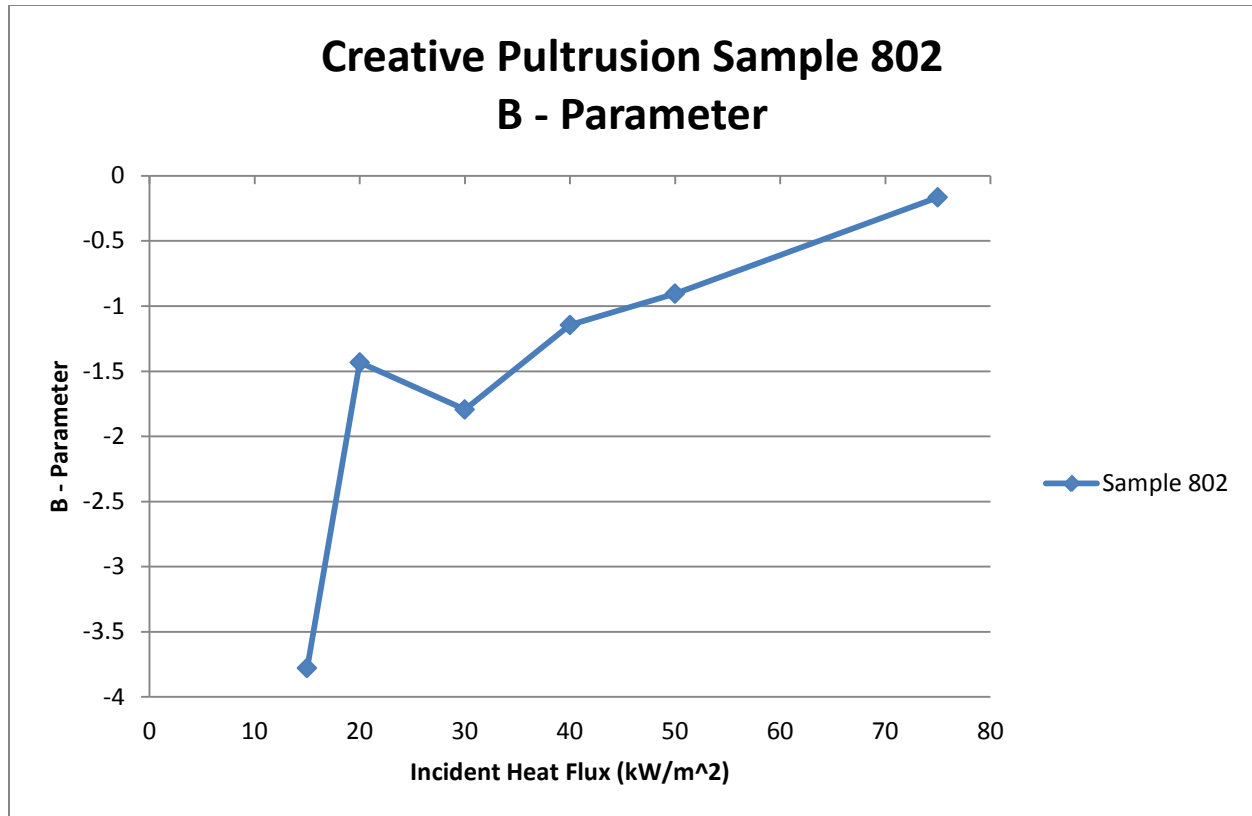
Figure 45: CP 802 Sample B Parameter Graph

It can be seen in the figures above the B-Parameter increases as the incident heat flux increases which is to be expected. A similar analysis was done for a 30 sec Peak HRRPUA but was not included here because the results were very similar.

It can be seen that the flame spread parameter does not rise above 0. The B-Parameter is useful if we know a sample does not spread flame and one that does spread so we can create a B-Parameter range for flame spread. This is useful data but will only be used further if we do not have success with a fixed pyrolysis length method of spread.

5.8.1   References

Mowrer, F.W., and Williamson, R.B.. "Flame Spread Evaluation for Thin Interior Finish
Materials". *Fire Safety Science-Proceedings of the Third International Symposium*, p. 689-698. [1]

5.9 Appendix - Cone Analysis Database

Primary Compiler: Christian Acosta
Secondary Compiler: Nicholas Nava
Primary Chart Creators: Shawn Mahoney, Nicholas Nava
Secondary Chart Creator: Christian Acosta

The following database shows data from testing in the Cone.

Note: For reader to be able to relate more to size, graphs are labeled in English units i.e. 4"x4", which is 100mm by 100mm, and 7"x7", which is 175mm by 175mm).

5.9.1   HRRPUA: 100 mm x 100 mm Specimens
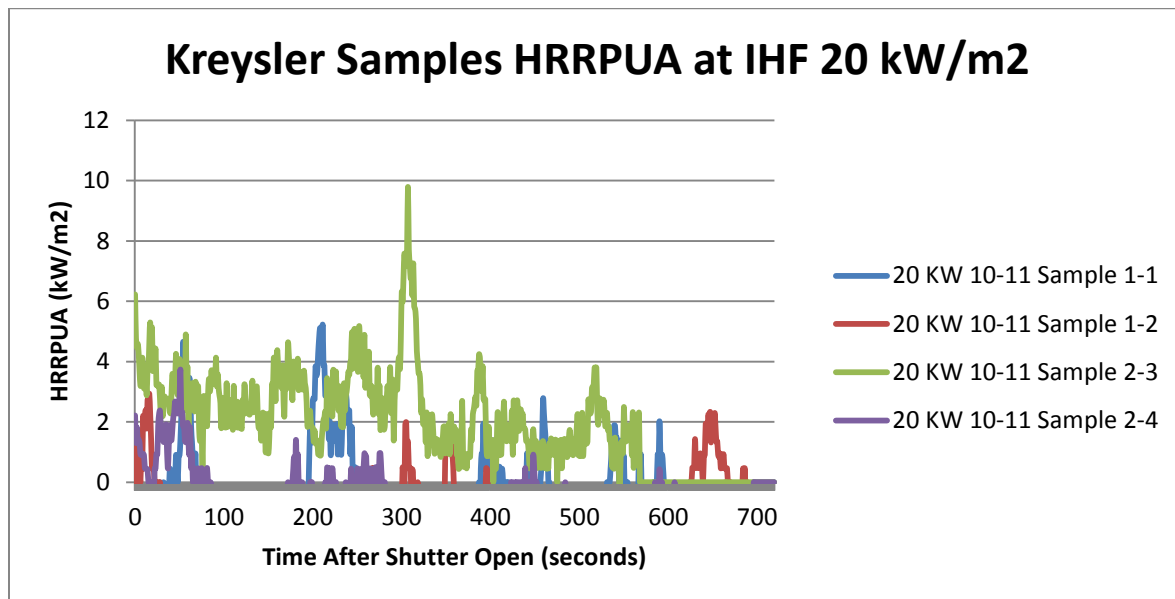
Figure 46: Standard Size Kreysler HRRPUA IHF 20kW/m^2
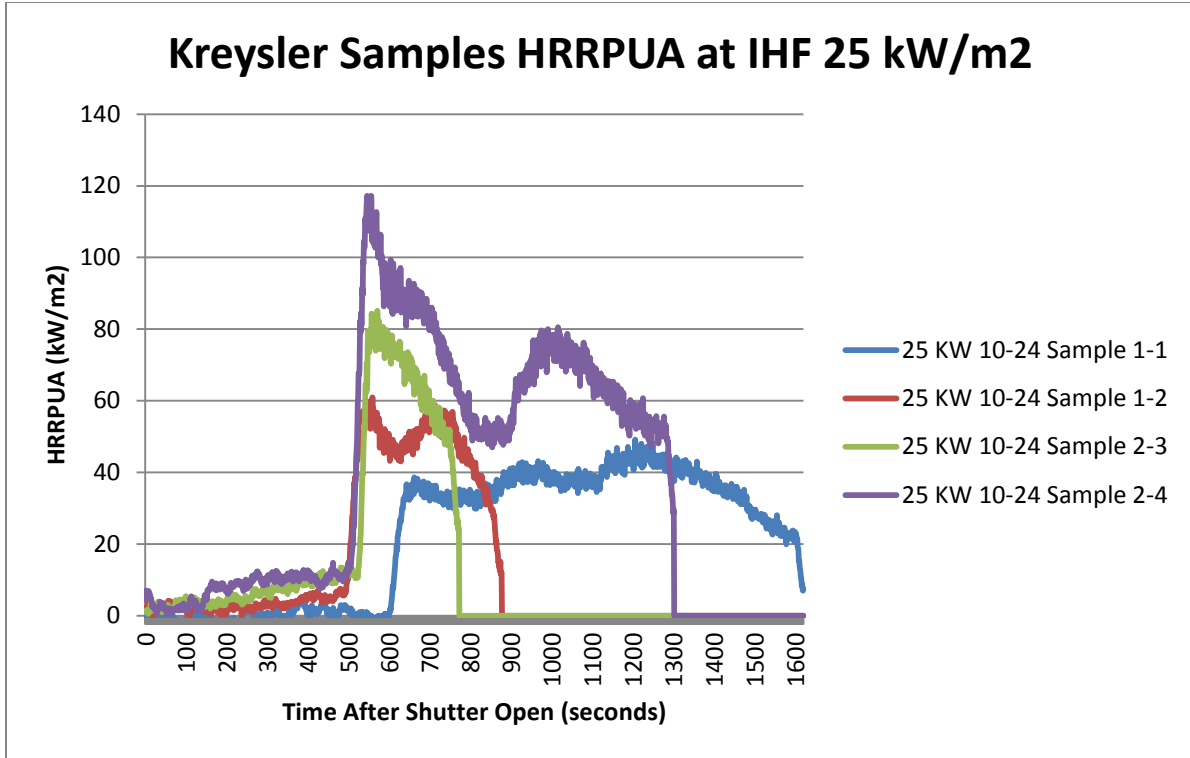
Figure 47: Standard Size Kreysler HRRPUA IHF 25kW/m^2
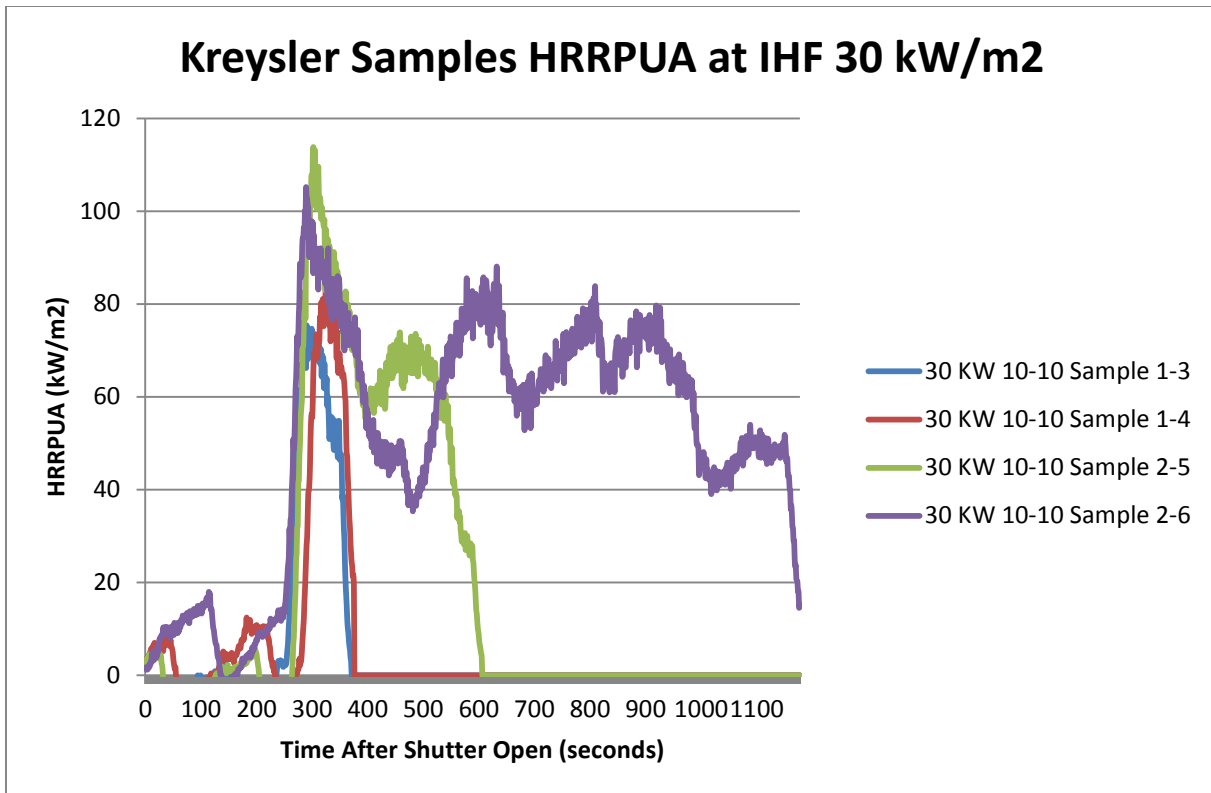
Figure 48: Standard Size Kreysler HRRPUA IHF 30kW/m^2
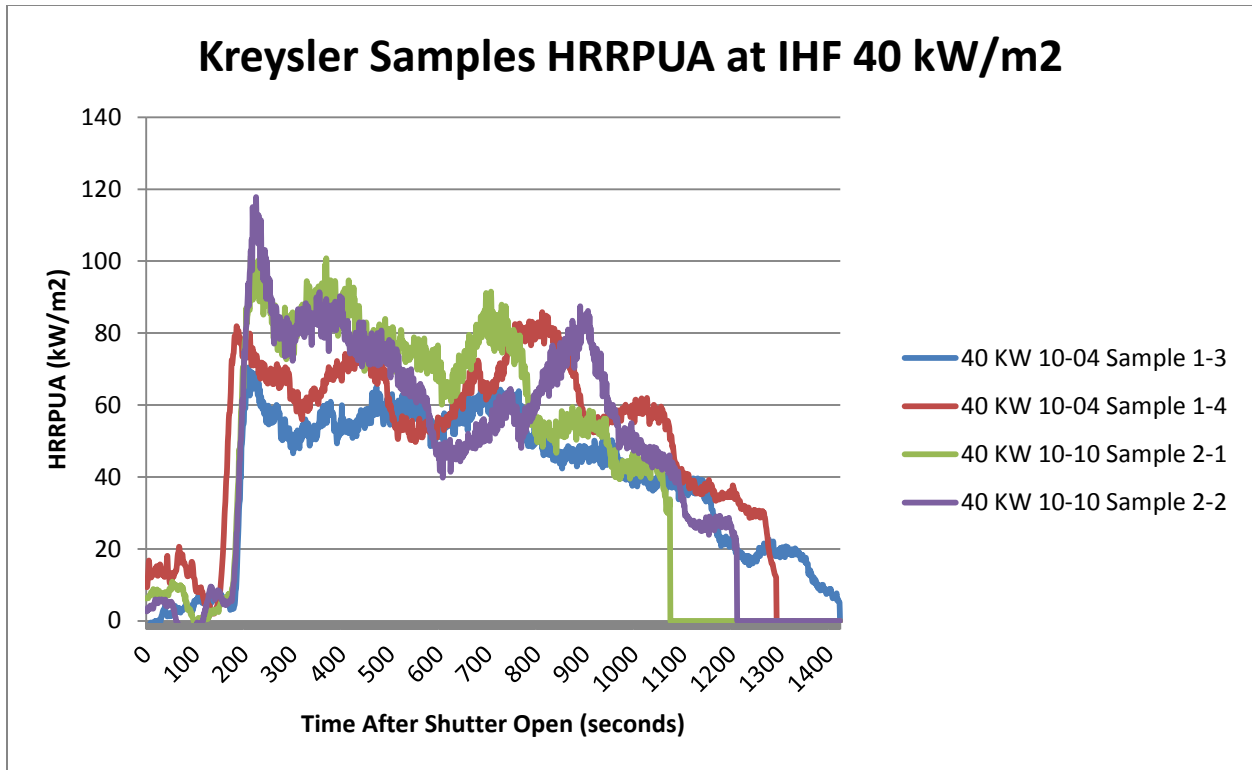
Figure 49: Standard Size Kreysler HRRPUA IHF 40kW/m²
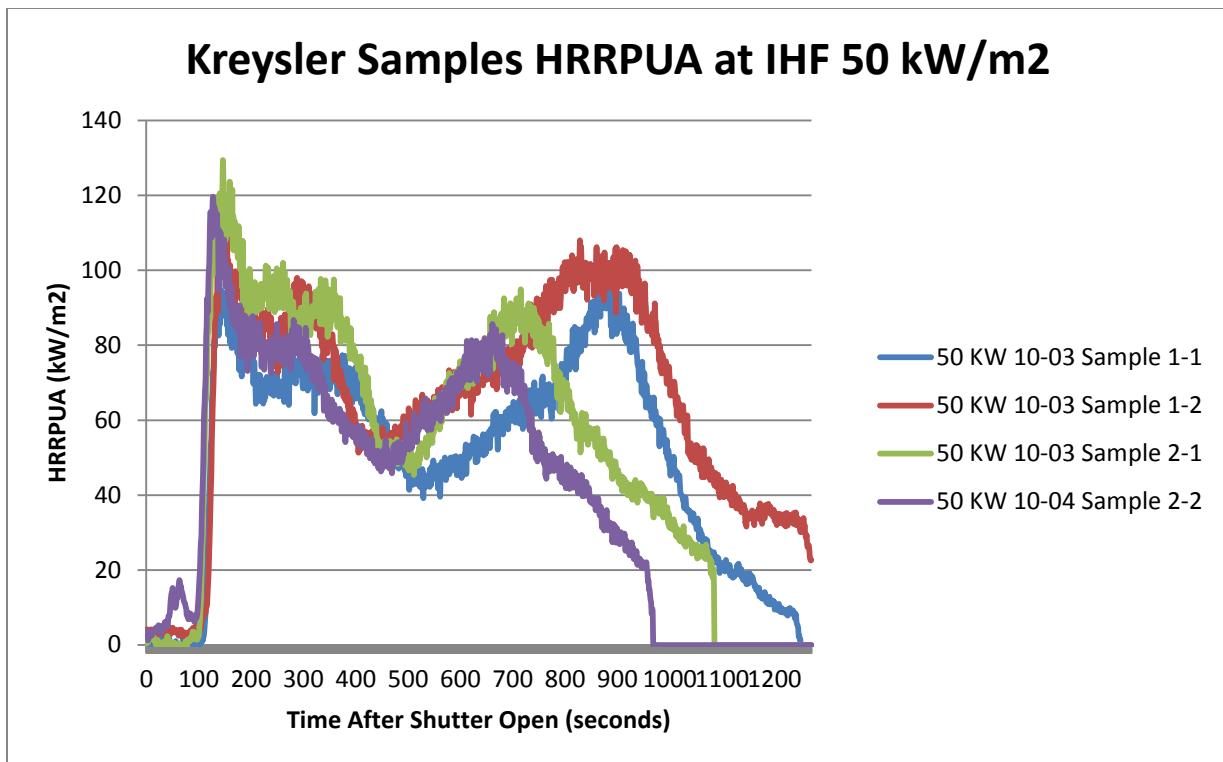
Figure 50: Standard Size Kreysler HRRPUA IHF 50kW/m²
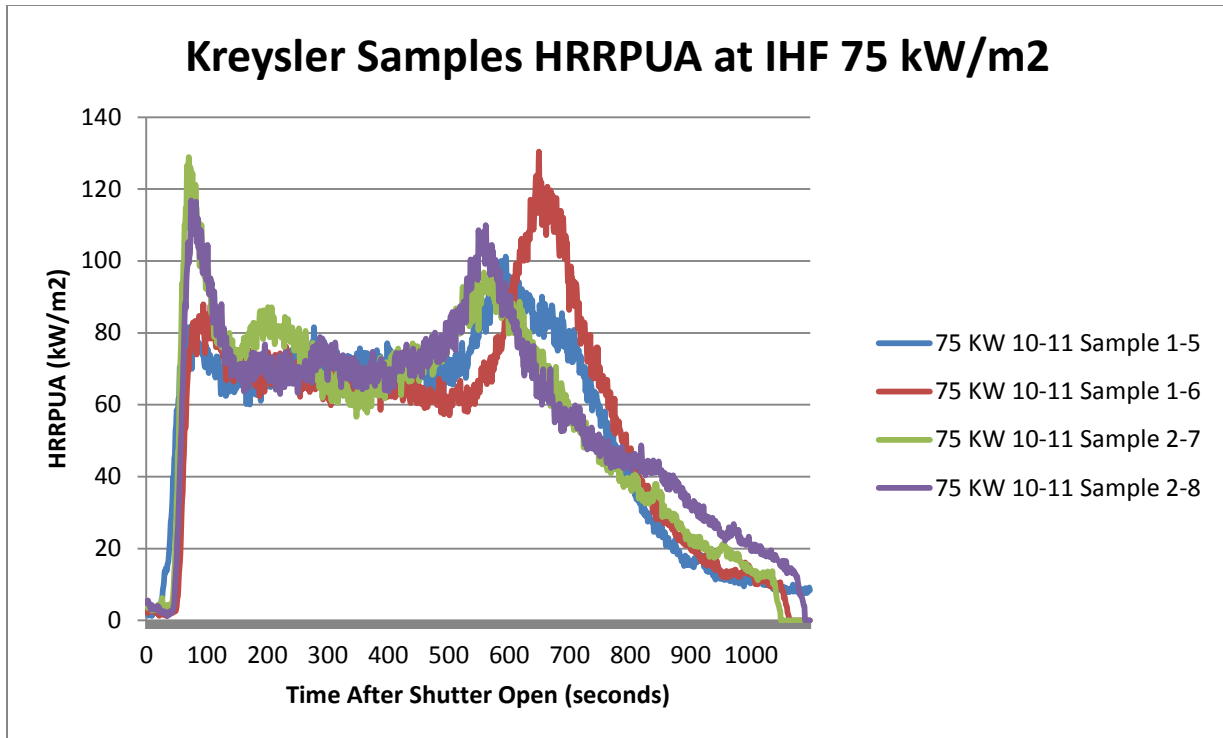
Figure 51: Standard Size Kreysler HRRPUA IHF 75kW/m²
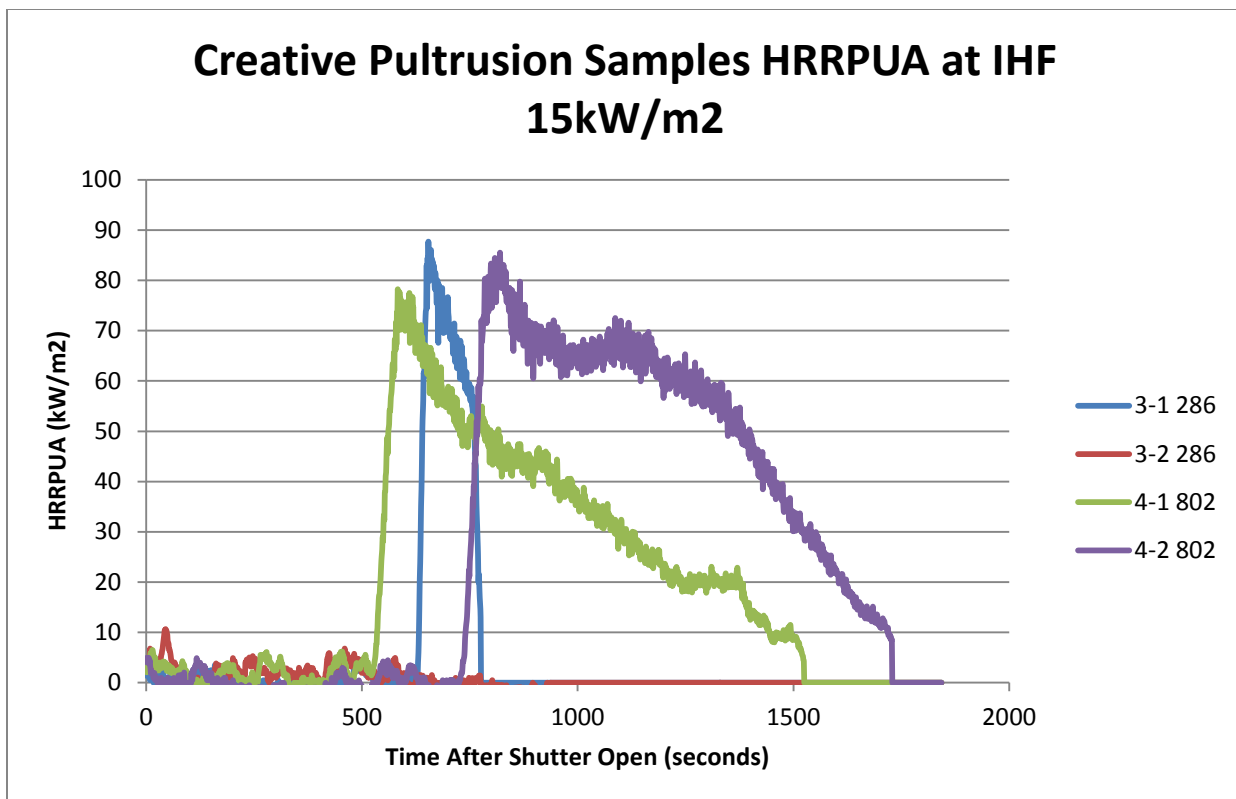
Figure 52: Standard Size CP HRRPUA IHF 15kW/m²
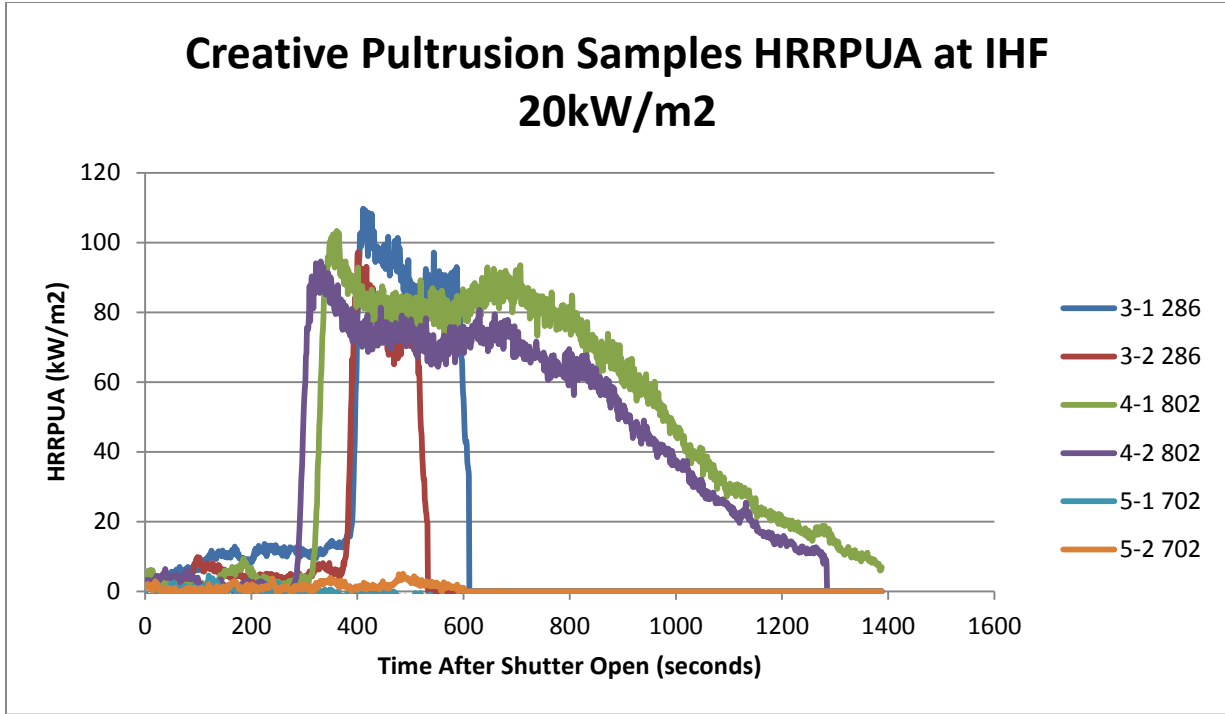
Figure 53: Standard Size CP HRRPUA IHF 20kW/m^{2}
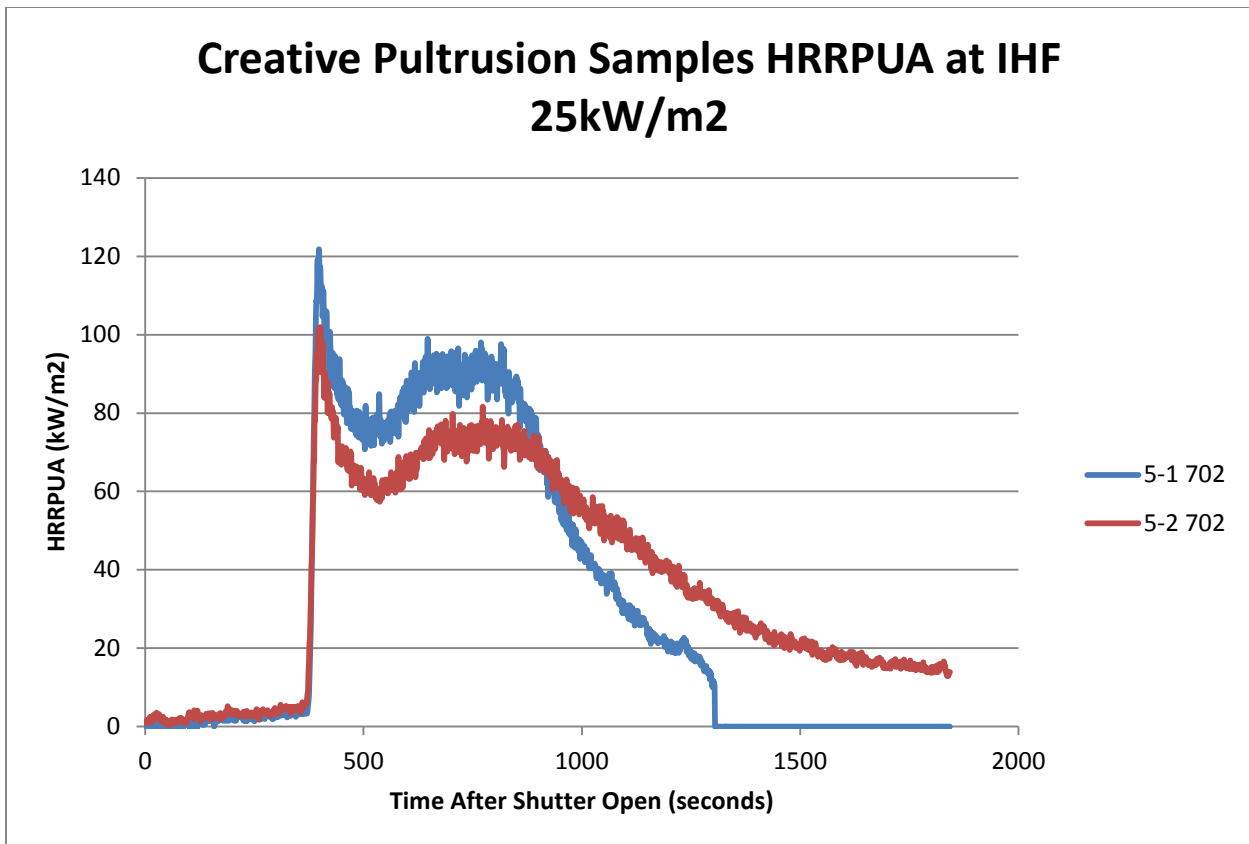
Figure 54: Standard Size CP HRRPUA IHF 25kW/m^{2}
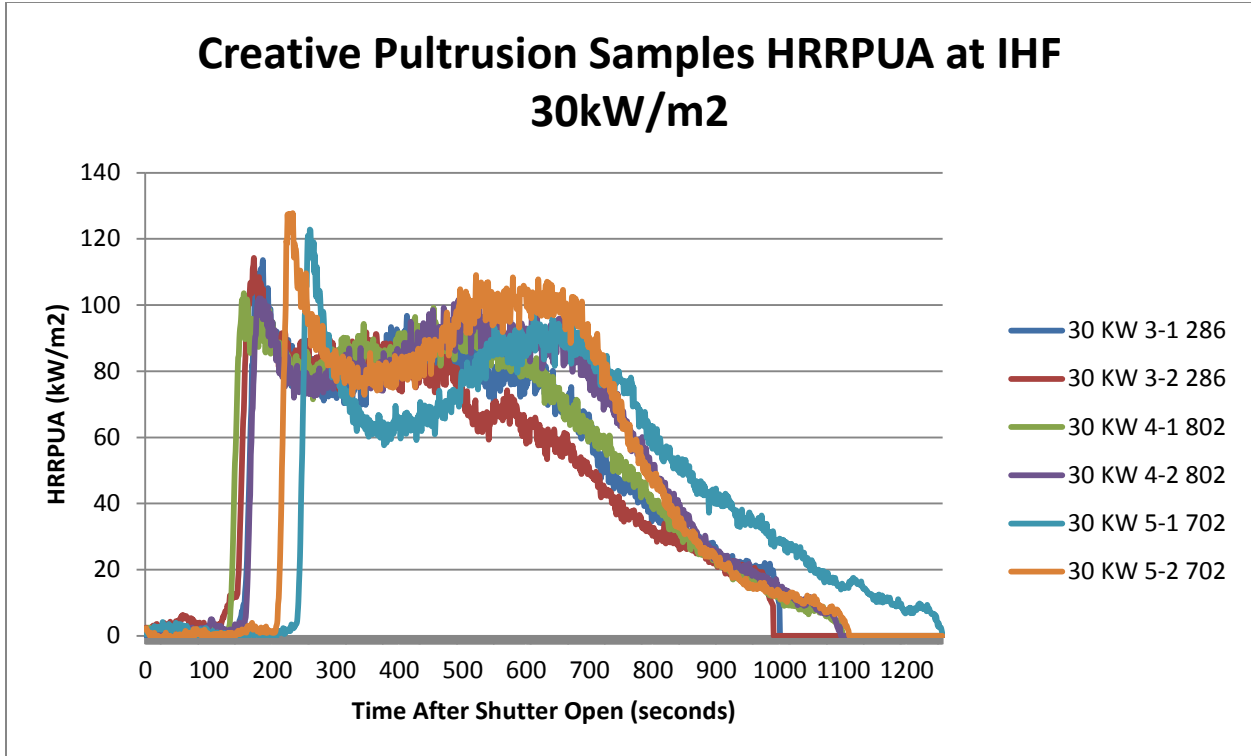
Figure 55: Standard Size CP HRRPUA IHF 30kW/m^{2}
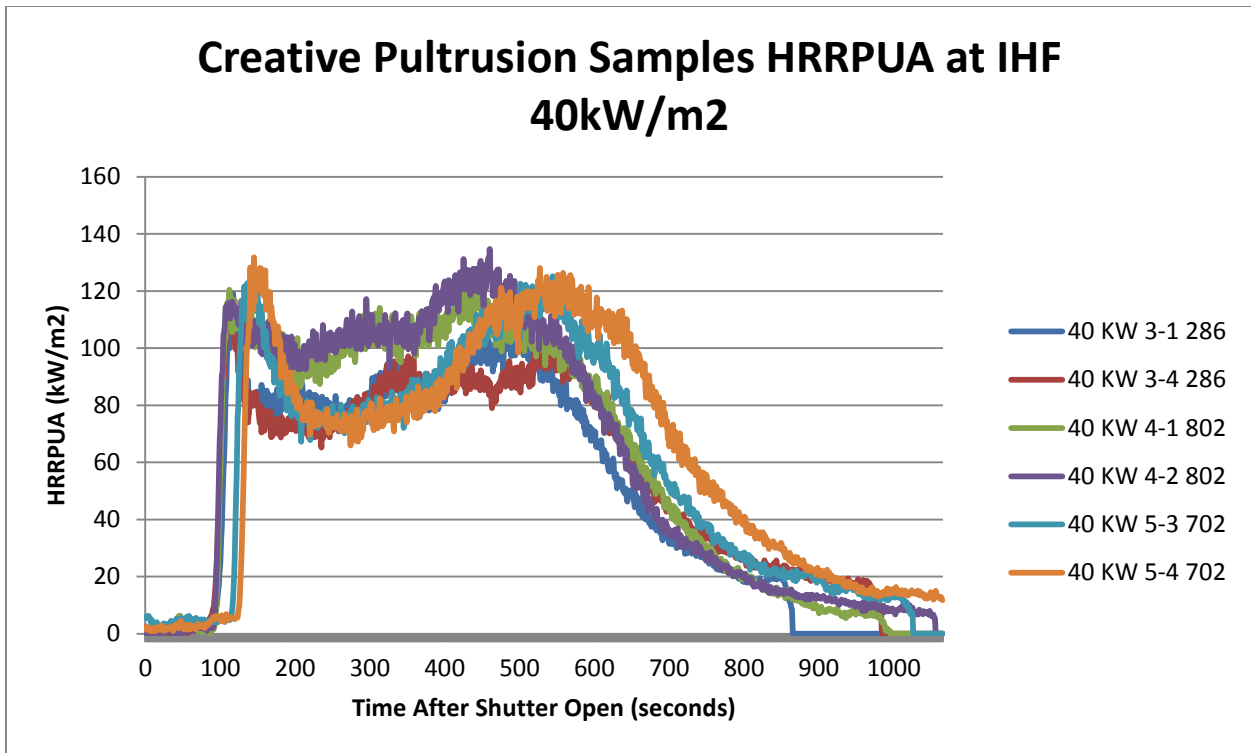
Figure 56: Standard Size CP HRRPUA IHF 40kW/m^{2}
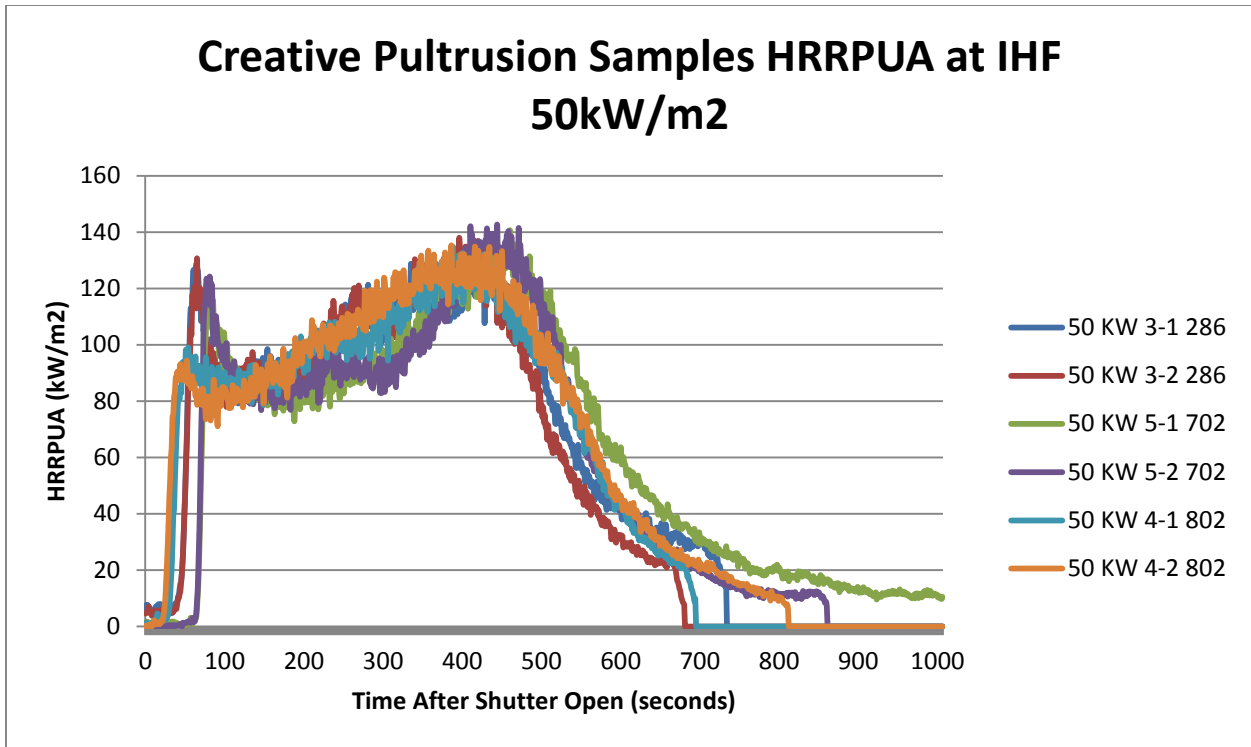
Figure 57: Standard Size CP HRRPUA IHF 50kW/m²
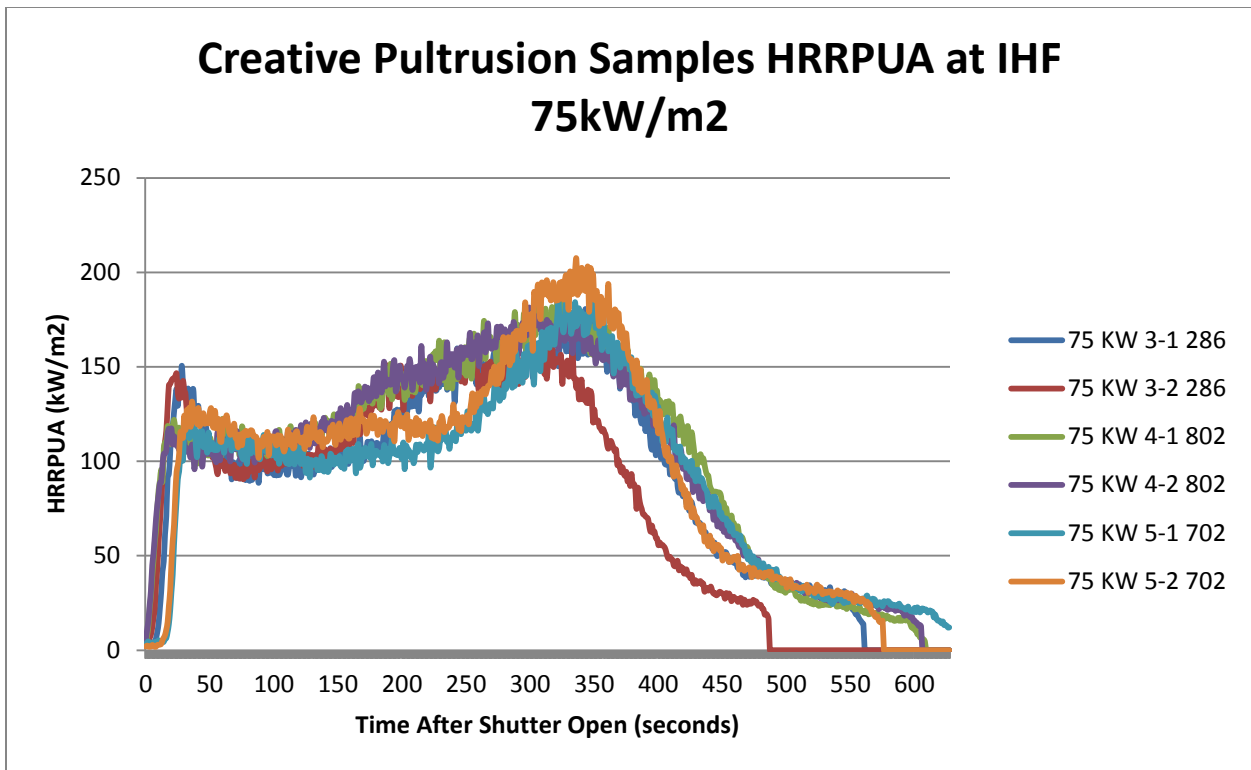
Figure 58: Standard Size CP HRRPUA IHF 75kW/m²

5.9.2 HRRPUA: 175 mm x 175 mm Specimens

Creative Pultrusion Sample 286 (7"x7")
HRRPUA at IHF 25 kW/m2
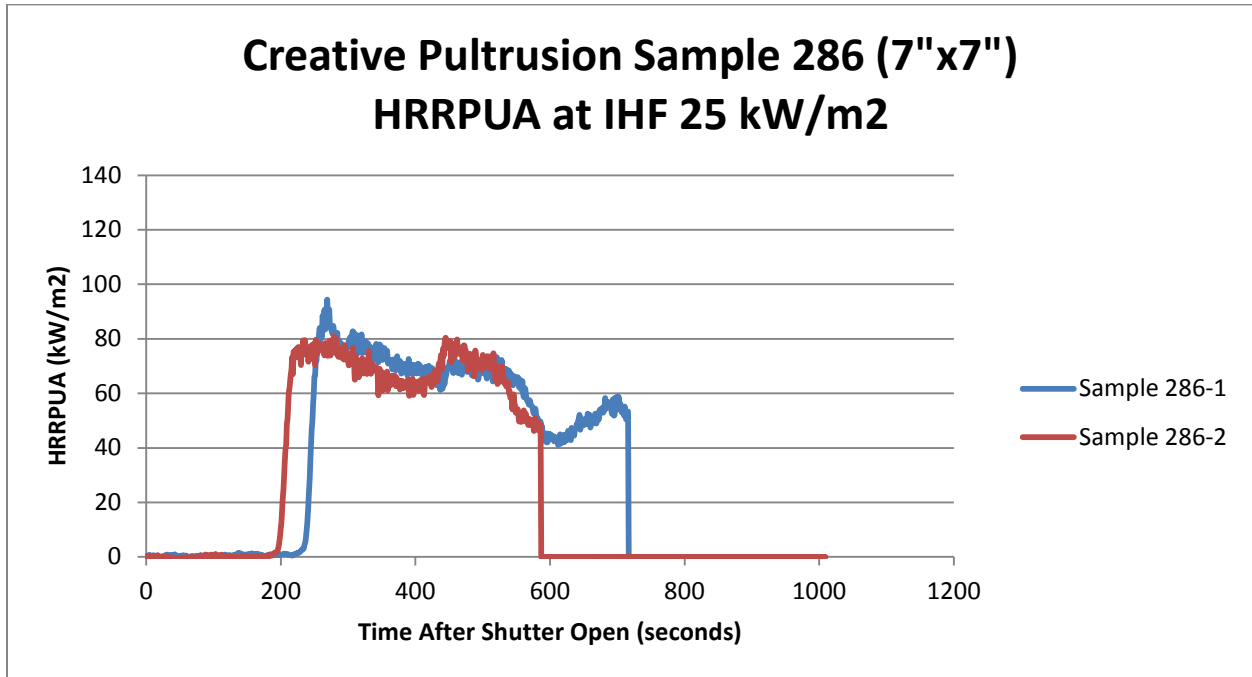
Figure 59: Extended Size CP 286 HRRPUA IHF 25kW/m^{2}

Creative Pultrusion Sample 702 (7"x7")
HRRPUA at IHF 25 kW/m2
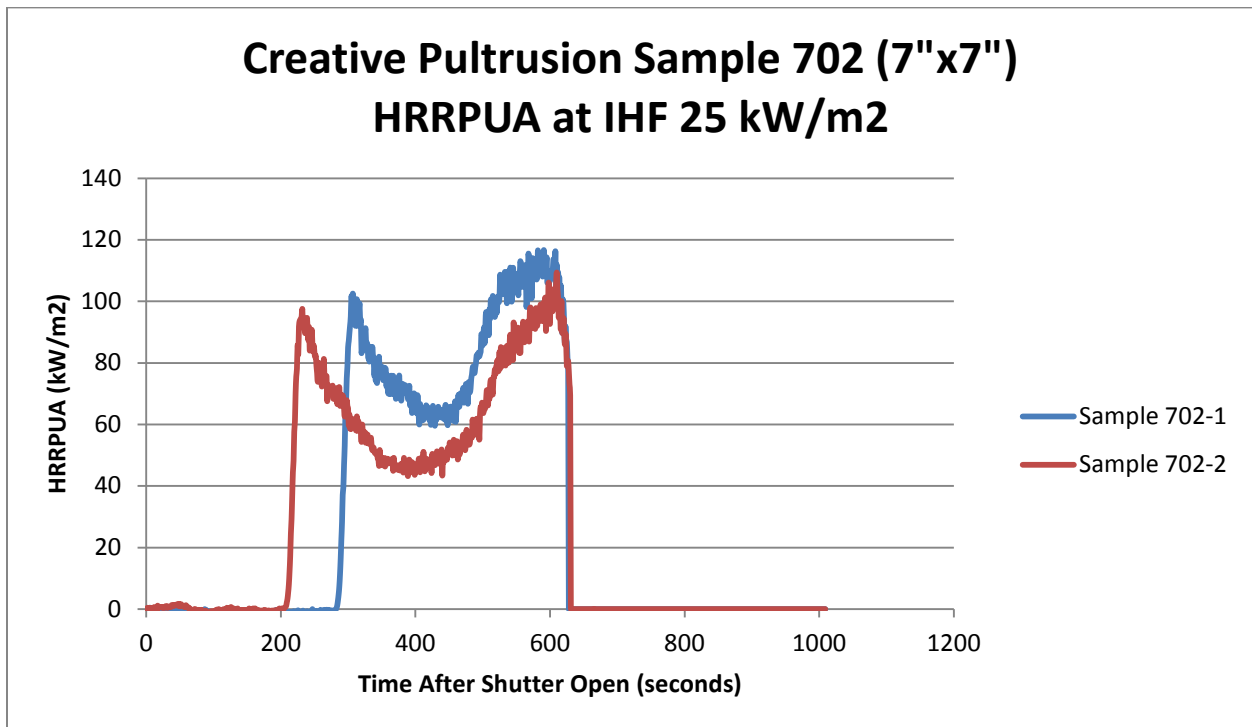
Figure 60: Extended Size CP 702 HRRPUA IHF 25kW/m^{2}
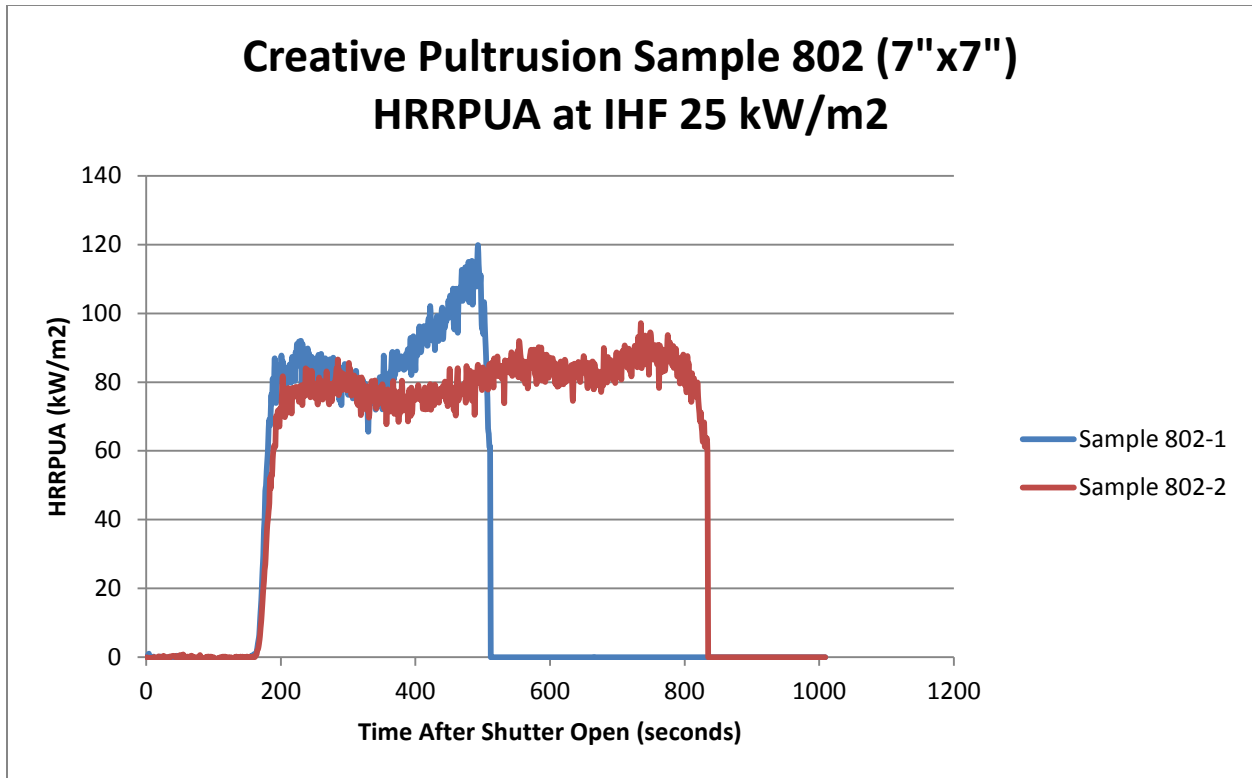
Figure 61: Extended Size CP 802 HRRPUA IHF 25kW/m²
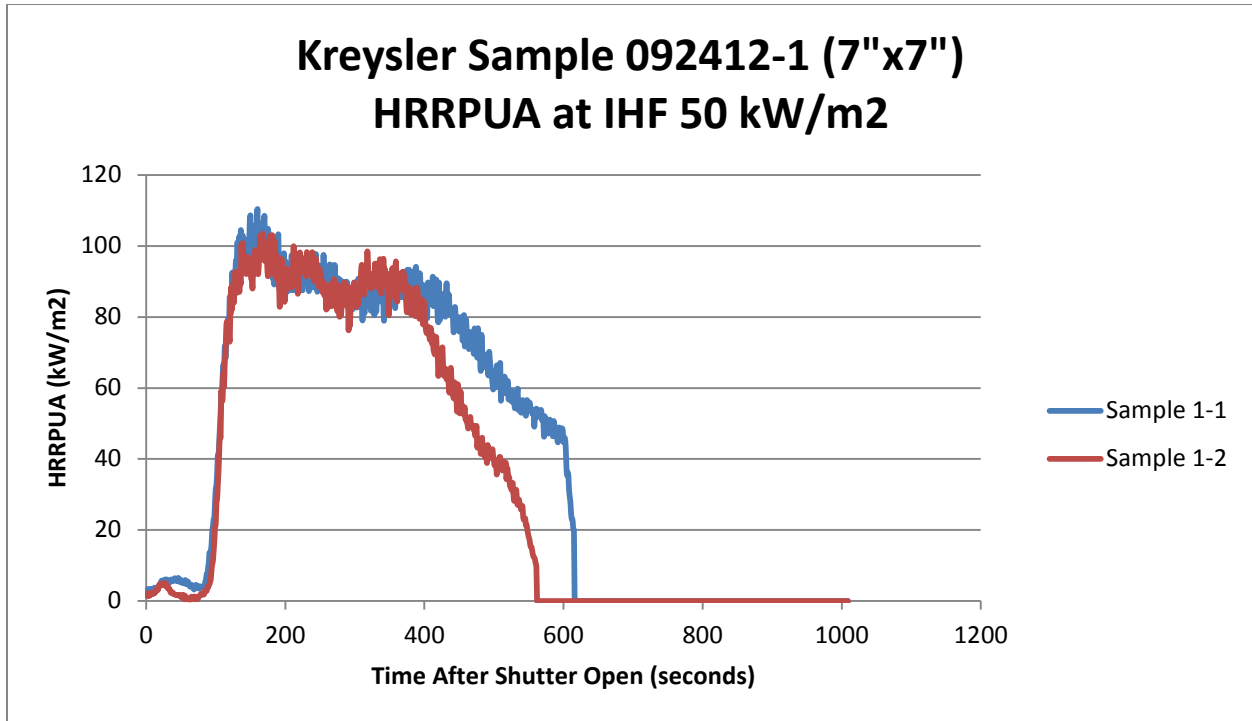
Figure 62: Extended Size Kreysler 1 HRRPUA IHF 50kW/m²
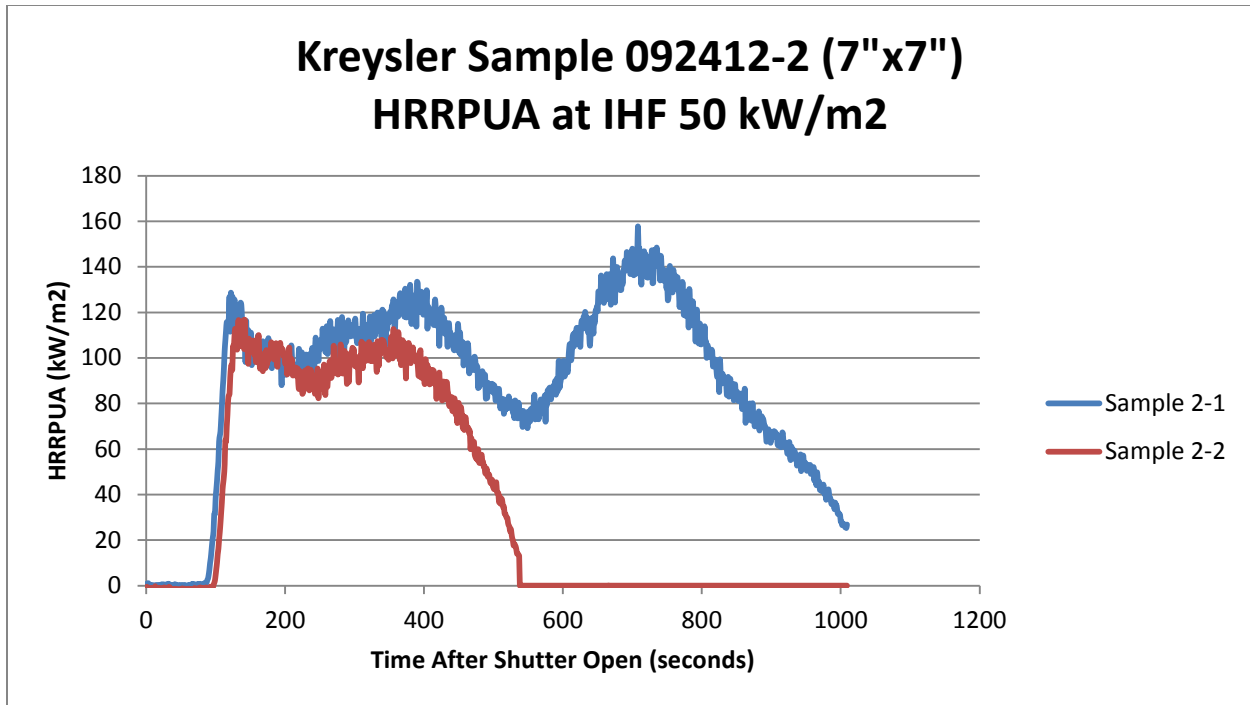
Figure 63: Extended Size Kreysler 2 HRRPUA IHF 50kW/m^2
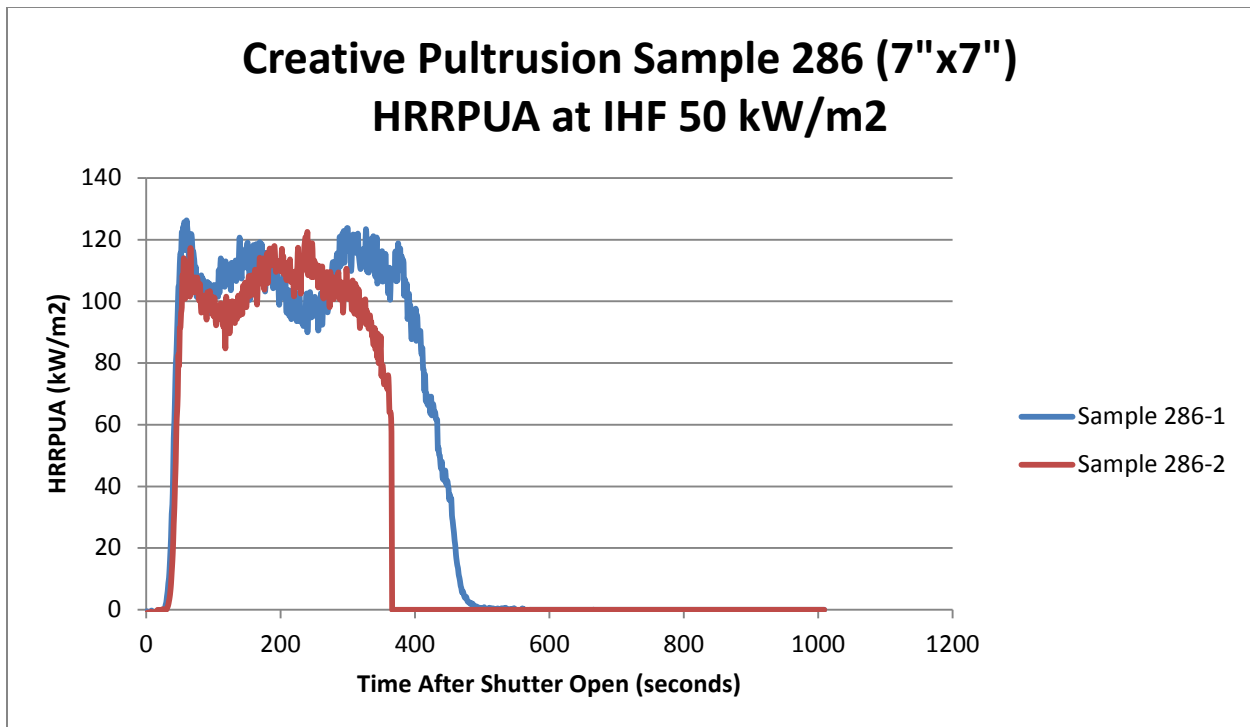
Figure 64: Extended Size CP 286 HRRPUA IHF 50kW/m^2
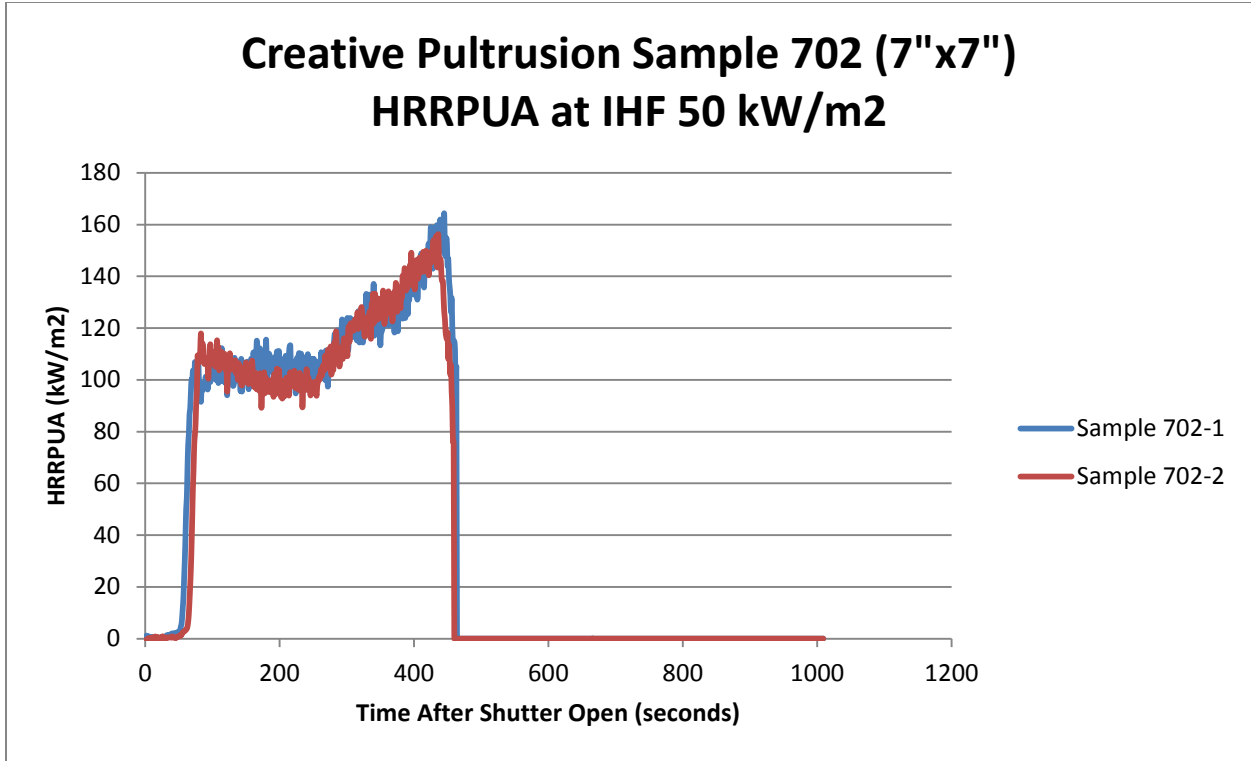
Figure 65: Extended Size CP 702 HRRPUA IHF 50kW/m²
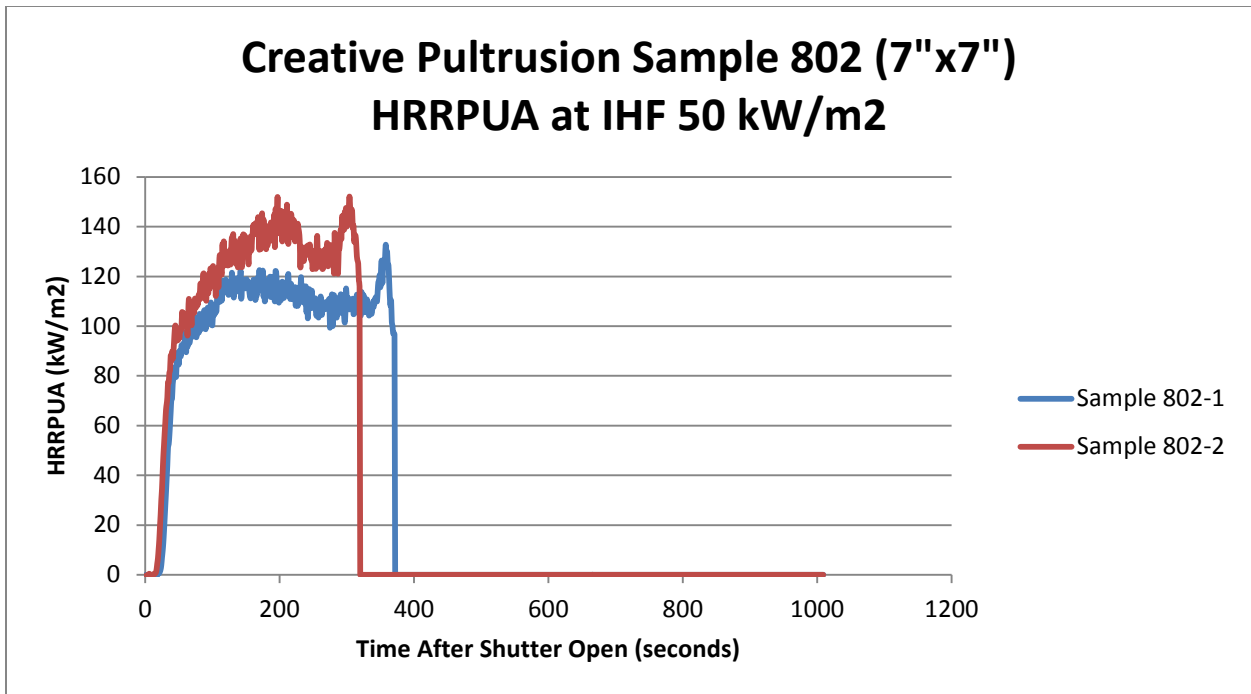
Figure 66: Extended Size CP 802 HRRPUA IHF 50kW/m²
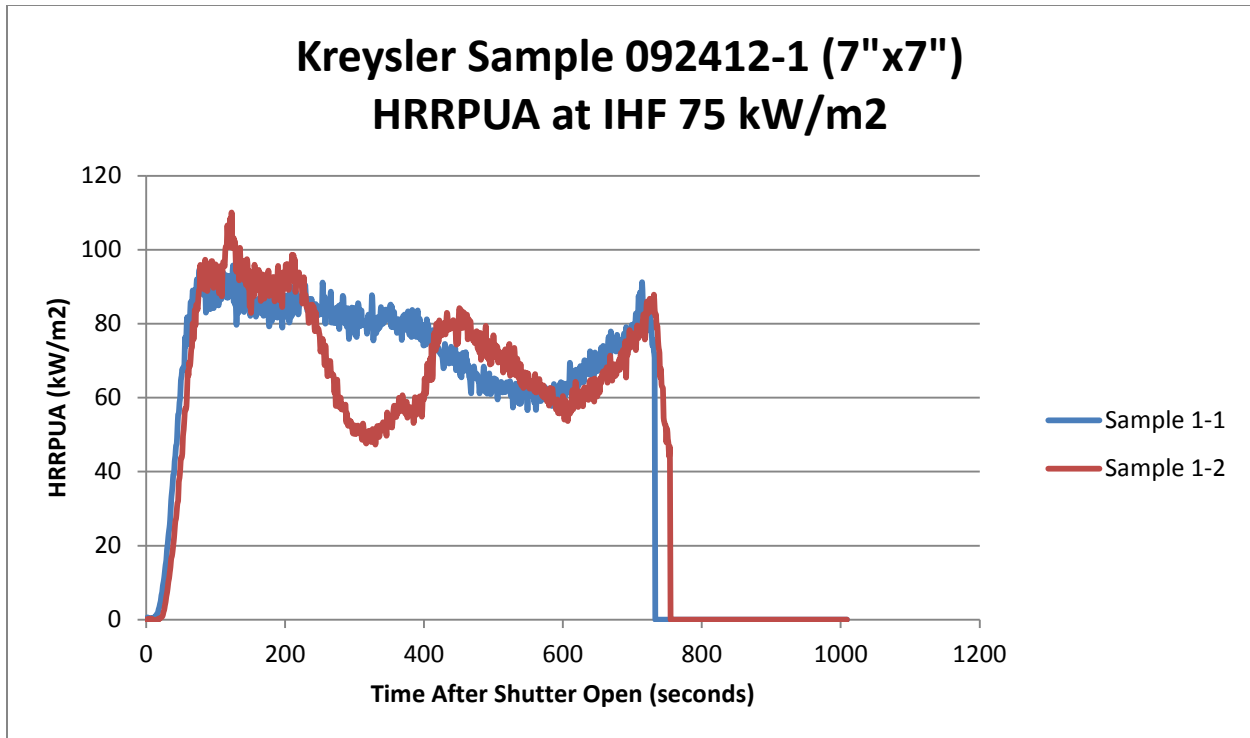
Figure 67: Extended Size Kreysler 1 HRRPUA IHF 75kW/m²
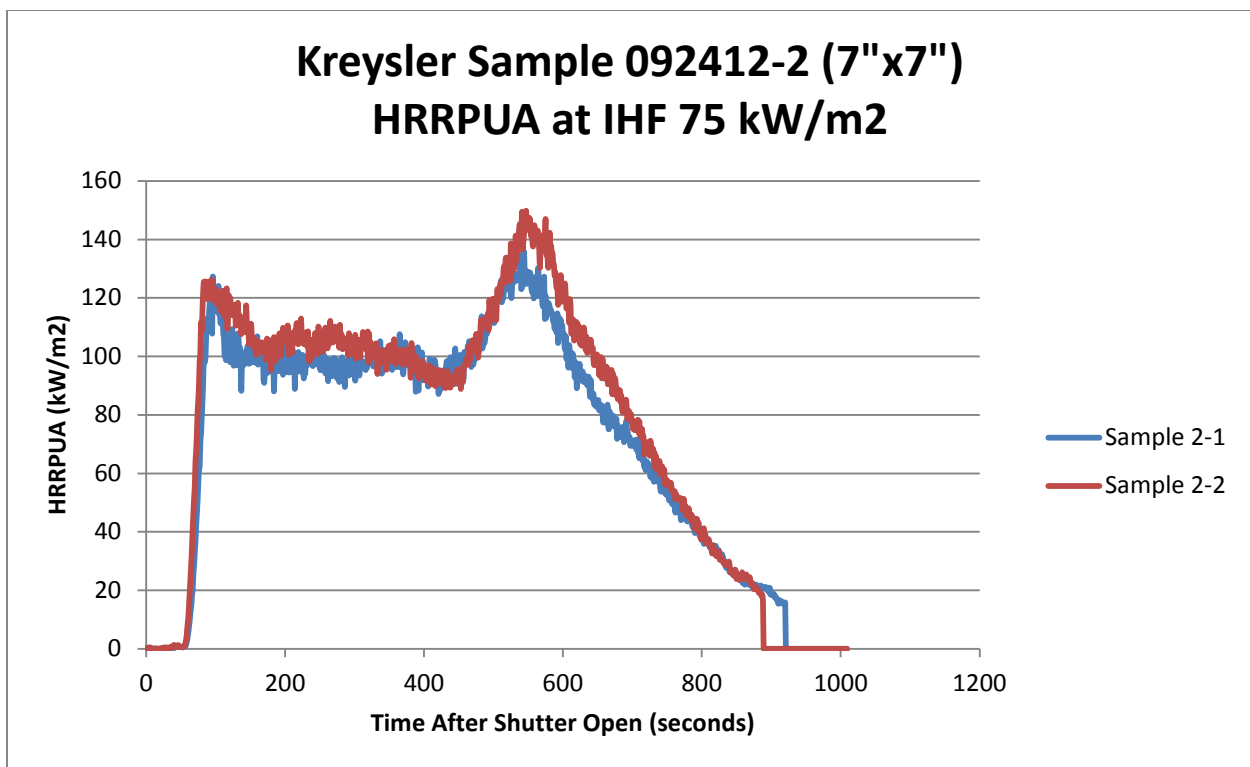
Figure 68: Extended Size Kreysler 2 HRRPUA IHF 75kW/m²
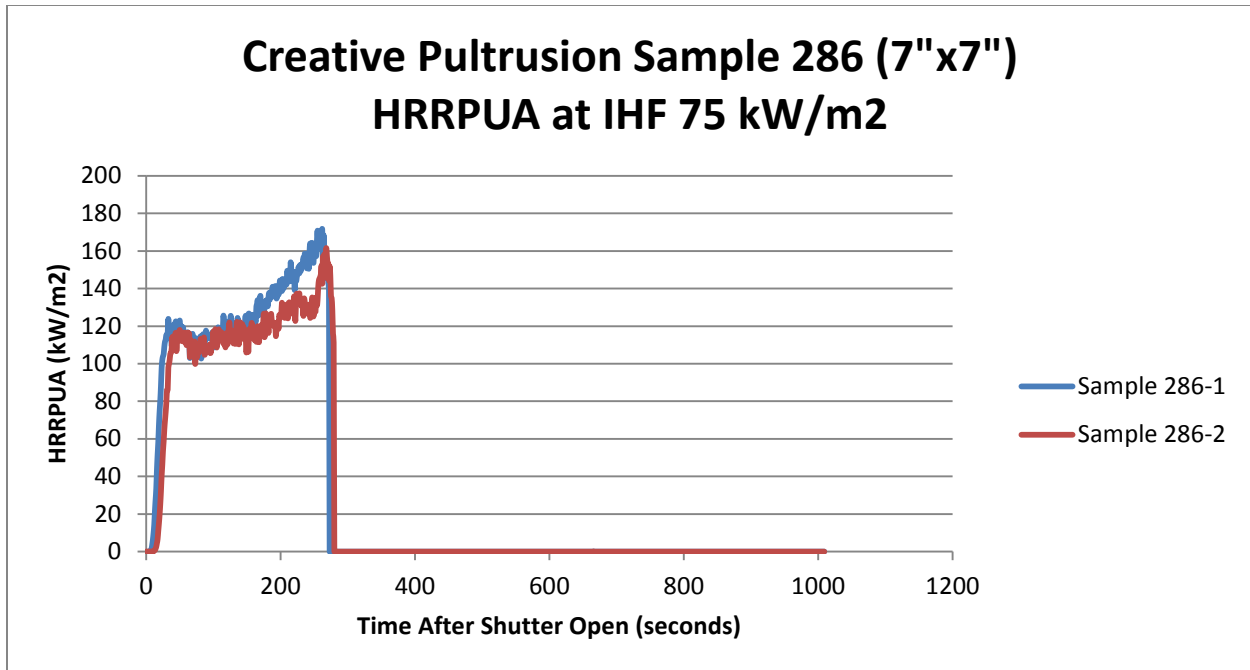
Figure 69: Extended Size CP 286 HRRPUA IHF 75kW/m²
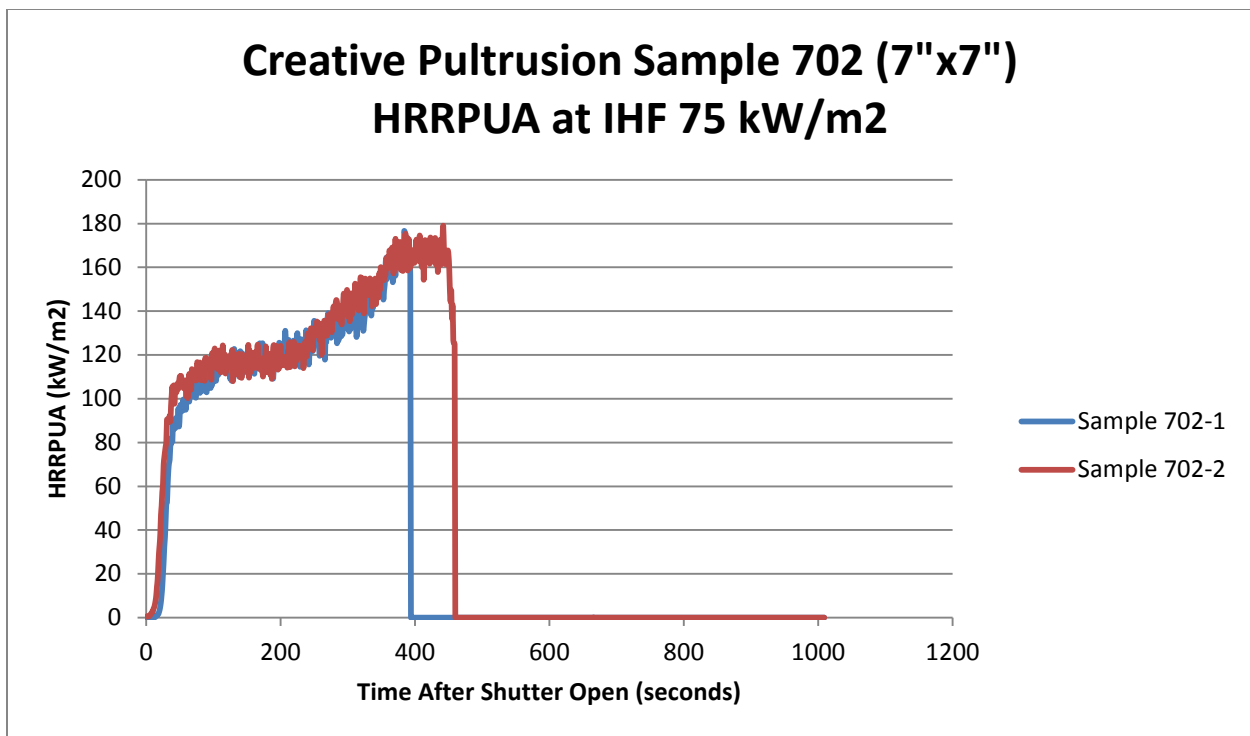
Figure 70: Extended Size CP 702 HRRPUA IHF 75kW/m²
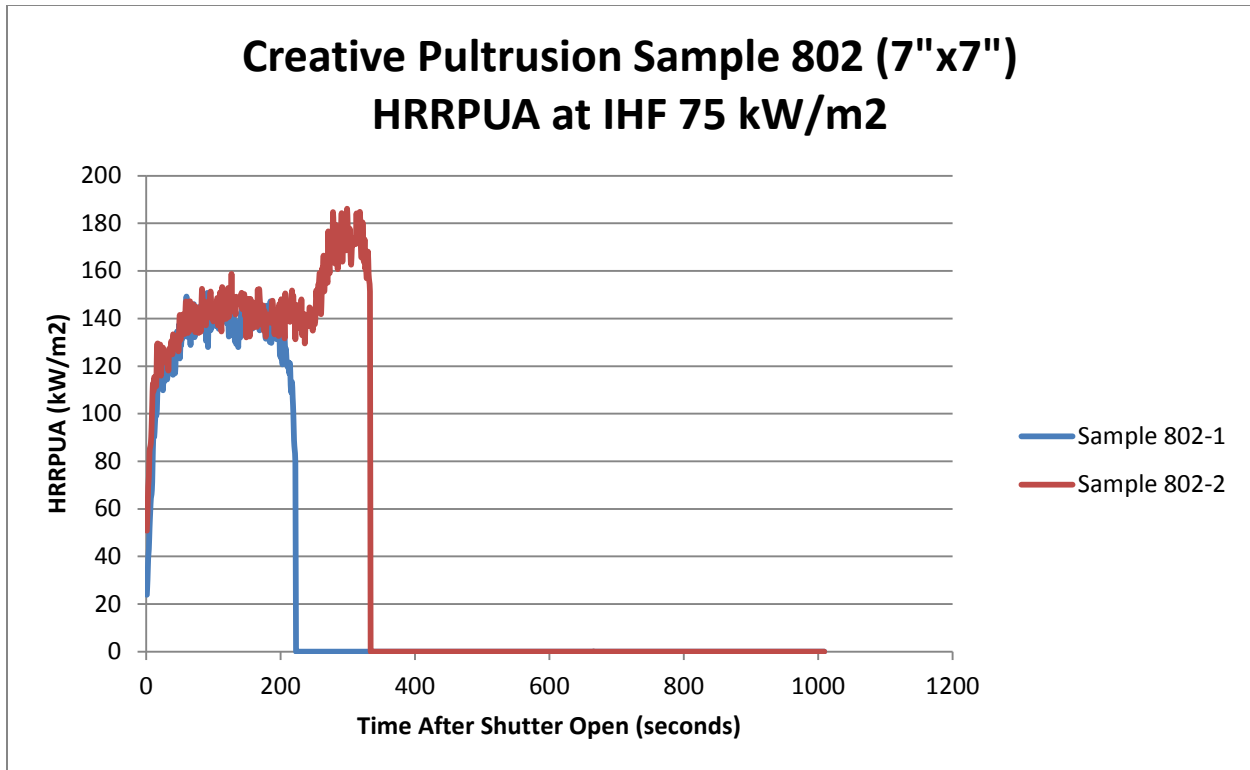
Figure 71: Extended Size CP 802 HRRPUA IHF 75kW/m^2

5.9.3 Cone Analysis: 100mm x 100mm & 175mm x 175mm comparison
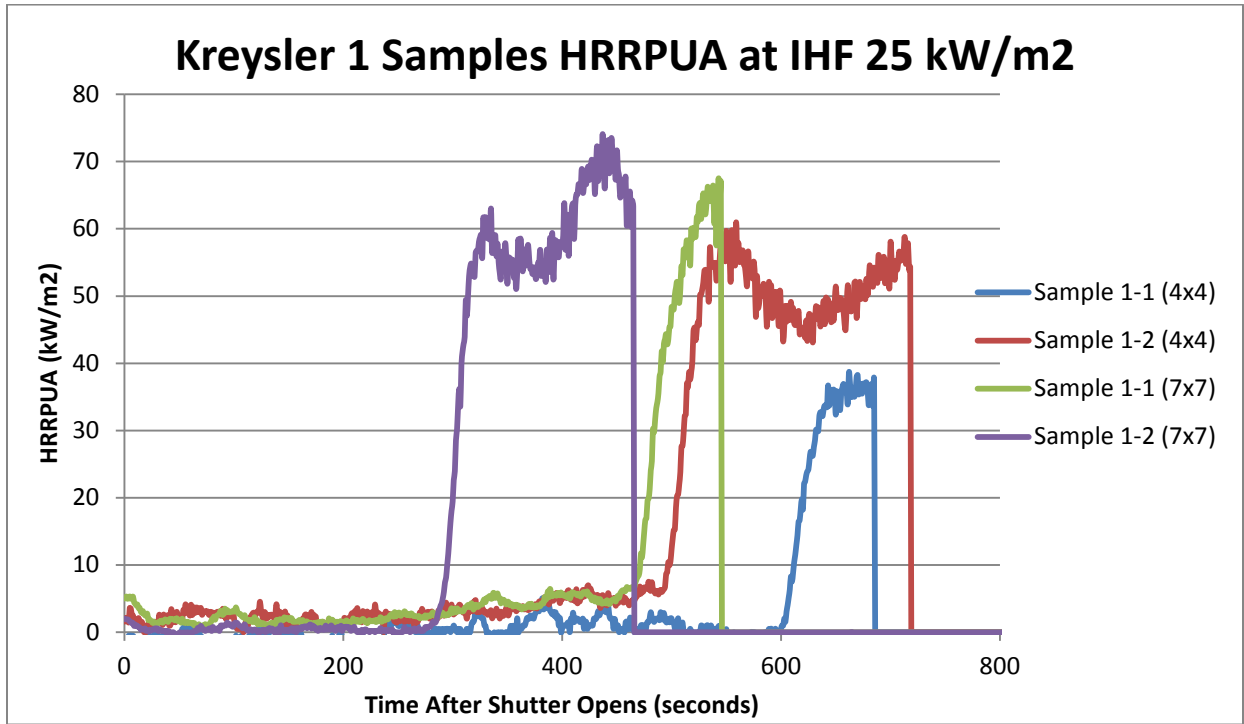
Figure 72: Kreysler 1 HRRPUA Comparison between Sizes IHF 25kW/m^{2}
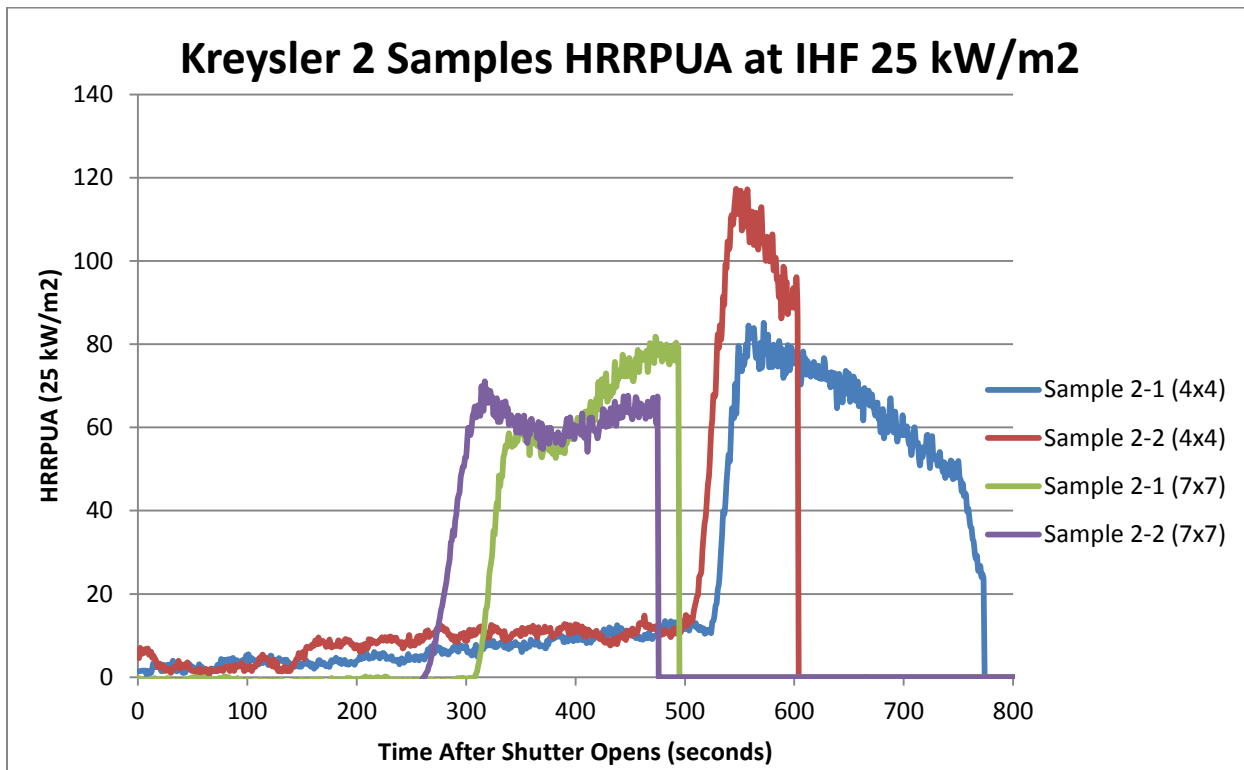
Figure 73: Kreysler 2 HRRPUA Comparison between Sizes IHF 25kW/m^{2}
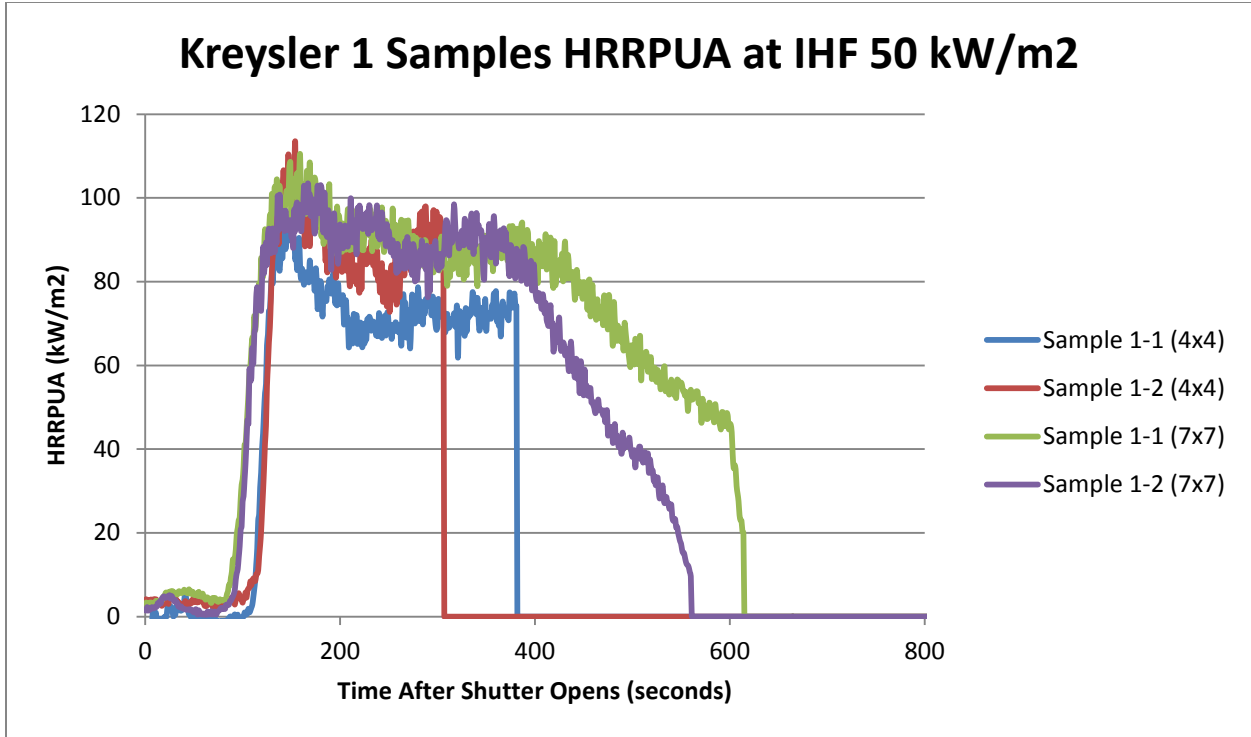
Figure 74: Kreysler 1 HRRPUA Comparison between Sizes IHF 50kW/m^2
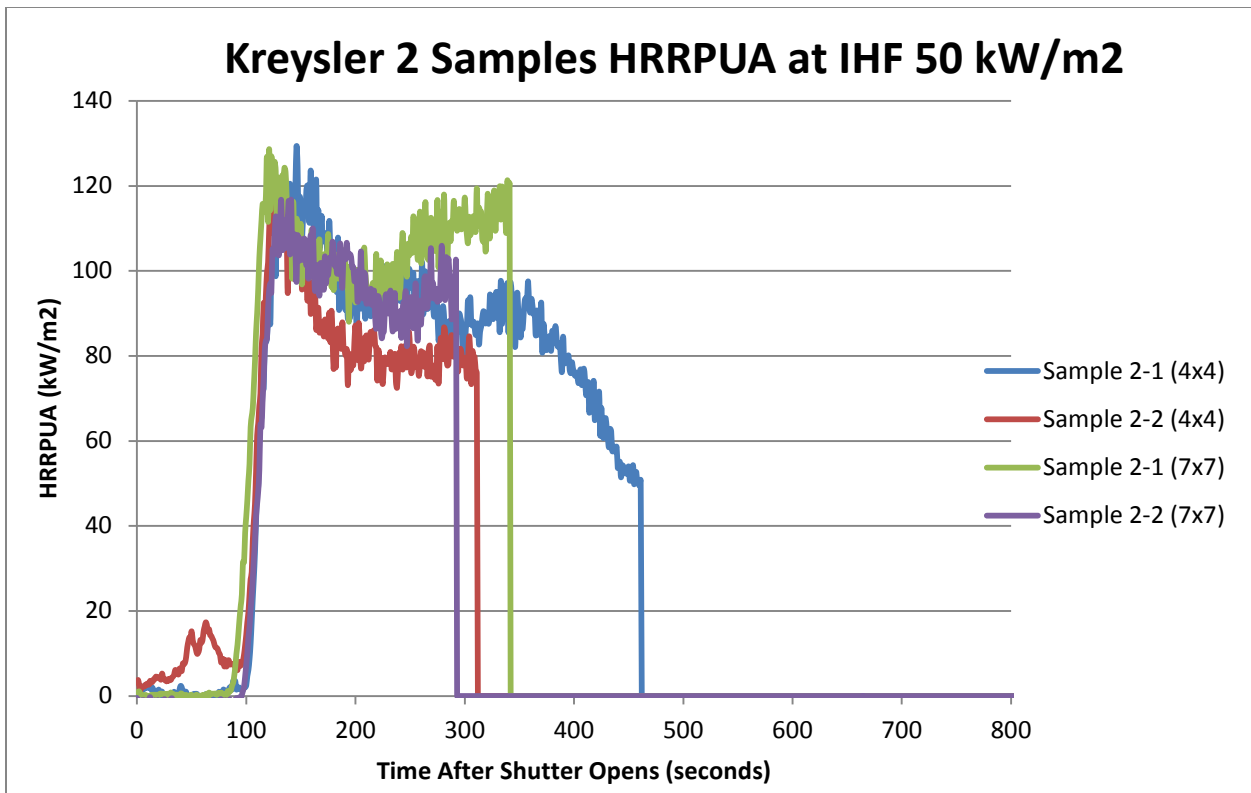
Figure 75: Kreysler 2 HRRPUA Comparison between Sizes IHF 50kW/m2
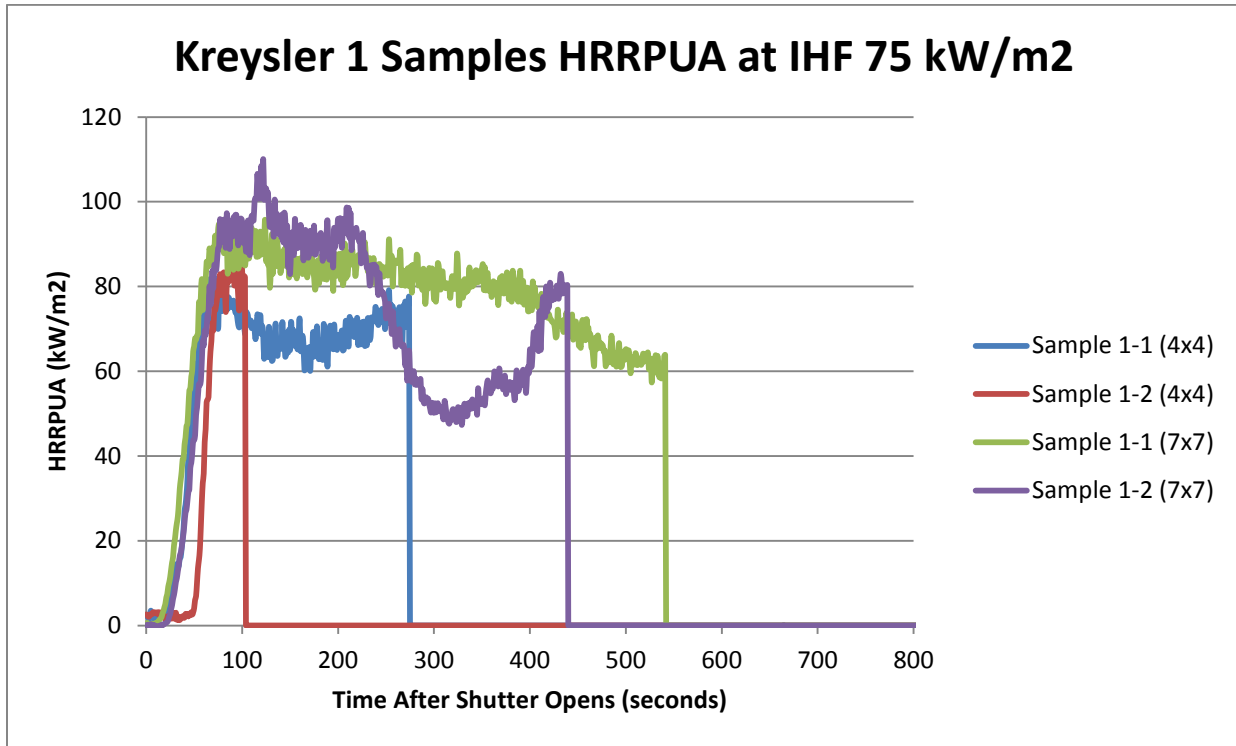
Figure 76: Kreysler 1 HRRPUA Comparison between Sizes IHF 75kW/m^{2}
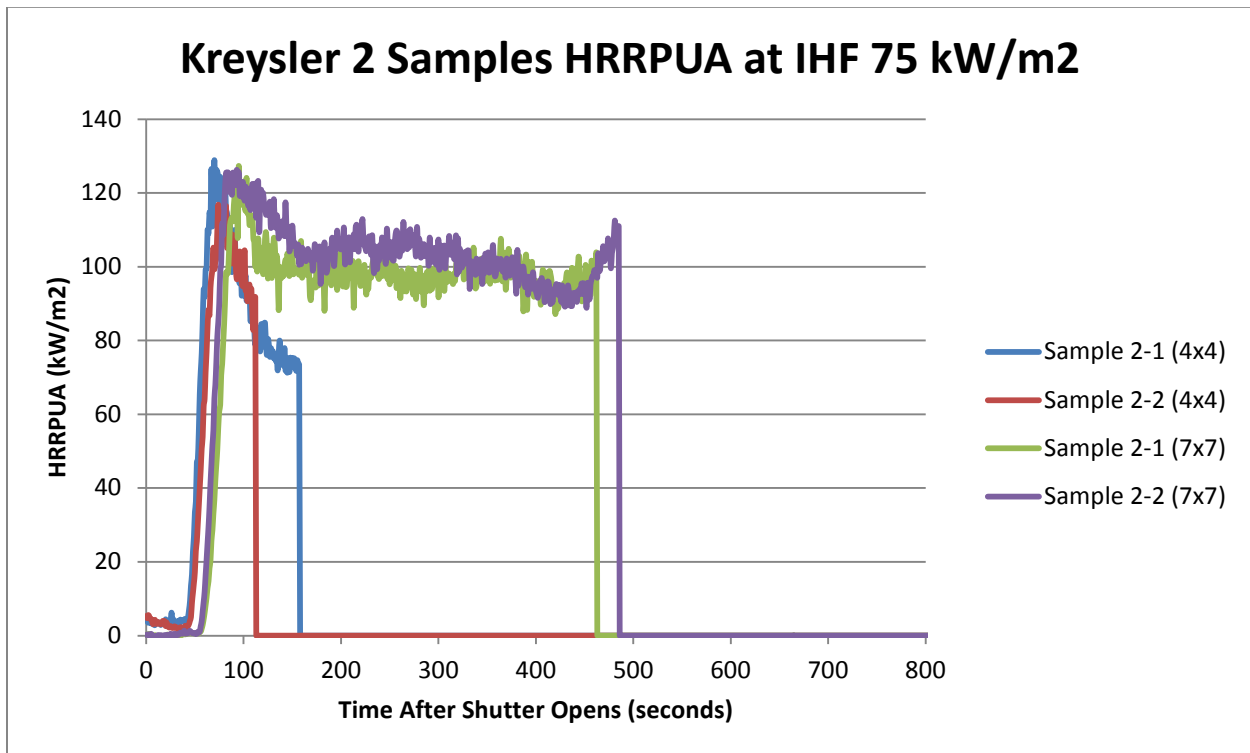
Figure 77: Kreysler 2 HRRPUA Comparison between Sizes IHF 75kW/m^{2}
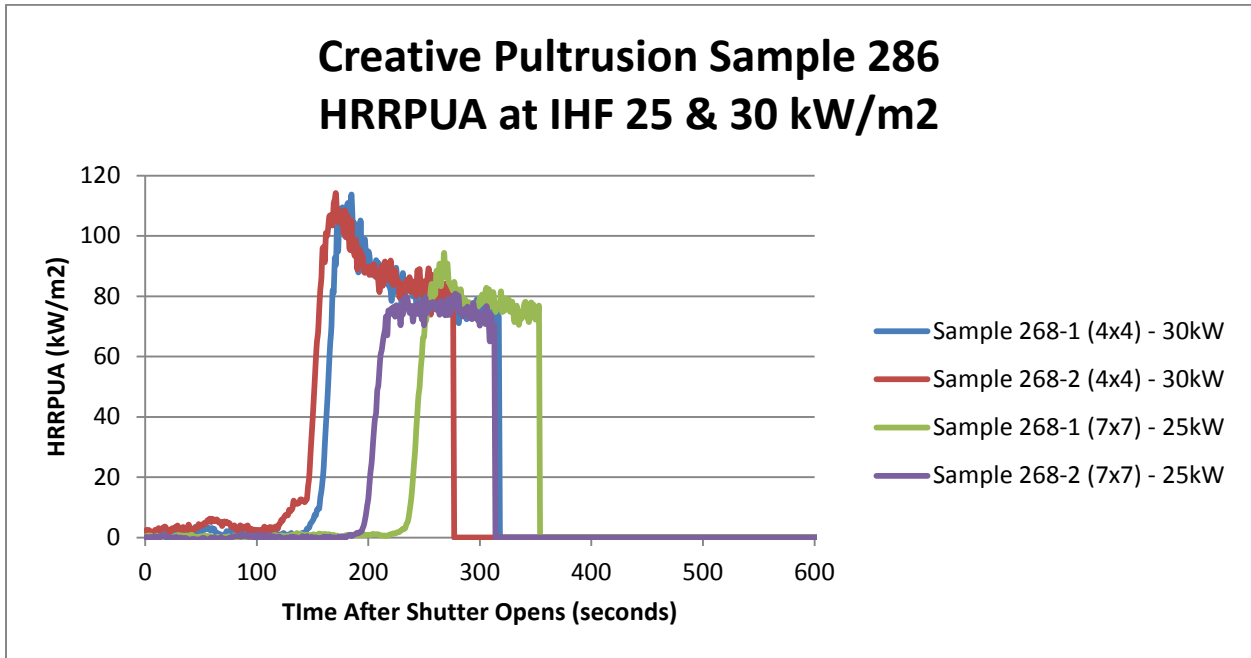
Figure 78: CP 286 HRRPUA Comparison between Sizes IHF 25/30 kW/m^2
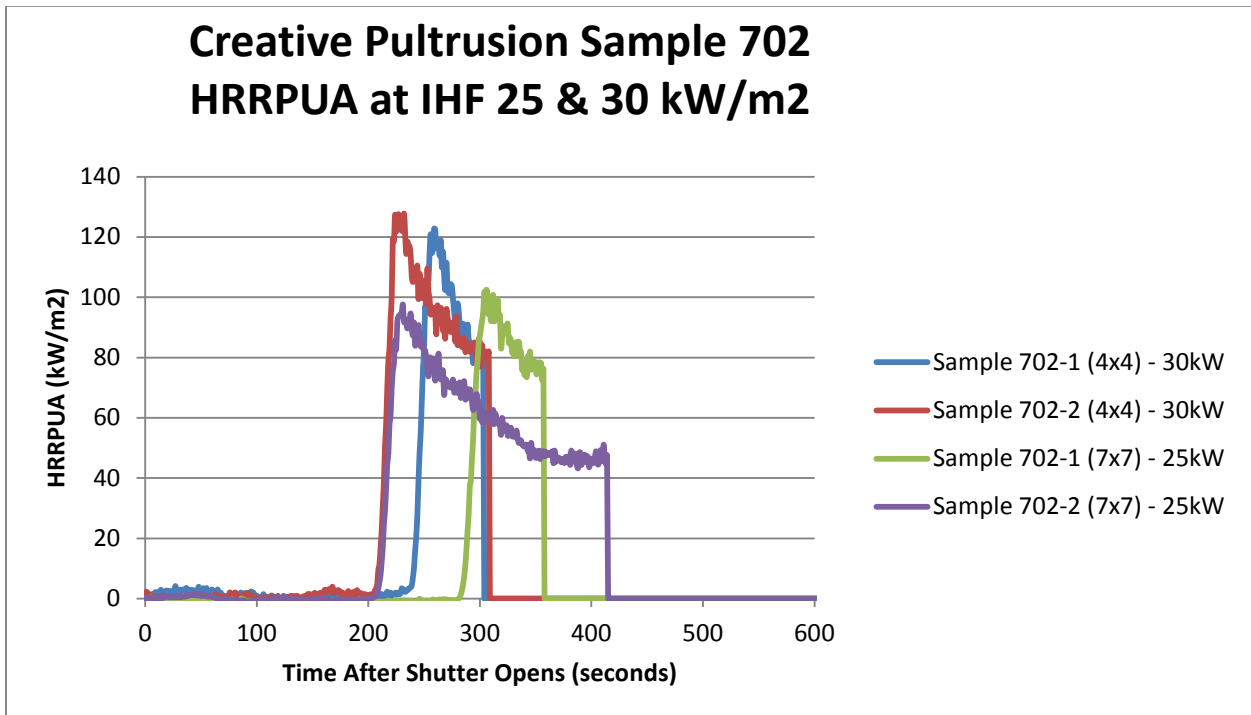
Figure 79: CP 702 HRRPUA Comparison between Sizes IHF 25/30 kW/m^2
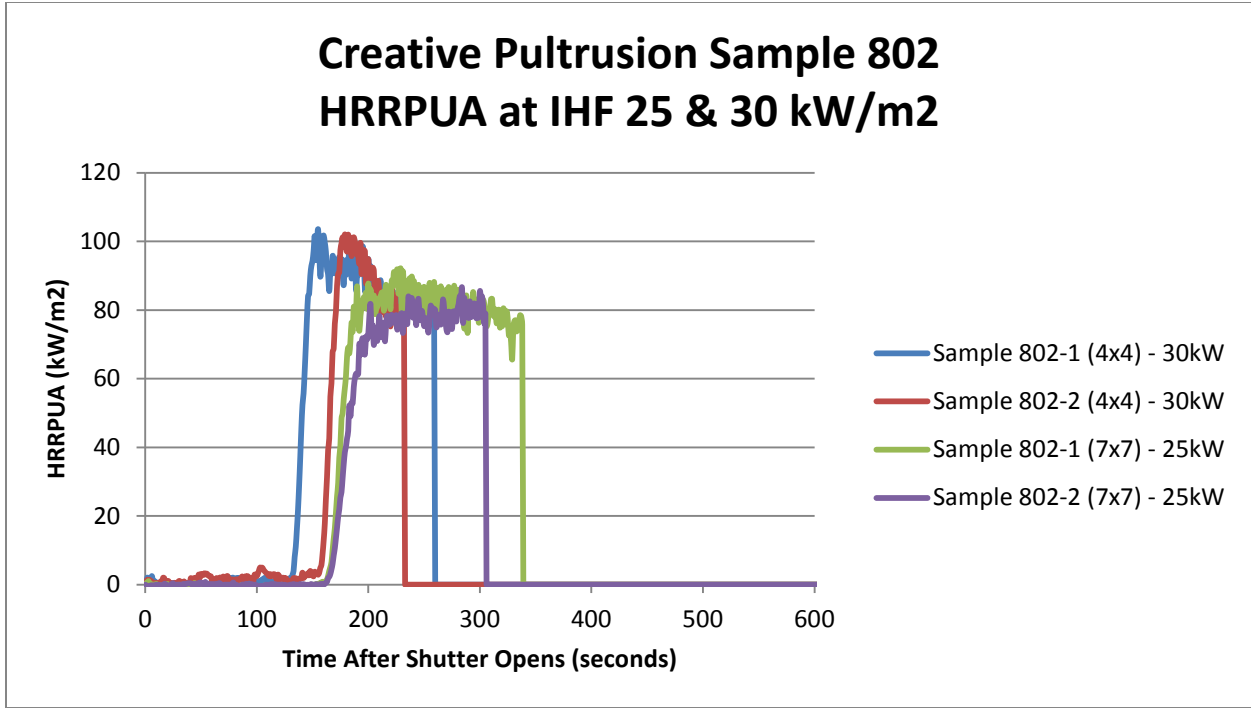
Figure 80: CP 802 HRRPUA Comparison between Sizes IHF 25/30 kW/m²
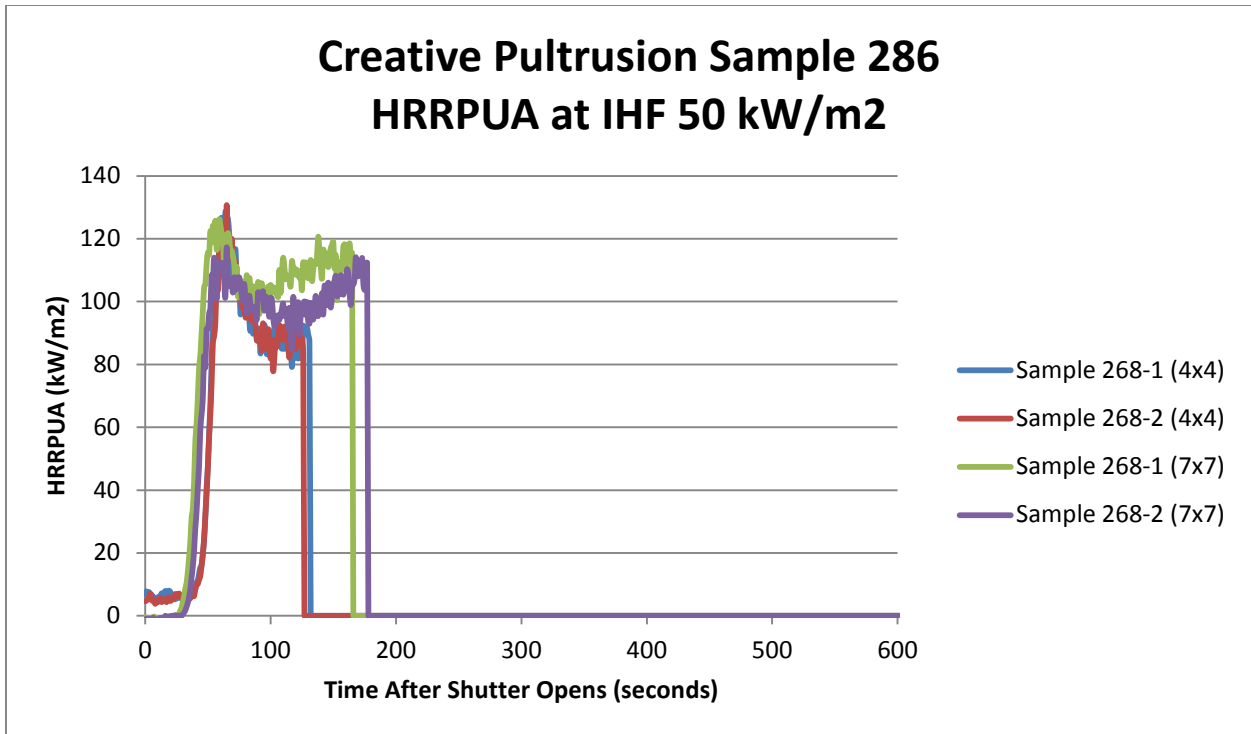
Figure 81: CP 286 HRRPUA Comparison between Sizes IHF 50 kW/m²
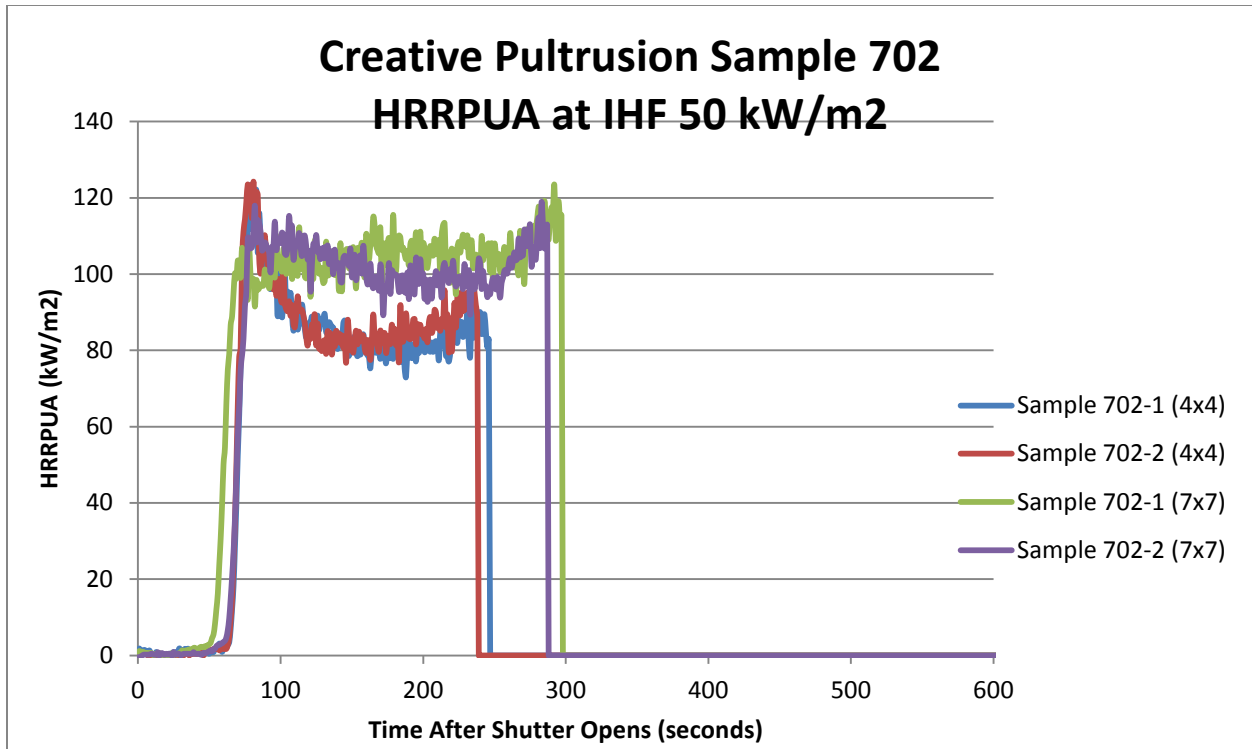
Figure 82: CP 702 HRRPUA Comparison between Sizes IHF 50 kW/m^2
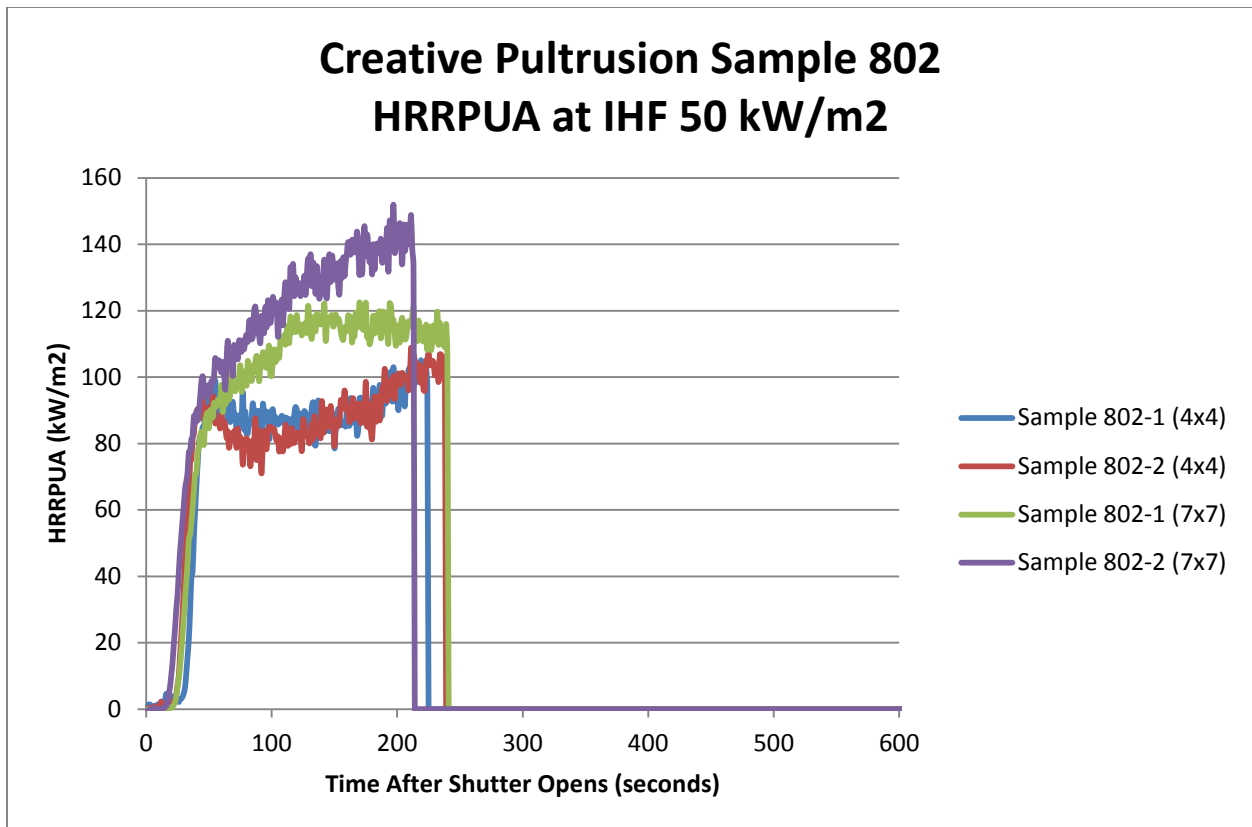
Figure 83: CP 802 HRRPUA Comparison between Sizes IHF 50 kW/m^2
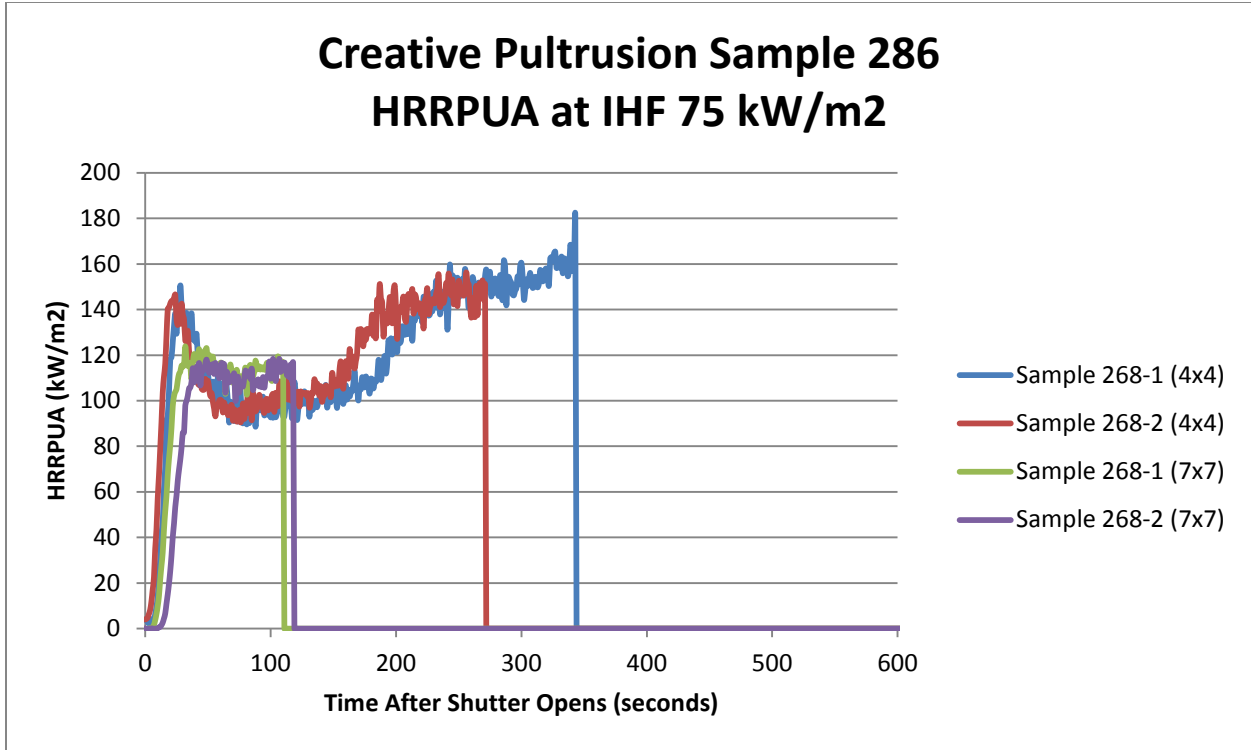
Figure 84: CP 286 HRRPUA Comparison between Sizes IHF 75 kW/m²
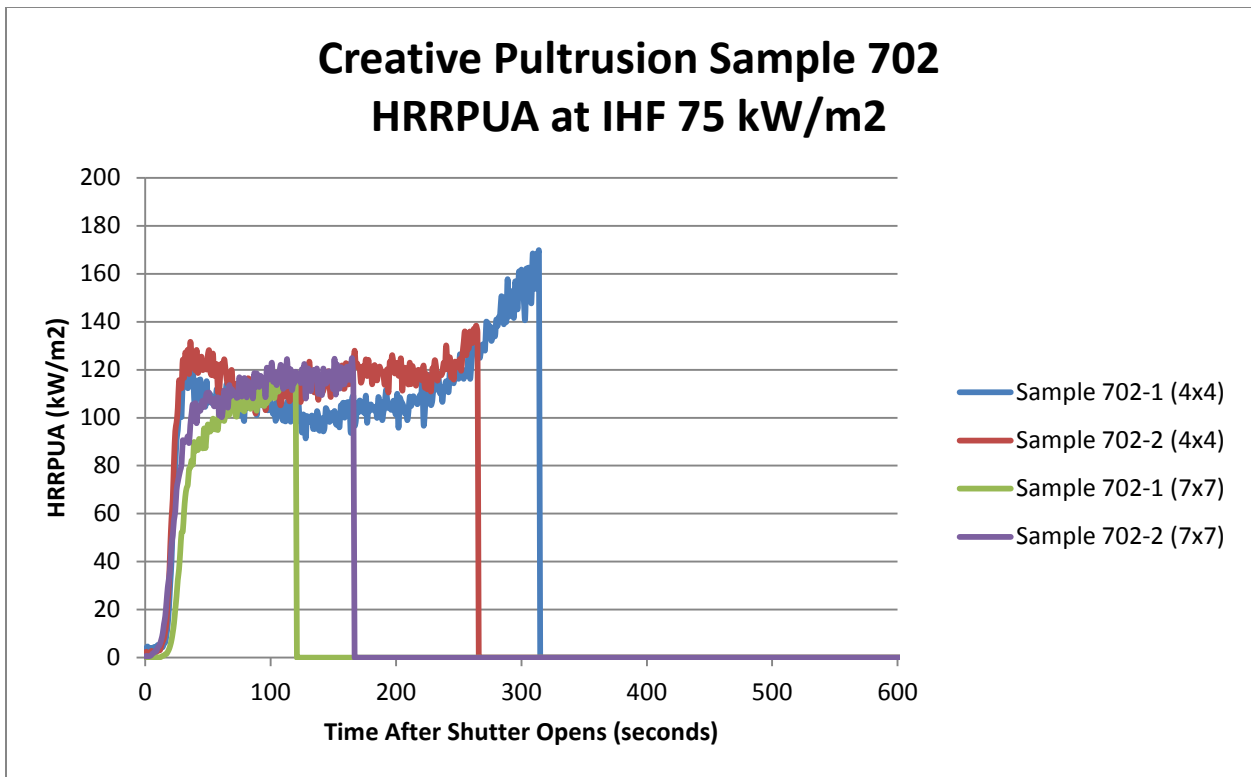
Figure 85: CP 702 HRRPUA Comparison between Sizes IHF 75 kW/m²
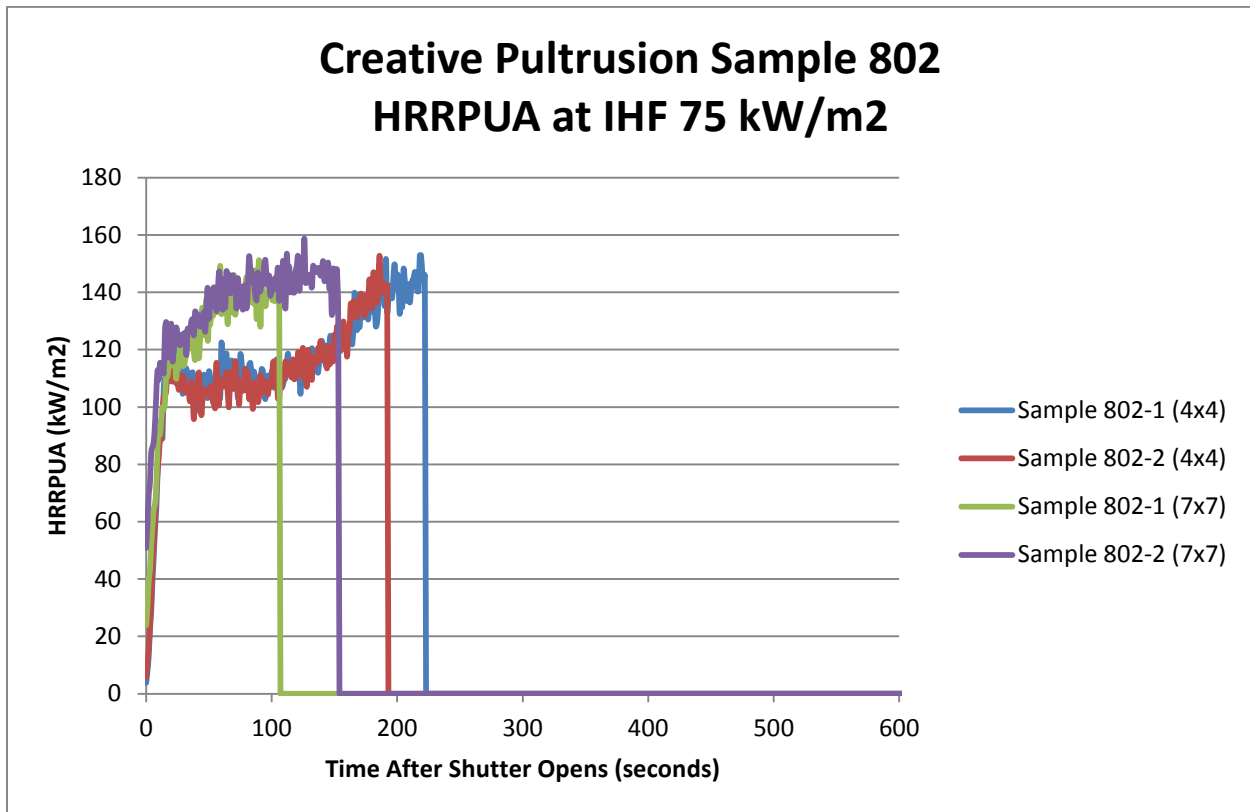
Figure 86: CP 802 HRRPUA Comparison between Sizes IHF 75 kW/m²

5.9.4 Time to Ignition and End of 1d Burning Data
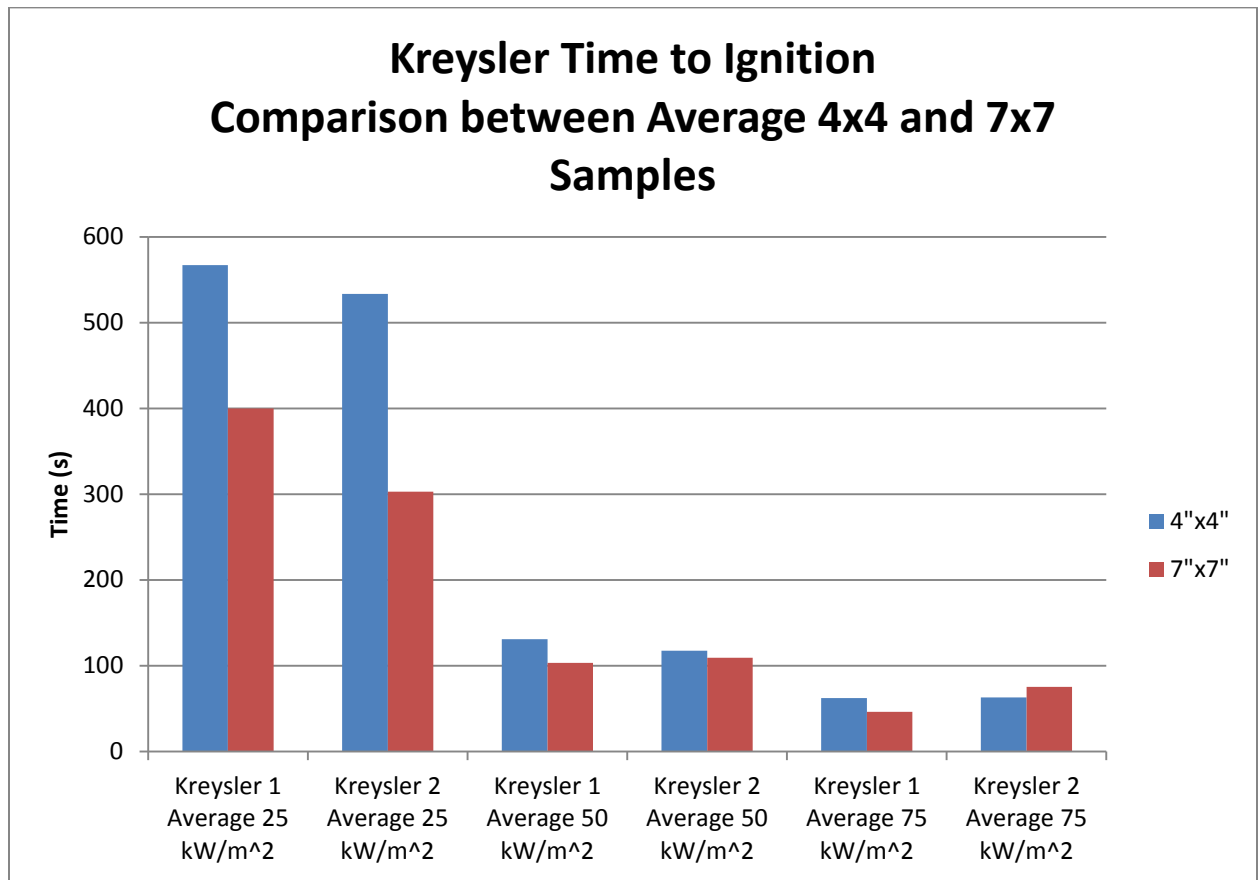
Figure 87: Kreysler Sample Average Time to Ignition Comparison
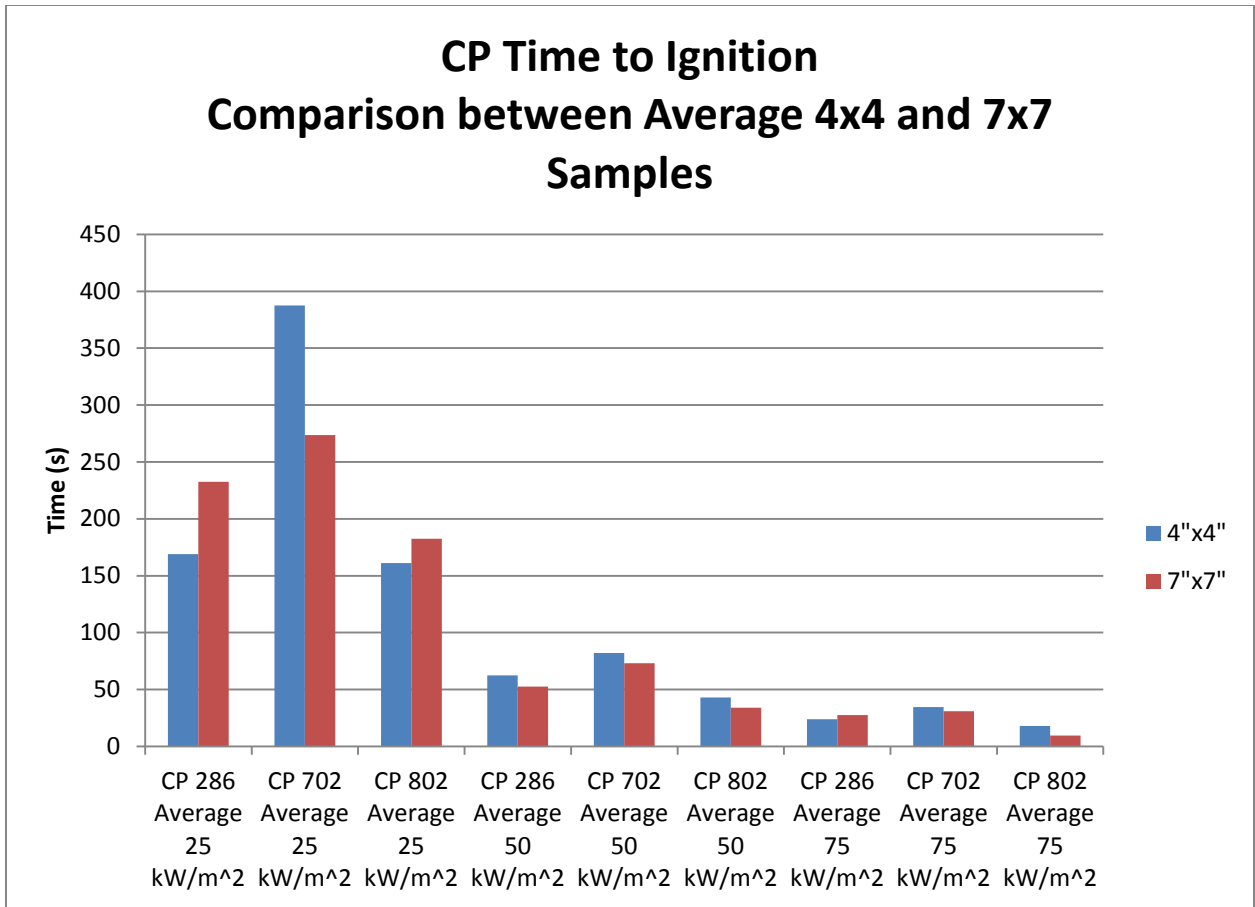
Figure 88: CP Sample Average Time to Ignition Comparison
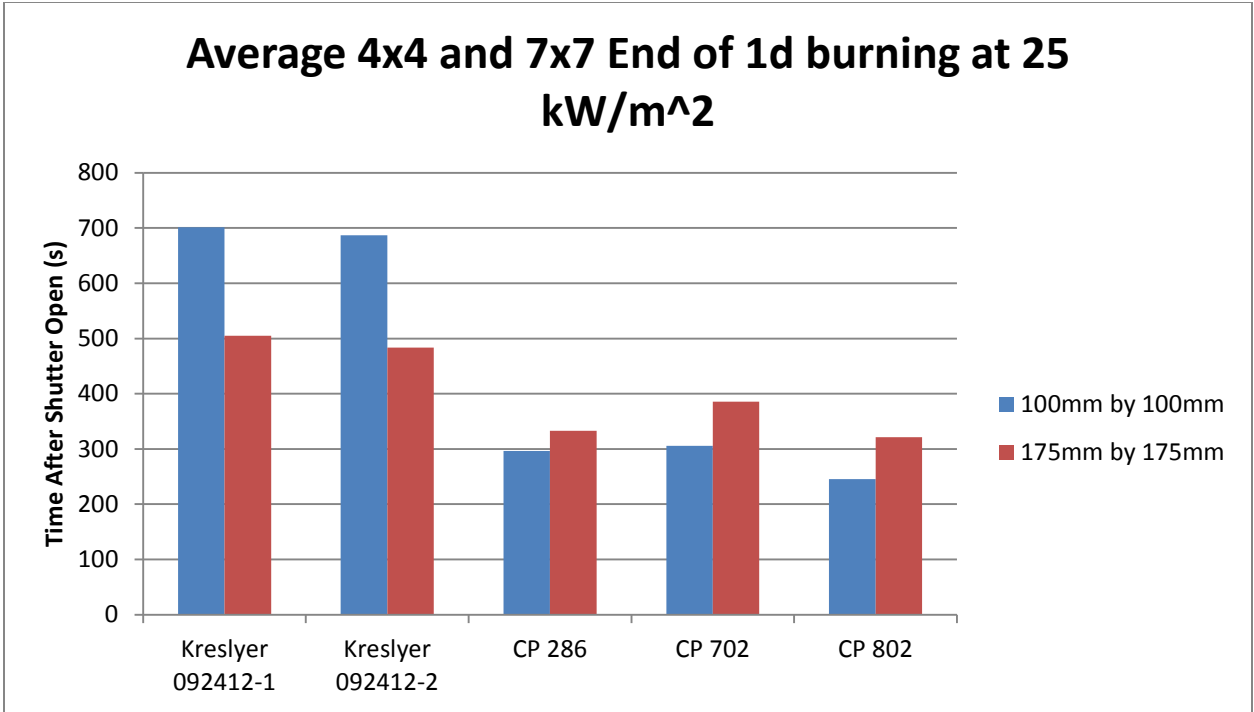
Figure 89: Average End of 1D Burning Time Comparison at IHF of 25 kW/m²
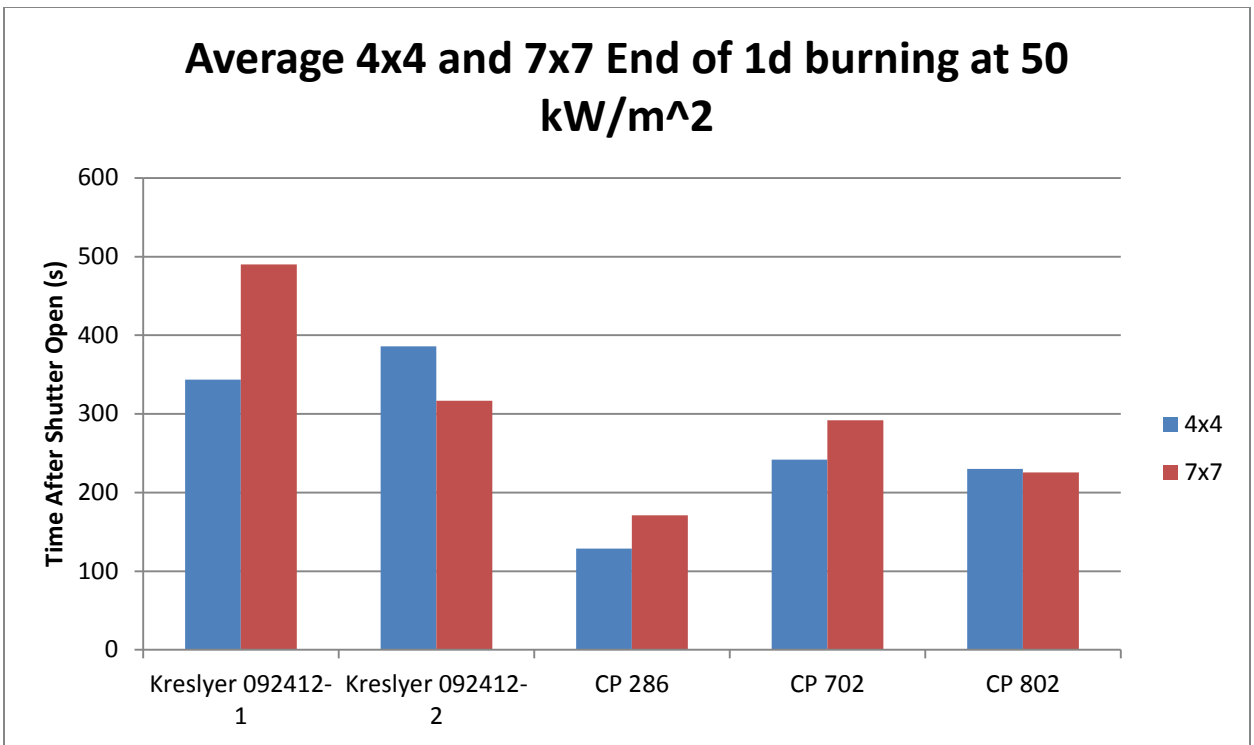
Figure 90: Average End of 1D Burning Time Comparison at IHF of 50 kW/m²
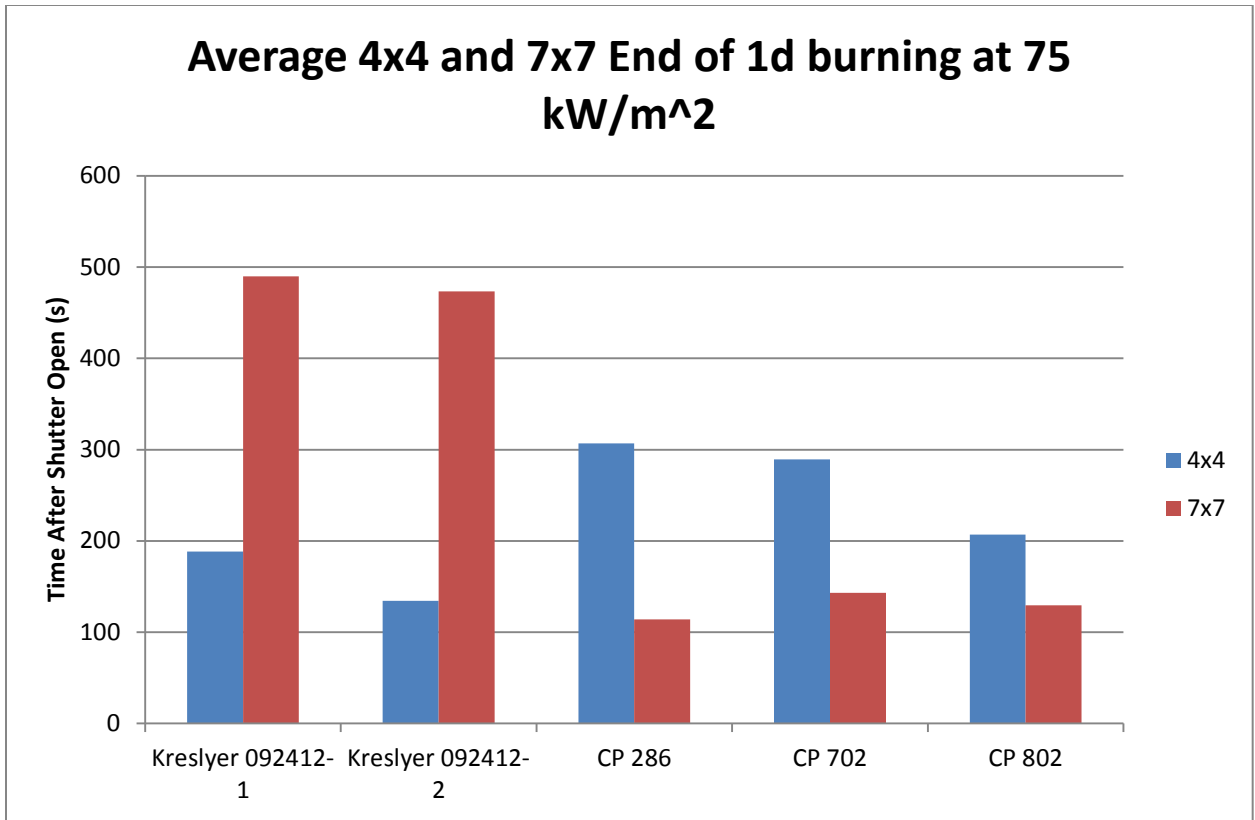
Figure 91: Average End of 1D Burning Time Comparison at IHF of 75 kW/m²

5.9.5 HRRPUA: No Edge Frame 100 mm x 100 mm Specimens
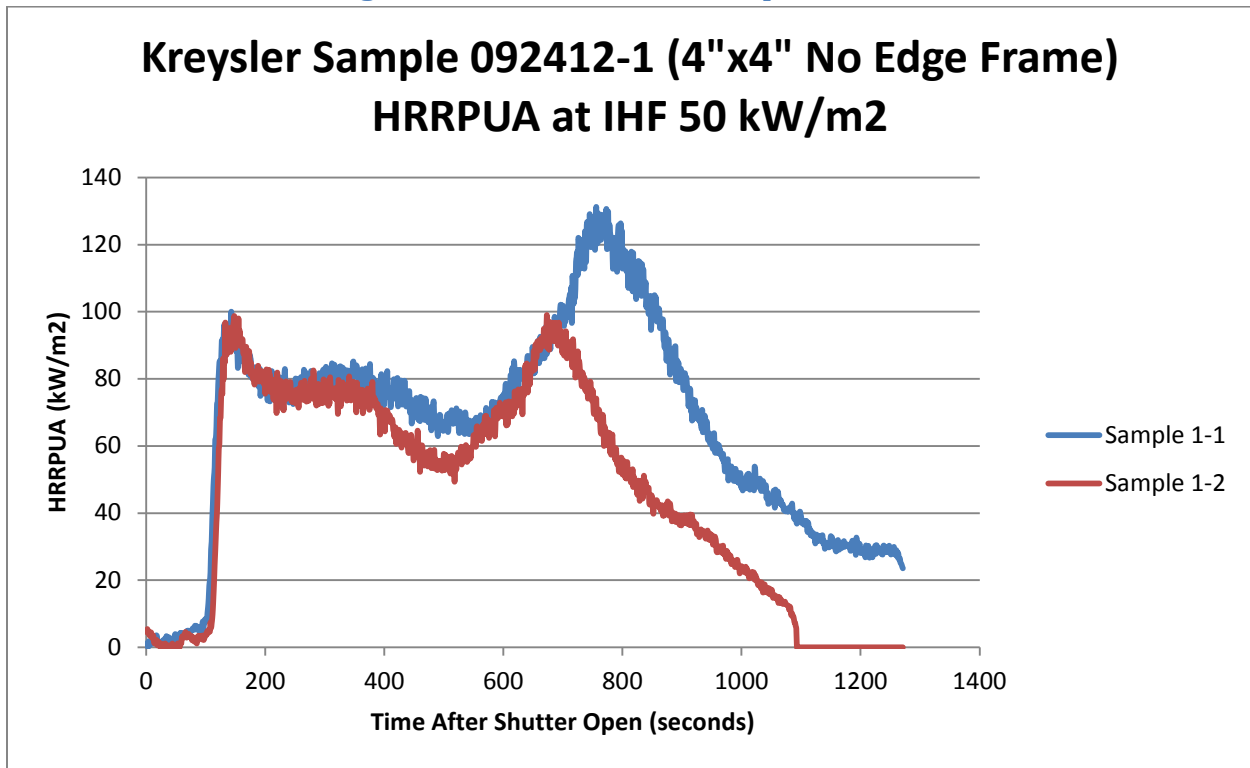
Figure 92: No Edge Frame HRRPUA Kreysler 1 at IHF of 50 kW/m²
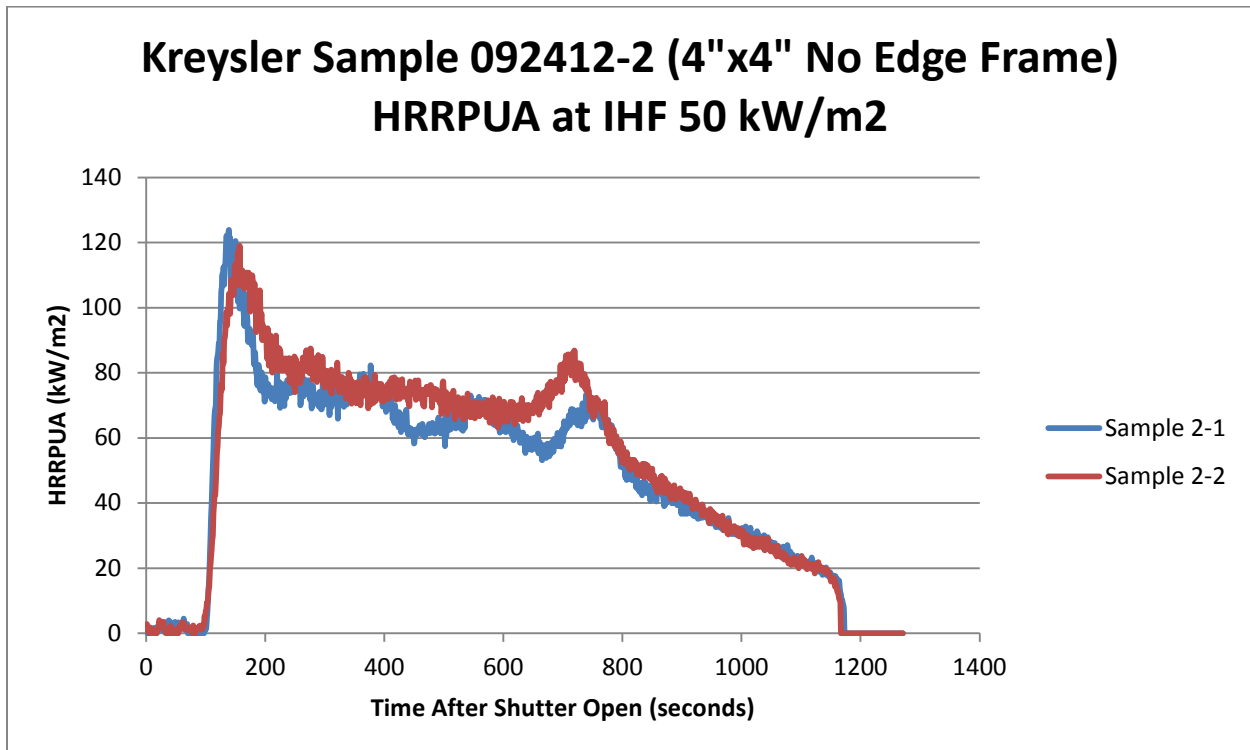
Figure 93: No Edge Frame HRRPUA Kreysler 2 at IHF of 50 kW/m²
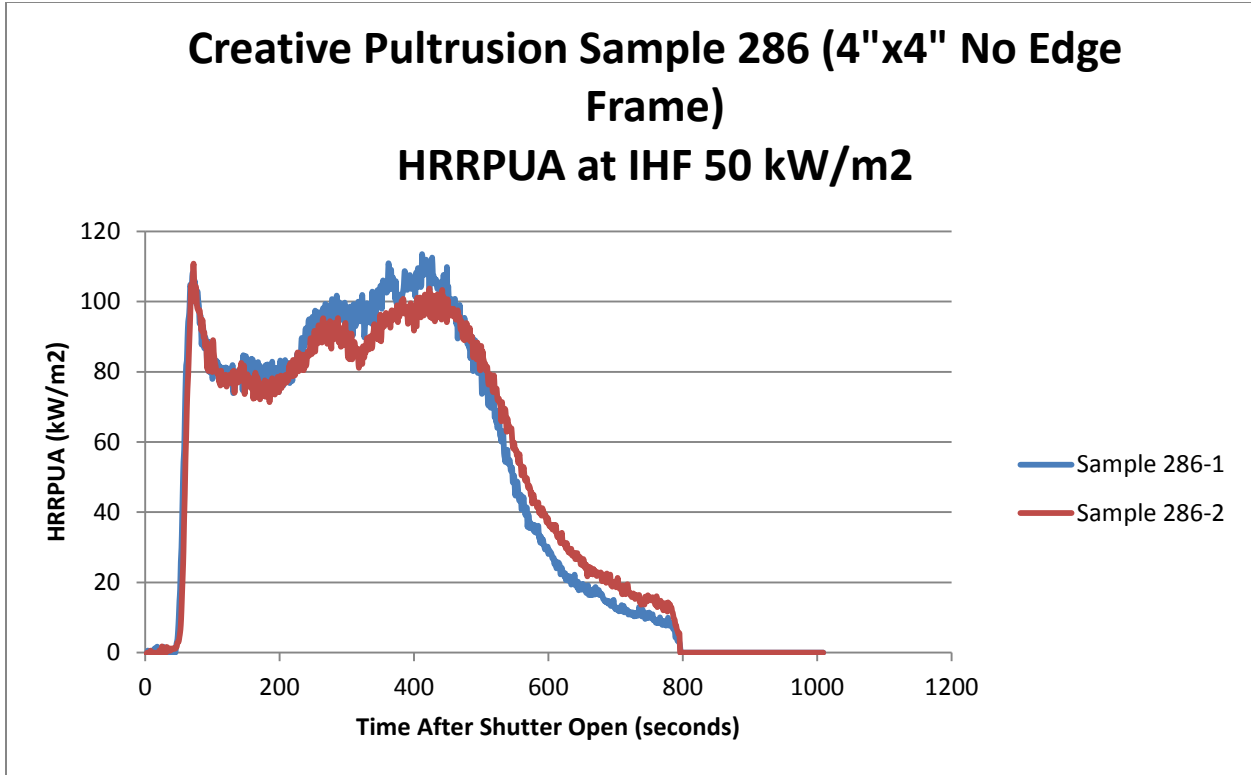
Figure 94: No Edge Frame HRRPUA CP 286 at IHF of 50 kW/m^2
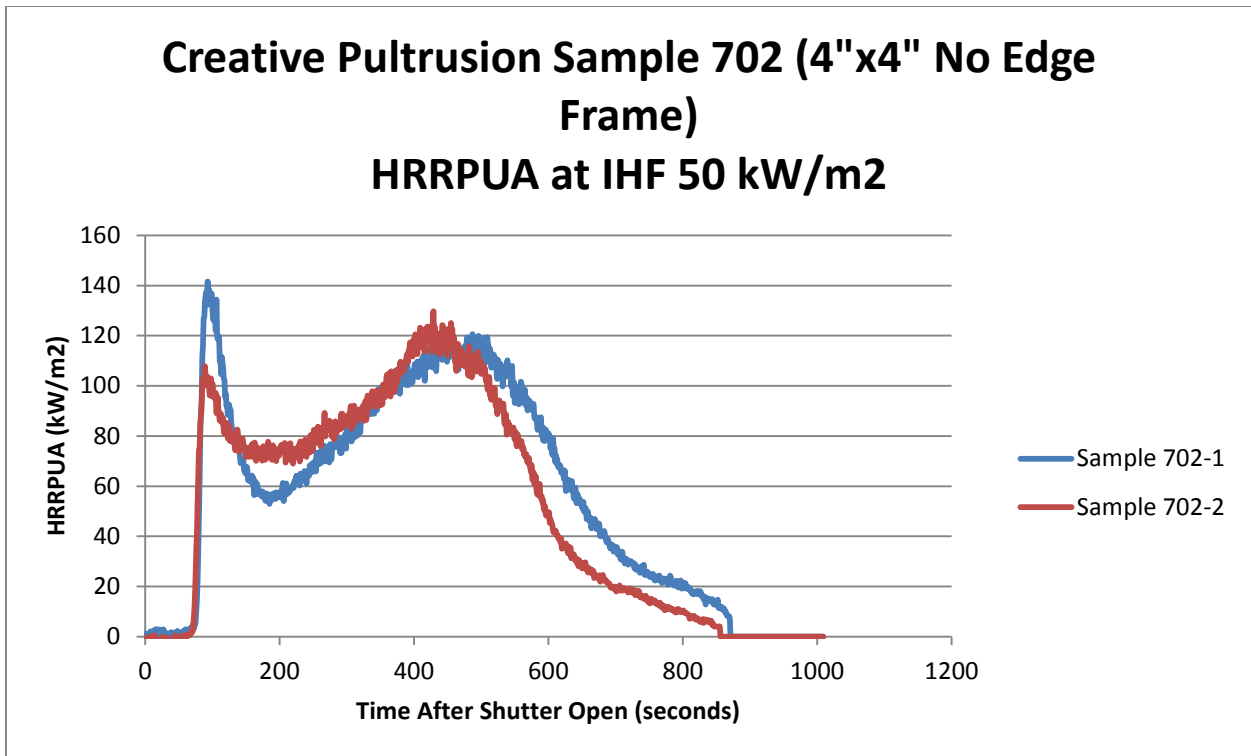
Figure 95: No Edge Frame HRRPUA at IHF of 50 kW/m^2
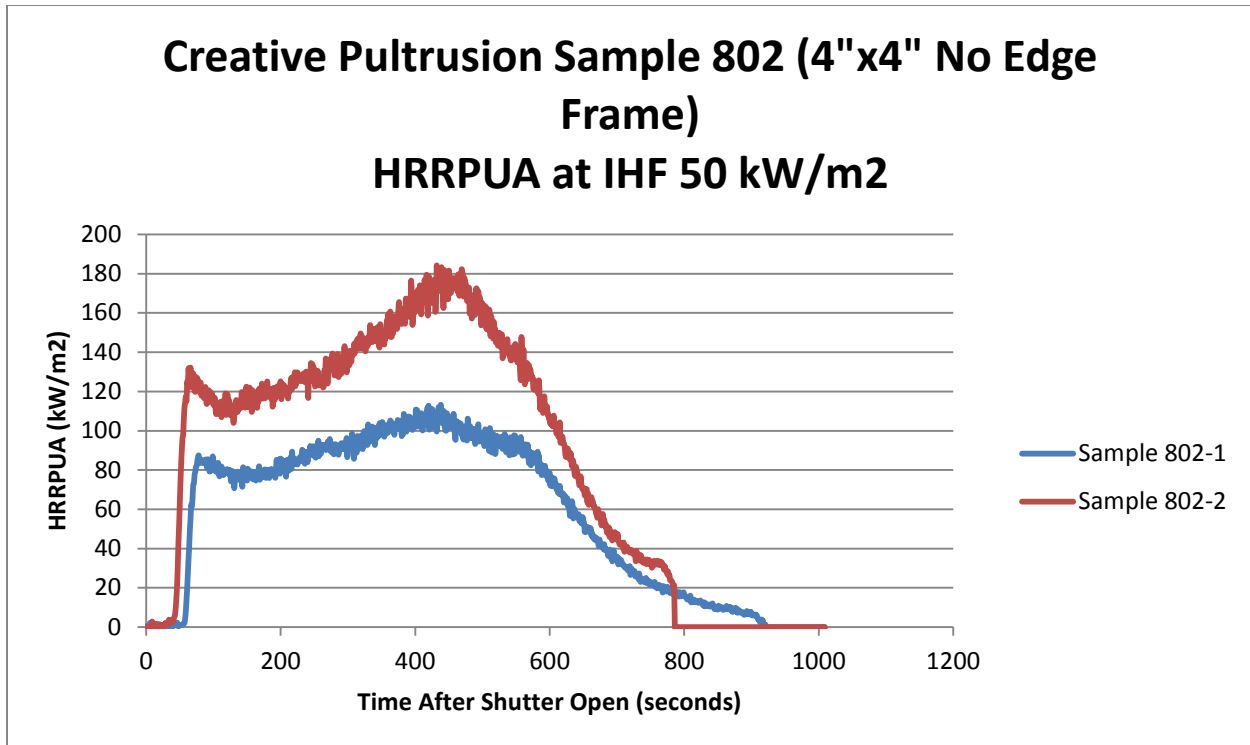
Figure 96: No Edge Frame HRRPUA CP 802 at IHF of 50 kW/m^2

5.9.6 Cone Analysis: No Edge Frame vs. Standard Comparison
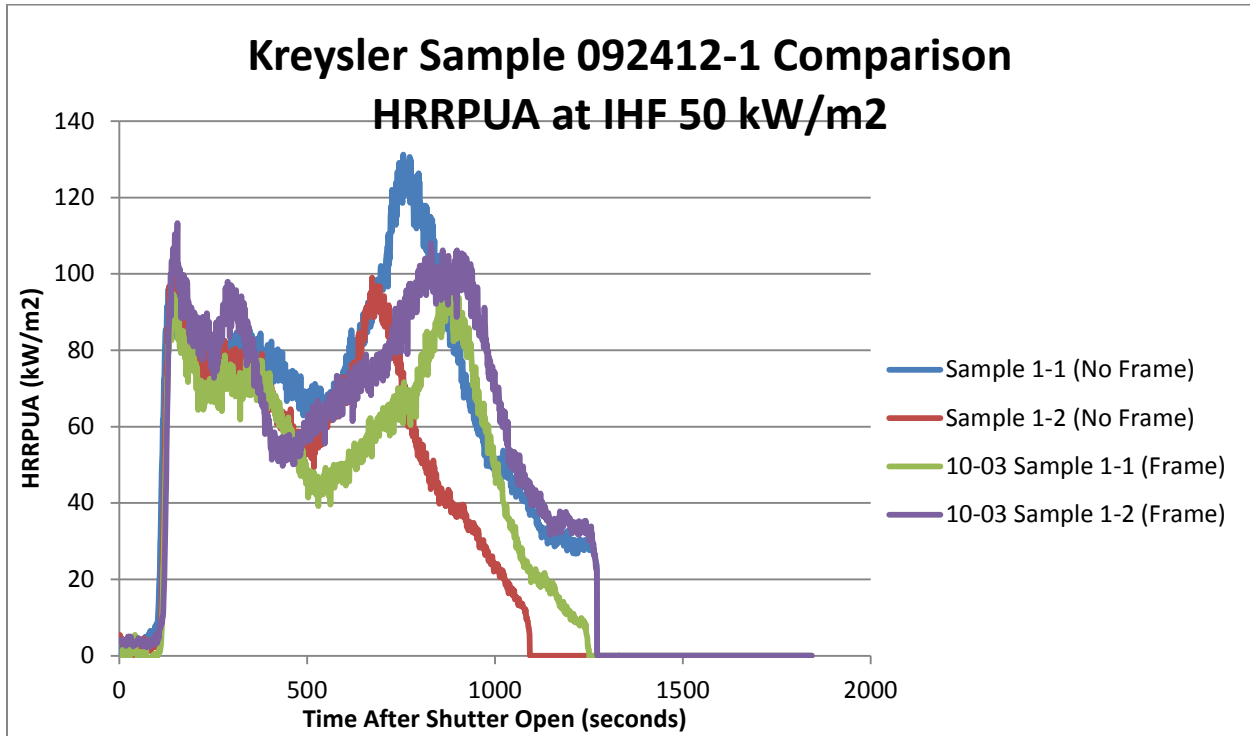
Figure 97: Kreysler 1 No Edge Frame to Edge Frame Comparison HRRPUA at 50 kW/m²
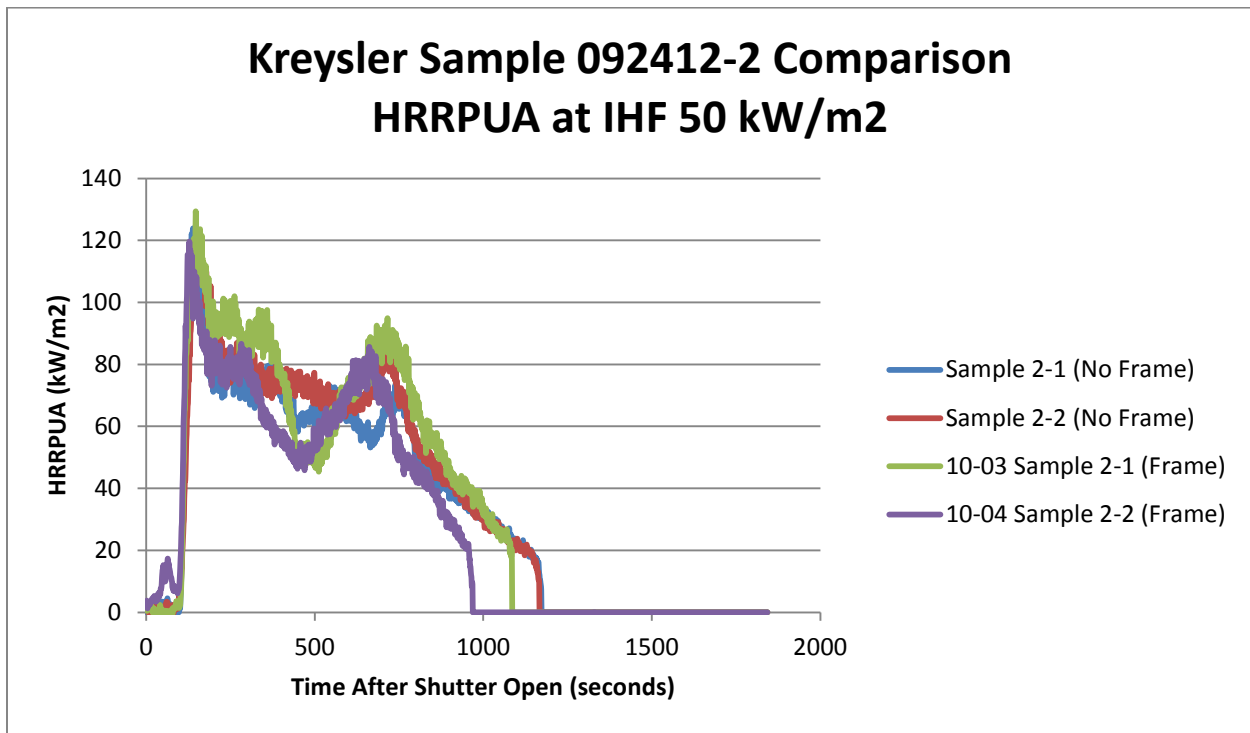
Figure 98 Kreysler 2 No Edge Frame to Edge Frame Comparison HRRPUA at 50 kW/m²
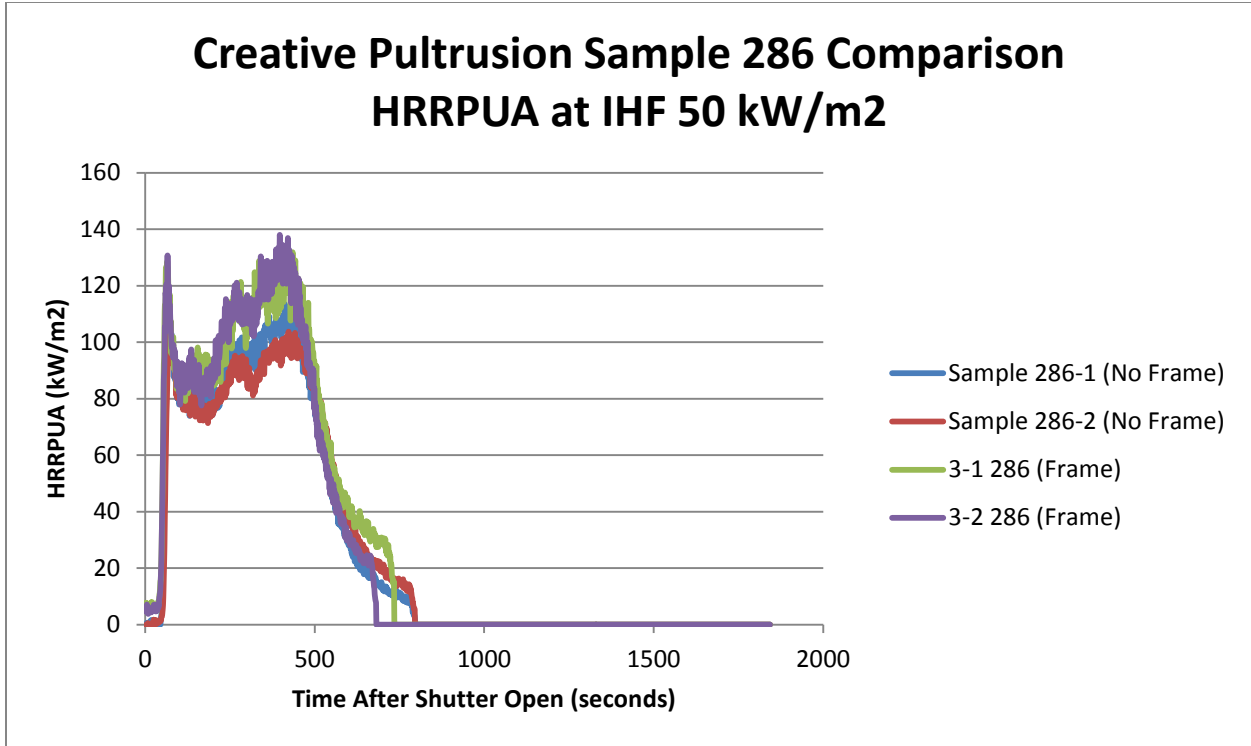
Figure 99: CP 286 No Edge Frame to Edge Frame Comparison HRRPUA at 50 kW/m²
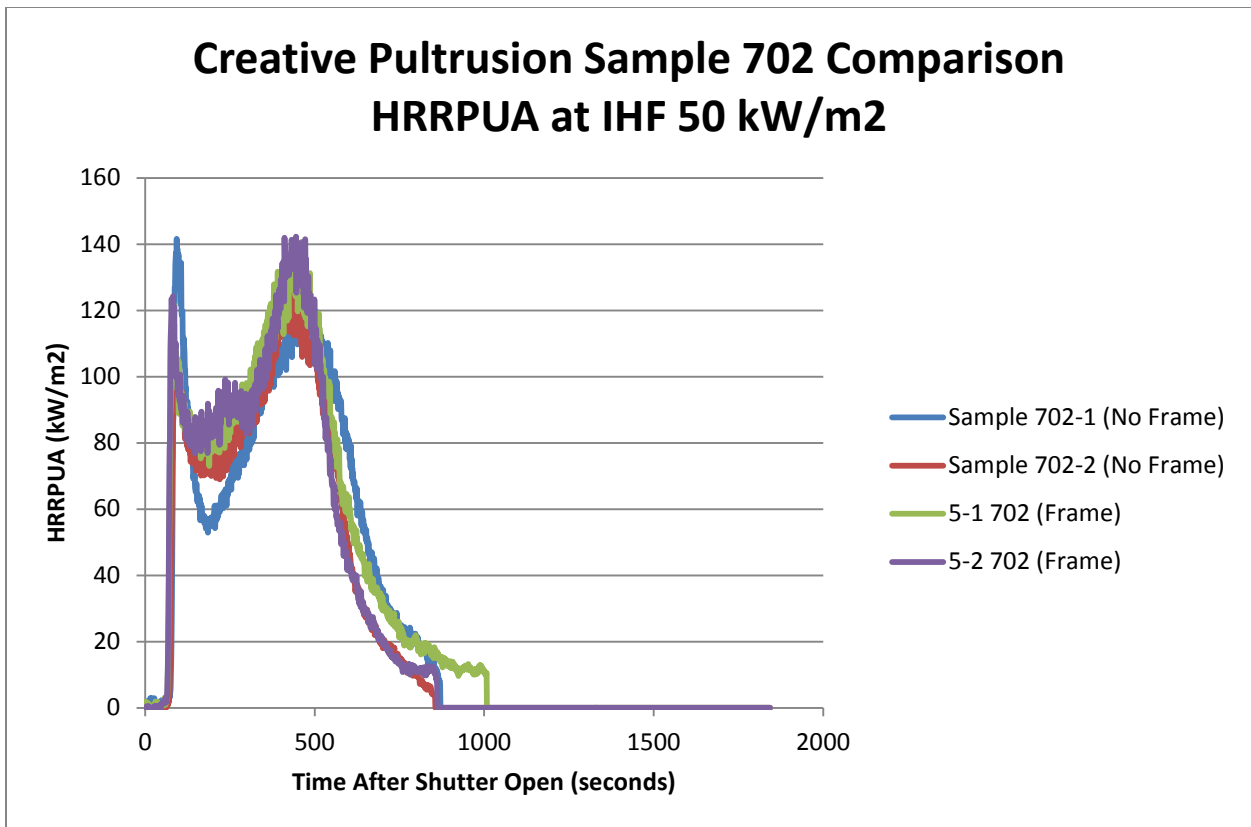
Figure 100: CP 702 No Edge Frame to Edge Frame Comparison HRRPUA at 50 kW/m²

Creative Pultrusion Sample 802 Comparison HRRPUA at IHF 50 kW/m2
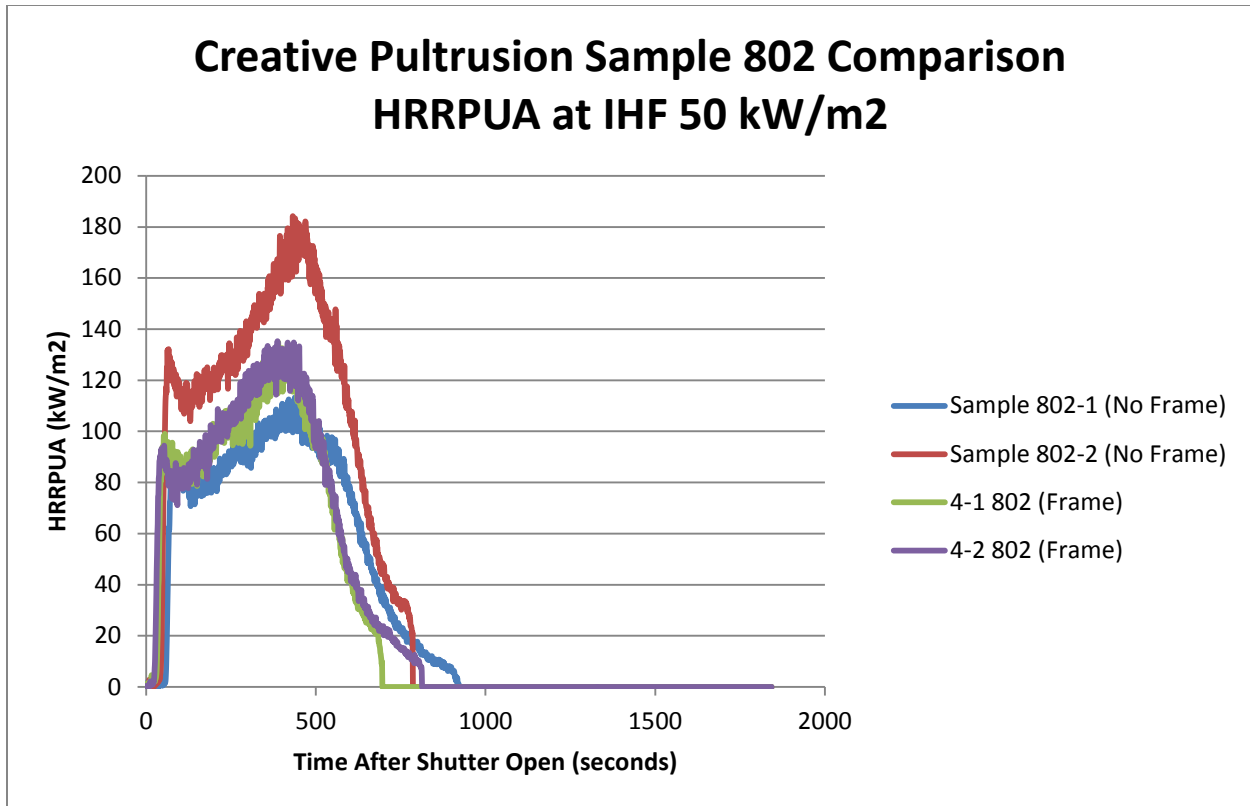
Figure 101: CP 802 No Edge Frame to Edge Frame Comparison HRRPUA at 50 kW/m^2

5.9.7   HRRPUA: Additional Tests
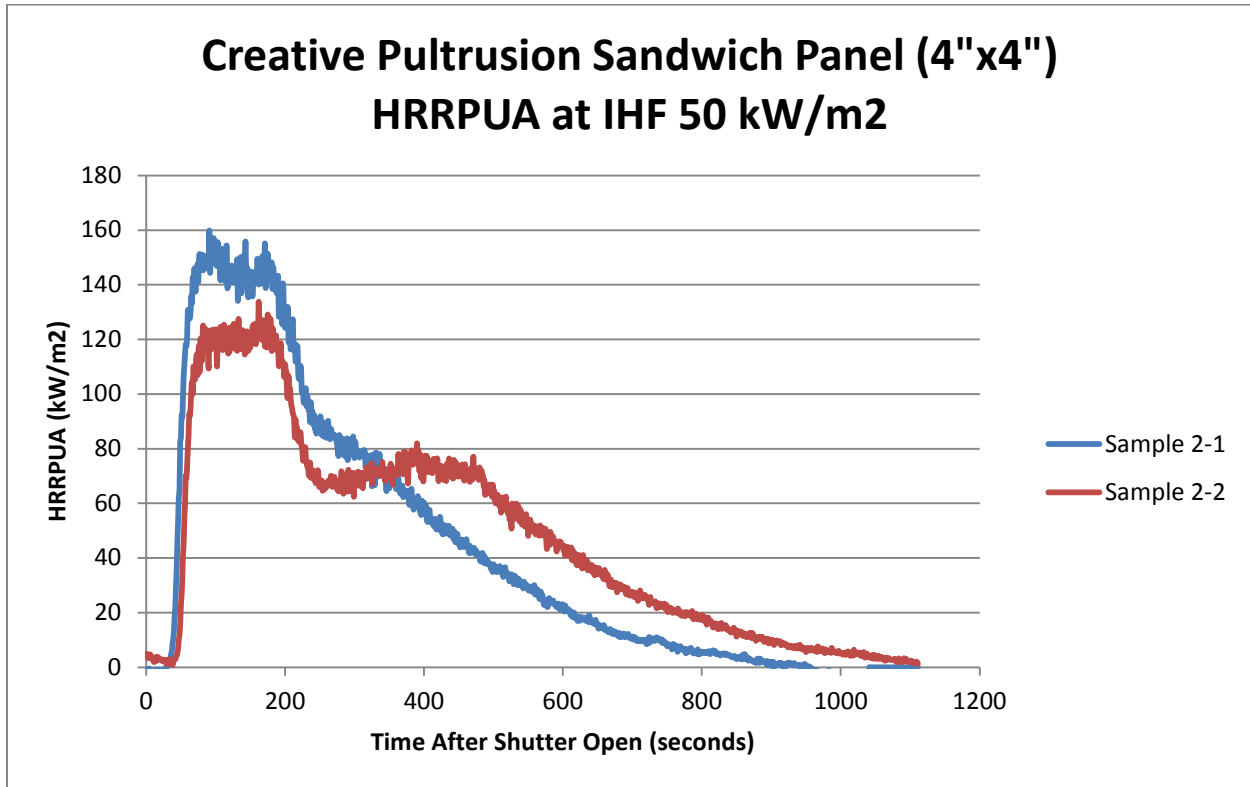
Figure 102: Standard Size CP Sandwich Panel HRRPUA at IHF of 50 kW/m^{2}
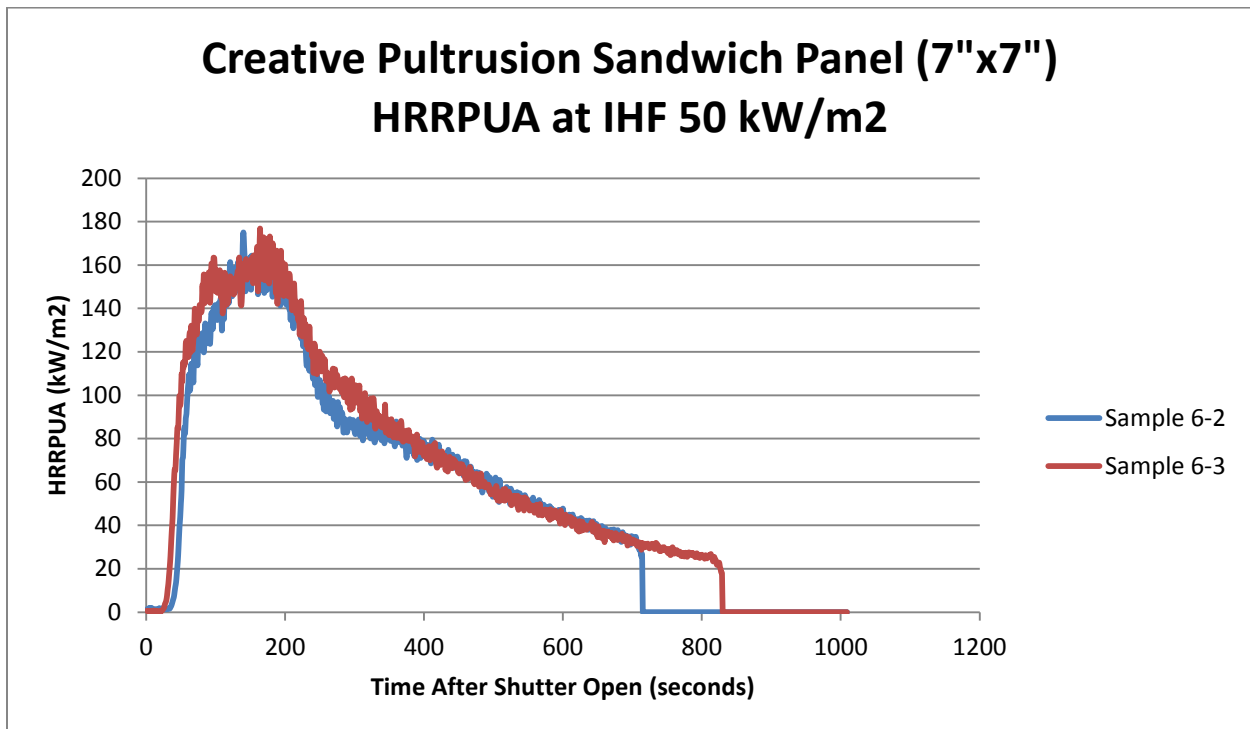
Figure 103: Extended Size CP Sandwich Panel HRRPUA at IHF of 50 kW/m^{2}
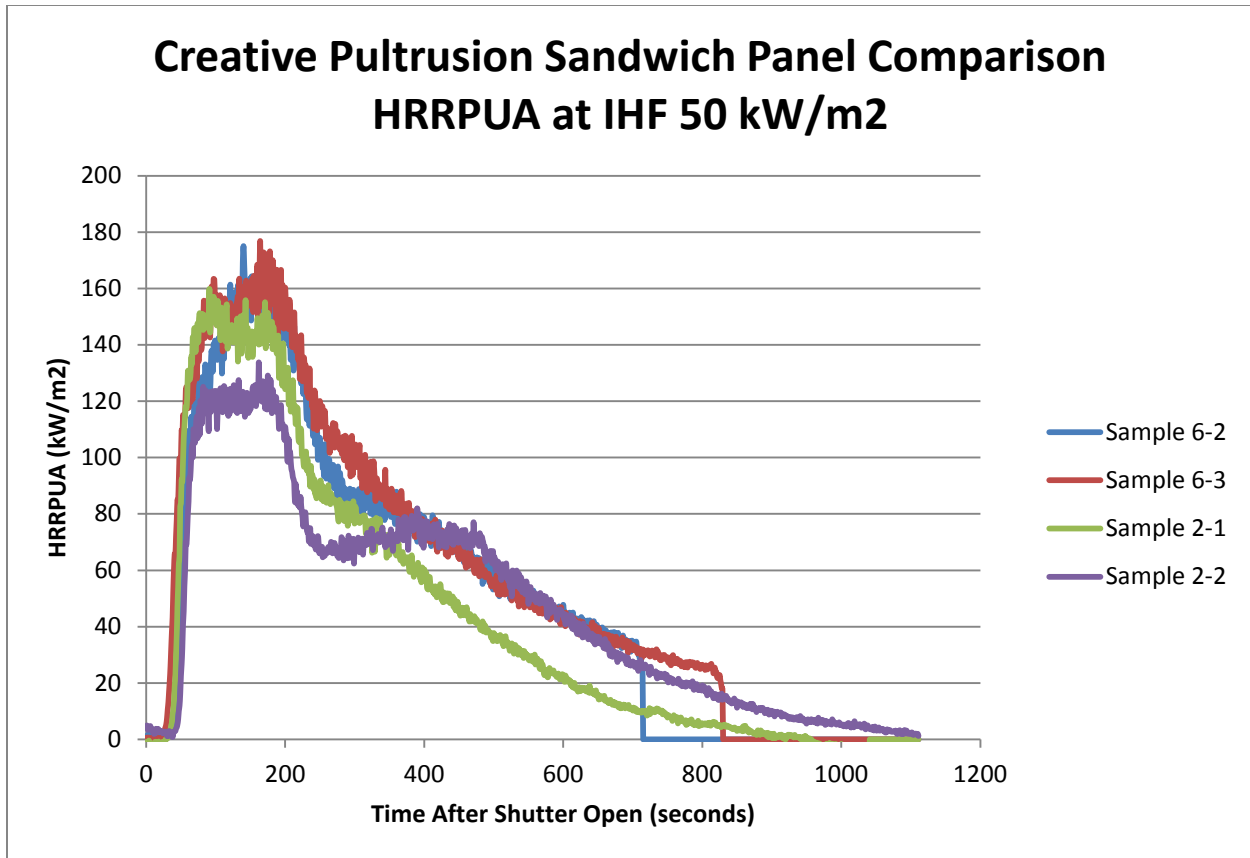
Figure 104: Size Comparison CP Sandwich Panel HRRPUA at IHF of 50 kW/m^{2}

5.9.8 Stair Step IHF Cone Test Data
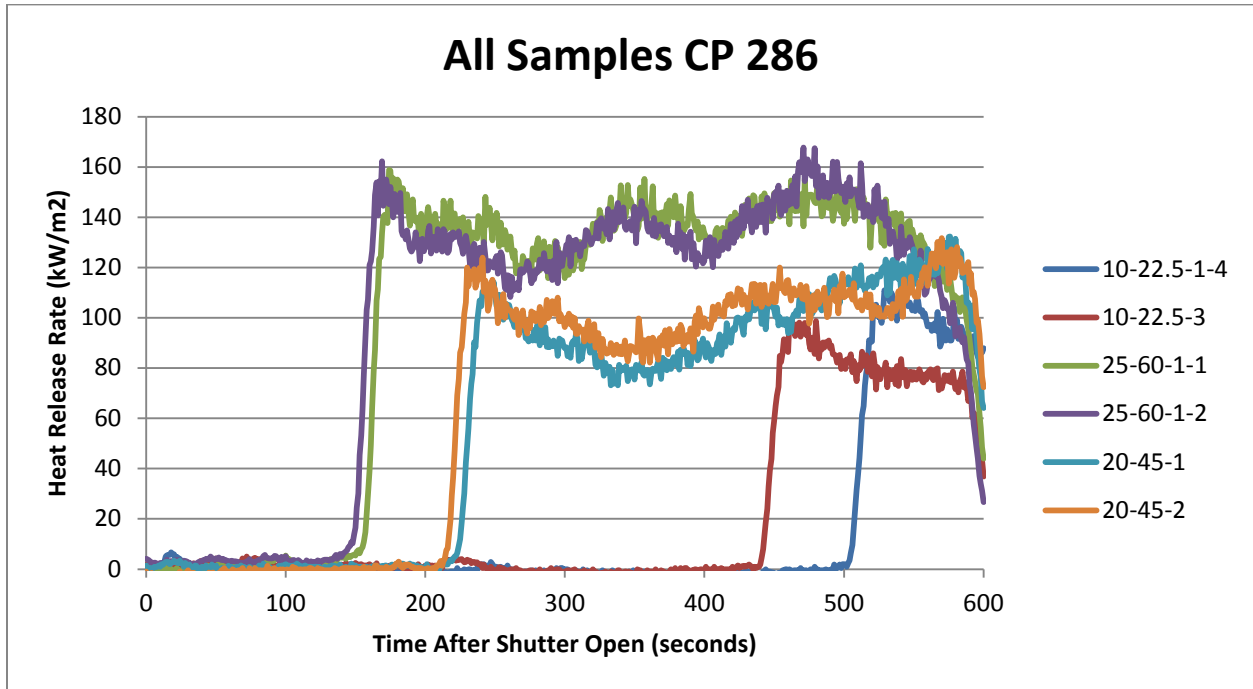
Figure 105: HRRPUA CP 286 Stair Step Heating
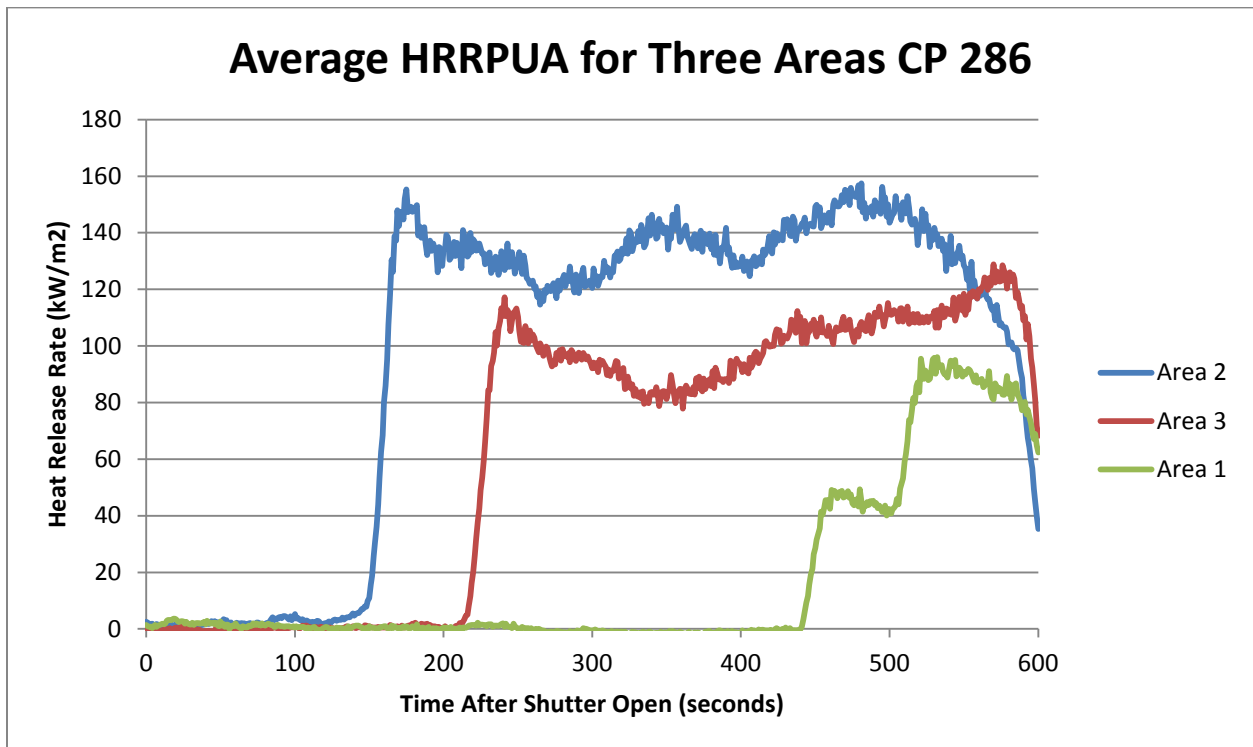
Figure 106: Average HRRPUA CP 286 Stair Step Heating
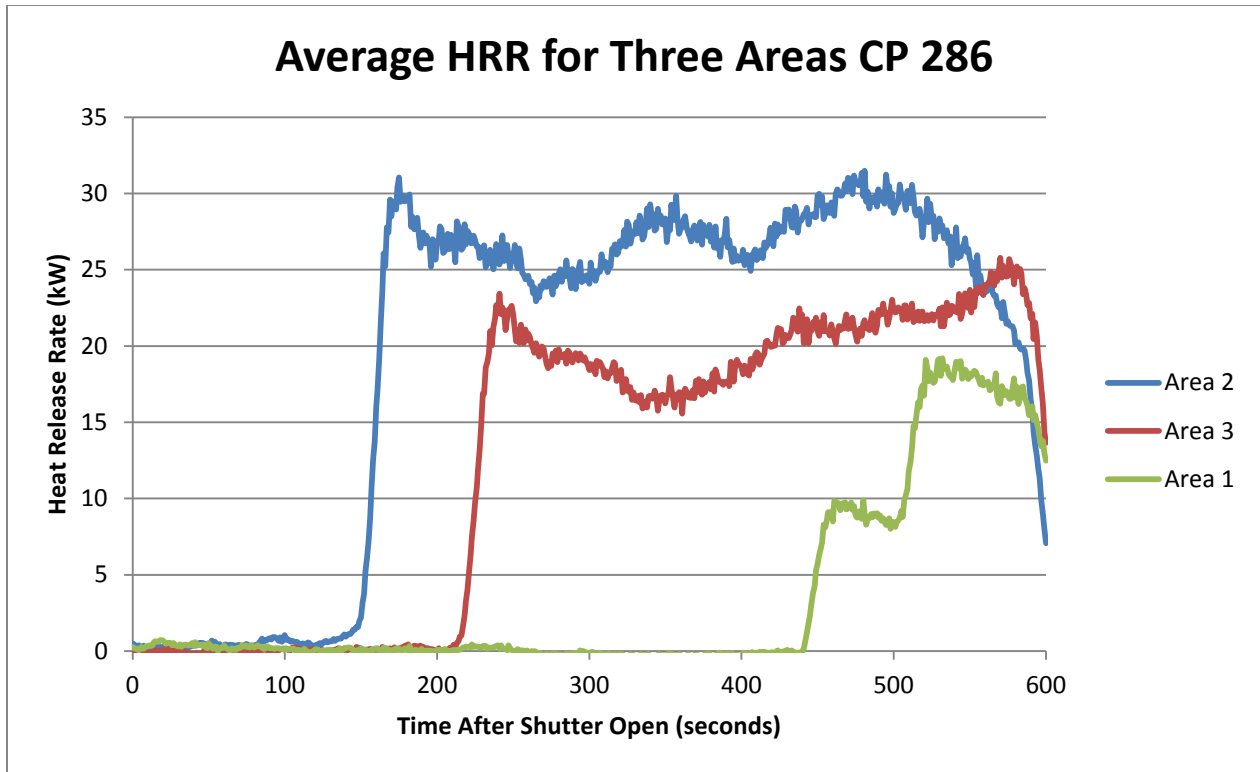
Figure 107: Average HRR CP 286 Stair Step Heating
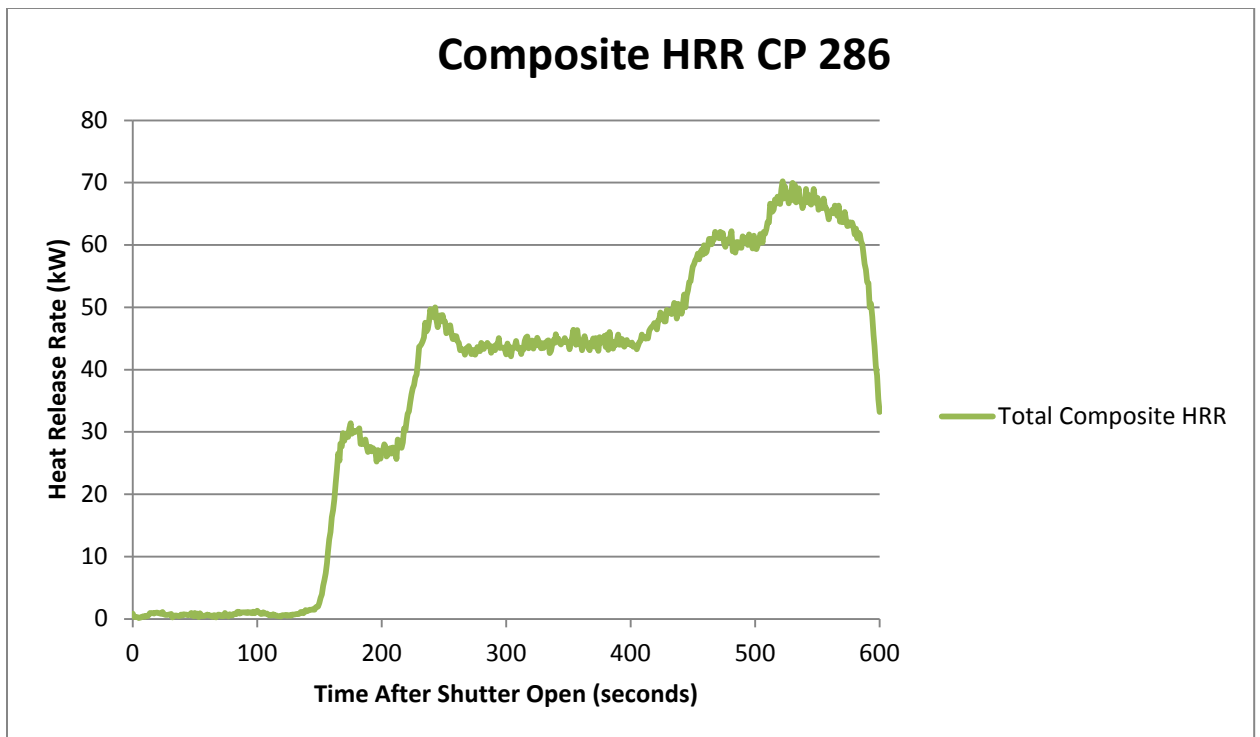
Figure 108: Composite HRR CP 286 After Condensing Stair Step Heating
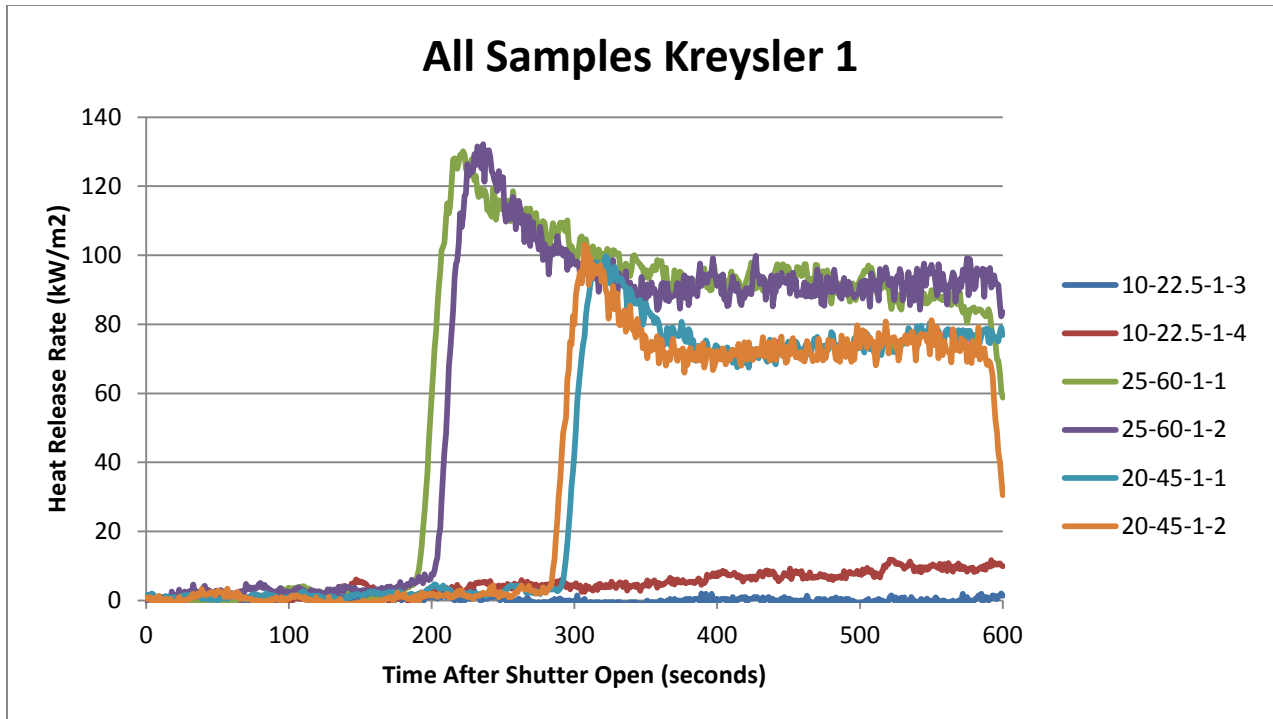
Figure 109: HRRPUA Kreysler 1 286 Stair Step Heating
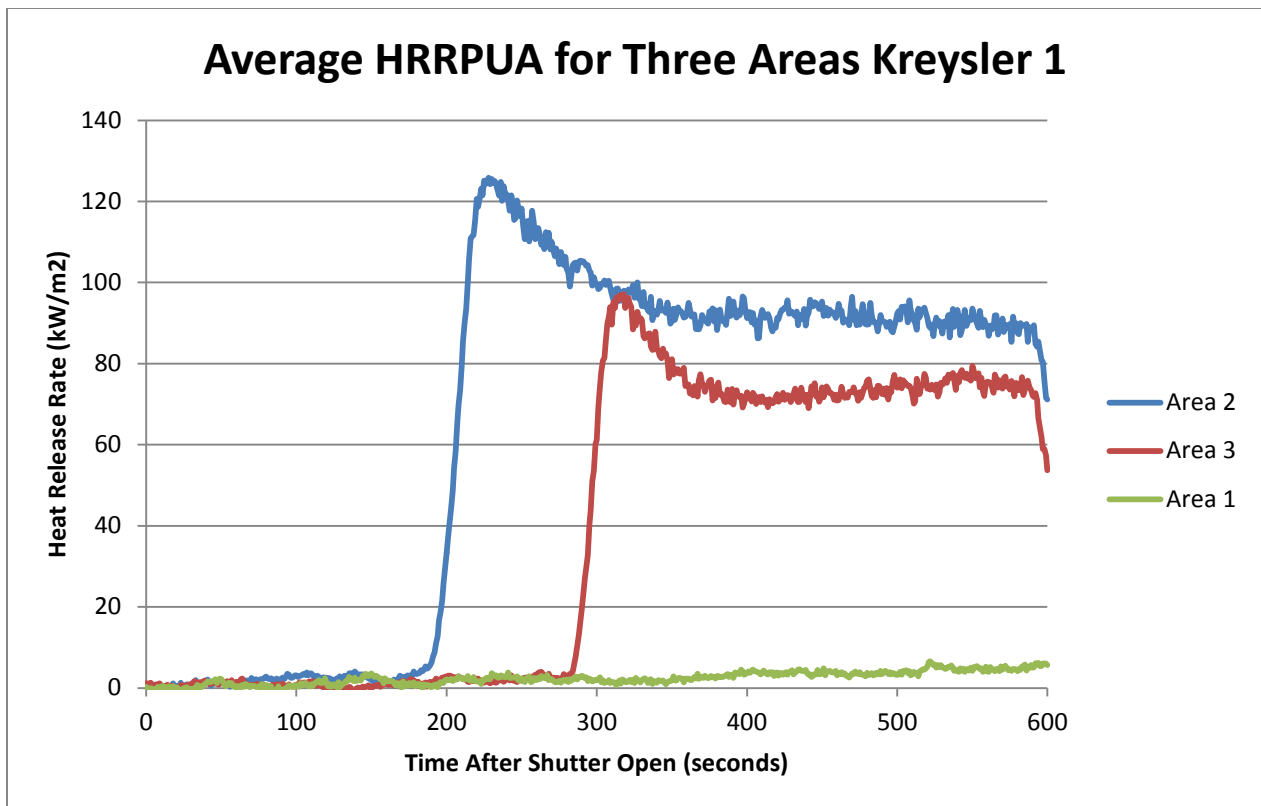
Figure 110: Average HRRPUA Kreysler 1 Stair Step Heating
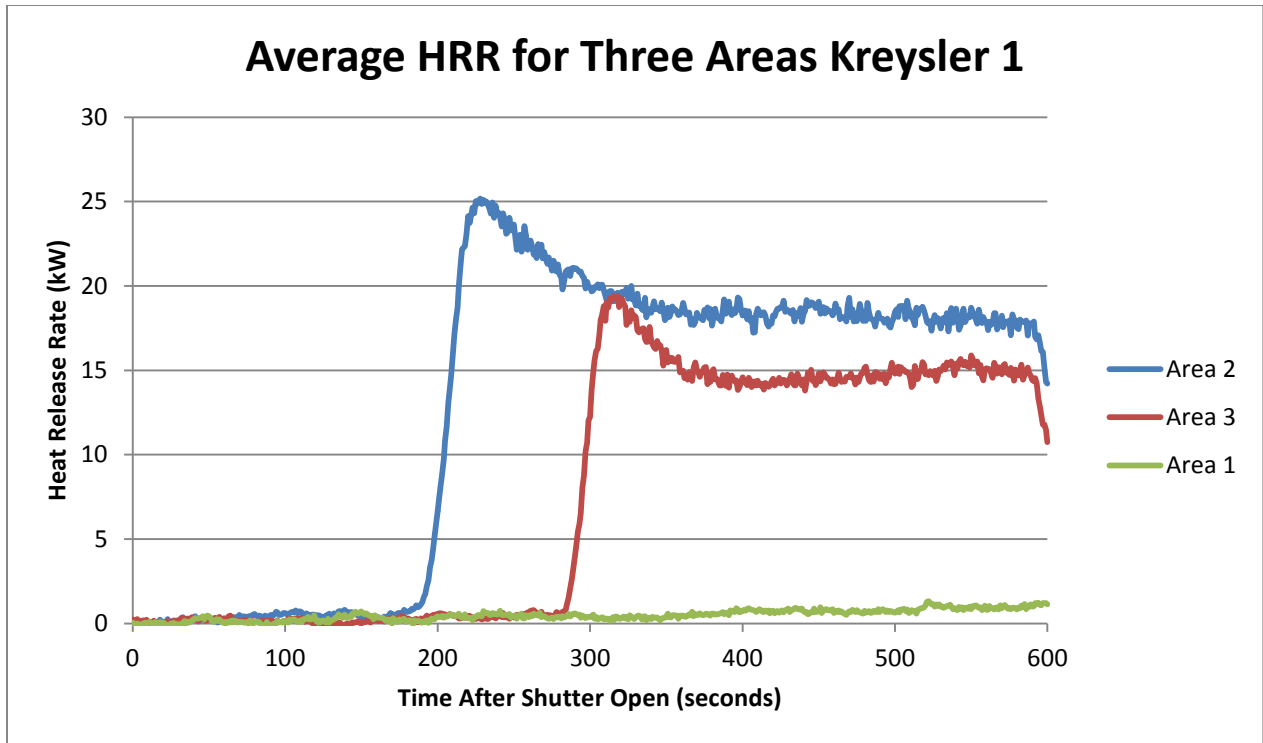
Figure 111: Average HRR Kreysler 1 Stair Step Heating
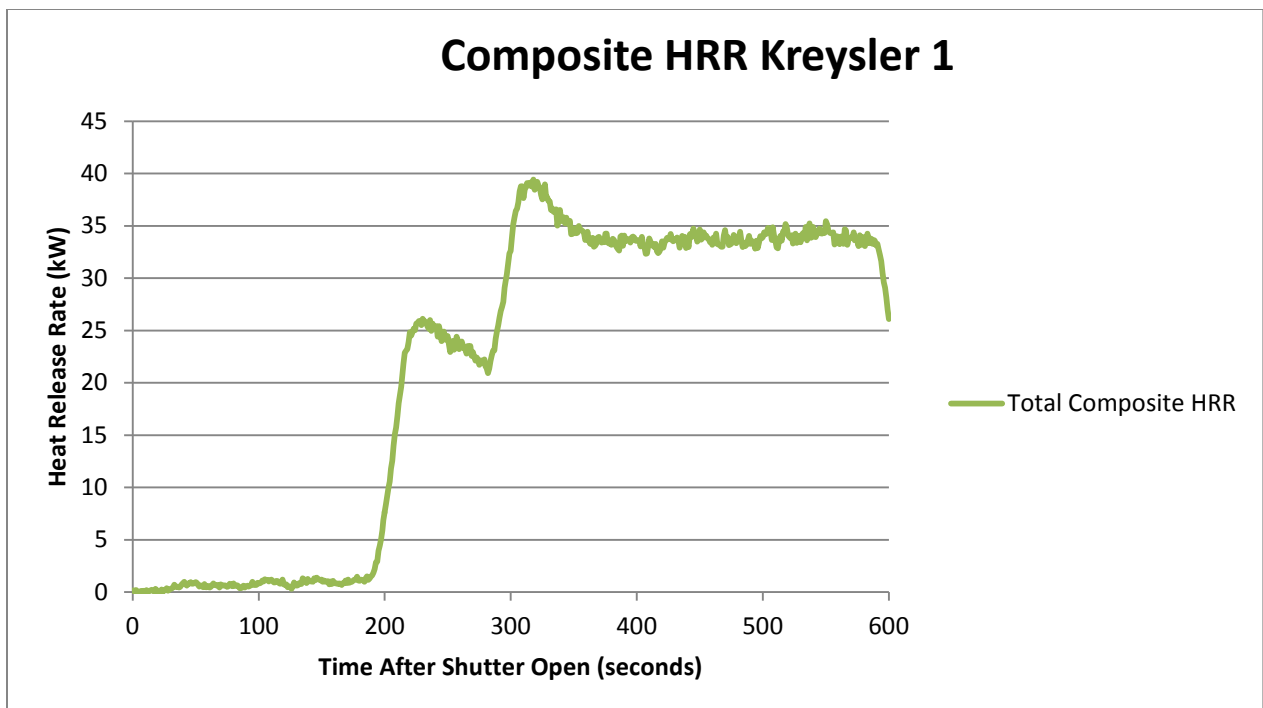
Figure 112 : Composite HRR Kreysler 1After Condensing Stair Step Heating
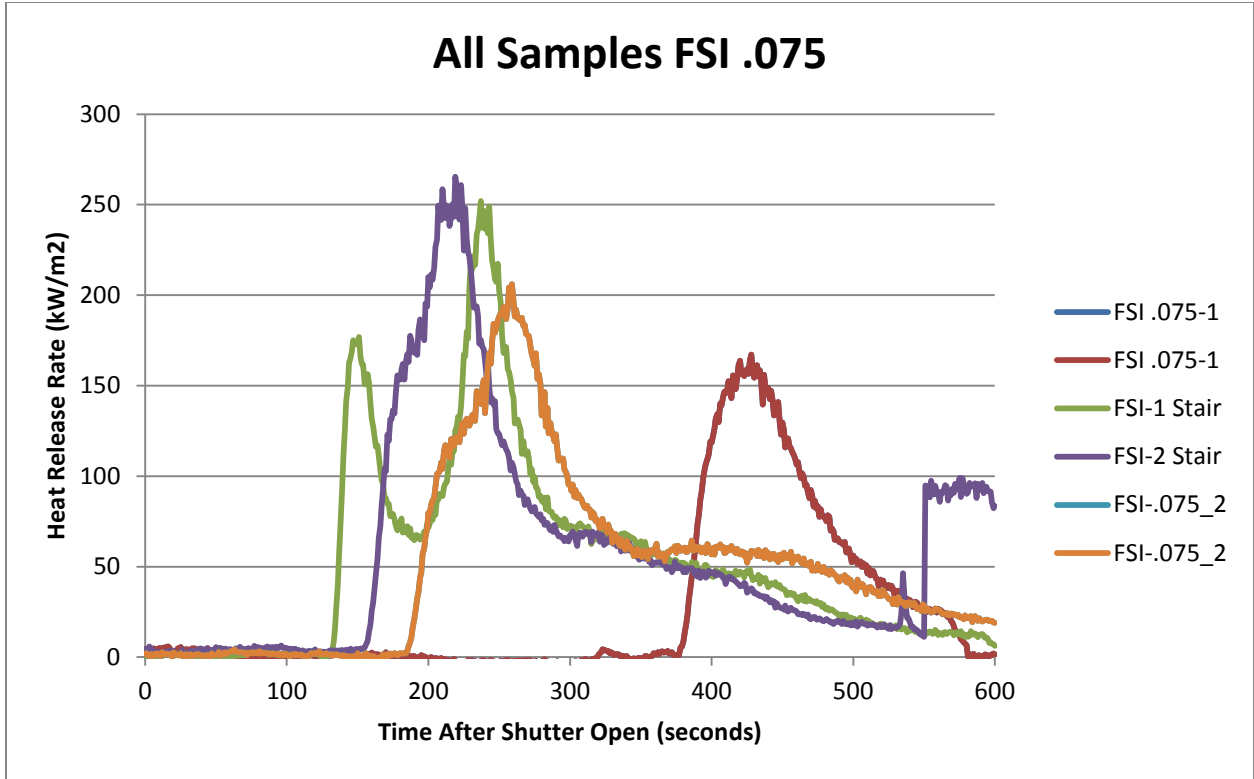
Figure 113 : HRRPUA FSI .075 Stair Step Heating
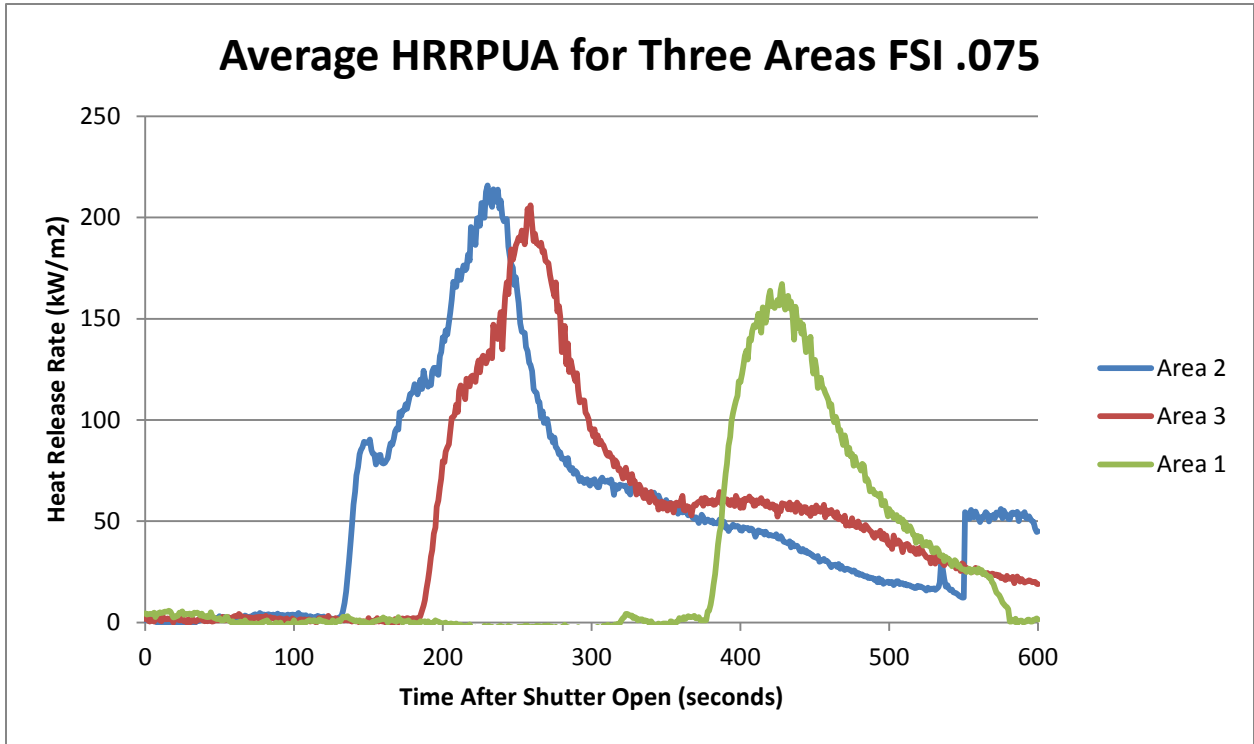
Figure 114 : Average HRRPUA CP 286 Stair Step Heating
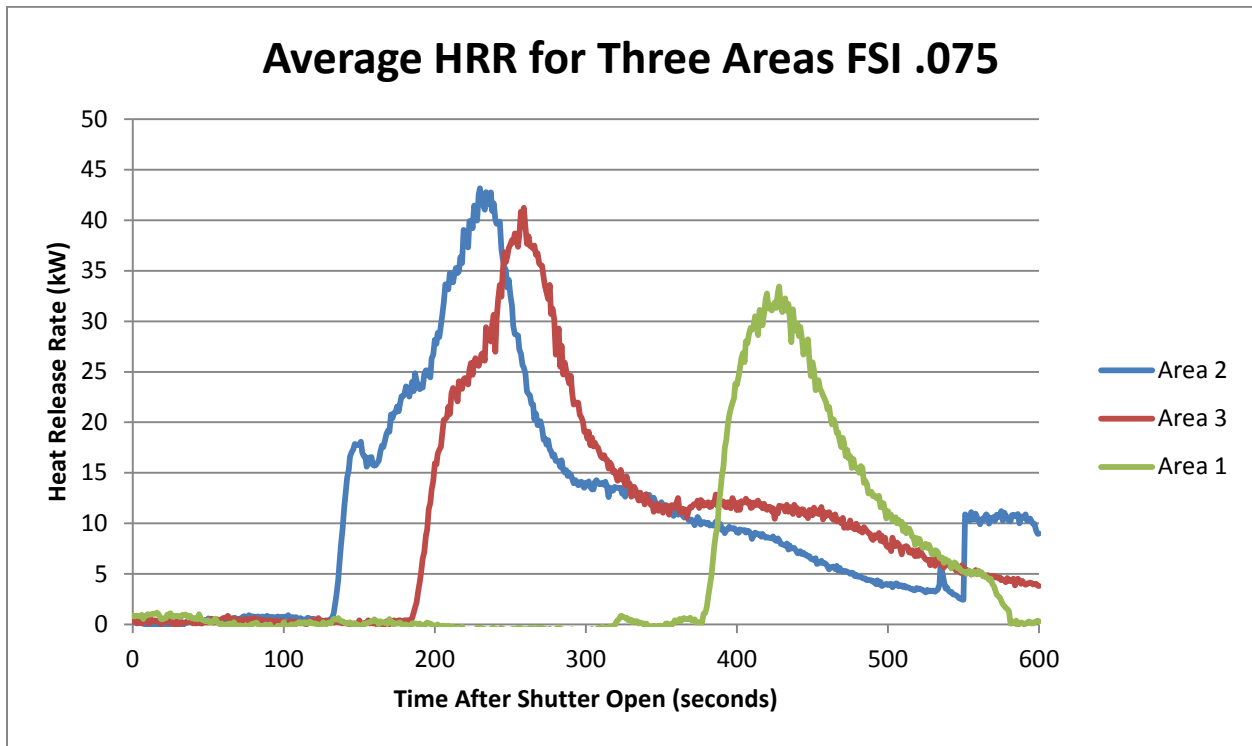
Figure 115 : Average HRR FSI .075 Stair Step Heating
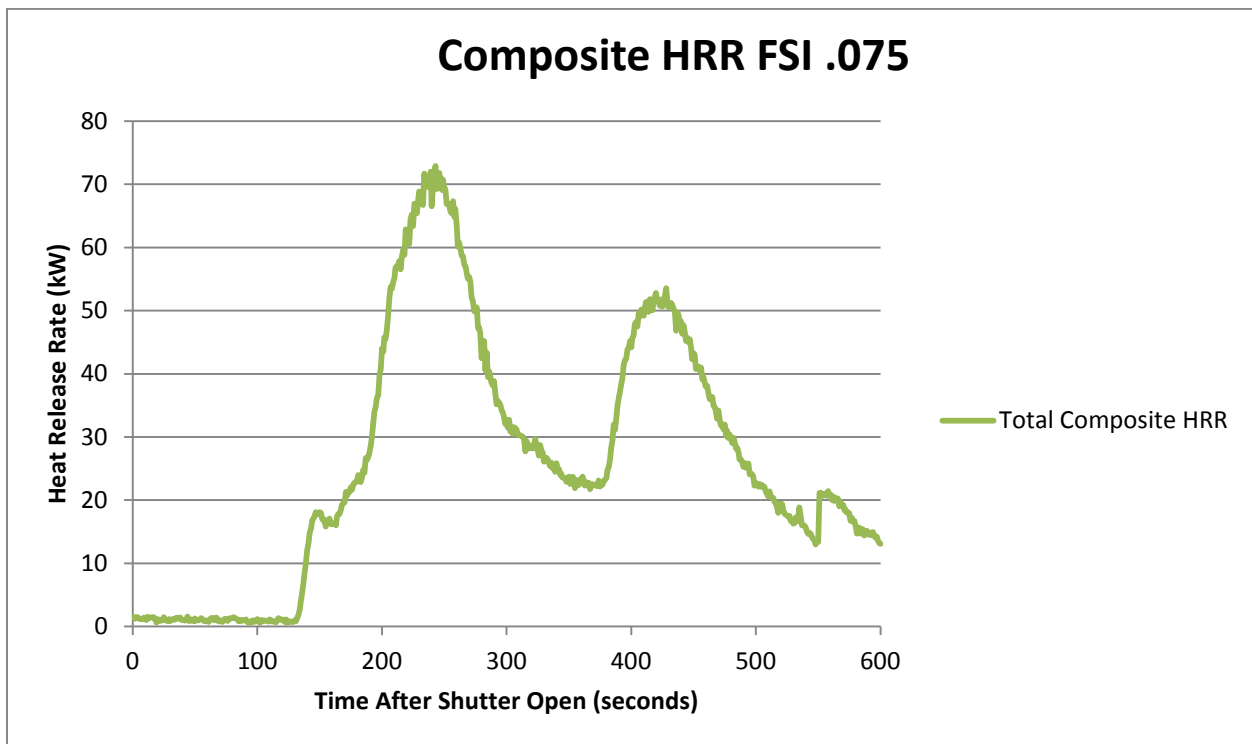
Figure 116: Composite HRR FSI .075 After Condensing Stair Step Heating
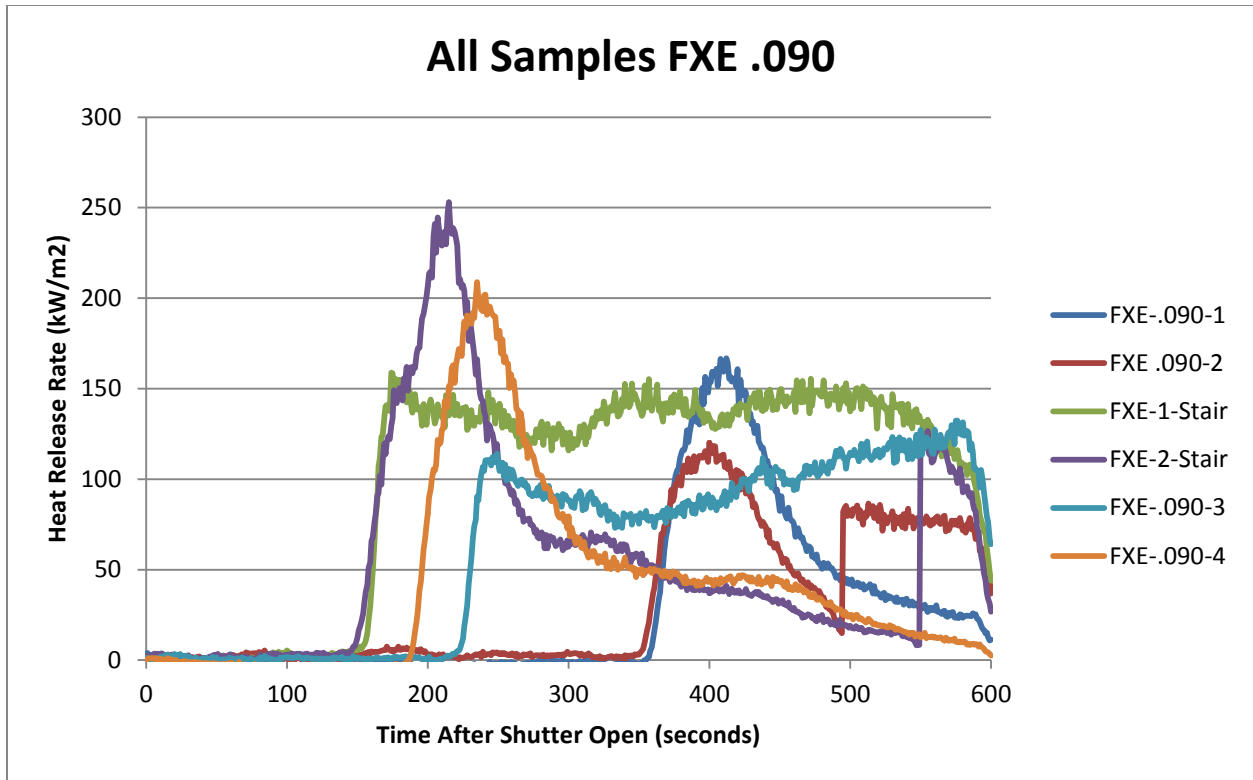
Figure 117: HRRPUA FXE .090 Stair Step Heating
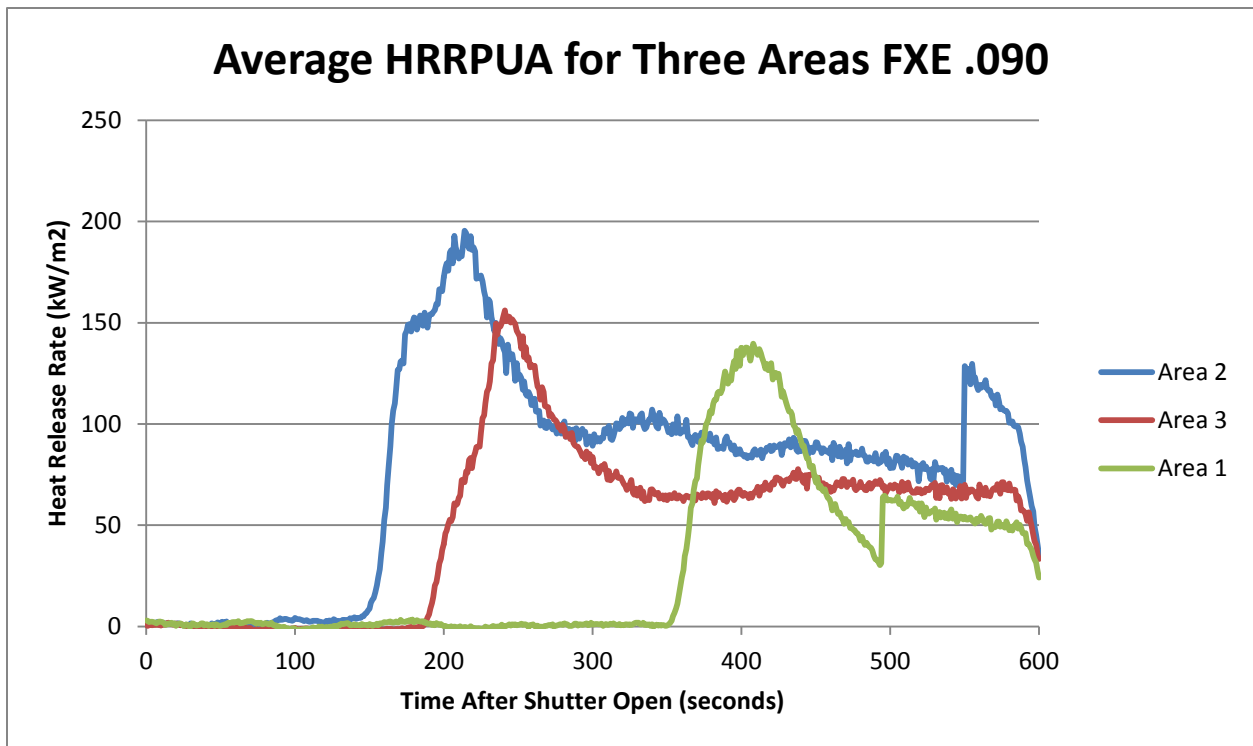
Figure 118 : Average HRRPUA FXE .090 Stair Step Heating
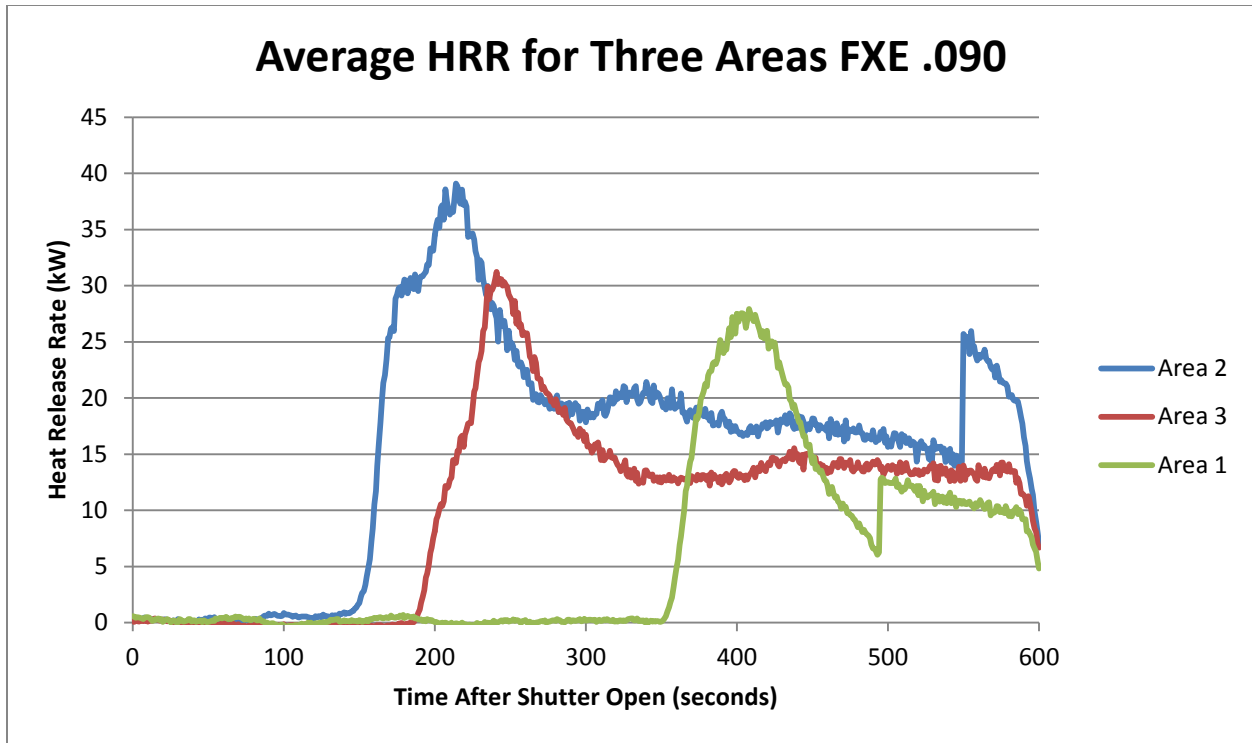
Figure 119 : Average HRR FXE .090 Stair Step Heating
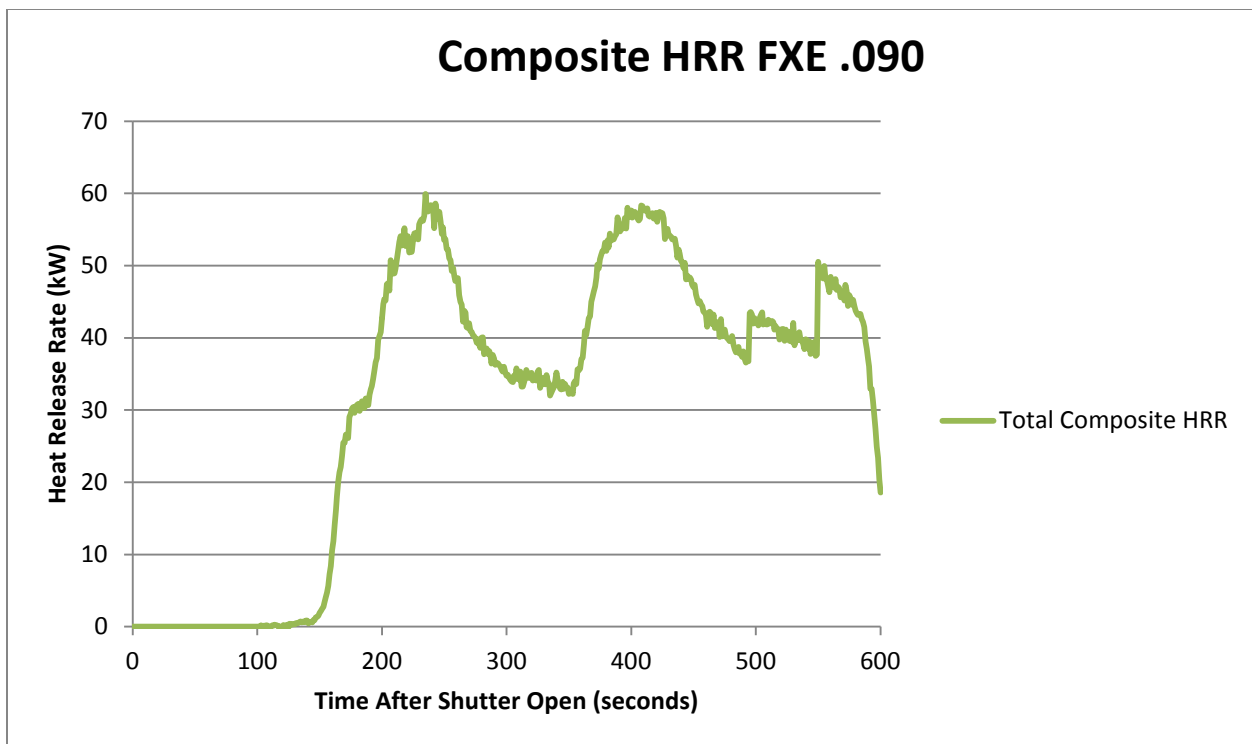
Figure 120 : Composite HRR FXE .090 After Condensing Stair Step Heating

5.10   Appendix - E-84 Flame Length Correlations from Cone Calorimeter Data

Primary Author: Shawn Mahoney

For our project, we will create a correlation for the flame height produced in the ASTM e84 Tunnel Test of a given material from data collected in the ASTM 1354 Cone Calorimeter Test. In order to create this correlation, we will be exploring existing flame height correlations and adjusting them to fit the parameters in the ASTM e84 Tunnel Test. This is important because flame height has been proven to be one of the two most important parameters that control the rate in which a flame spreads [3]. This correlation will help us determine the ability for a material to pass the ASTM e84 tunnel test with only running the material through the much less invasive ASTM 1354 test. This is possible because the determination of passing this ASTM e84 test is based upon the flame length created. In the case of the ASTM e84 test, it is measured through the distance a flame will travel down a tunnel given a material on the ceiling that is combusted. This brief will explain the different approaches that we took in order to end up at the final correlation described in the conference paper.

5.10.1 Flame Height

In order to be able to utilize these calculations we must first understand the study of flame heights. The most basic part of flame height seems to be the determination of the height itself. Most studies are based upon the visual observation of the flame itself [2]. This is determined by the average position of the luminous flame by eye, but the use of digital images has allowed this method to become more systematic. But the use of visual determination still depends on the establishment of a luminous flame[2]. Because of this, some scientists such as Hasemi and Quintiere began to determine the tip of the flame by detecting a temperature rise of 10 degrees C, and furthermore, chemical height of the flame as well. The chemical flame height was defined by Hawthorne as "the distance to the point of 99% complete combustion [1]. But in the scope of our project we will be focusing on the luminous flames because the e 84 tunnel test depends on the luminous flame. We will also be focusing on determining the flame height based upon the heat release rate determined in the cone calorimeter.

Empirical studies were completed in order to derive an equation that relates flame height to the dimensionless number known as the Froude number. The Froude number is a ratio of the inertia force on an element of fluid in to the weight of the fluid element. It is calculated as seen below.

$$Fr = \frac{v}{\sqrt{gl}}$$

Fr=Froude number
v= Velocity
g= Gravity
l= Characteristic Length

This dimensionless ratio has been incorporated with the heat release in order to create a value known as Q*. This value has then been used to help find a correlation between the height of the flame and the heat released. The value for Q* can be seen below.

$$Q^* = \frac{Q}{\rho c_p T_0 \sqrt{gD^3}} \text{ [3]}$$

Q=Heat Release rate per unit width (kW/m)
Rho= Density of the Fuel (kg/m[3)]
C_p= Specific Heat of the Fuel (kJ/kg)
T_0=Ambient Temperature (K)
g= gravitational acceleration (m/s^2)
D= Diameter of fuel source (m)

The Froude number will prove to be a very important variable in most of the flame height equations that we consider for our correlation.

5.10.2 Equations to Be Used

In order to help us establish a correlation we need to find an existing flame height equation that we can adjust to determine the flame length in the ASTM e84 tunnel test based upon the Heat Release Rate. From our research we have found numerous equations that relate flame height to the Heat Release Rate, but each equation is based upon different burning configurations. The burning configuration that best fits the burning in the Tunnel Test is known as concurrent flow flame spread. Equations that model the concurrent flow flame spread work under the assumption that the flame is extending in the direction of the flow of air. This is analogous to the conditions in the Tunnel Test because there is an imposed air flow of 2 m/s in the direction that the flame is to spread. Equations modeling concurrent flow flame spread are created by correlating a flame height created from a concurrent flow, which is usually air flow created by natural convection. This flame height is then correlated to a known heat release rate of the fire. These equations have been compiled in order to find one that can best be adapted in order to model the flame height in the Tunnel Test.

Equation 1

Studies completed by Delicharsios, Quintiere, Acklund, and Yuji Hasemi concluded that the flame height on a wall proportional to the rate of heat release rate per unit width. These correlations for flame height were developed from existing data and simple source theory based on conservation of mass, momentum, and energy in the fire plume.[6] These studies were also completed using line burners which makes this equation extremely pertinent towards our research.

$$\frac{L}{D} = a(Q^*)^n \text{ [3,5,7] Q is in kW/m}$$

As found by Zuskoski and presented by Newman, for values of Q^* less than .15, a=40 and n=2 (1). This basic flame height equation will be a consideration for a basis of our flame length correlation in the ASTM-e84 tunnel test because the ceiling of the tunnel can be construed as a horizontal wall.

Equation 2

The next equation that we will be considering for our correlation is an equation developed by Delichatsios and verified further by King-Mon Tu and James Quintiere [9]. This equation was specifically verified with multiple types of wall materials mounted vertically. It was proven by King-Mon Tu and Quintiere that the flame height is proportional to the heat release rate per unit width of the material to

the 2/3 power. As noted in their paper they state that the initial slope as denoted in the equation as W can vary with fire conditions, but found to be around 004.33 and 006.66.

$$X_f = W\left(\frac{Q}{C_p T_\infty \rho_\infty g^{1/2}}\right)^{2/3} Q \text{ is in } kW \text{ [9]}$$

The values for specific heat, temperature, and density are for air. This equation proves to be a very good option for a use as our correlation. The value of W is a coefficient that we can be determined for the Tunnel Test from experimental data.

Equation 3
The final equation that we will be using in our analysis is an equation developed by William Parker as a correlation for heat release rate to distance down an ASTM e84 tunnel test, which was determined through oxygen depletion calorimetry in the ASTM e84 Tunnel. The equation is as follows

$$d = (0.61 + 49\, Q) \text{ Q is in MW[11]}$$

Q is the total heat release rate production in MW. This is obtained by multiplying the Heat Release per unit area found in the cone calorimeter by the area of the specimen burning in the tunnel.

5.10.3 Materials Collected for Correlation
For our correlation, it will be necessary to collect the heat release curves for multiple materials and compare that to available flame lengths in the ASTM e-84 tunnel test. In order to do this we have consulted existing FRP companies, and through great cooperation they sent us samples of their most populate class A FRPs along with the ASTM e-84 results.

5.10.3.1   Crane Composites
Crane composites was founded as a Kemlite Company in 1954, and is now currently the world's leading manufacturer of fiber-reinforced plastics. They have been extremely kind, and have sent us two of their most popular class A FRPs. These include two products from their Glasbord with Surfaseal line. One sample is their FSI- 0.075 Class A Fire-Rated 85 White Smooth FRP and the other sample is their FX-0.090 Class A Fire-Rated 85 White Pebbled Embossed FRP. With much generosity, they have sent us one 1 foot by one foot sample of each style. This will allow us to collect around 9 sets of heat release data to be compared with the flame lengths found in the ASTM e-84 tunnel test.

5.10.4 ASTM 1354 Test Procedure
In order to use these equations we need to find a heat release rate from the material that can be analogous to the heat release rate created in the ASTM e84 tunnel. To do this we need to better represent the conditions in the tunnel in the cone calorimeter. In order to do this we must find a test procedure for this specimen that matches the imposed heat flux of the tunnel test. To determine this test procedure we will be utilizing two data acquisitions made by William Parker [11], the first being the heat flux in the tunnel over time at 2 feet from the tunnel. This measurement was made using a water-cooled Gardon total heat flux gauge. The graph of this information can be seen below in Figure 121.
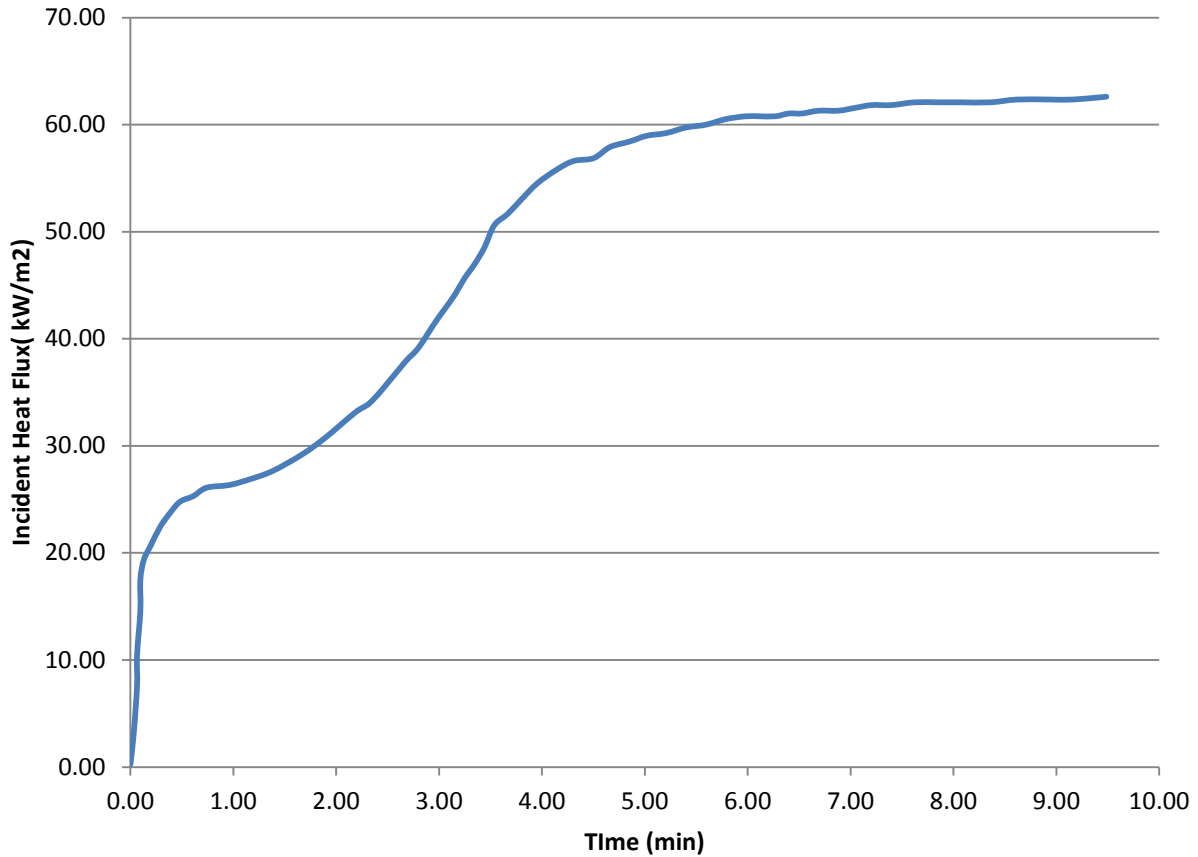
Figure 121: Incident Heat Flux at Two Feet Over Time

From this graph it can be seen that the incident heat flux imposed on the specimen is a function of time from the beginning of the test. We will use this data to help us create a test sequence in the cone that represents the imposed heat flux on the sample inside the Steiner Tunnel. The next aspect of the imposed heat flux that we will look at is the imposed heat flux on the sample as the distance from the burner increases. We obtained this data from William Parker as well and it can be seen below in Figure 122.
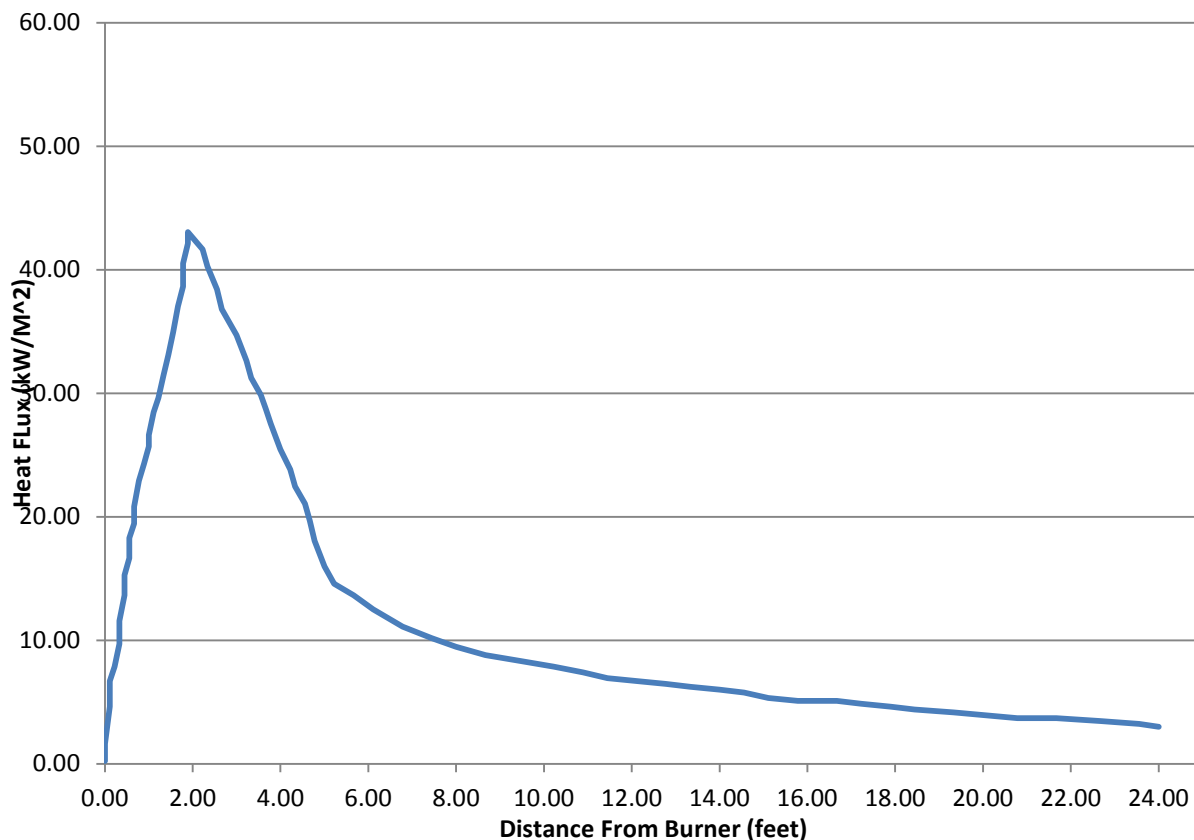
Figure 122: Incident Heat Flux per Distance in E-84 Tunnel

From this graph it can be seen that the imposed heat flux on the specimen is also a function of the distance from the burners. It was noted in Parkers research that he used thermocouples mounted on the front and rear surface of asbestos millboard every .1 meters in order to calculate the heat flux from the temperature differences rather than a water cooled heat flux gauge. This accounts for the lower peak heat flux in the distance graph because the thermocouple technique does not measure total heat flux. For our correlation we need to use the heat flux measured with the water cooled heat flux gauge because the incident heat flux in the cone calorimeter is measured using a water cooled heat flux gauge. Because of this, we have decided to combine the two sets of data. In order to do this we took the shape created by the thermocouples mounted every .1 meters and scaled it to match the heat flux measured with the water cooled heat flux gauge. In order to this we made three incident heat flux charts per distance as time increases in the tunnel. This was used by taking the maximum incident heat flux of 60 kW/m^2 and the minimum heat flux of 25 kW/m^2 from Parkers incident heat flux over time graphs and using them for the peaks of three time intervals. The three time intervals that we chose are 0-1.5 min, 1.5-4.75 min, and 4.75-10 min. Finally, we have also only focused on the first 4.5 feet of the tunnel because this is the area that is affected most by the burners. This is a good estimation for class A materials because they do not tend to spread as the test goes on. We are assuming a static pyrolysis area that is equivalent to the area of the specimen impinged by the flame. The three heat flux over distance graphs can be seen below in Figure 123.
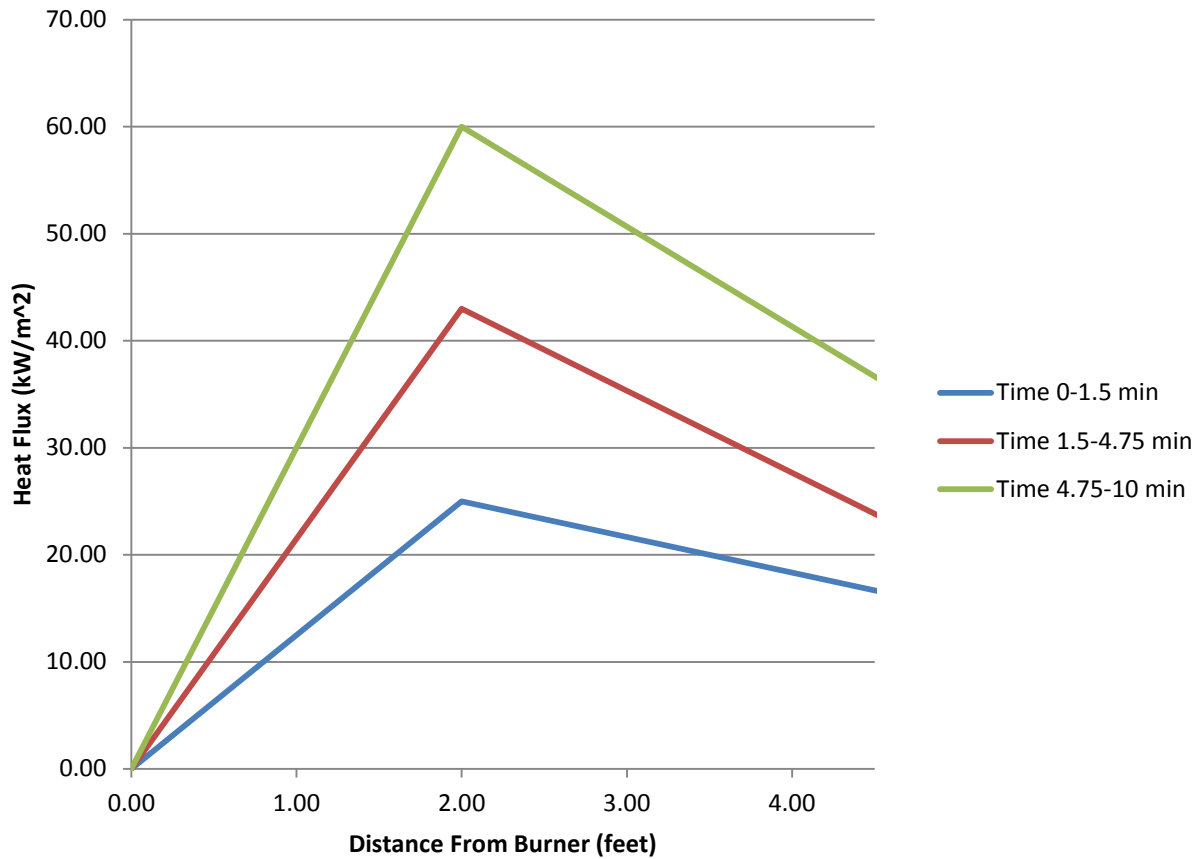
Figure 123: IHF Over The First 4.5 Feet per Time

After we created these graphs we needed to divide the 4.5 feet into areas that we could determine a heat flux over time graph to run in the cone. We decided to make this test easier; we need to choose the lowest number of areas to get accurate data because each area will ultimately account for a different heat flux step run in the cone. From Figure 124 seen below you can see that we divided the first 4.5 feet into three, foot and a half long areas along the 17 inch width of the tunnel.
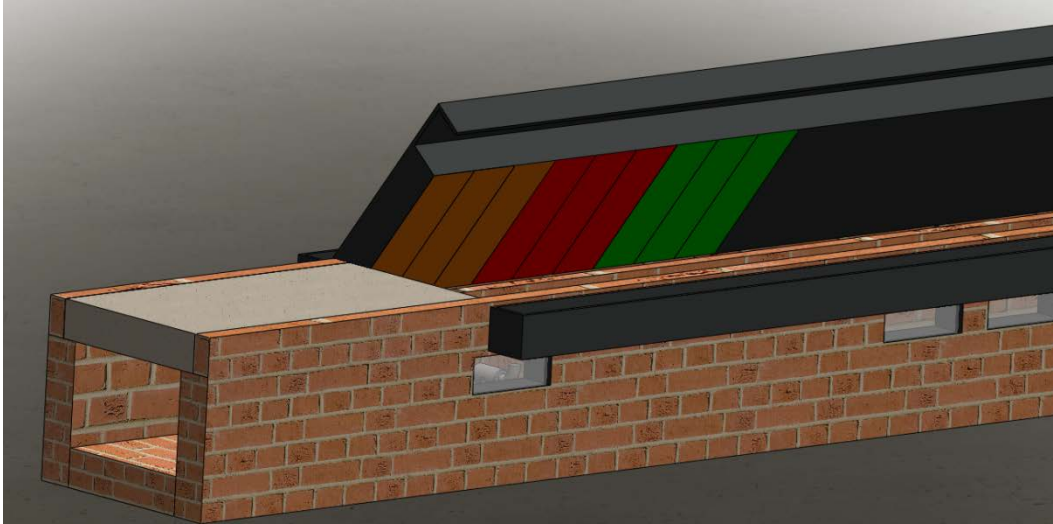
Figure 124: Tunnel Test Burn Areas

After dividing the 4.5 feet into three testing areas we looked at the graph to try and decide average values for each of the three time steps that we chose. The estimated average values that we chose can be seen below in Figure 125.
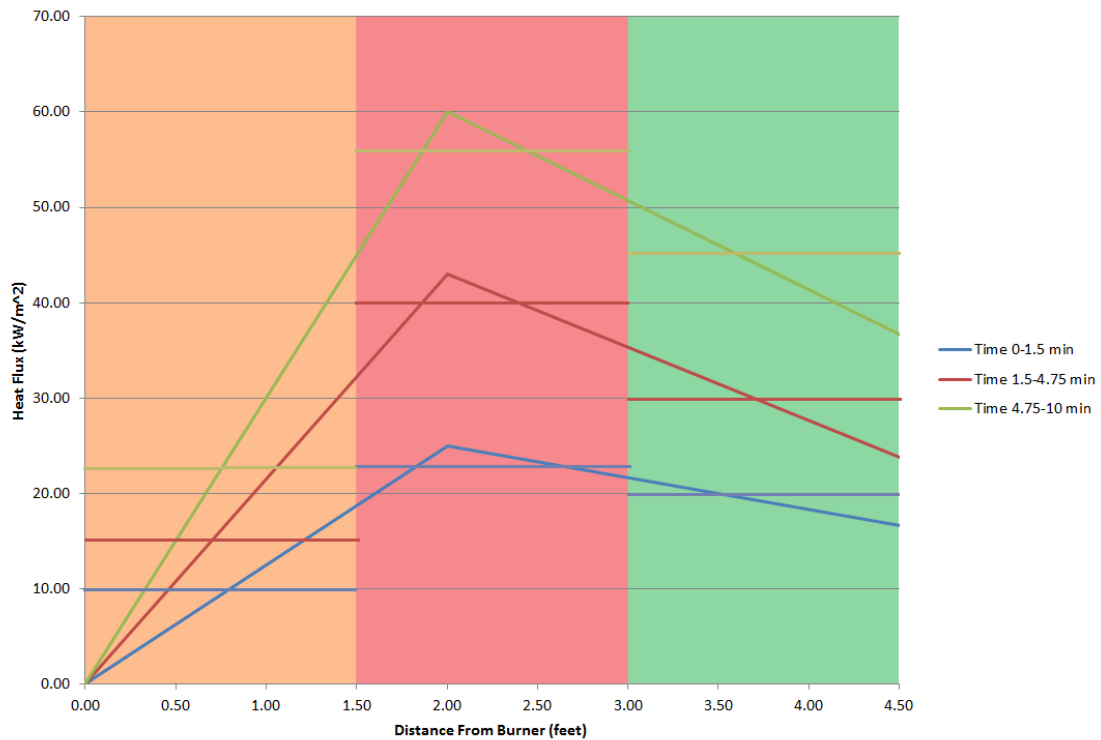
Figure 125: Incident Heat Flux over The First 4.5 Feet per Time

Next, from each of the three average values for each of the three testing areas we were able to construct an incident heat flux step curve that best represents the conditions in the cone. These three step curves can be seen below in Figure 126.
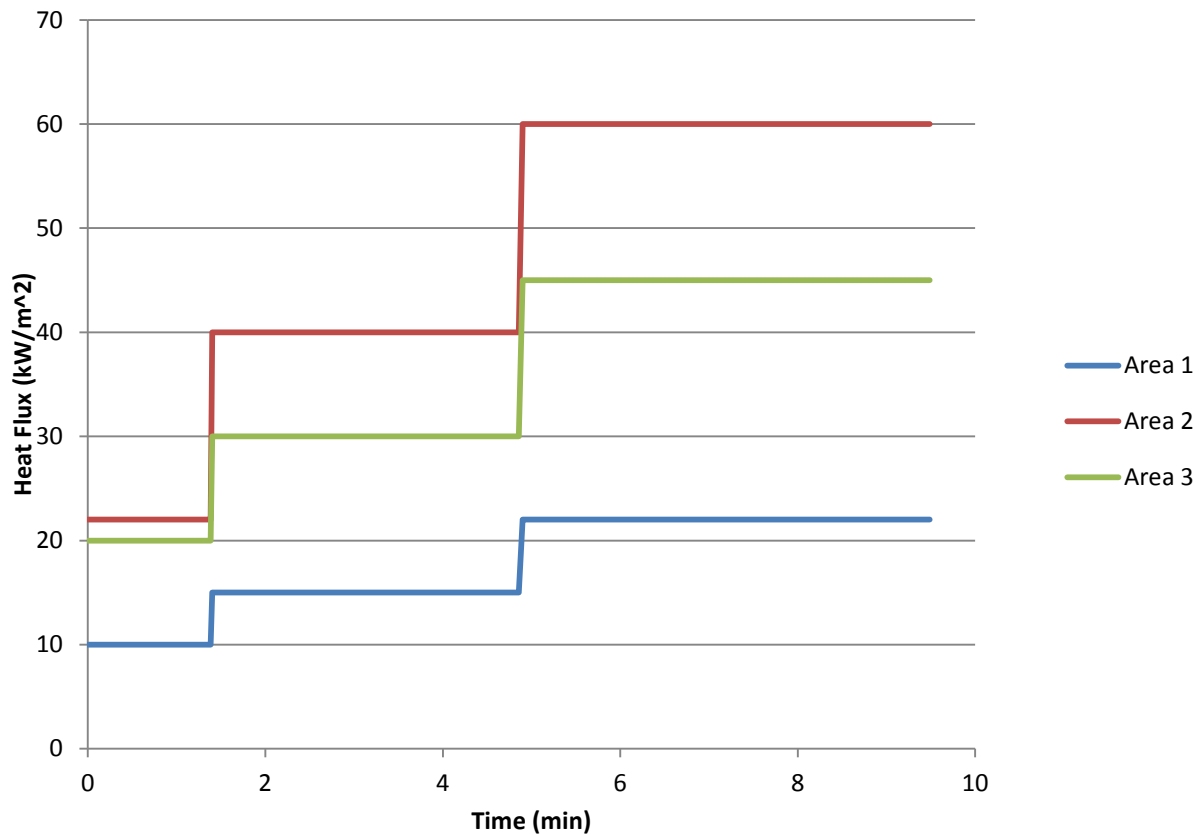
Figure 126: IHF for 3 Burn Sections in Burn Area over Time

After attempting to recreate these steps in the Cone Calorimeter it was obvious that these steps could not be recreated because the cone heater takes time to heat up. We also would like these steps to look more like the graph generated by William Parker in which the Incident Heat Flux in increasing with time rather than stepping up. From this information we revised the curves to allow for the cone heater to heat up and this in turn follows the heat flux mapping created by William Parker. The graph of the revised curves can be seen below in Figure 127.
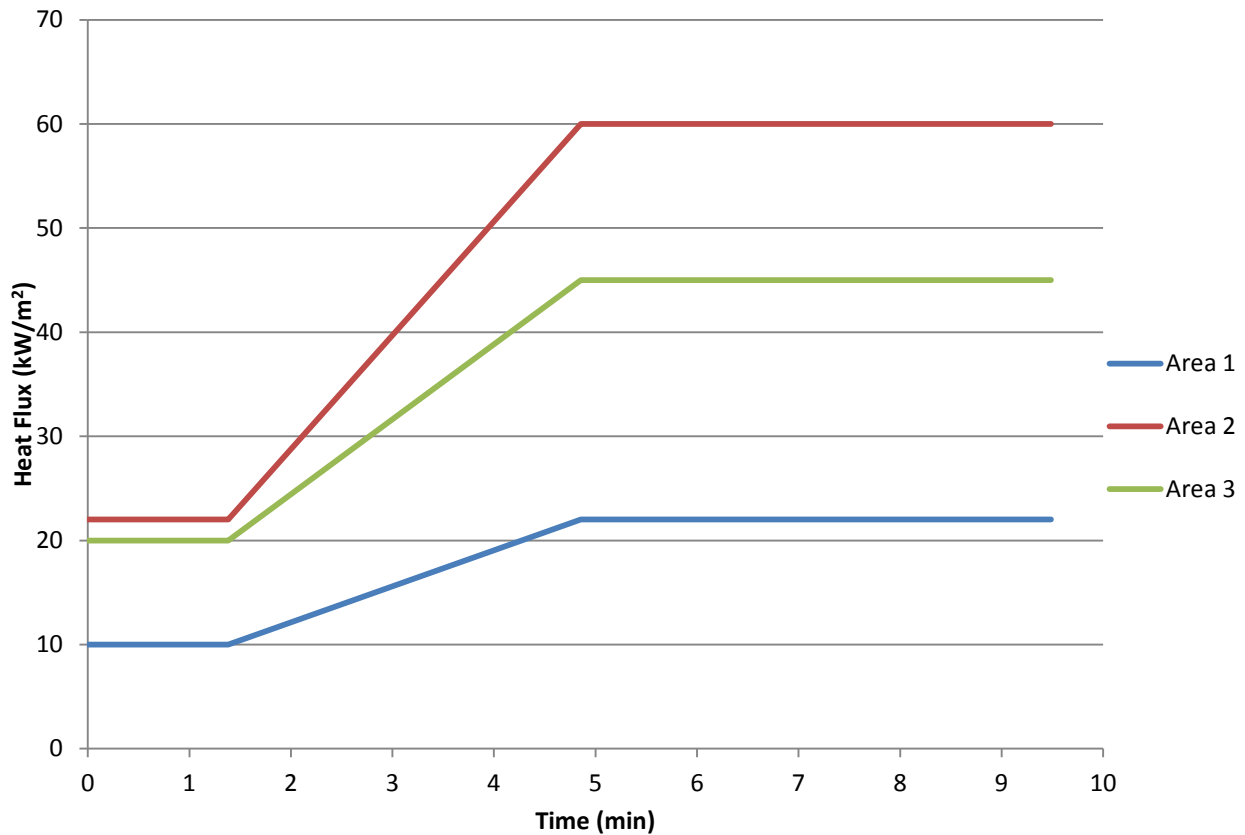
Figure 127: IHF for 3 Burn Sections in Burn Area Over Time

After we created the ideal heat flux curves we needed to then create the three steps in the cone. In order to do this we mounted a heat flux one inch below the cone heater and recorded the incident heat flux over time. After some trials we created the three different curves by changing the temperature on the cone controller over the 10 minutes of the test. These three temperature steps can be seen below in Table 30. The temperatures noted are average temperatures, in order to keep our data consistent we would constantly check these temperatures with a heat flux gauge to ensure the proper heat flux as the temperature probe inside the cone heater had a tendency to move around during heat cycles.

Table 30: Heat Flux Curves in Cone

Area 1			Area 2			Area 3		
Heat Flux (kW/m2)	Start Time (seconds)	End Time (seconds)	Heat Flux (kW/m2)	Start Time (seconds)	End Time (seconds)	Heat Flux (kW/m2)	Start Time (seconds)	End Time (seconds)
10 kW	0	1:25	25kW	0	1:00	20 kW	0	1:25
15 kW	1:25	3:40	60kW	1:00	10:00	30 kW	1:25	3:25
22.5 kW	3:40	10:00				45 kW	3:25	10:00

While creating these three different heat flux curves we were also recording the incident heat flux over time and repeated each step twice. The data that we collected versus the ideal curves can be seen below in Figure 128.
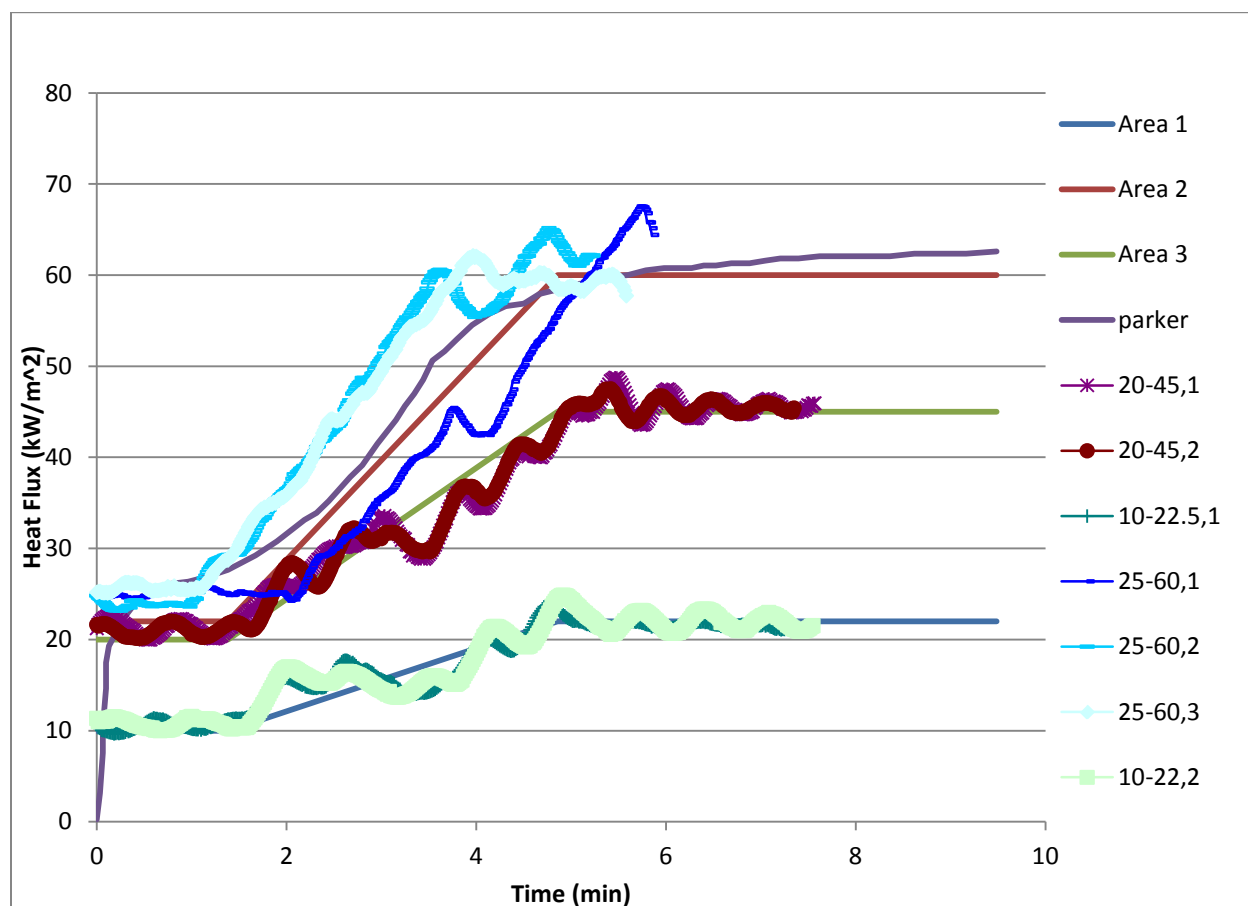
Figure 128: IHF for 3 Burn Sections in Burn Area Over Time

From looking at these curves it can be seen that there is some significant oscillation in the incident heat flux created by the cone heater. This is due to the nature of the temperature controller trying to increase and decrease the temperature in order to level out at a constant level. The oscillation becomes a bit more apparent while the cone is heating up, this is also due to the nature of the temperature controller that we are using.

After we created the curves it was time to run our specimens in the cone calorimeter utilizing them. We ran two samples of each specimen that we had with each of the three curves that we created for a total of 6 tests per specimen. We then took the heat release rates generated from the cone calorimeter and calculated an overall heat release rate for the entire 4.5 length utilizing a method described below.

5.10.5 Composite Heat Release Rate Calculations

In order to use the equations that were discussed before in our correlations we will need to generate a single heat release rate over time for each specimen to put into the calculations. To do this we first

averaged the heat release rate per unit areas of the two samples run at each of the three incident heat flux curves. All of my sample calculations will be using values found for CP 286 at 100 seconds

$$\frac{(HRRPUA\ sample\ 1) + (HRRPUA\ sample\ 2)}{2} = Average\ HRRPUA$$

$$\frac{(.4759\ kw/m^2) + (.4671\ kw/m^2)}{2} = .4715\ ^{kW}/_{m^2}$$

This equation was completed for each second of all three of the incident heat flux curves for a total of three average heat release rates per unit area curves for each specimen that was run in the test. This gave us three different heat release rate per unit area curves, one for each of the three areas in the 4.5 foot (1.4 meter) distance. After this was completed we needed to convert the heat release rate per unit area into a heat release rate. This was done by multiplying each heat release rate curve that was created by the area of one third of the first 4.5 foot (1.4 meter) section of the curve. This is because each heat release rate per unit area curve is only applied to the section of the burn area that is affected by that incident heat flux. The area was calculated in meters because the heat release rates given from the cone calorimeter are in units of KW/m².

$$\frac{1.4\ m * .43\ m}{3\ areas} = .20\ m^2\ per\ area$$

$$HRRPUA * .20\ m^2 = Heat\ Release\ Rate$$

$$.4715\ ^{kW}/_{m^2} * .20\ m^2 = .0943\ kW$$

After converting each curve for each area to a Heat Release Rate we then added them together in order to create a total heat release rate for the first 4.5 feet (1.4 meters) of the tunnel.

$$HRR\ of\ Area\ 1 + HRR\ of\ Area\ 2 + HRR\ of\ Area\ 3 = Composite\ HRR\ for\ Specimen$$

$$.0943\ kW + 1.0574\ kW + .1486\ kW = 1.3003\ kW$$

For the first two equations that we will be looking at, the Heat Release Rate must be converted to a Heat Release Rate per unit Width. In the case of the Tunnel, the width is 17 inches. We converted this to meters and divided the total heat release rate in order to arrive at a heat release rate per unit width.

$$\frac{Composite\ Heat\ Release\ Rate}{.43\ meters} = Heat\ Release\ Rate\ per\ unit\ width\ (^{kW}/_m)$$

$$\frac{1.3003}{.43\ meters} = 3.0240\ ^{kW}/_m$$

These calculations were completed at each second for the first 600 seconds after shutter open in order to create a composite heat release rate per unit width over time. This heat release rate per unit width

over time curve was then used in the equations to determine which equation would become the best basis for our correlation. This Process of creating the composite heat release rate for CP 286 can be seen in Figure 129 through Figure 133.
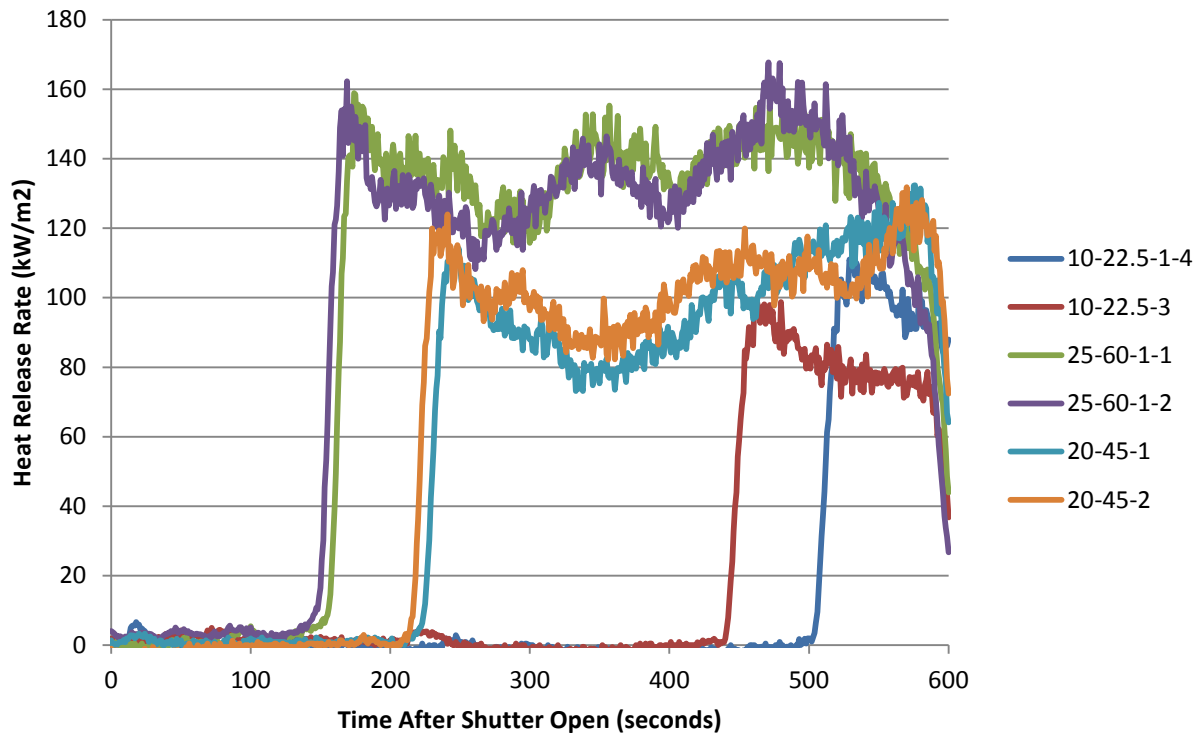
Figure 129: HRRPUA for All Samples CP 286
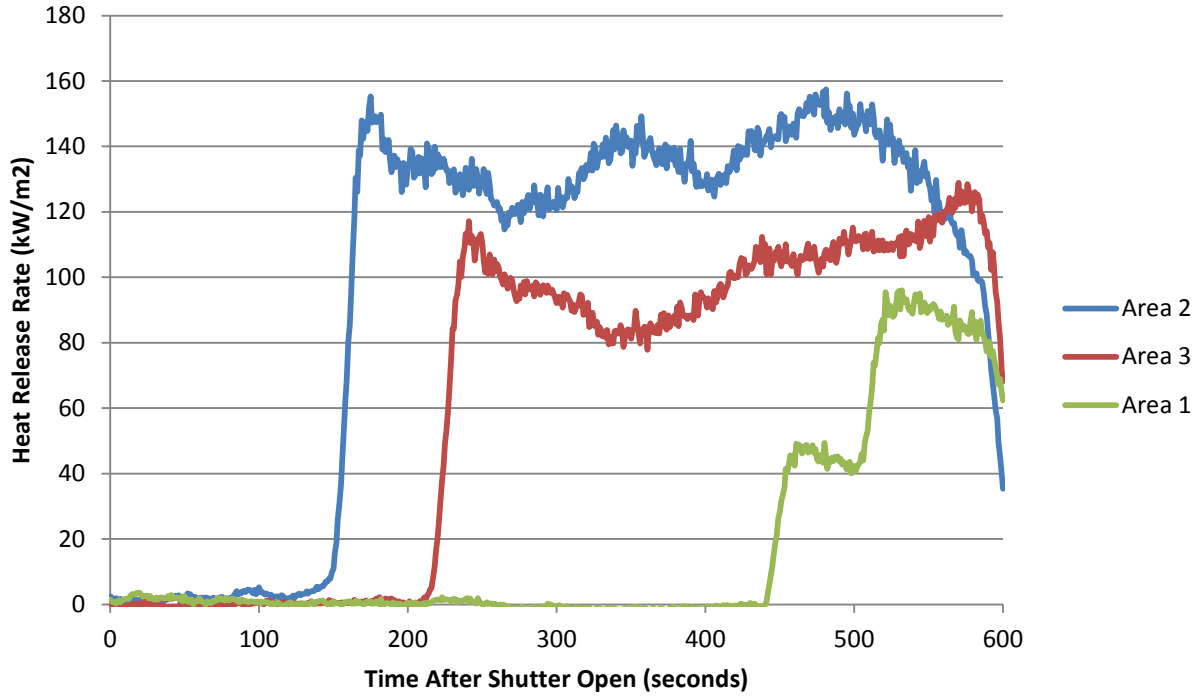
Figure 130: Average HRRPUA for Three Areas CP 286
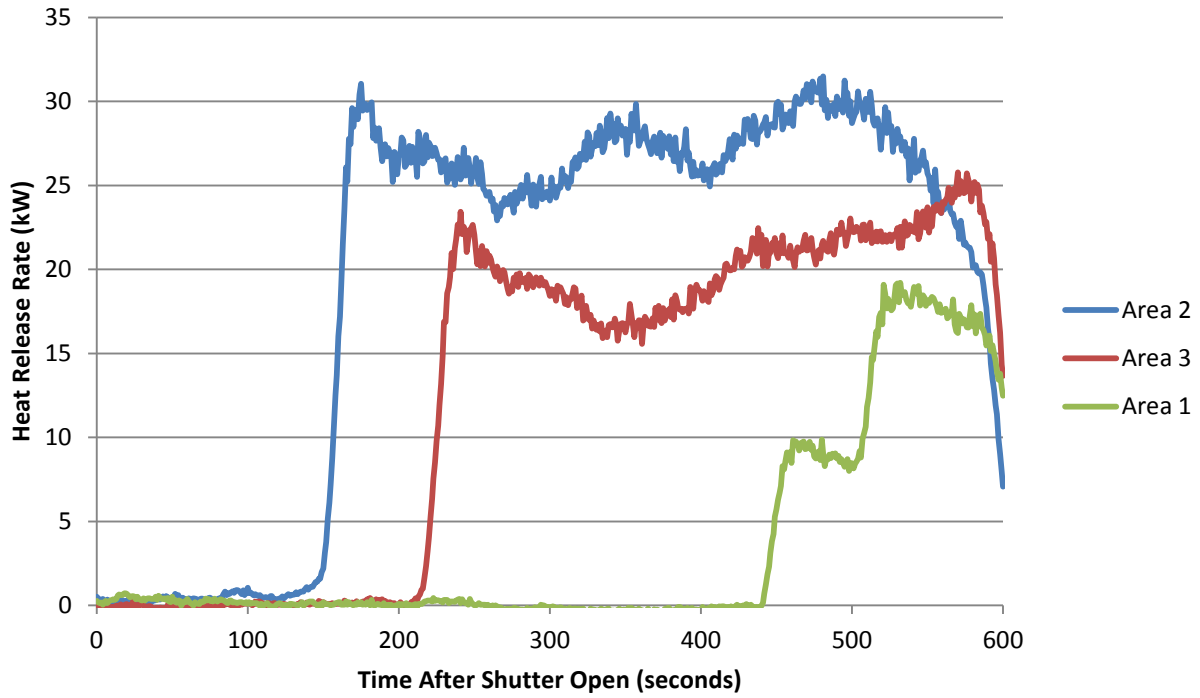
Figure 131: Average HRR for Three Areas CP 286
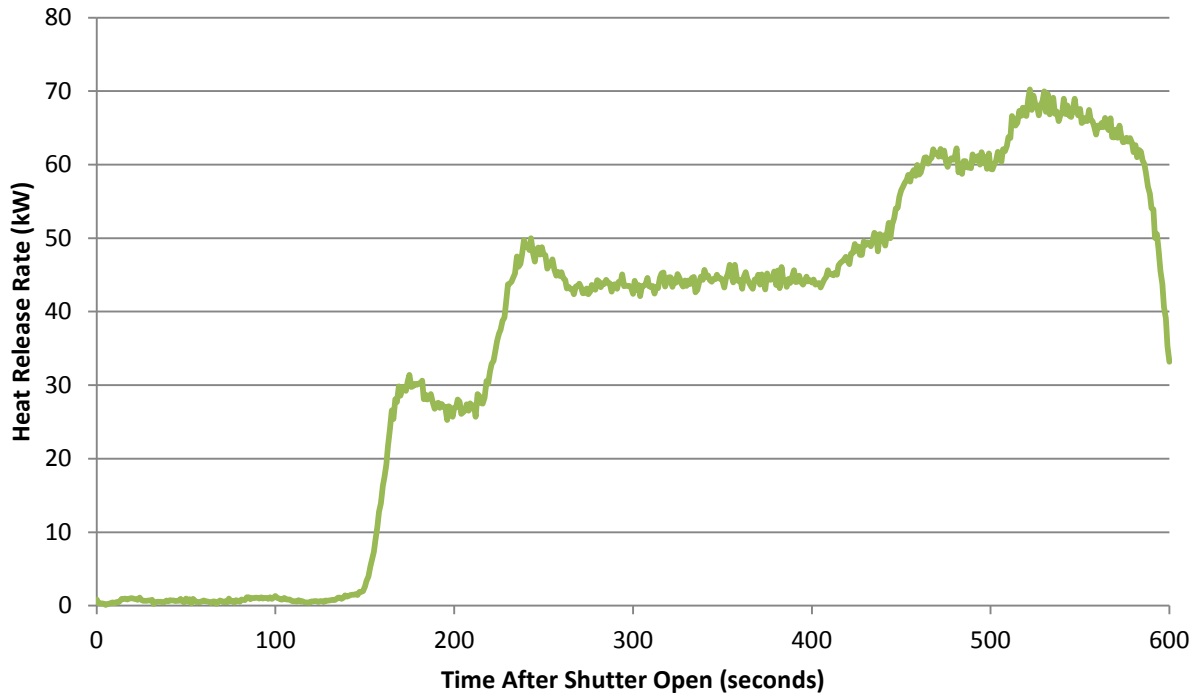
Figure 132: Composite HRR CP 286
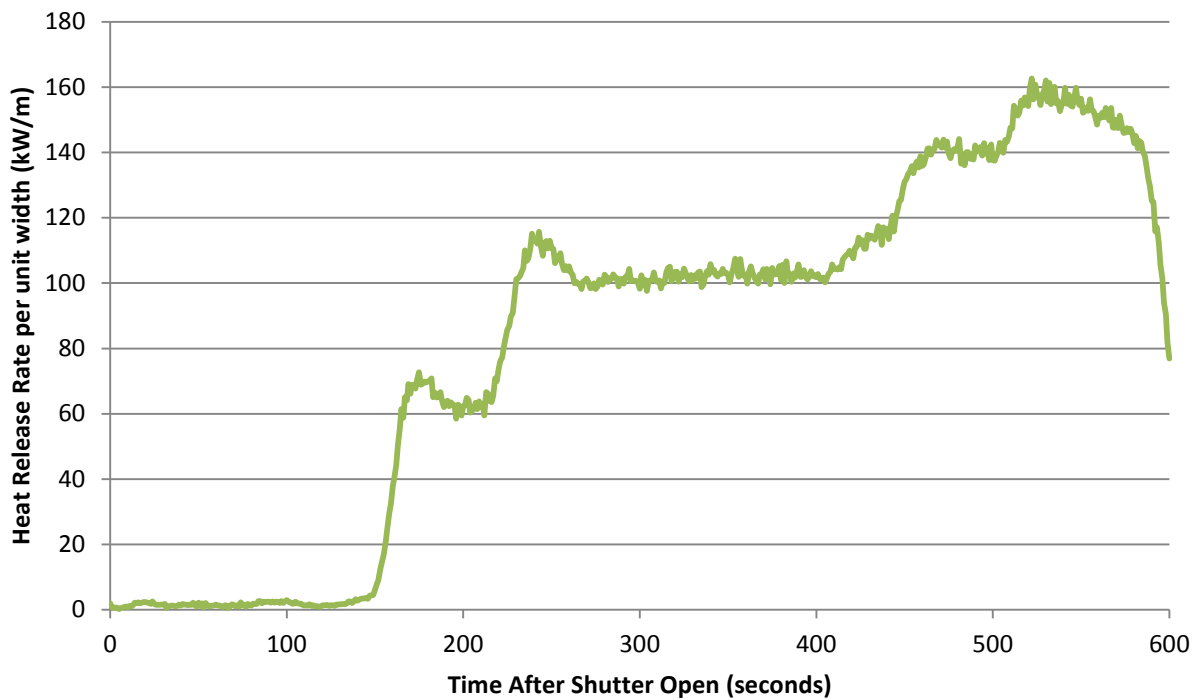
Figure 133: Composite HRR per unit width CP 286

5.10.6 Equation Analysis

Now that we have a composite heat release rate that represents the conditions in the tunnel, we needed to find a preexisting equation that could be adjusted to reflect the conditions in the tunnel. In order to do that we will use the tree equations discussed earlier. These three equations are

$$\textbf{Equation 1: } \frac{L}{D} = a(Q^*)^n$$

$$Q^* = \frac{Q}{\rho c_p T_\infty \sqrt{gD^3}}$$

Q= Rate of Heat Release per unit width (kW/m)
L=Flame Length (m)
D= Characteristic Length (.4316 m)
α= Constant (6.0)
n= Constant (.8 for Q*<1)

$$\textbf{Equation 2: } X_f = W \left(\frac{Q}{c_p T_\infty \rho_\infty g^{1/2}} \right)^{2/3}$$

Q= Rate of Heat Release per unit width (kW/m)
Xf= Flame Length (m)
W= Constant (4.6)
Q= Rate of Heat Release per unit width (kW/m)

$$\textbf{Equation 3: } d = (0.61 + 49\,Q)$$

d= Flame Extension (m)
Q= Total Rate of Heat Production (MW)

For equation three all we needed to do was convert the composite HRR from kilowatts to megawatts and plug it into the equation. This is because the equation was found by William Parker from oxygen depletion calorimetry in the tunnel, it already accounts for all of the factors.

HRR (kW) / 1000 = HRR (MW)

1.3004 kW / 1000 = .0013004 MW

$$d = (0.61 + 49\,Q)$$

$$d = (0.61 + 49\,.0013004) = .6737 \text{ meters}$$

For equations one and two on the other hand, there are some extra variables that we need to account for. This is the specific heat, temperature, and density of air as well as gravity. For these equations we will be using ambient conditions.

$$C_p = 1 \, \frac{kJ}{kg} \, K$$

$$T_\infty = 273\ K$$

$$\rho_\infty = 1.18\ \frac{kg}{m^3}$$

$$g = 9.81\ \frac{m}{s^2}$$

We used these values in equations one and two to calculate the flame lengths. Before we calculate the flame length for equations one and two we must account for the heat release from the burners in the ASTM e-84 tunnel. This was found by converting the given flow found in the ASTM e-84 standard [12].

$$\frac{5000\ BTU}{Min} * \frac{1\ Min}{60\ Secconds} * \frac{1055.06\ Joules}{1\ BTU} * \frac{1\ Watt}{1\frac{J}{s}} * \frac{1\ Kiliowatt}{1000\ Watts} = 87.92\ Kilowatts$$

This now needs to be converted to a heat release rate per unit width in the tunnel.

$$\frac{88\ kW}{.43\ meters} = 204.4651\ {kW}/{m}$$

For simplicity we will round this to 204 kW/m. Due to this additional heat release rate creating a flame in the tunnel, we must add 204 kW/m to the heat release rate of the material to arrive at the heat release rate that contributes to the flame length. The first thing we needed to do for equation one is compute Q*. Keeping in mind that Q for equation one is a heat release per unit width.

$$Q^* = \frac{Q}{\rho c_p T_\infty \sqrt{gD^3}}$$

$$Q^* = \frac{3.0240\ {kW}/{m} + 204\ {kW}/{m}}{1.18\ \frac{kg}{m^3} * 1\ \frac{kJ}{kg}\ K * 273\ K\ \sqrt{9.81\ \frac{m}{s^2} * .4316\ ^3m}} = .6604$$

We then put Q* into equation one to receive a flame length.

$$\frac{L}{D} = a(Q^*)^n$$

$$L = D * a(Q^*)^n$$

$$L = .4316 * 6.0\ (.6604\ )^{.8} = 1.8512\ meters$$

Equation two is the same method, however we did not need to compute Q*.

$$X_f = W(\frac{Q}{C_p T_\infty \rho_\infty g^{{1}/{2}}})^{{2}/{3}}$$

$$X_f = 4.6 \left(\frac{3.0240\ kW\ /\ m + 204\ {kW}/{m}}{1.18\ \frac{kg}{m^3} * 1\ \frac{kJ}{kg}\ K * 273\ K\ \sqrt{9.81\ \frac{m}{s^2}}} \right)^{2/3} = 1.5000\ meters$$

After the length was calculated for each second of the Heat Release Curve for the first 600 seconds, we converted from meters to feet in order to compare to the known values found in the ASTM e-84 tunnel test which is in English units.

$$Meters * \frac{3.2808\ Foot}{1\ meter} = feet$$

$$.6737\ meters * \frac{3.2808\ Foot}{1\ meter} = 2.2103\ feet$$

$$1.8512\ meters * \frac{3.2808\ Foot}{1\ meter} = 6.0734\ feet$$

$$1.5000\ meters * \frac{3.2808\ Foot}{1\ meter} = 4.9212 feet$$

Due to the nature of William Parkers equation, this is as far as we will go with it. This correlation already accounts for the velocity in the tunnel and already gives the flame length as an extension past 4.5 feet. For equation one and two on the other hand, we want to adjust them to account for both the velocity of air in the tunnel and the fact that the flame length must be converted to an extension past the 4.5 feet burn area.

5.10.6.1   *Air Velocity Correction*

In the ASTM e-84 standard it is noted that the velocity in the tunnel must be 1.22 m/s ± .0233 m/s. We have concluded that this velocity in the tunnel will have an effect on the length of the flame, ultimately increasing it. In order to determine how much the flame will increase when imposed by wind, we have consulted work completed by Fernandez-Pello [13]. We specifically used his Pyrolysis Length vs Flame Length for several flow velocities. This graph can be seen below in Figure 134.
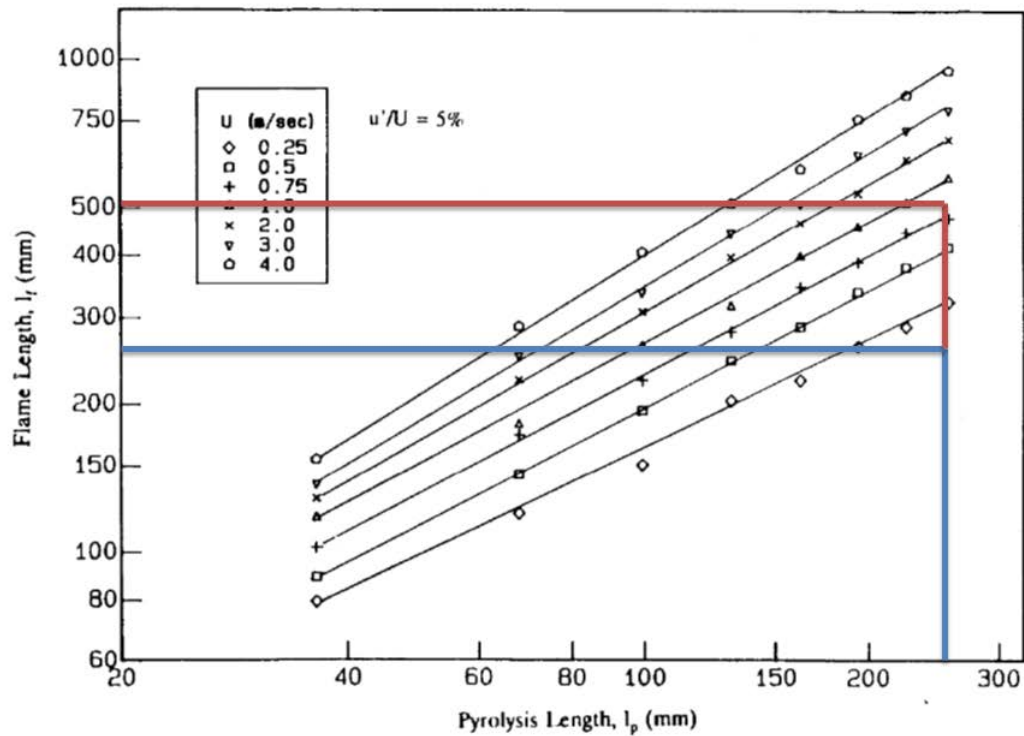
Figure 134: Flame Length vs Velocity of Air Movement

After estimating a flame length for a velocity of zero it can be seen that the flame length increase from 275 mm to 500 mm with a velocity of 1.25 m/s, because of this notion we will increase the flame lengths produced by equations one and two by a factor of 1.8 which was found using the equation below.

$$\frac{500 \; mm}{275 \; mm} = 1.8$$

The lengths were then increased using the following equation.

$$Length \; (feet) * 1.8 = Length \; Corrected \; for \; Wind$$

$$6.0734 \; feet * 1.8 = 10.9321 \; feet$$

$$4.9212 \; feet * 1.8 = 8.8582 \; feet$$

5.10.6.2   Flame Extension

The final correction that needed to be made to equations one and two is the fact they calculate the total flame length, however in the ASTM e-84 tunnel test they measure extension past 4.5 feet of the specimen. In our correlations we have assumed an origin that occurs 4.5 behind the line that the ASTM e-84 standard considers zero. Because of this we need to subtract 4.5 feet from our calculated flame lengths in order to arrive at an extension past the ASTM e-84 zero line.

$$Calculated \; Flame \; Length - 4.5 \; feet = Flame \; Extension$$

$$10.9321 \, feet - 4.5 \, feet = 6.4321 \, feet \, of \, extension$$

$$8.8582 \, feet - 4.5 \, feet = 4.3582 \, feet \, of \, extension$$

5.10.6.3   Comparison

After completing the calculations for all four of our specimens, it was time to compare the results to pick the best flame equation to use. The three flame length equations can be seen graphed against known distances found in the ASTM e-84 tunnel test for all four of our specimens in Figure 135 through Figure 138.
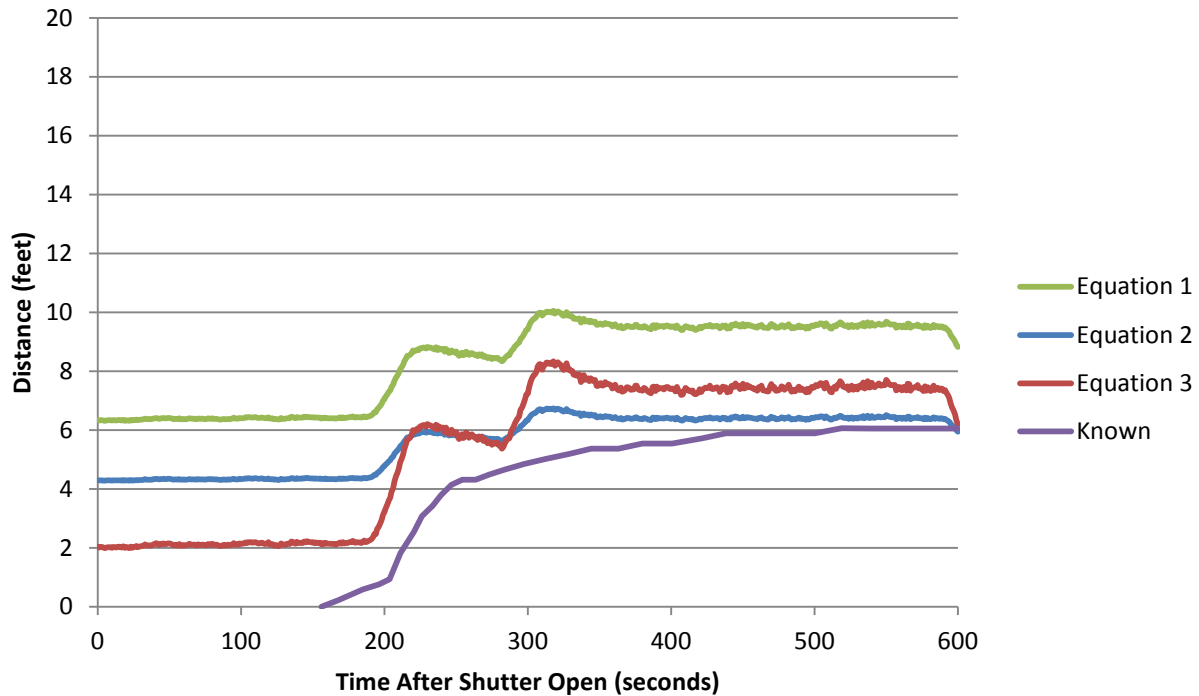
Figure 135: Flame Length Extension Kreysler 1
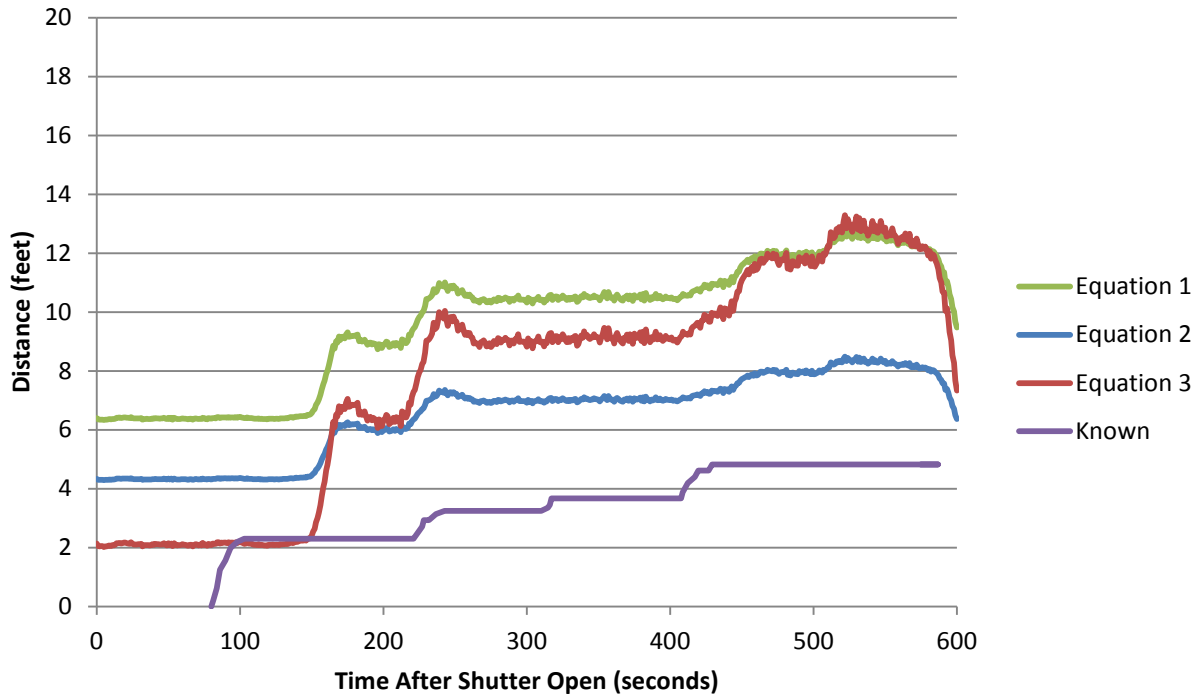
Figure 136: Flame Length Extension CP 286
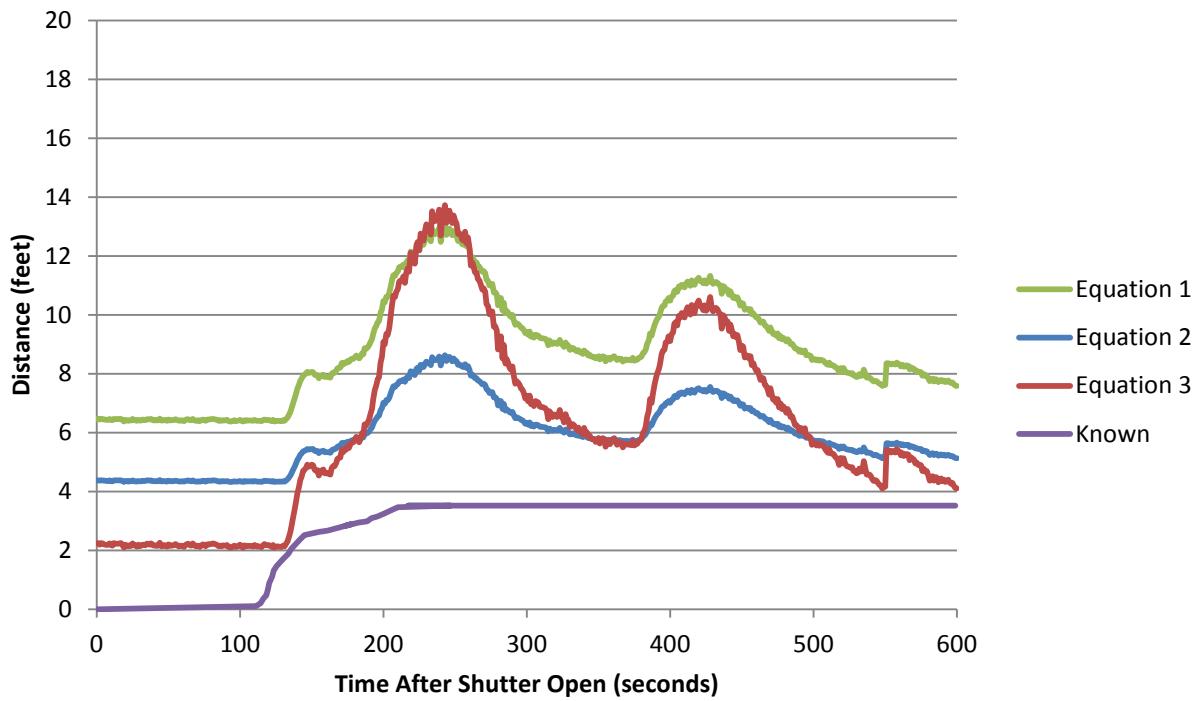
Figure 137: Flame Length Extension FSI .075
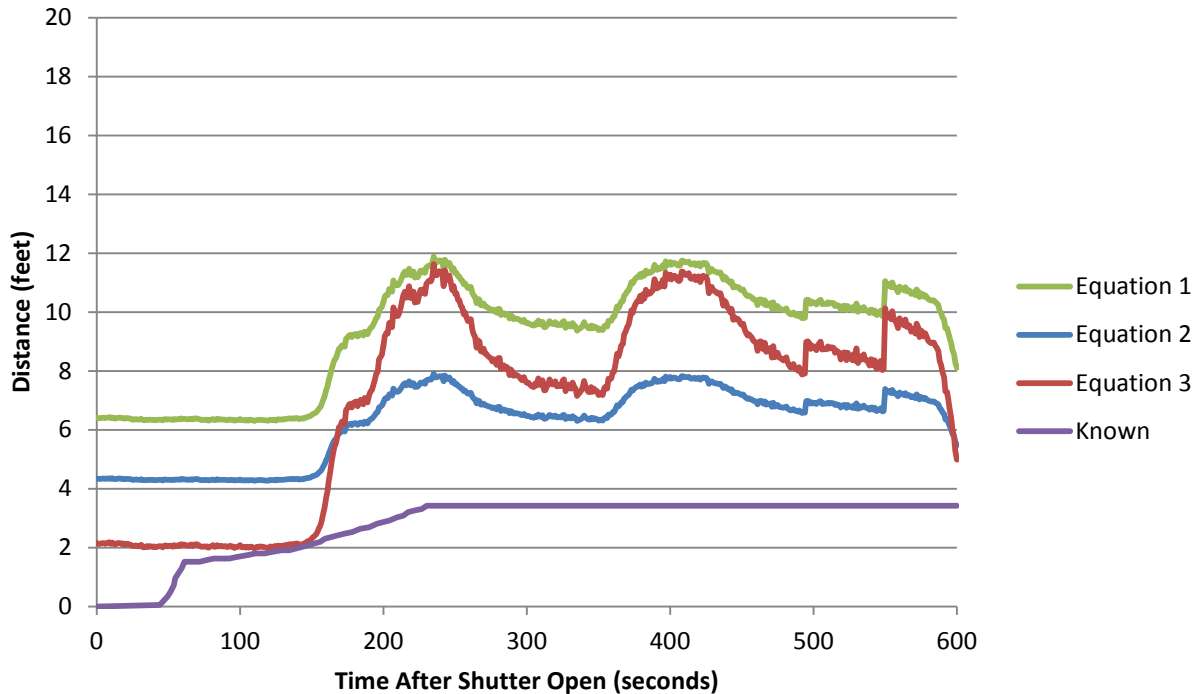
Figure 138: Flame Length Extension FXE .090

After comparing all of the results, it can be seen that equation 2 gives us the best correlation of flame length for all four specimens. The fact that it may not be exact for all of them will be adjusted for next by determining the best value for W in the equation.

5.10.6.4   *Flame Spread Index Calculations*

After deciding to use equation two as a basis it was important to decide how to calculate the flame spread index from the flame lengths. For this procedure we consulted the ASTM e-84 standard to determine the guidelines. The first thing that must be done in our correlation is not allow the flame to recede down the tunnel. This was completed in excel by using a simple if statement. The set up can be seen below in Figure 139.

Figure 139: Setting Up No Flame Back in Excel

This formula gave use flame extension over time that looked more like the ASTM e-84 results which did not show flame back. These graphs can be seen in Figure 140 through Figure 143.
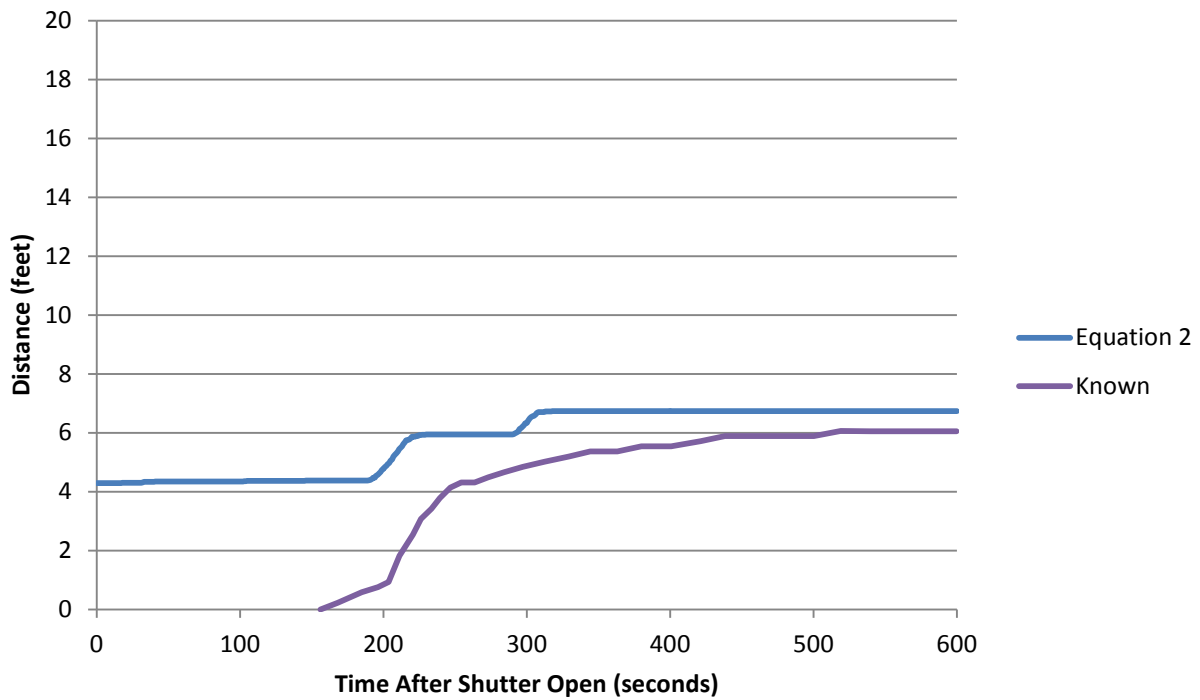
Figure 140: Flame Length Extension with No Flame Back Kreysler 1
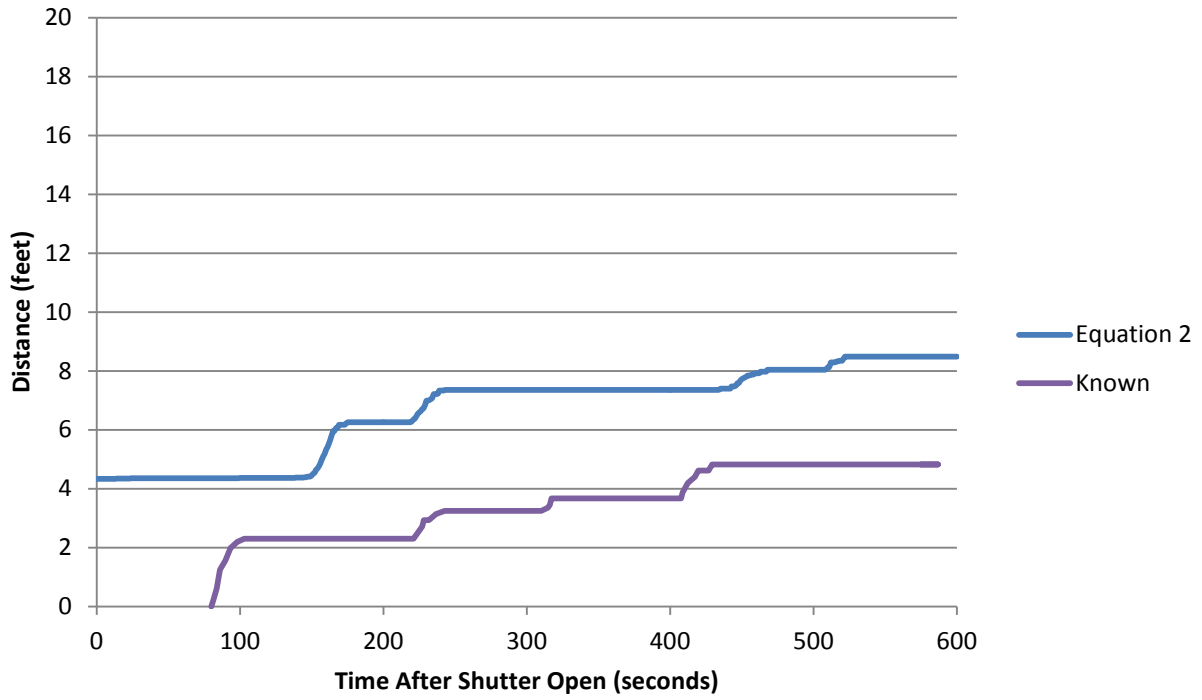
Figure 141: Flame Length Extension with No Flame Back CP 286
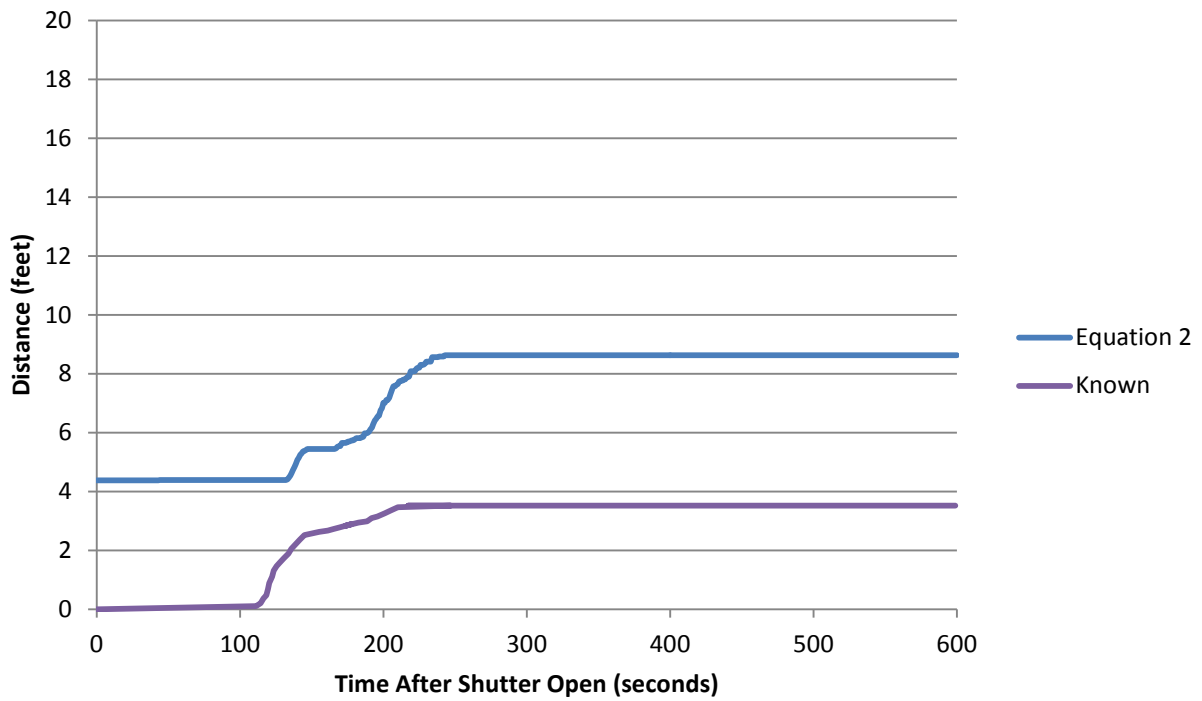
Figure 142: Flame Length Extension with No Flame Back FSI .075
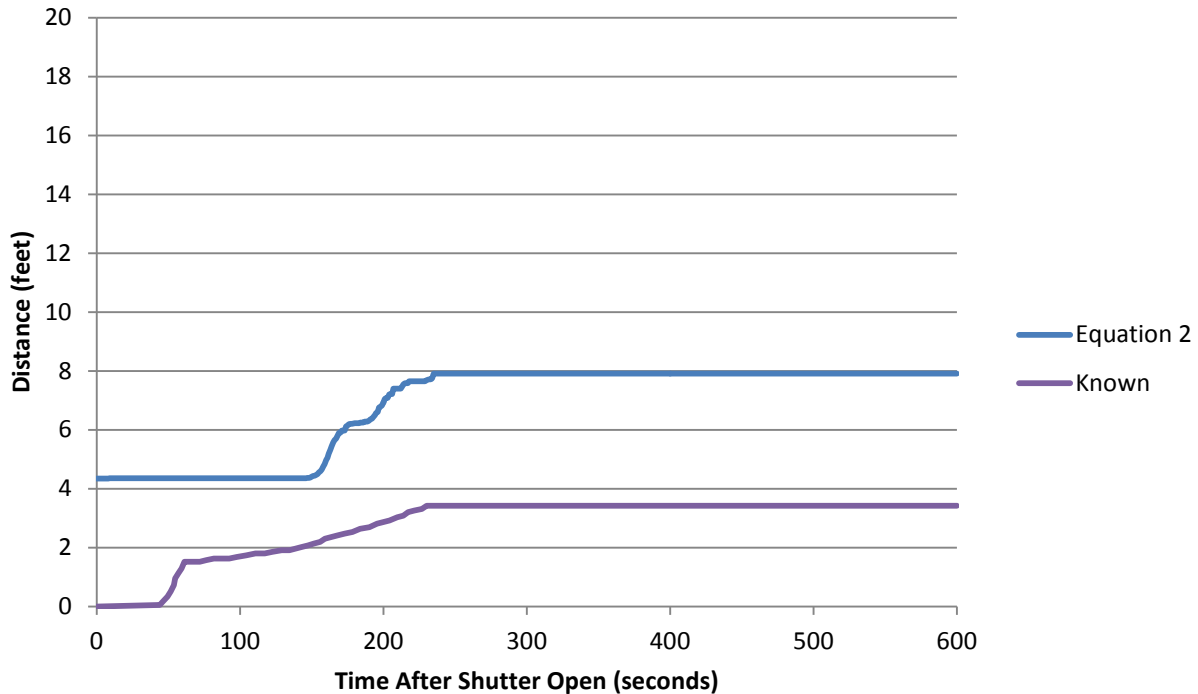
Figure 143: Flame Length Extension with No Flame Back FXE .090

The next part to calculating the Flame Spread Index is to calculate the area under the curve. This was done by using the Trapezoid Rule for approximating integrals. In order to complete this method the average of the first two values must be taken, after that the average is multiplied by the distance between the two points to create an area. This is then completed for each point along the curve and added together to create a total area under the curve.

$$\frac{Point\ 1 + Point\ 2}{2} * \frac{1}{60}\ min = area\ (ft * \min)$$

$$\frac{4.3585\ feet + 4.3585\ feet}{2} * \frac{1}{60}\ min = 0.0726\ (ft * \min)$$

Once the area under the curve is found it is then multiplied by a factor supplied in ASTM e-84. The factor is .515 if the area is less than 97.5 ft.*min. All of our specimens had areas well below 97.5 ft.*min, so this is the only equation we need.

$$Area\ Under\ Curve * .515 = FSI$$

$$66.6324\ (ft * \min) * .515 = 34.3157$$

5.10.6.5   *Adjustment of Equation*

Now that we have a basis to judge that accuracy of our flame length model, it is time to adjust the equation to best fit all four of our specimens, in order to do that we will adjust the W in the following equation.

$$X_f = W\left(\frac{Q}{C_p T_\infty \rho_\infty g^{1/2}}\right)^{2/3}$$

To find the best value we adjusted the W for each specimen separately until we arrived at a calculated flame spread index that equals the flame spread index measured in the ASTM e-84 tunnel test. The found values for W can be seen below in Table 31.

Table 31: Values for W

	Value for W
Kreysler 1	3.576
CP 286	3.140
FSI .075	2.790
FSI .090	2.957

All four of these values were then averaged to arrive at the best value for W for all four of these specimens. The value for W was found to be 3.116. When this value of W was used in the equation, the following flame spread indexes were found and compared to the known unrounded values. The percent error can be seen in Table 32.

Table 32: Percent Error

	Calculated	Known	Percent Error	
Kreysler 1	12.73	18.00	29.26	
CP 286	15.77	16.00	1.45	
FSI .075	18.02233332	13.7	31.55	
FSI .090	16.33504454	14.35	13.83	
			19.02	**Average Error**

After the value for W was determined, it was time to take a look at the flame extension over time graphs. These graphs can be seen below in Figure 144 through Figure 147.
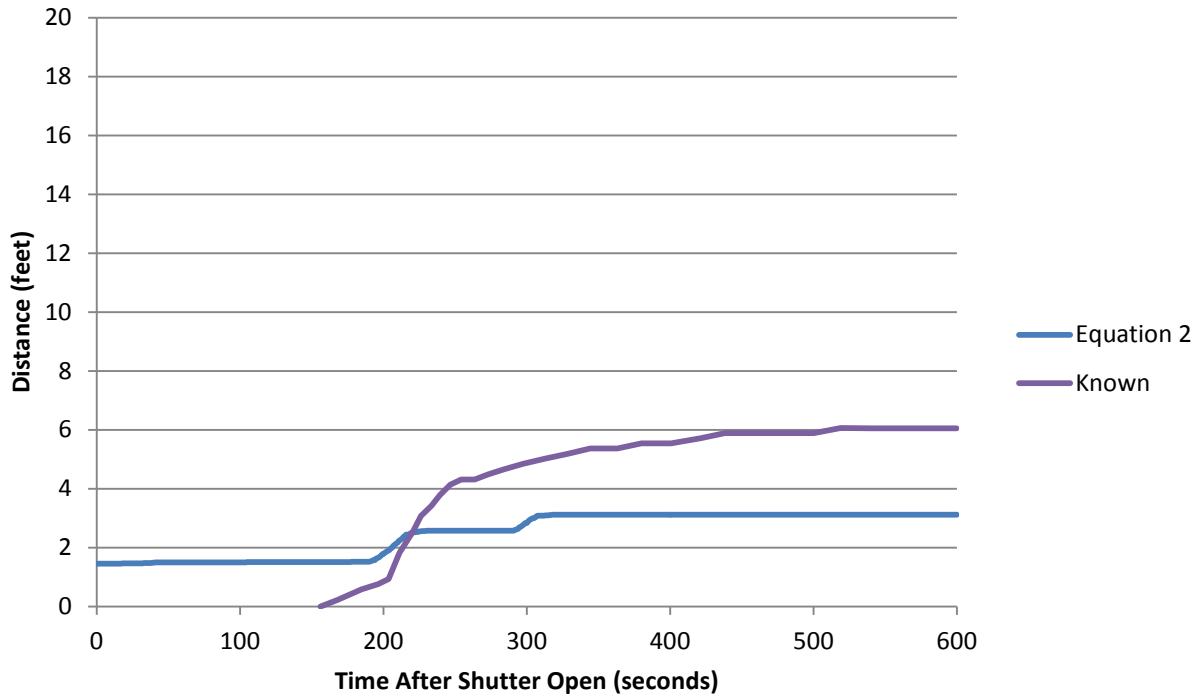
Figure 144: Flame Length Extension With No Flame Back Kreysler 1
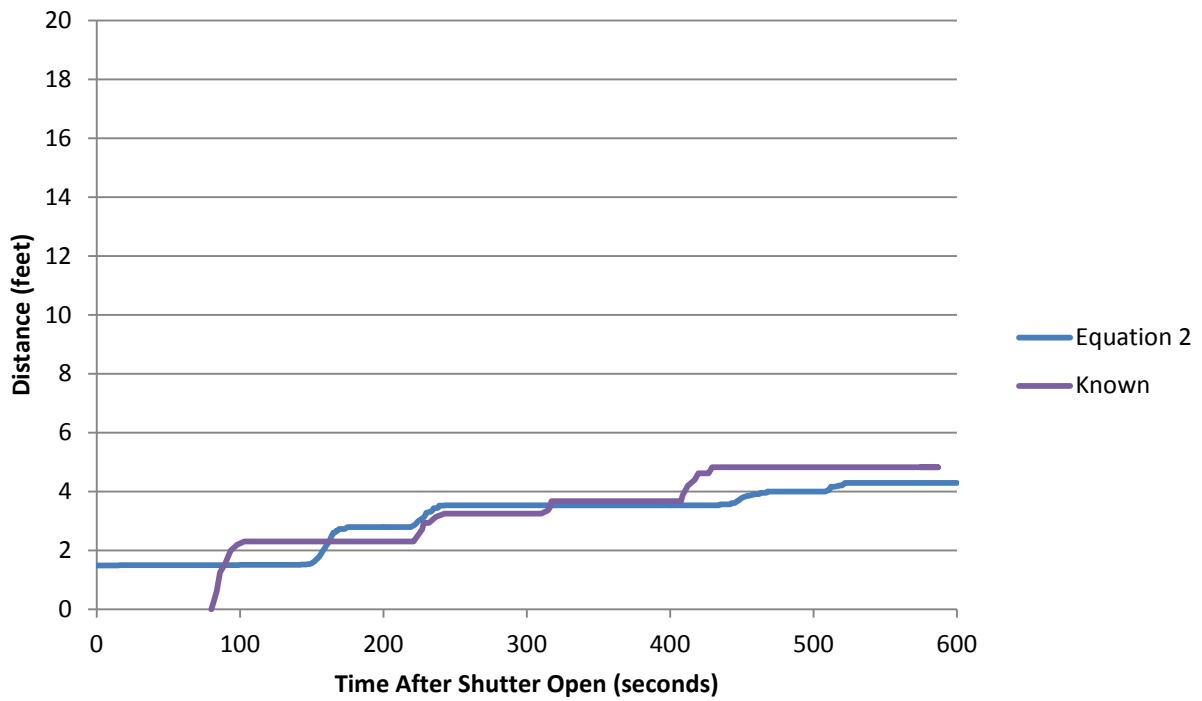
Figure 145: Flame Length Extension With No Flame Back CP 286
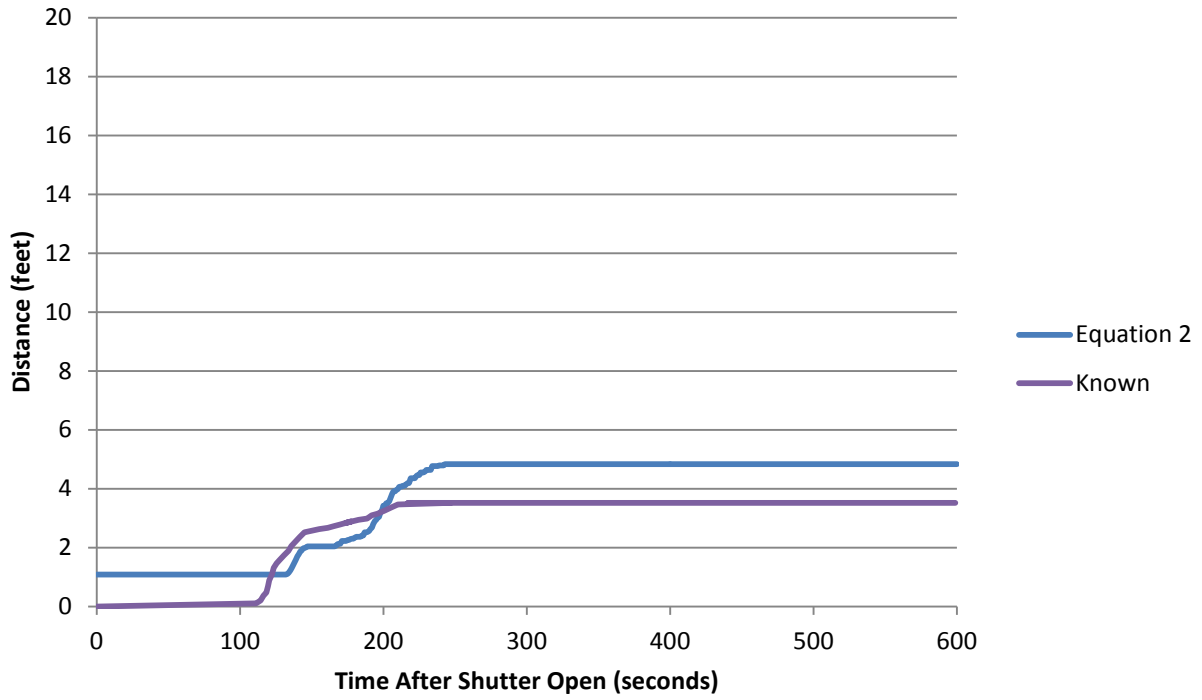
Figure 146: Flame Length Extension with No Flame Back FSI .075
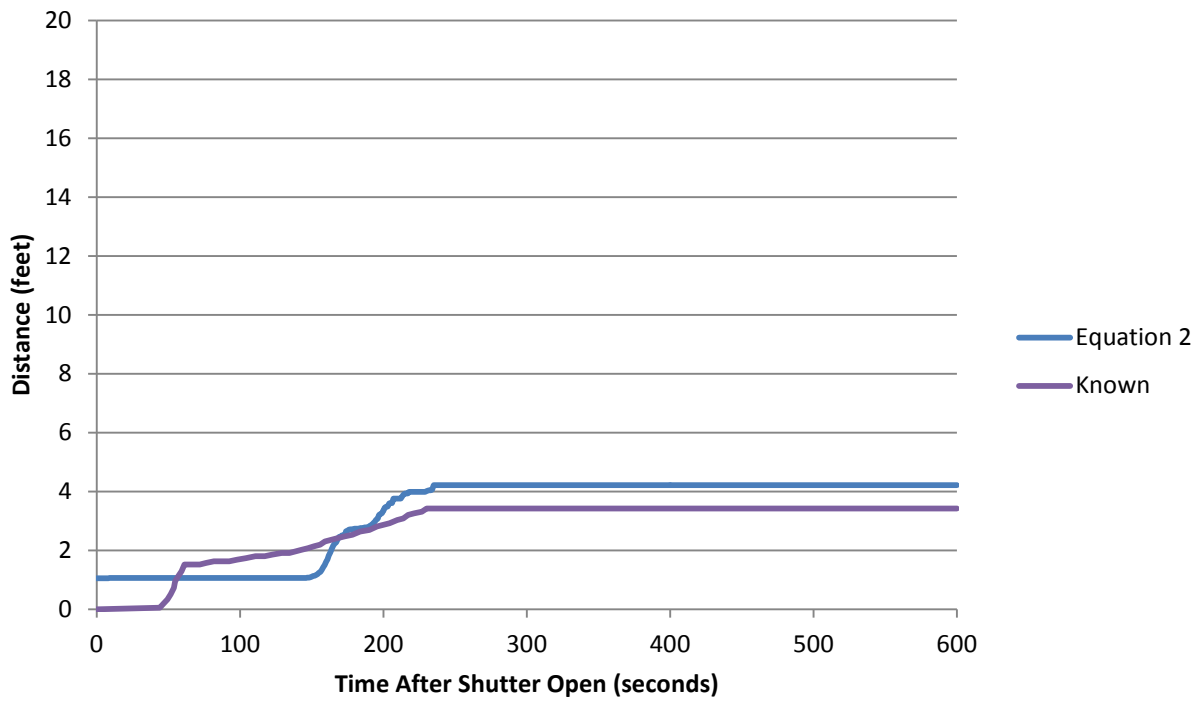
Figure 147: Flame Length Extension with No Flame Back FXE .090

After looking at these graphs it can be seen that the zero of the correlation is 1.45 feet above the zero of the known values. I believe that this can be attributed to adding too high of a Heat Release for the burners. To determine the correct amount I will solve the equation for the heat release rate when the length is 1.37 meters (4.5 feet), W is 3.116, and adding in the velocity adjustment term of 1.8 . This will give us the heat release rate per unit width that should be added for the burners.

$$X_f = V * W (\frac{Q}{C_p T_\infty \rho_\infty g^{1/2}})^{2/3}$$

$$1.37 = 1.8 * 3.11 (\frac{Q \; kW/m}{1.18 \frac{kg}{m^3} * 1 \frac{kJ}{kg} K * 273 K \sqrt{9.81 \frac{m}{s^2}}})^{2/3}$$

$$Q = 1.63.8878 \; kW/m$$

$$Q \; of \; Burners = 70.7668 \; kW$$

After completing this adjustment, the new heat release rate was added to the heat release rate. After looking at the curves it was seen that the zero was still high by about ¾ of a foot. In turn, the heat release from the burners was reduced to 60 kW. After this correction was made, a new value for W needed to be determined. This was completed using the same steps above. The value for each specimen can be seen below in Table 33.

Table 33: Values for W

	Value for W
Kreysler 1	4.350
CP 286	3.750
FSI .075	3.250
FSI .090	3.500

From these values, the average was found to be 3.713. When this value of W was used in the equation, the following flame spread indexes were found and compared to the known unrounded values. The percent error can be seen in Table 34.

Table 34: Percent Error

	Calculated	Known	Percent Error
Kreysler 1	12.08	18.00	32.91
CP 286	16.01	16.00	0.03
FSI .075	18.89097731	13.7	37.89
FSI .090	16.7338552	14.35	16.61
			21.86 Average Error

After making this change, the average error went up, this signifies that the correlation is not aiding from the change. To double check it is time to take a look at the new flame extension over time graphs. These graphs can be seen below in Figure 148 through Figure 151.
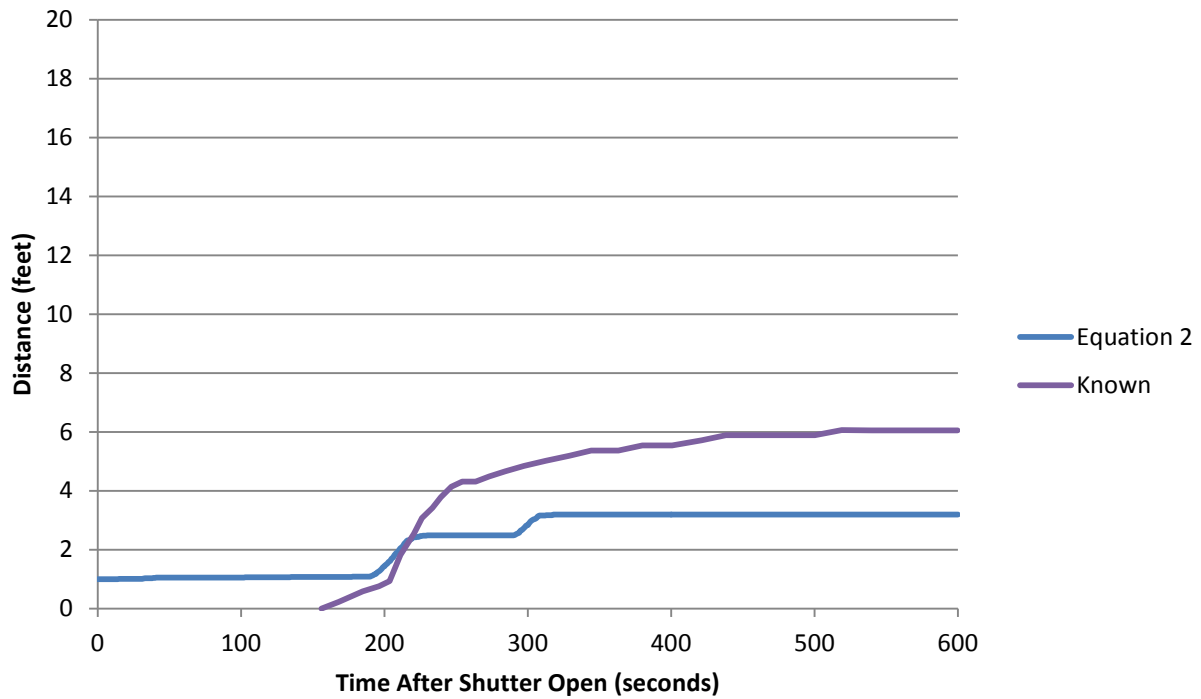
Figure 148: Flame Length Extension with No Flame Back Kreysler 1
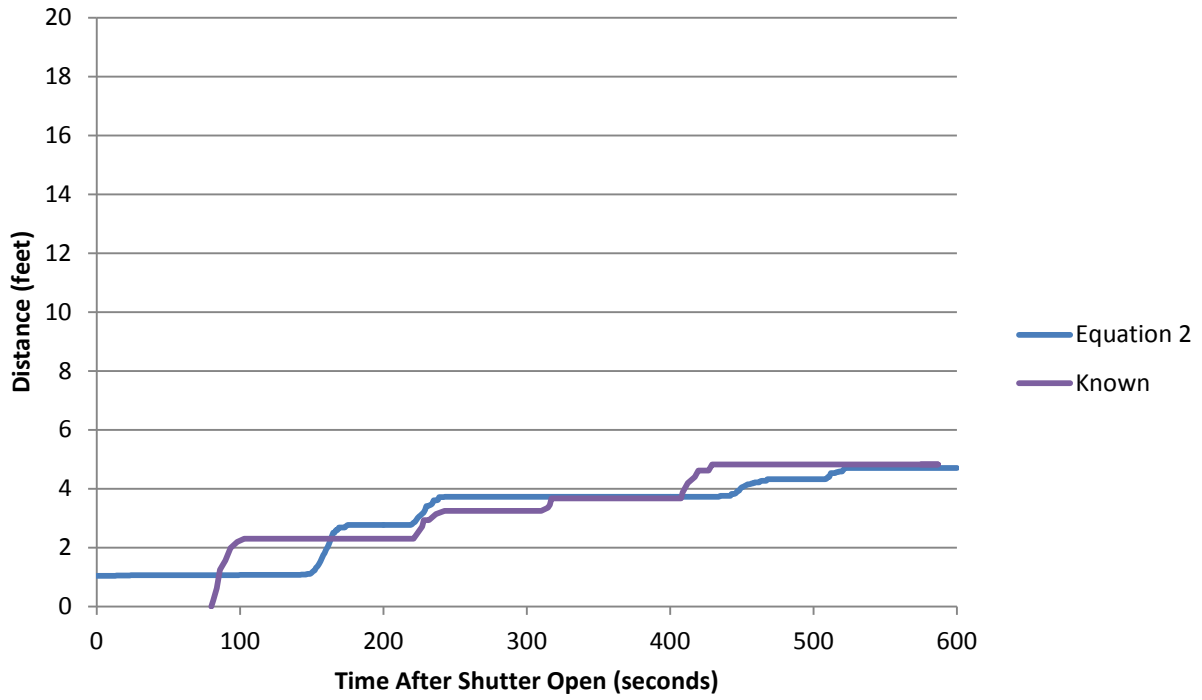
Figure 149: Flame Length Extension with No Flame Back CP 286
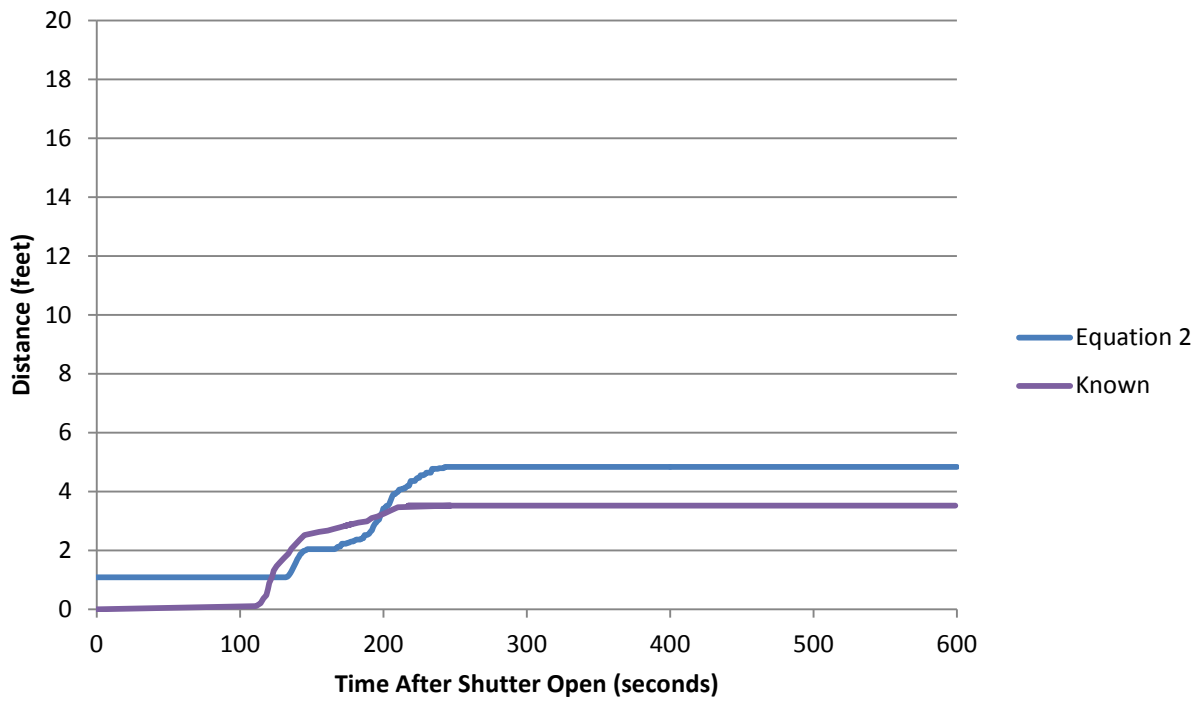
Figure 150: Flame Length Extension with No Flame Back FSI .075
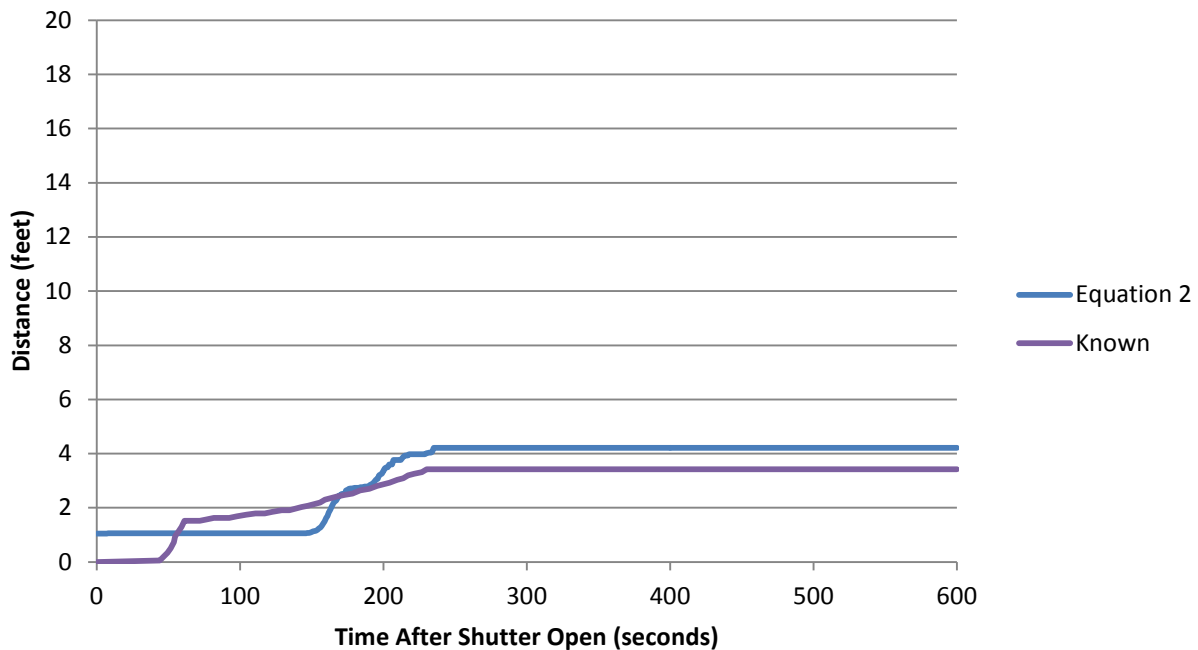
Figure 151: Flame Length Extension with No Flame Back FXE .090

These graphs have the same issue as the iteration above; because of the higher average percent error on the second iteration I will be reverting back to the equation that utilizes a value of 3.116 and adding a value of 88 kW for the burners.

5.10.6.6   *Pyrolysis Length Sensitivity*

One discussion that comes up about this flame length correlation is whether or not assuming that only the first 4.5 feet of the specimen is adding to the heat release rate from burning. We have assumed that any part of the specimen past 4.5 feet will not be burning in the correlation above. In order to deduce the effects of assuming a larger burning area, I will increase it by one foot to see if that makes the model more accurate. In order to begin, I must decide what the imposed incident heat flux is on the 4.5 – 5.5 foot section. To determine this we have consulted William Parkers data again [11]. Specifically we have looked at the imposed heat flux over distance from the burner for the 4.5 – 5.5 foot section. This graph can be seen below in Figure 152.
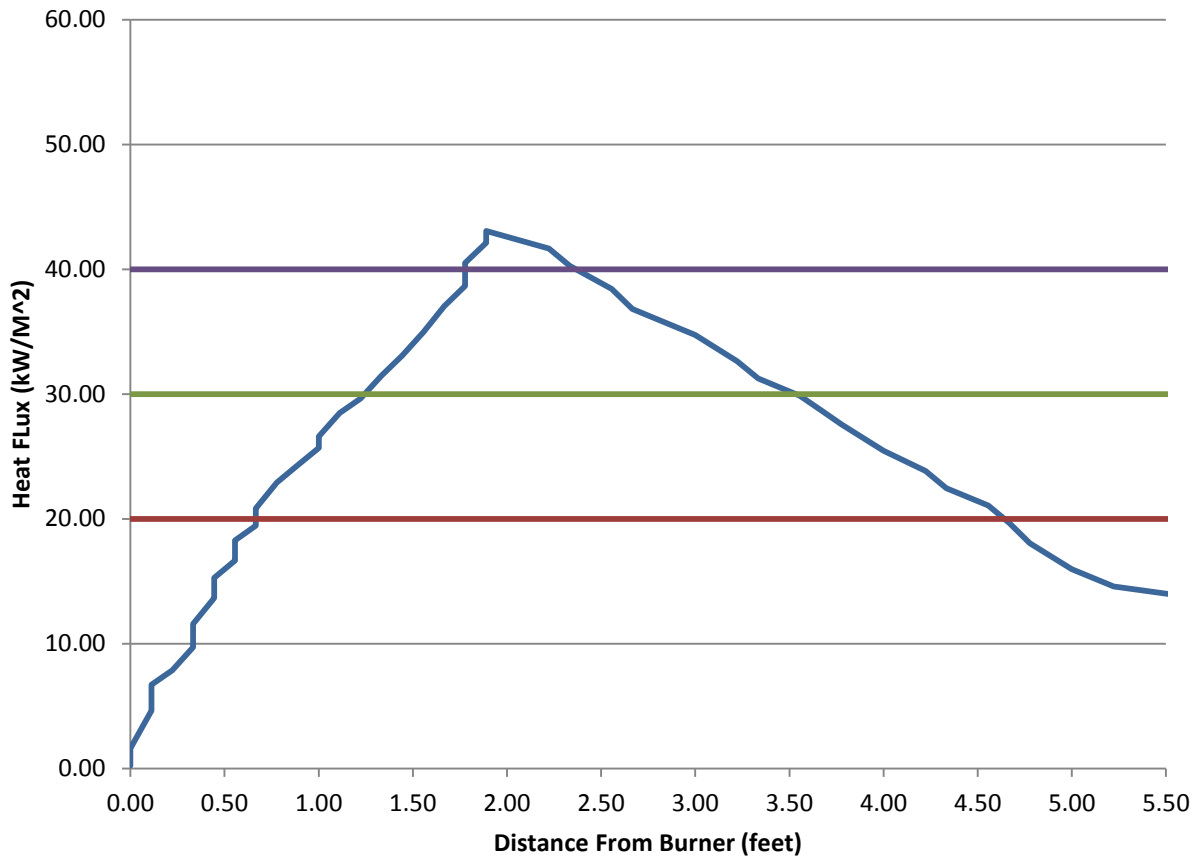
Figure 152: Incident Heat Flux per Distance in E84 Tunnel

From this graph it can be seen that the imposed heat flux on the first foot section is nominally the same as the imposed heat flux on the 4.5 to 5.5 foot section. Because of this I will the heat release rate of a 1 foot section that is exposed to the same incident heat flux as area 1. This means that the data from the 10 kW/m^2-22.5 kW/m^2 stair step will be used. First the average HRR for Area 1 must be taken and multiplied by the area of this new section which is .1316 m^2. I will complete all sample calculations using CP 286 at 400 seconds.

$$Area = 0.3048 \ m * .4318 \ m = \ .1316 \ m^2$$

$$HRR \ Average \ Area \ 1 * .1316 \ m^2 = Added \ Heat \ Release \ Rate$$

$$27.5050 \frac{kW}{m^2} * .1313 \ m^2 = 27.6363 \ kW$$

This is then converted to a heat release rate per unit width to get added to the total heat release per unit width.

$$\frac{Heat \ Release \ Rate}{.43 \ meters} = Heat \ Release \ Rate \ per \ unit \ width \ (^{kW}/_m)$$

$$\frac{27.6363 \; kW}{.43 \; meters} = 64.2705 \; {kW}/{m}$$

This was then added to the total heat release per unit width and entered into the equation using the method explained above. The next computation needed is to find a new value for W which can be seen in Table 35.

Table 35: Values for W

	Value for W
Kreysler 1	3.560
CP 286	3.100
FSI .075	2.780
FSI .090	2.870

The average value for W was found to be 3.078. From using this value in the equation, the following flame spread indexes were found and compared to the known values. The percent error can be seen below in Table 36.

Table 36: Percent Error

	Calculated	Known	Percent Error	
Kreysler 1	12.35	18.00	31.37	
CP 286	15.79	16.00	1.34	
FSI .075	17.68268878	13.7	29.07	
FSI .090	17.02778672	14.35	18.66	
			20.11	**Average Error**

Comparing this to the static model explained previously, the average error is higher. This means that assuming a static burn area will yield a more accurate correlation to class A material flame spread. For consistency, the flame extension graphs can be seen below in Figure 153 through Figure 156.
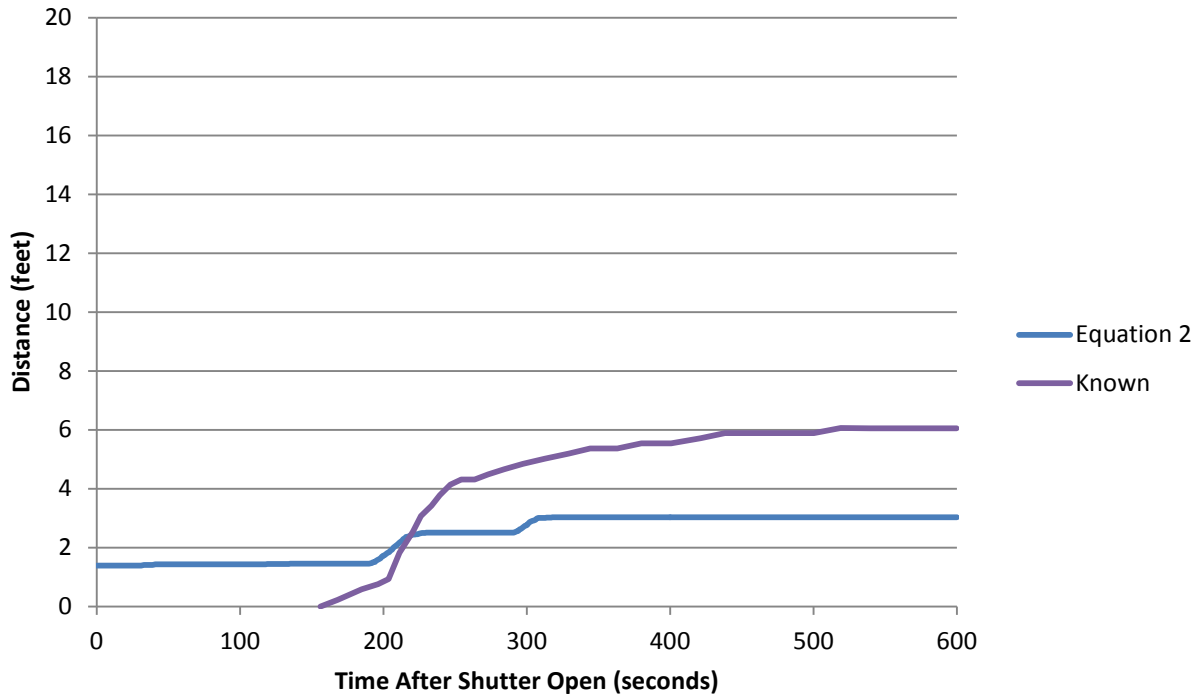
Figure 153: Flame Length Extension with No Flame Back Kreysler 1
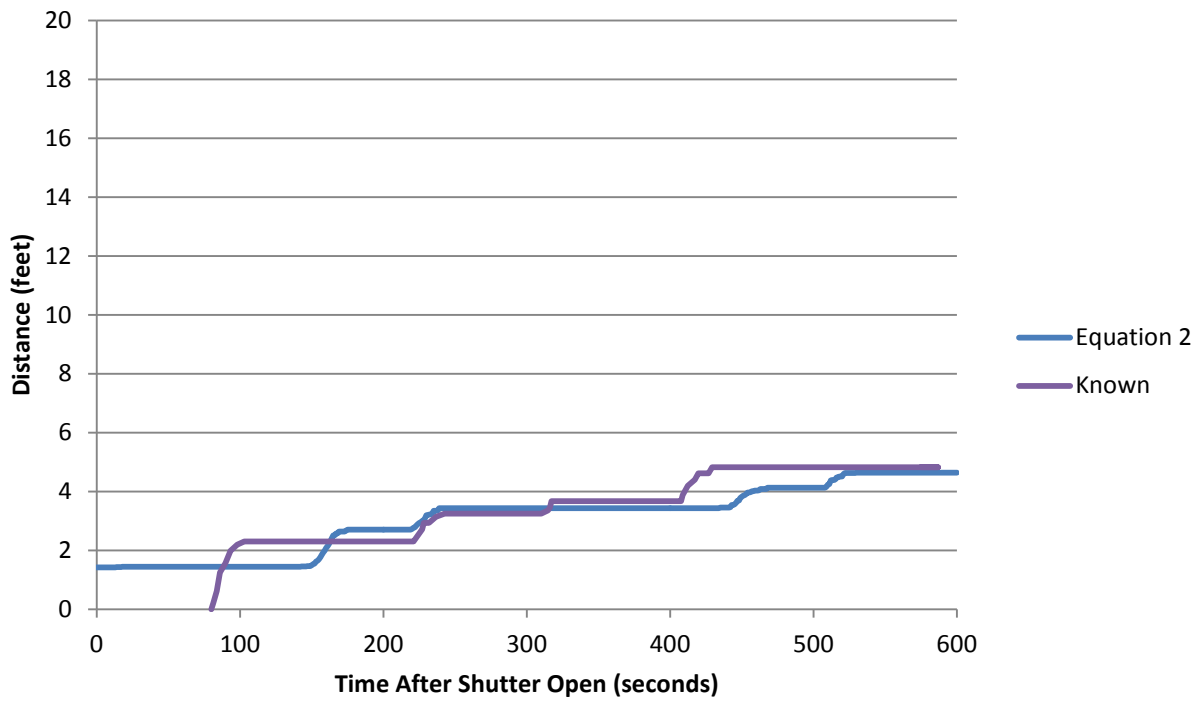
Figure 154: Flame Length Extension with No Flame Back CP 286
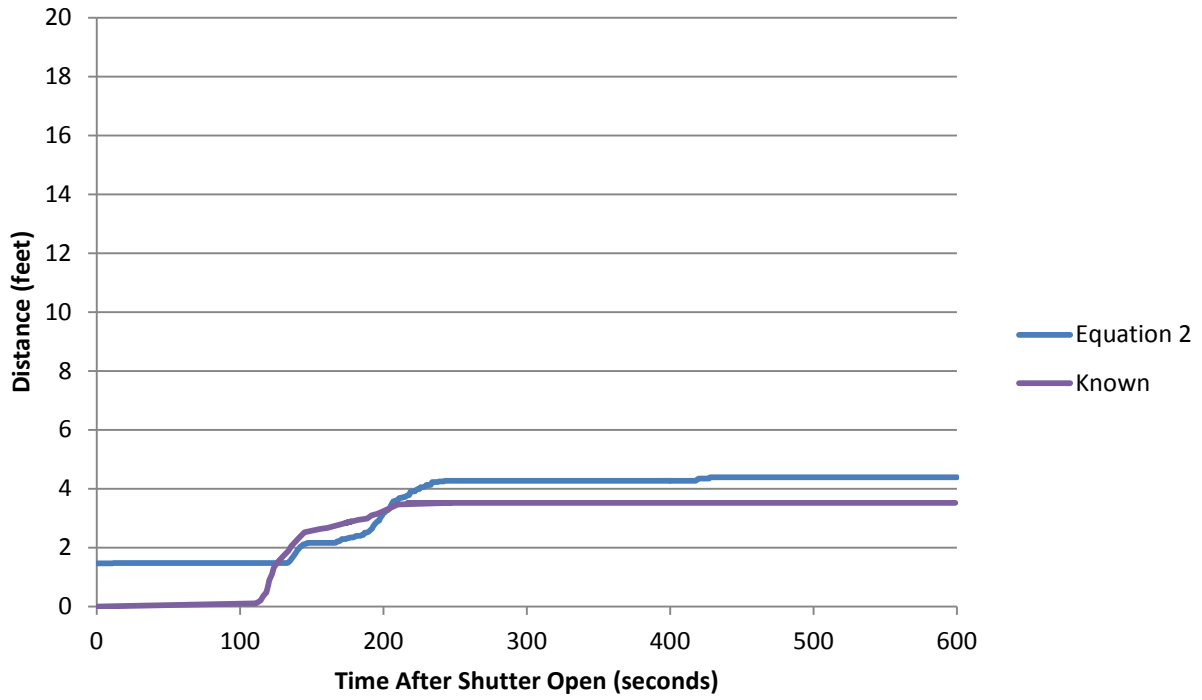
Figure 155: Flame Length Extension with No Flame Back FSI .075
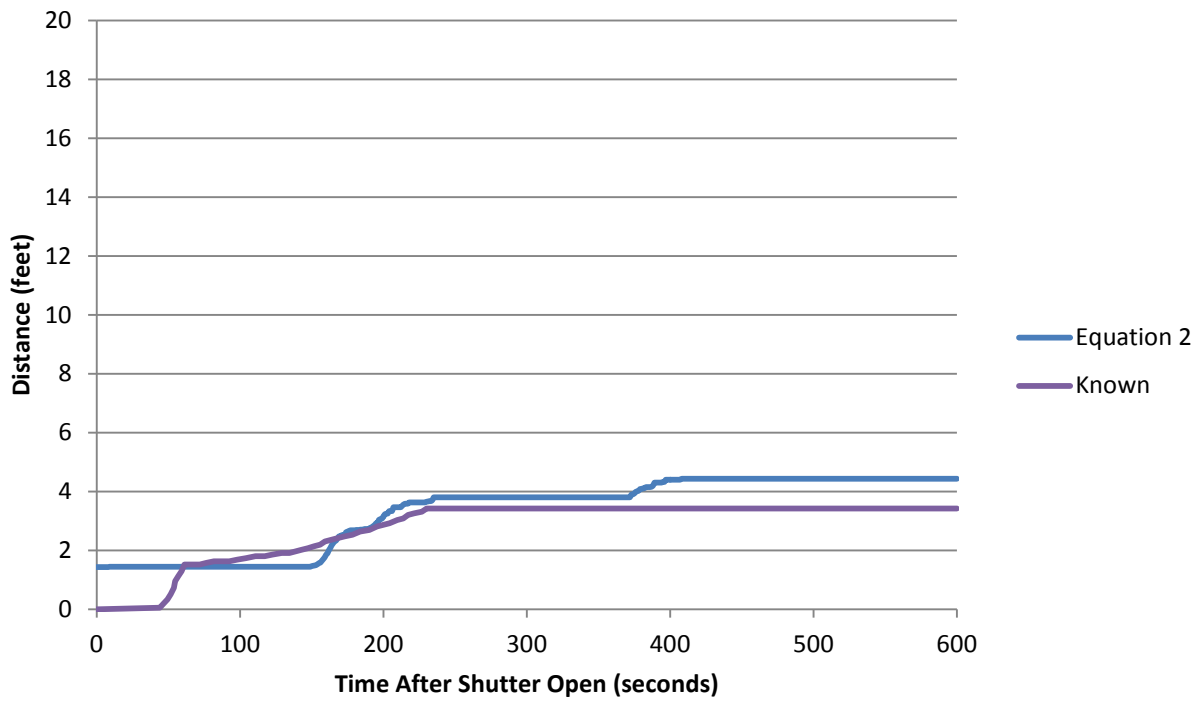
Figure 156: Flame Length Extension with No Flame Back FXE .090

5.10.7 Final Adjustment to Model

After working with these equations, it became apparent that there needed to be a change to eliminate the 1.5 foot flame indicated by the model while there was no flame indicated in the ASTM e84 Tunnel Test. This is believed to be caused by the different burning nature of the burners and the specimen being tested. When the burner flame is created, it can be considered a point source originating at the burner. The burning specimen on the other hand, cannot be construed as a point source coming from the same location as the burners. When the specimen begins to ignite, the average point source of the combined burners and material begins to move further down the tunnel. In order to account for this we have decided to change the equation used. The new equation can be seen below.

$$L_{f=}(\beta + \gamma) * \dot{Q}'^n$$

Beta is a constant that will be found to create a flame length of 4.5 feet when just the burners are on. Gama is a constant that will be found to add in when the specimen begins to burn. $\dot{Q}'$ will remain the heat release per unit width of the specimen and the burners. Finally, the value of n will be adjusted as well to create a more accurate model.

5.10.7.1 Ignition Delay

In order to have a model that best represents the Tunnel Test, we must have two separate equations to account for the different burning characteristics of the burners and specimen. In order to define a time to switch the equations it is necessary to define a time for ignition of the specimen in the Tunnel Test. This was completed by comparing the ignition times in the Tunnel Test and the ignition times when testing each specimen at varying incident heat fluxes in the Cone Calorimeter. The results of this can be seen below in Table 37 through Table 40.

Table 37: Time to Ignition Kreysler 1

Time to Ignition in ASTM e 84 = 175 seconds

	IHF (kW/m^2)	Sample	Tig (s)	Tig_avg (s)
	25	Kreysler System 1, Sample 1	619	567
	25	Kreysler System 1, Sample 2	515	
	30	Kreysler System 1, Sample 1	251	274.5
	30	Kreysler System 1, Sample 2	298	
Krey 1	40	Kreysler System 1, Sample 1	201	188
	40	Kreysler System 1, Sample 2	175	
	50	Kreysler System 1, Sample 1	128	131
	50	Kreysler System 1, Sample 2	134	
	75	Kreysler System 1, Sample 1	55	62.5
	75	Kreysler System 1, Sample 2	70	

Between 40 & 50 kW/m^2

Table 38: Time to Ignition CP286

Time to Ignition in ASTM e 84 = 90 seconds

	IHF (kW/m^2)	Sample	Tig (s)	Tig_avg (s)
CP 286	15	3-1 286	646	789.5
	15	3-2 286	933	
	20	3-1 286	407	402.5
	20	3-2 286	398	
	25	CP 286-1	176	169
	25	CP 286-2	162	
	30	3-1 286	176	169
	30	3-2 286	162	
	40	3-1 286	115	113
	40	3-4 286	111	
	50	3-1 286	63	62.5
	50	3-2 286	62	
	75	3-1 286	23	24
	75	3-2 286	25	

Between 40 & 50 kW/m^2

Table 39: Time to Ignition FSI 0.075

Time to Ignition in ASTM e 84 = 110 seconds

	IHF (kW/m^2)	Sample	Tig (s)	Tig_avg (s)
FSI .075	20	FSI .075 2-1	350	354.5
	20	FSI .075 2-2	359	
	30	FSI .075 2-1	127	180
	30	FSI .075 2-2	233	
	40	FSI .075 2-3	85	102
	40	FSI .075 2-4	119	
	50	FSI .075 2-1	28	28
	50	FSI .075 2-2		

Between 30 & 40kW/m^2

Time to Ignition in ASTM e 84 = 50 seconds

	IHF (kW/m^2)	Sample	Tig (s)	Tig_avg (s)
FXE .090	20	FXE .090 1-1	378	378.5
	20	FXE .090 1-2	379	
	30	FXE .090 1-1	182	171
	30	FXE .090 1-2	160	
	40	FXE .090 1-1	101	100.5
	40	FXE .090 1-2	100	
	50	FXE .090 1-1	59	66
	50	FXE .090 1-2	73	
	60	FXE .090 1-1	50	50.5
	60	FXE .090 1-2	51	

About 60 kW/m^2

The compiled incident heat fluxes that represent an approximate time to ignition can be seen below in Table 41

Table 41: Incident Heat Flux Representing Time to Ignition

Specimen	IHF (kW/m^2)
Kreysler 1	40
CP 286	40
FSI .075	40
FXE .090	60

Due to the unusual ignition characteristics in FXE .090, a time to ignition to be used in the correlation will be taken as the time to ignition of the specimen when run at an incident heat flux of 40 kW/m^2. The respective time to ignitions can be seen below in Table 42.

Specimen	Time to Ignition (seconds)
Kreysler 1	188
CP 286	113
FSI .075	102
FXE .090	100

These times indicate the time at which we will switch from the equation that only accounts for the burners to the equation that accounts for the specimen burning.

5.10.7.2   Equation for Burners

In order to calculate the equation for the burners a value of 2/3 will be assumed for n, a flame length of 1.37 meters (4.5 feet) will be used, and the value for Q' will be calculated by converting the known heat release of the burners of 88 kW/m^2 to a heat release per unit width.

$$\frac{Heat\ Release\ Rate}{.43\ meters} = Heat\ Release\ Rate\ per\ unit\ width\ (kW/m)$$

$$\frac{88\ kW/m^2}{.43\ meters} = 204.65\ (kW/m)$$

These values will then be put into the equation below and the equation will then be solved for beta.

$$L_{f=}(\beta) * \dot{Q}'^n$$

$$\frac{L_f}{\dot{Q}'^n} = \beta$$

$$\frac{1.37\ m}{204.65\ kW/m^{2/3}} = \beta$$

$$\beta = 0.0395$$

Now to check this equation, a value of 1.37 meters shall be obtained.

$$L_{f=}(\beta) * \dot{Q}'^n$$

$$L_{f=}(0.0395) * 204.65^{\frac{2}{3}} = 1.37\ m$$

This equation will be used for the time up to ignition of specimen as indicated by testing it at a 40 kW/m^2 incident heat flux in the Cone Calorimeter. For simplicity, a flame length of 4.5 feet will be assumed for all time before ignition in the correlation.

5.10.7.3   Equation for Burning Specimen

For the next part of this correlation it is necessary to find an appropriate gamma for our equation. In order to do this, the composite heat release per unit width as found above will be used as $\dot{Q}'$. This composite heat release per unit width will have an added 204.65 kW/m to account for the burners. These composite heat releases per unit widths were put into excel and ran through the equation below.

$$L_{f=}(0.0395 + \gamma) * \dot{Q}'^{2/3}$$

The same calculations as discussed in the equation analysis section will be used to first convert from meters to feet, then account for flame extension, next account for no flame back, and finally calculate the flame spread index. The flame length before ignition will be assumed as 4.5, and the value of gamma will then be found to best represent the Flame Spread Index found in the Tunnel Test. Before this is completed it is necessary to discuss the differences in the Kreysler 1 specimen as compared to CP 286, FSI .075, and FXE 0.090. It can be seen in the iterations above that Kreysler 1 performs differently than the other three samples; this is due to the nature of the Proprietary Case Stone Coating on the surface of the FRP. In order to account for this we will be calculating a separate gamma for the Kreysler 1 specimen. Also the value for gamma of the other three FRPs without a Proprietary Case Stone Coating will be found only utilizing CP 286 and FSI 0.075. FXE 0.090 will then be used to test the correlation made. The results from this can be seen below in Table 43 and Table 44.

Table 43: Calculated Gama for Kreysler 1

	Calculated	Known	Percent Error
Kreysler 1	18.00	18.00	0.02

Gama	0.0279

Table 44: Calculated Gama for CP286 and FSI .075

	Calculated	Known	Percent Error
CP 286	12.92	16.00	19.25
FSI .075	15.18	13.70	10.79
			15.02 Average Error

Gama	0.0107

From the Table 43 and Table 44 above, it can be seen that a value of 0.0279 has been found for gamma for Kreysler 1, and a value of 0.0107 has been found for gamma for CP 286 and FSI .075. Now I will use the values of FXE 0.090 to test the accuracy of the gamma found from CP 286 and FSI 0.075. The results can be seen below in Table 45.

Table 45: Value of Gama Checked Against FXE .090

	Calculated	Known	Percent Error
FXE .090	13.58	14.35	5.34

Gama	0.0107

As can be seen above in Table 45, the value of gamma found from CP 286 and FSI 0.075 creates a great correlation for FXE 0.090. The percent error in FXE 0.090 is significantly lower than the average percent error of CP 286 and FSI 0.075. This shows that the value found for gamma would work in the correlation. In order to see the correlation of these two equations, below is the generated graphs showing the calculated flame extension versus the known flame extension in the tunnel test in Figure 157 through Figure 160.
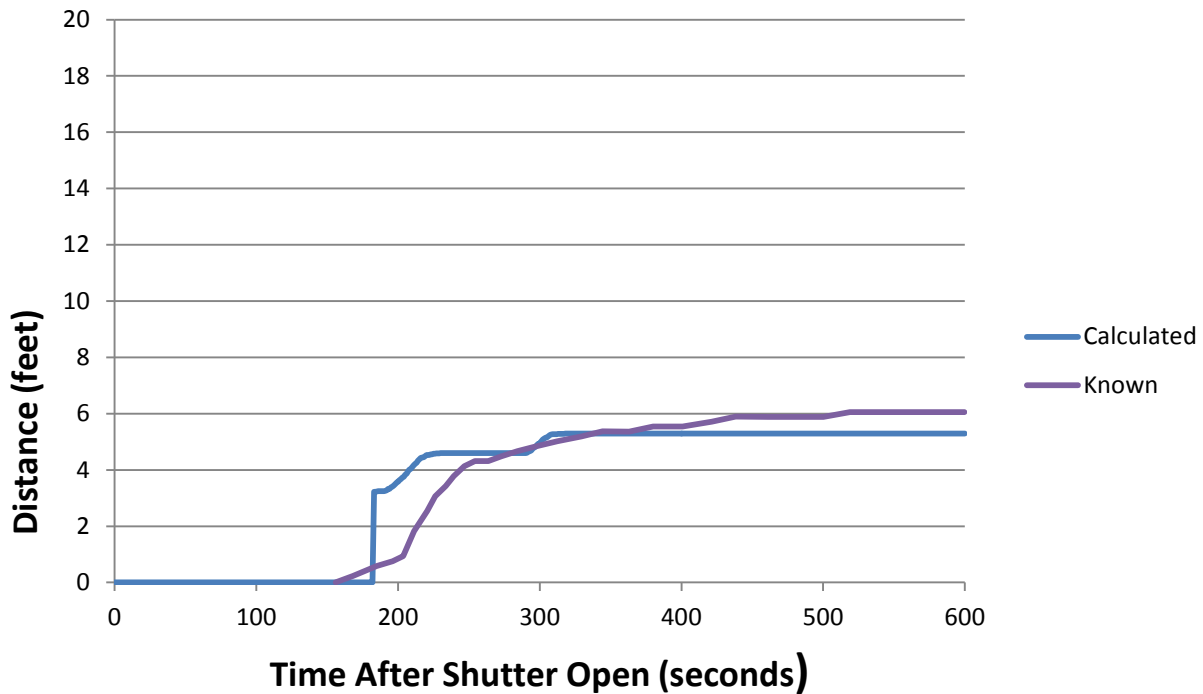
Figure 157: Calculated Flame Length Extension Kreysler 1
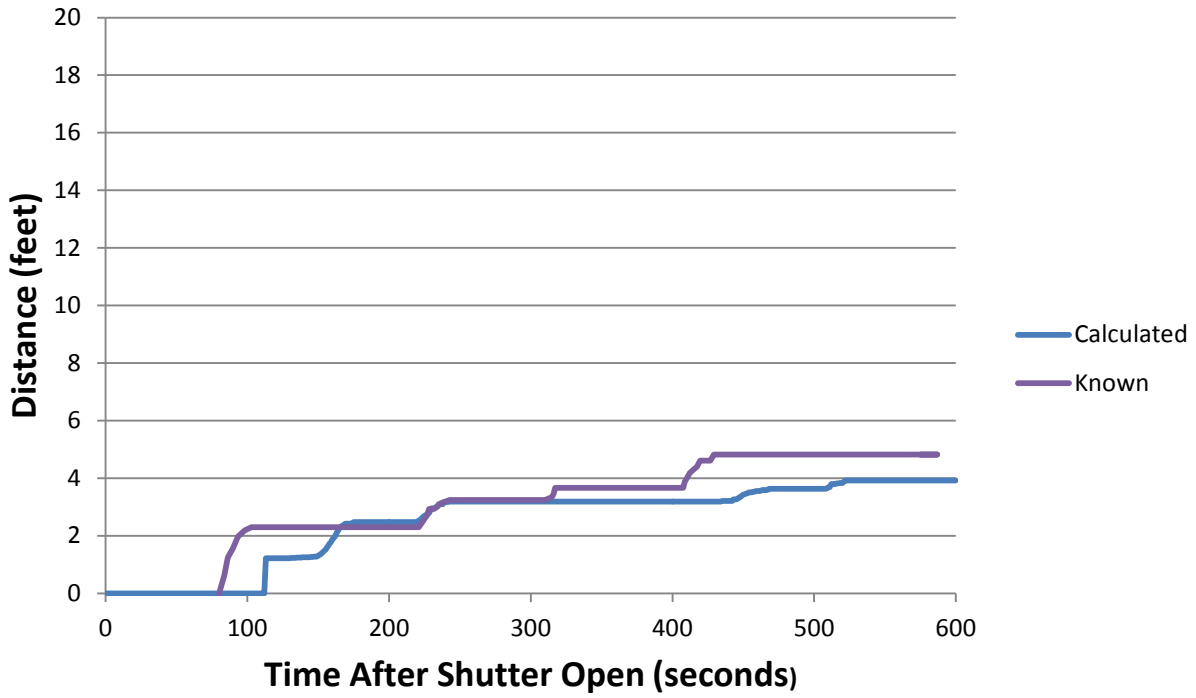
Figure 158: Calculated Flame Length Extension CP 286
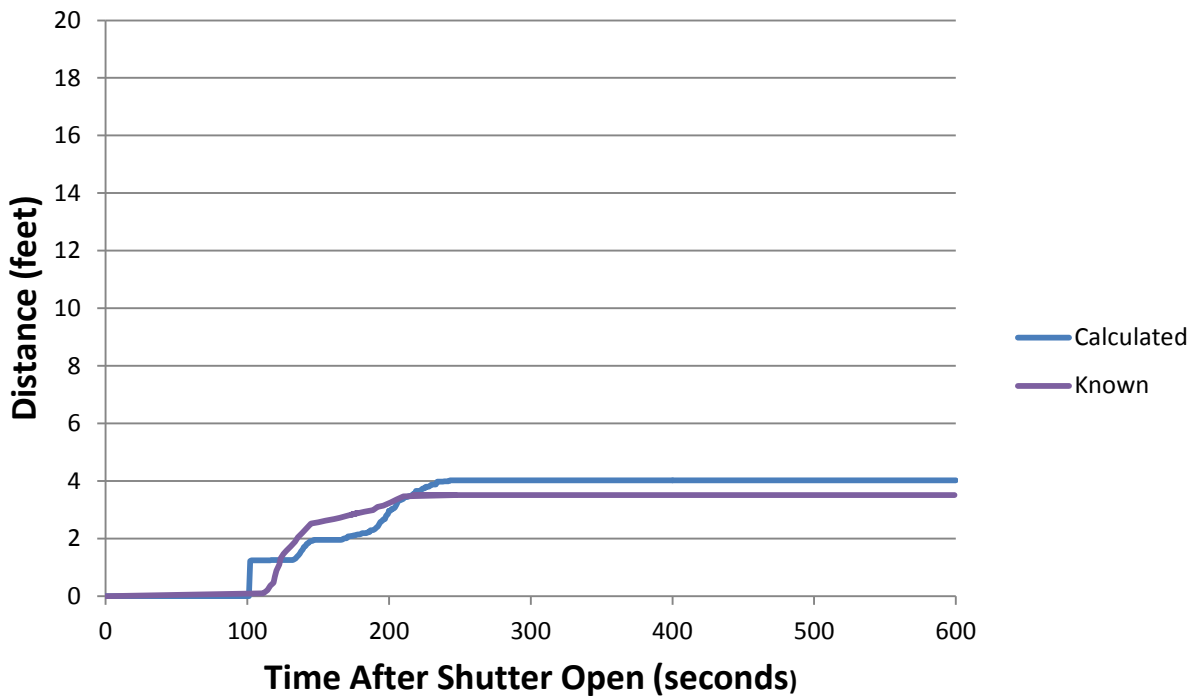
Figure 159: Calculated Flame Length Extension FSI .075
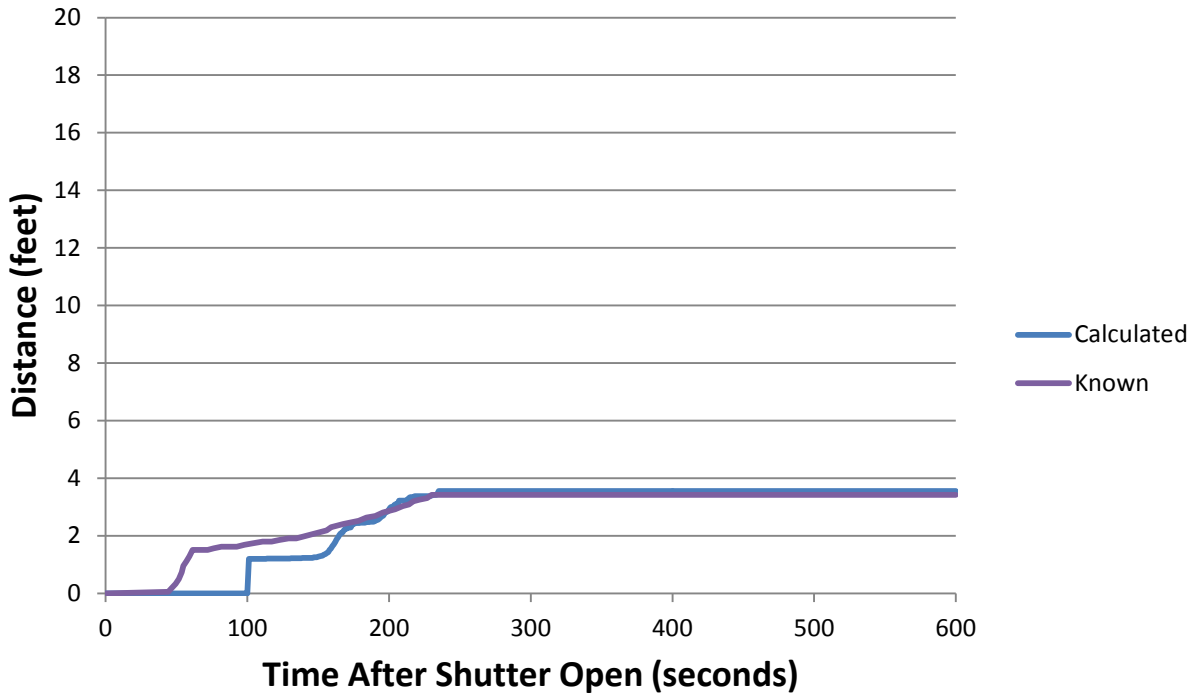
Figure 160: Calculated Flame Length Extension FXE .090

The next thing to check in this equation would be an adjustment to the value of n. In order to check to see if adjusting n will help the accuracy of this correlation, I will adjust the value of n for CP 286 and FSI .075 while keeping gamma the same and see if that lowers the average error. Unfortunately because there is only one specimen with a Proprietary Case Stone Coating, I cannot test the value of n for this. After adjusting the value of n to minimize the percent error for both CP 286 and FSI 0.075 and averaging them it has been found that the best value for n is 0.6709, which is not far from .6667 which is 2/3. Changing the value of n slightly increases the average error of CP 286 and FSI yet decreases the percent error of FXE .090 significantly. This can be seen in the Table 46 below.

Table 46: Percent Error- n Adjust

	Calculated	Known	Percent Error
CP 286	13.70	16.00	14.36
FSI .075	16.04	13.70	17.09
			15.72 Average Error

n	0.6709

	Calculated	Known	Percent Error
FXE .090	14.40	14.35	0.32

n	0.6709

From this information our new equations can be written as

$$\text{Proprietary Case Stone Coating Correlation } L_{f=}(0.0395 + 0.0279) * \dot{Q}'^{0.6709}$$

$$\text{Non-Coated FRP Correlation } L_{f=}(0.0395 + 0.0107) * \dot{Q}'^{0.6709}$$

$$where: L_f \text{ is in meters and } \dot{Q}' \text{ is in } kW/m$$

5.10.7.4   *Pyrolysis Length Sensitivity*

Our flame length correlation so far has assumed a pyrolysis of 4.5 feet (1.37 meters) when calculating the composite heat release rate for the specimen. After reviewing core samples taken from Kreysler 1 after it was burnt in the ASTM E84 Tunnel Test there was substantial decomposition from 0-5 feet and partial decomposition from 5-7 feet. Because of this it is necessary to test the sensitivity of this model to a larger pyrolysis zone while creating the composite heat release rate. In order to do this we will add to the composite heat release the heat release that we believe would be generated in the 4.5 foot to 5.5 foot section. The equation will then be adjusted and the percent error of the model will be calculated. The procedure in creating the new composed heat release rate is repeated from the same procedure discussed in Equation Analysis under Pyrolysis Length Sensitivity. Due to the nature of Kreysler 1 being the only specimen that we have with a Proprietary Case Stone Coating, the pyrolysis sensitivity can only be tested using CP 286 and FSI 0.075 then validated using FXE 0.090. The first thing done after calculating the new composite heat release rate was to calculate a new value for gamma while keeping n at 2/3.Then the value for n was calculated after finding gamma. The results can be seen in the tables below in Table 47.

Table 47: Calculated Values for Gama and n

	Calculated	Known	Percent Error	
CP 286	13.90	16.00	13.16	
FSI .075	15.86	13.70	15.73	
			14.45	Average Error

gama	0.0115
n	0.6664

	Calculated	Known	Percent Error
FXE .090	15.25	14.35	6.25

gama	0.0115
n	0.6664

From these results it can be seen that adding one foot to the pyrolysis zone does not change the values significantly. The average error of CP 286 and FSI .075 has decreased by 1.27 percent, but the percent error on FXE 0.090 has increased by 5.93 percent. From this information a conclusion has been made to

keep the pyrolysis zone at 4.5 feet because the correlation is not made any more accurate by adjusting the pyrolysis zone.

5.10.8 Single Incident Heat Flux Model

The correlation that we have created utilizes a fairly complicated testing procedure in the cone calorimeter. Most material manufacturers want to be able to test a specimen at a single Incident Heat Flux in order to get an idea how the material would perform in the ASTM E84 Tunnel Test. In order to make the testing procedure easier but sacrifice accuracy a new model was created to allow the use of heat release data from a single Incident Heat Flux test. To do this an Incident Heat Flux must be chosen that gives Heat Release data that best represents the composite heat release rate we created for the model earlier. An incident heat flux of 40 kW/m^2 has already been found to estimate the time to ignition in the tunnel test. Now an incident heat flux must be found that represents the composite heat release rate curve. To do this a comparison was made to the peak heat release of the composite heat release rate and the specimens tested at varying incident heat fluxes after multiplying the peak heat release by 0.60 m^2 which is the area of the pyrolysis zone in the tunnel test. The results can be seen in Table 48 below.

Table 48: Peak Heat Release Comparison

Specimen	Composite Peak Heat Release Rate (kW)	Average Peak Heat Release Rate from Single IHF (kW)		
		20 (kW/m2)	30 (kW/m2)	40 (kW/m2)
Kreysler 1	39	2	47	46
CP 286	70	62	68	71
FSI 0.075	73	119	106	120
FXE 0.090	60	110	96	107

From this table it can be seen that testing at an incident heat flux of 40 kW/m^2 also gives the best representation of the peak heat release rate in the composite heat release rate. The only problem is that the average peak heat release rate of FSI 0.075 and FXE 0.090 are much larger than that of Kreysler 1 and CP 286. It is believed that this could be due to the smaller thickness of FSI 0.075 and FXE 0.090 as compared to Kreysler 1 and CP 286; this causes the material to burn much faster in the cone and creates a higher peak heat release rate. This is something that is accounted for when finding the values for the constant gamma. Also to be noted is that Kreysler 1 will be calculated separately in order to create a separate correlation for materials with a Proprietary Case Stone Coating and the other three specimens will be used to create a correlation for specimens without a Proprietary Case Stone Coating layer.

The first thing completed when calculating the new model is to create an average heat release rate for each specimen by averaging the two samples that we analyzed in the cone calorimeter and multiplying them by the pyrolysis area which is (0.60 m^2). These curves can be seen below in Figure 161.
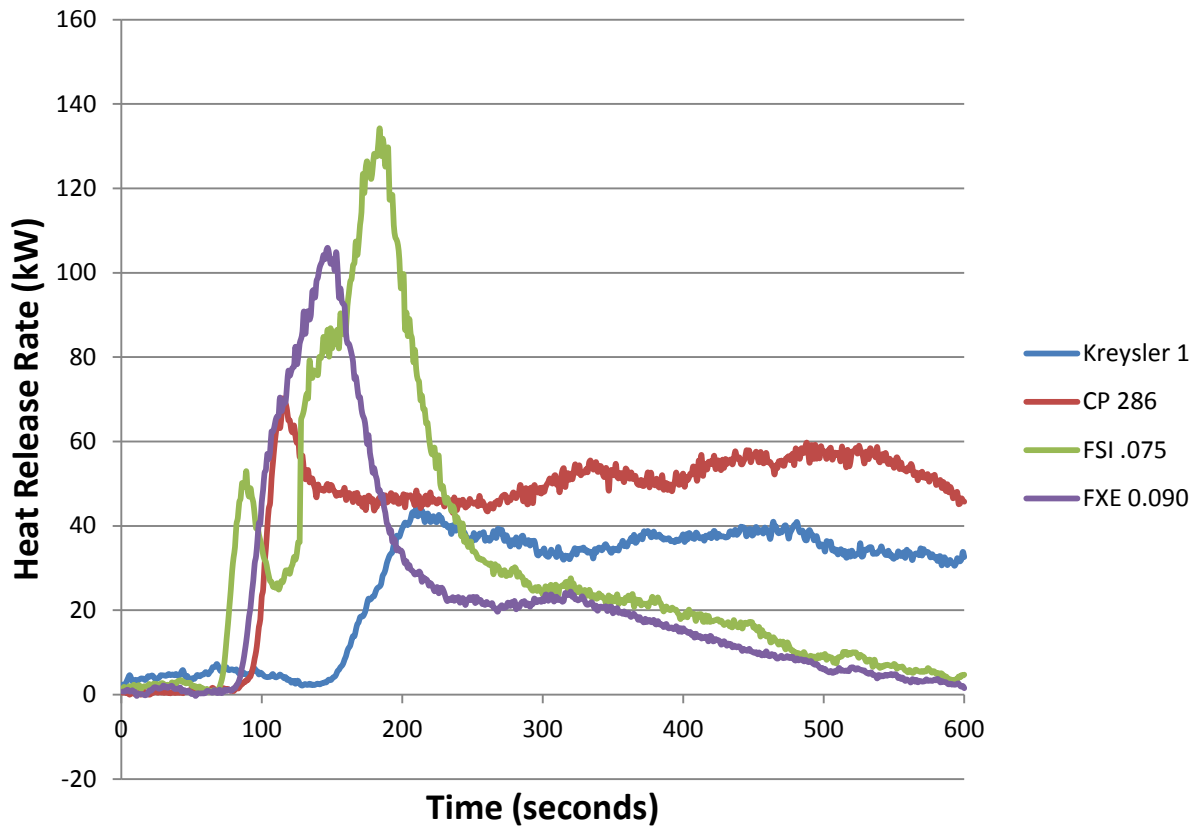
Figure 161: Average Heat Release Rates Created at IHF of 40 kW/m^2

The next thing to do to this data is to add the heat release of 88 kW for the burners and convert to heat release per unit width by dividing by .43 meters. This creates a heat release per unit area that we can then use for our correlation. A graph of the heat release rate per unit width curves can be seen below in Figure 162.
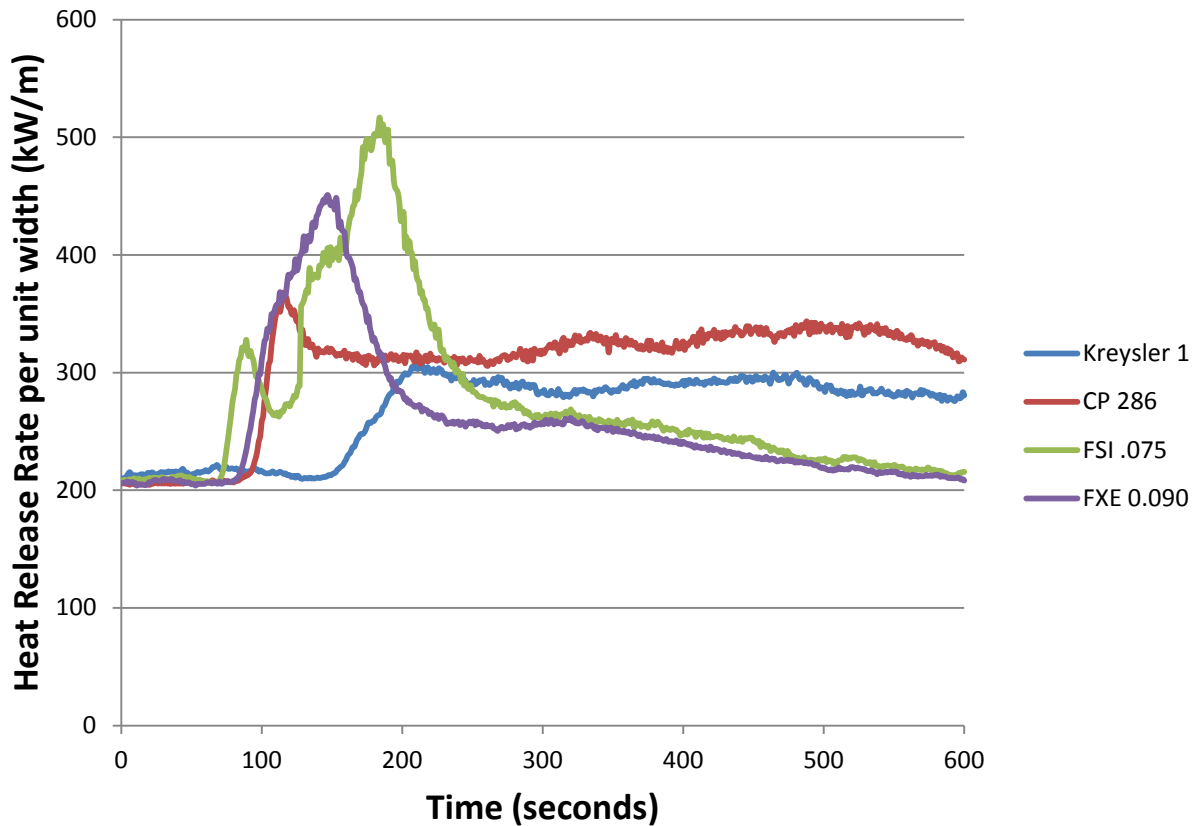
Figure 162: Heat Release Rate Per Unit Width

The following equation was then applied to the heat release per unit width curve for the time after ignition. The flame length before ignition was set to 4.5 feet. Gama was left as a constant to be determined later.

$$L_{f=}(0.0395 + \gamma) * \dot{Q}'^{2/3}$$

After this equation was applied the flame length was converted to feet, a distance of 4.5 feet was subtracted to calculate extension, and an if statement was applied in order to compensate for no flame back. After that the same calculations as discussed in equation analysis were used in order to calculate the flame spread index. Once this was completed, the value for gamma was determined with a slight preliminary adjustment to n. These results have been tabulated below in Table 49.

Table 49: Calculated Values for Gama and Percent Error

	Calculated	Known	Percent Error
Kreysler 1	17.99	18.00	0.08

gama	0.0310
n	0.6500

	Calculated	Known	Percent Error	
CP 286	11.87	16.00	25.84	
FSI .075	18.69	13.70	36.39	
			31.11	Average Error

gama	0.0085
n	0.6500

After finding a good value for gamma, the data from CP 286 and FSI 0.075 were used to find a better value for n.

Table 50: Calculated Value for n for CP286 and FSI .075

	Calculated	Known	Percent Error	
CP 286	11.76	16.00	26.52	
FSI .075	18.54	13.70	35.36	
			30.94	Average Error

gama	0.0085
n	0.6494

The new value for n which was found to be 0.6494 was then put into the Kreysler 1 correlation and a new value for gamma was found.

Table 51: Calculated Value for Gama for Kreysler 1

	Calculated	Known	Percent Error
Kreysler 1	18.01	18.00	0.07

gama	0.0313
n	0.6494

And finally, the values for gamma and n in the non-Proprietary Case Stone Coating coated correlation was checked against FXE 0.090.

Table 52: Checking Values for Gama and n

	Calculated	Known	Percent Error
FSI .090	16.16901298	14.35	12.68

gama	0.0085
n	0.6494

From this correlation it can be seen that accuracy has been sacrificed in order to make the correlation easier to use and to reduce the amount of tests needed in a cone calorimeter. The results of this correlation can be seen in the graphs below.
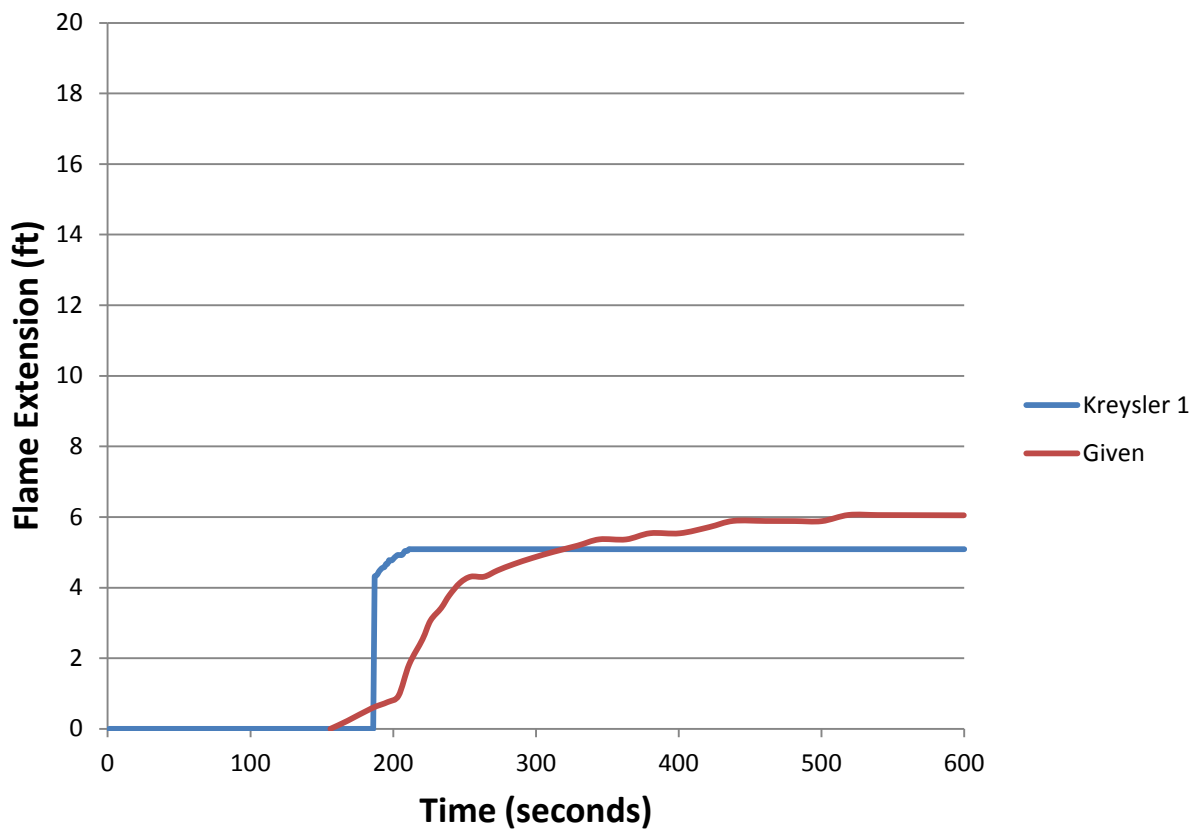
Figure 163: Calculated Flame Extension Kreysler 1
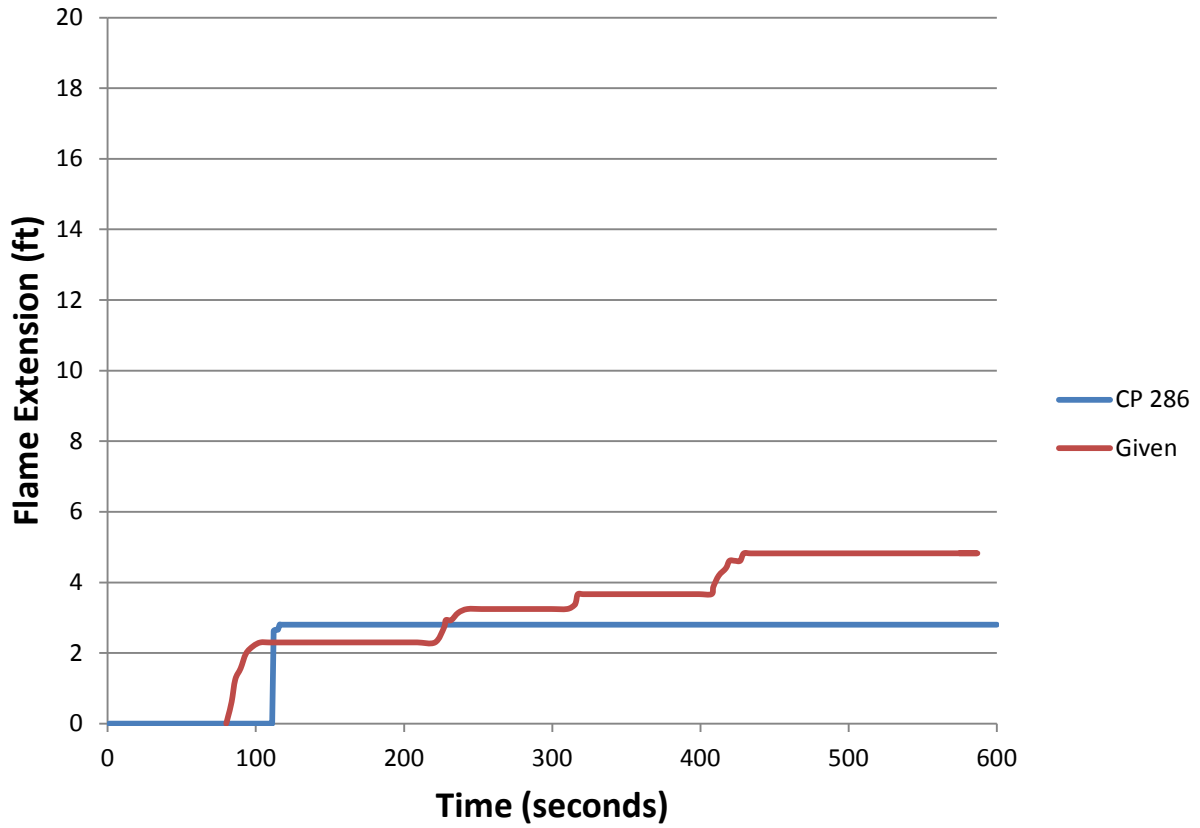
Figure 164: Calculated Flame Extension CP 286
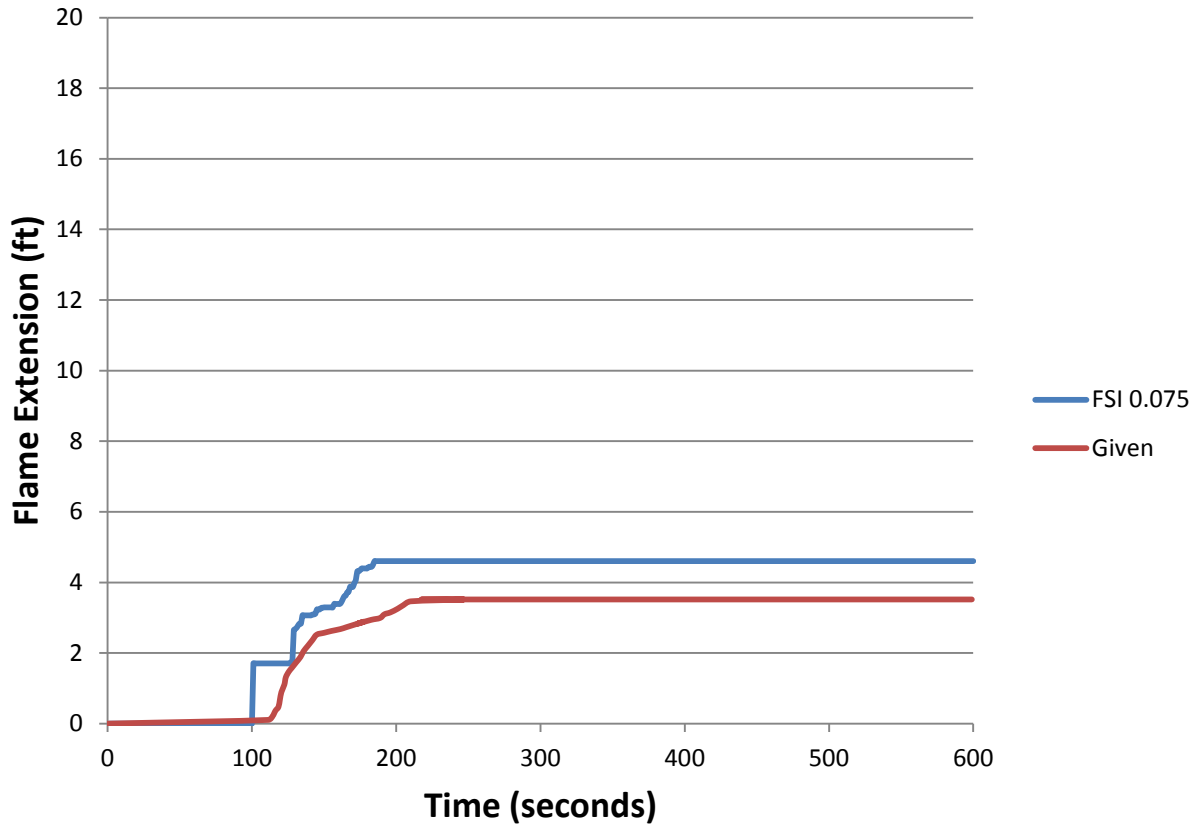
Figure 165: Calculated Flame Extension FSI 0.075

5.10.9 Ability to Pass ASTM E84 Quick Screen

Now that there is a correlation to relate the heat release rate of a specimen when tested in the ASTM 1354 Cone Calorimeter and a constant incident heat $40\frac{kW}{m^2}$ we can create a way to quick screen a material based upon both the peak heat release rate and the ignition temperature. In order to do this the assumption is made that as soon as the specimen ignites it reaches its peak heat release rate. This creates a rectangular area to be calculated under the flame extension time curve, the height of the rectangle being the calculated flame height and the width being 10 minutes minus time to ignition. The area under the curve was then multiplied by .515 to convert this area to a Flame Spread Index. The equation was then set equal to 25 and solved for Q in order to obtain the equations below.

Non-Proprietary Case Stone Coating

$$Qpeak = \left(\left(\left(\left(\left(\left(\frac{25}{10-tig}\right)+4.5\right)*\left(\frac{1}{0.1574}\right)^{\frac{1}{0.6494}}\right)*0.43\right)-88\right)*\frac{1}{60}\right)$$

Proprietary Case Stone Coating

$$Qpeak = \left(\left(\left(\left(\left(\left(\frac{25}{10-tig}\right)+4.5\right)*\left(\frac{1}{0.2322}\right)^{\frac{1}{0.6494}}\right)*0.43\right)-88\right)*\frac{1}{60}\right)$$

Tig is Time to Ignition in minutes

$Qpeak$ is maximum peak heat release rate in $\frac{kW}{m^2}$

The graphing of these two equations can be seen below in Figure 167 and Figure 168.
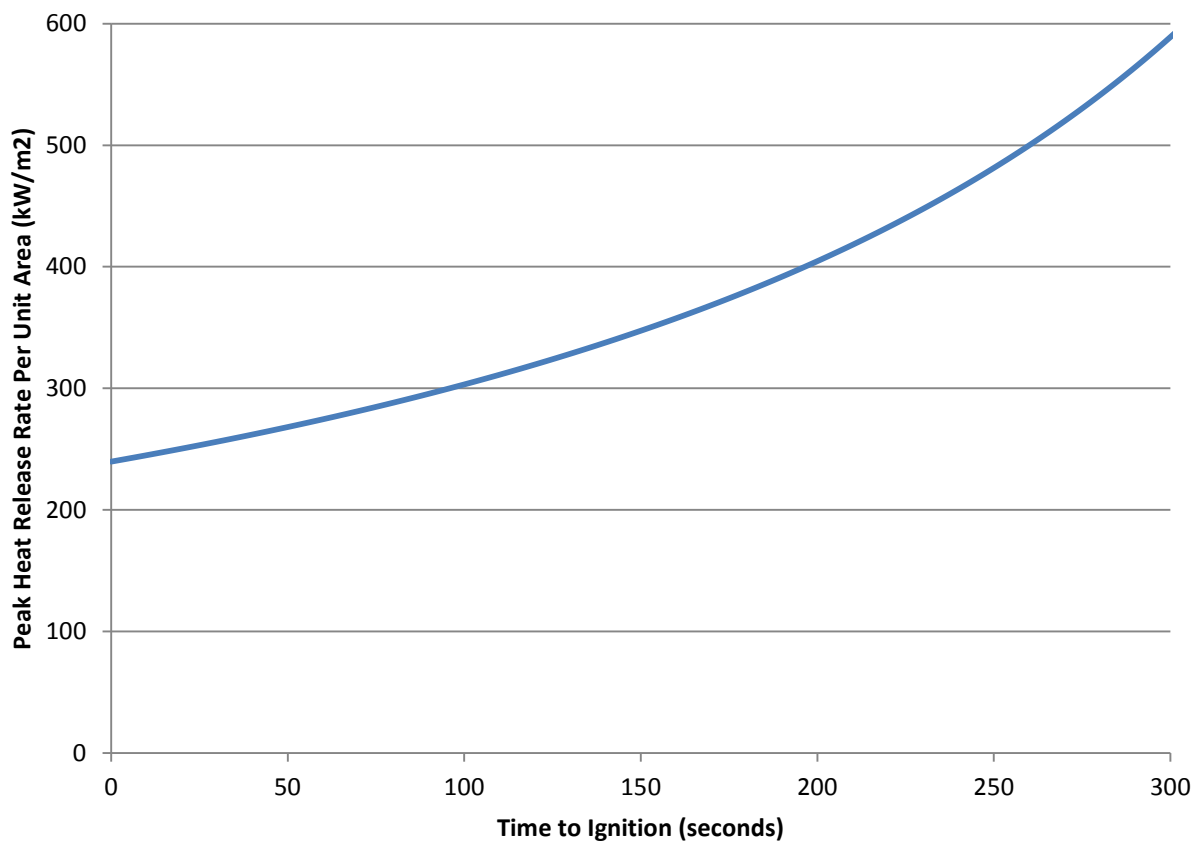
Figure 167: Peak HRR PUA versus Time to Ignition to Receive FSI of 25 for Non-Coated FRPs
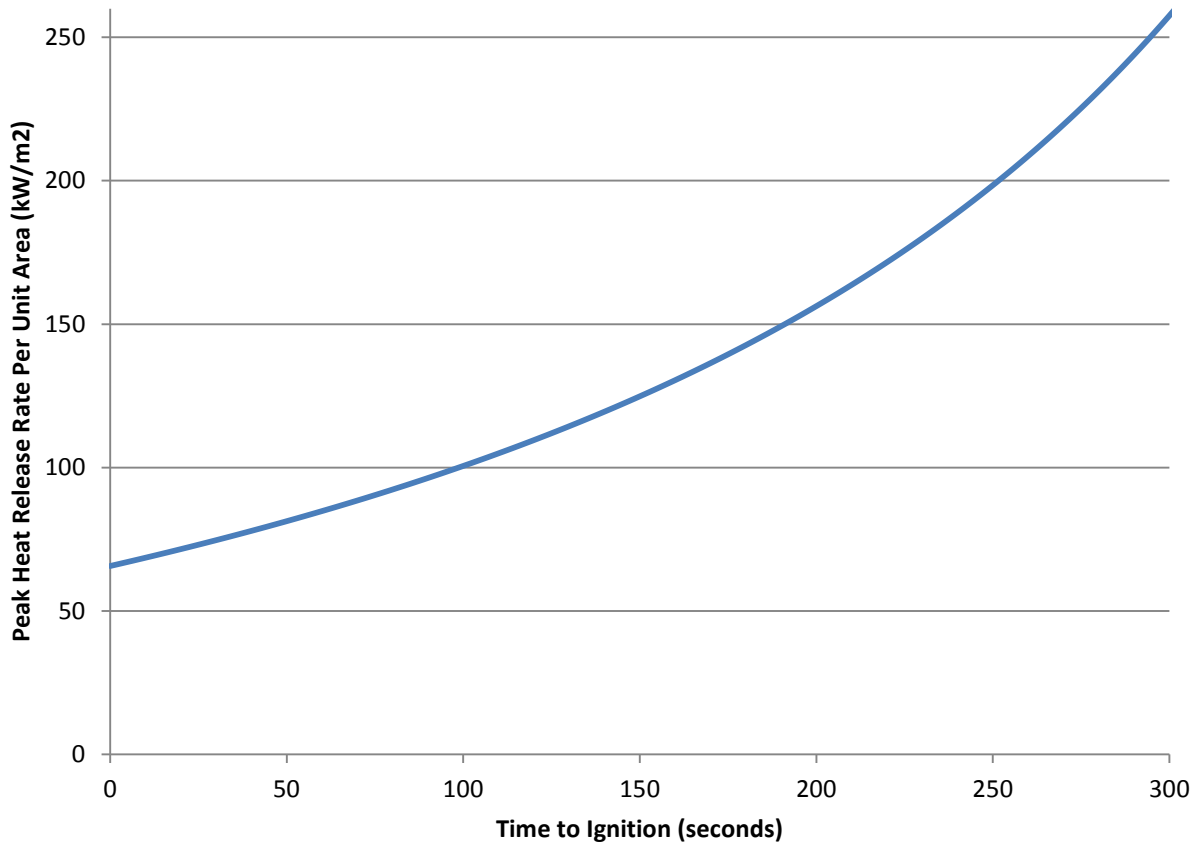
Figure 168: Peak HRR PUA versus Time to Ignition to Receive FSI of 25 for Proprietary Case Stone Coated FRPs

From this data it can be seen that as the time to ignition increases, the allowable peak heat release rate is increased at an exponential rate. Due to the nature of our correlation there is about a 30 percent error in the constants that were calculated while finding a single incident heat flux model. Also all of the specimens that we used in our correlation had a relatively low time to ignition which makes our model bias towards FRPs with lower ignition temperatures and the percent uncertainty will increase as ignition temperature is increased, because of this we have decided to truncate the curve at a maximum time to ignition of 300 seconds.

5.10.10   Conclusion

We have arrived at two sets of equations to predict the flame extension down an ASTM E84 Tunnel Test. One set of equations requires testing the specimen at three different incident heat flux steps. The resulting Heat Release rate per unit area must then be converted to a heat release rate by multiplying by the area of each section. These three heat release rate curves must be added together and a term of 88 kW be added. After that is completed the Heat Release rate must be converted to a heat release rate per unit width by dividing the rate by the width of the tunnel. Finally in order to calculate the distance the flame traveled down the tunnel, insert the heat release rate per unit width into the following equation and apply a flame extension of zero feet for all time before ignition as predicted from testing the specimen in an ASTM 1354 Cone Calorimeter at an incident heat flux of $40\frac{kW}{m^2}$.

Proprietary Case Stone Coating Correlation $L_{f=}\left((0.2211)*(Q'+\dot{2}04.47)^{0.6709}\right)-4.5$

Non-Coated FRP Correlation $L_{f=}\left((0.1647)*(Q'+20\dot{4}.4651)^{0.6709}\right)-4.5$

L_f is Flame Extension in Tunnel Test (ft)

$\dot{Q}'$ is a composite heat release rate per unit width of the specimen $\left(\dfrac{kW}{m}\right)$

The next set of equations that were created utilize Heat Release Rate data collected from running a sample at a single incident heat flux in the ASTM 1354 Cone Calorimeter. As before apply a flame extension of zero feet for all time before ignition as predicted from testing the specimen in an ASTM 1354 Cone Calorimeter at an incident heat flux of $40\,\dfrac{kW}{m^2}$.

Proprietary Case Stone Coating Correlation $L_{f=}\left((0.2322)*(\dfrac{(Q*.6\dot{0})+88}{.43})^{0.6494}\right)-4.5$

Non-Coated FRP Correlation $L_{f=}\left((0.1574)*(\dfrac{(Q*.6\dot{0})+88}{.43})^{0.6494}\right)-4.5$

L_f is Flame Extension in Tunnel Test (ft)

$\dot{Q}$ is the heat release per unit area retrieved from testing the specimen at an IHF $(\dfrac{kW}{m^2})$

5.10.11   References

1) Jeffrey S Newman, Christopher J Wieczorek, Chemical flame heights, Fire Safety Journal, Volume 39, Issue 5, July 2004, Pages 375-382, ISSN 0379-7112, 10.1016/j.firesaf.2004.02.003.

(http://www.sciencedirect.com/science/article/pii/S0379711204000244)

2) J.L. Consalvi, Y. Pizzo, B. Porterie, J.L. Torero, On the flame height definition for upward flame spread, Fire Safety Journal, Volume 42, Issue 5, July 2007, Pages 384-392, ISSN 0379-7112, 10.1016/j.firesaf.2006.12.008.

(http://www.sciencedirect.com/science/article/pii/S0379711207000057)

3) Chung Tsai, K.-. and Drysdale, D. (2002), Flame height correlation and upward flame spread modeling. Fire Mater., 26: 279–287. doi: 10.1002/fam.809

4) F. Tang, L.H. Hu, M.A. Delichatsios, K.H. Lu, W. Zhu, Experimental study on flame height and temperature profile of buoyant window spill plume from an under-ventilated compartment fire, International Journal of Heat and Mass Transfer, Volume 55, Issues 1–3, 15 January 2012, Pages 93-101, ISSN 0017-9310, 10.1016/j.ijheatmasstransfer.2011.08.045.

(http://www.sciencedirect.com/science/article/pii/S001793101100490X)

5)National Institute of Standards and Technology (NIST) and Society of Fire Protection Engineers (SFPE). International Conference on Fire Research and Engineering (ICFRE). Proceedings. September 10-15, 1995, Orlando, FL, SFPE, Boston, MA, Lund, D. P.; Angell, E. A., Editor(s)(s), 166-171 pp, 1995.

6) Grove, Brian, and James Quintiere. "Calculating Entrainment and Flame Height in Fire Plumes of Axisymmetric and Infinite Line Geometries. Linear and axisymmetric fires." Journal of Fire Protection Engineering 12 (2002): 117-137. Print

7) Hasemi, Y., 1986. Thermal Modeling Of Upward Wall Flame Spread. Fire Safety Science 1: 87-96. doi:10.3801/IAFSS.FSS.1-87

8) DiNenno, P. J. (2008). SFPE handbook of fire protection engineering (4th ed.). Quincy, Mass.: National Fire Protection Association pg 2-4, 3-122

9) Tu, King-Mon (08/01/1991). "Wall flame heights with external radiation". *Fire technology (0015-2684)*, 27 (3), p. 195.

10) Dietenberger, Mark A., White, Robert H. Reaction-to-fire testing and modeling for wood products. IN: Twelfth Annual BCC Conference on Flame Retardancy, May 21-23, 2001, Stamford, CT. Norwalk, CT: Business Communications Co., Inc., 2001. pp. 54-69

11) Parker, William. "An Investigation of the Fire Environment in the ASTM E 84 Tunnel Test." National Bureau of Standards technical note 945 (1977): 28. Print.

12) ASTM Standard e-84,2012, "Standard Test Method for Surface Burning Characteristics of Building Materials," ASTM International, West Conshohocken, PA, 2012 DOI : 10.1520/E0084-12A, www.astm.org.

13) Zhou, L.; Fernandez-Pello, A. C. Turbulent, Concurrent, Ceiling Flame Spread: The Effect of Buoyancy. Combustion and Flame, Vol. 92, No. 1-2, 45-59, 1993.